Paleoenvironmental Interpretations of the Lower Taylor Group, Olympus Range Area, southern Victoria Land, Antarctica

---

A thesis submitted in partial fulfillment of

the requirements for the degree

of

Master of Science in Geology

At the University of Canterbury

By

Greer J. Gilmer

University of Canterbury
2008

Frontispiece

Olympus Range

Right to left: Mt Circe, Mt Dido, Mt Electa

Abstract

The Devonian Taylor Group, in the Olympus Range area, southern Victoria Land (SVL), Antarctica, is separated from the basement by a regional nonconformity (Kukri Erosion Surface). A second localized unconformity within the Taylor Group called the Heimdall Erosion Surface separates the New Mountain Sandstone and older units from the younger Altar Mountain Formation. The depositional environment of the New Mountain Sandstone has long been under contention.

The New Mountain Sandstone Formation is a predominantly quartzose cross-bedded sandstone. Its newly defined Mt Jason Member is a coarse arkosic small scale cross-bedded pebbly sandstone that grades up section into the rest of the quartzose New Mountain Sandstone with large scale cross beds. The New Mountain Sandstone has been divided into five lithofacies including the Basal Conglomerate Lithofacies, Pebbly Sandstone Lithofacies, Granule Cross-bedded Lithofacies, Pinstripe Cross-bedded Lithofacies and Cross-bedded Sandstone Lithofacies. Deposition was in a shoreface environment with minor coastal aeolian deposition. The environment changed from upper shoreface to lower shoreface up section, forming transgressive to highstand systems tracts.

The Heimdall Erosion Surface truncates the Cross-bedded Sandstone Lithofacies and the Pinstripe Cross-bedded Lithofacies and was formed due to relative sea level fall leading to exposure and erosion of underlying sedimentary and basement rocks. It forms a type 1 sequence boundary. The New Mountain Sandstone was partially or totally lithified before erosion as shown by the jagged morphology of the eroded cross beds on the surface. It is not known when cementation of the NMS took place or how much of the formation has been eroded. The Heimdall Erosion Surface and Kukri Erosion Surface converge locally due to erosion on the Heimdall Erosion Surface and relief on the Kukri Erosion Surface.

The Heimdall Erosion Surface became a shore platform and the site of deposition as relative sea level rose. The Altar Mountain Formation with its Odin Member is a cross-bedded, massive and bedded feldspathic and quartzose sandstone that fines up section and is deposited on the erosion surface. The Altar Mountain Formation is divided into four lithofacies including the Conglomerate Lithofacies, Trough Cross-bedded Lithofacies, Cross-bedded Bioturbated Lithofacies and Bedded Fine Lithofacies. Deposition was in a shoreface environment, changing up section to an inner shelf environment with minor estuarine/tidal influence near the top of the section forming transgressive to highstand to regressive system tracts.

The sedimentary rocks are derived mainly from the Granite Harbour Intrusives and Koettlitz Group, which underlie the sandstones, but were exposed elsewhere in SVL. The sandstone clasts within the Conglomerate Lithofacies could be derived from underlying older Taylor Group rocks or exotic sources from outside the field area.

Correlation with data from adjacent areas suggests deposition of the New Mountain Sandstone occurred in a shallow sea that existed from the Olympus Range, southwards

into the Asgard Range and included Vashka Crag. The area around Sponsors Peak and to the north was exposed and supplying feldspathic and quartzose sediment and pebbles into the depositional basin. As relative sea level fell due to either tectonic uplift or eustatic processes a large area of southern Victoria Land was exposed including the Olympus and Asgard Ranges and Bull Pass-St Johns Range area. This lead to erosion of the New Mountain Formation and basement rocks. Deposition of the New Mountain Sandstone continued further south shown by the gradational contact between it and the overlying Altar Mountain Formation. Relative sea level rise led to deposition of the Altar Mountain Formation. Shallow seas once more dominated the southern Victoria Land with deltas in the east (in the Bull Pass-St Johns Range area) feeding feldspathic sediment into the depositional basin (Odin Member). Further sea level rise drowned the delta region and a shallow marine to inner shelf environment led to deposition of the rest of the Altar Mountain Formation.

Table of Contents

List of Figures

List of Tables

Acknowledgements

Firstly, I would like to thank John and Margaret Bradshaw (A.K.A Team J.A.M) for two great field seasons. Thank you both for teaching me the Antarctic ways, imparting priceless knowledge and telling great stories. I would also like to thank the other members of K051: Dr Robert Bolhar (2007) and Timothy O'Toole (2008).

Big thanks to Antarctica New Zealand for making the research possible and granting permission to enter ASPA 123, which proved invaluable. Thanks to all the Scott Base staff, especially Rob and HN0 for ferrying the team and our rocks around and providing news from the outside world and Jody for sending us surprise treats in our resupply.

Thanks to my supervisor Kari Bassett for teaching me about sedimentology and getting me to write like a grown up. Thank John Bradshaw for making sure everything made sense and Margaret Bradshaw for help with trace fossils and providing a wonderfully written and useful field notebook.

I would like to thank Dr Mike Palin from the University of Otago for initiating me into the mysteries of zircon dating and coaching me through copious spreadsheets.

Many thanks to Neil Andrews (Biology Department) for helping me with the SEM-CL; Rob Speirs for making my thin sections and cutting 'fun' rocks; Kerry Swanson for teaching me how to use the 'flash' microscope and camera; Chris Grimshaw and Jennifer Jackson for staining my thin sections.

Big ups to my classmates Jeremy, Myf, Tom, Richard, Neil, Kirsty, Henry and Brendan, who all went or are going through the ordeal. It has been heaps of fun though slightly insane. Thanks for always having time for a rant or procrastination.

Thanks to my boyfriend Chris for putting up with an absentee girlfriend (near the end) and editing all my chapters, which I am sure you found thoroughly stimulating.

Cheers to my present and past flatmates including Ella, Phil, Pete, Nita and Fiona. Thanks for providing a good excuse for being at home, having yummy food ready when I get there and putting up with a sometimes non-existent and unsociable flatmate.

Lastly, a big thanks to my family, Mum, Dad, Riley, Hugh, Zoë and Ella. Thanks for the care parcels and for being really supportive even though you think I am slightly mad.

Chapter One: Introduction

1.1 Introduction

The paleoenvironment of some of the lower formations in the Taylor Group have been much debated and the mechanisms that lead to formation of the Heimdall Erosion Surface are not well understood. The depositional environment of the New Mountain Sandstone Formation especially is a contentious issue due to different paleoenvironment interpretations suggested depending on the type of research undertaken (i.e. facies or trace fossil analysis). Extensive investigation of the Heimdall Erosion Surface has not been embarked on. The surface has been recorded throughout southern Victoria Land but no conclusions made as to how it formed or how it indicates changes in paleoenvironment.

The aim of this research is to determine the mechanisms that lead to the formation of the Heimdall Erosion Surface and the depositional environment of the lower formations of the Taylor Group in the Olympus Range map area (Isaac *et al*, 1995). The formations include the New Mountain Sandstone and Altar Mountain Formation including its Odin Arkose Member. The depositional features for each formation will be discussed in hope of resolving contentious issues concerning their depositional environment. This research uses a multidisciplinary approach combining facies, sedimentary structures and trace fossils. Additionally, dating of detrital zircons from the Taylor Group constrains the provenance of the sandstones and whether the source area changes up section. Overall, the research uses stratigraphy and provenance analysis to tie this area (Fig 1-1) to the regional stratigraphy to interpret the depositional environment across a wider area of southern Victoria Land. Most previous work done in the Olympus Range has been either broad reconnaissance mapping or detailed study and interpretation of small field areas and/or single formations.

Summary of research aims:

- Determination of depositional setting of New Mountain Sandstone and Altar Mountain Formation including the Odin Arkose Member

- Reconstruction of paleogeographic setting during deposition of the lower Taylor Group
- Understand the mechanisms that lead to the formation of the Heimdall Erosion Surface
- Identify the provenance of the New Mountain Sandstone and Altar Mountain Formation including the Odin Arkose Member.

1.2 Field Area

The study is located in southern Victoria Land between latitudes 77 15` and 77 35` S, mainly in the Olympus Range map area (Isaac *et al*, 1995) with one locality in the Bull Pass - St Johns Range map area (Turnbull *et al*, 1994). Field sites are located in the Olympus Range, Balham and Barwick Valleys and Sponsors Peak area (Fig 1-1). The sedimentary rocks of interest in this research are the formations within the lower part of the Taylor Group, which is part of the lower Beacon Supergroup in southern Victoria Land (Fig 2-1). The rocks are mainly medium to coarse cross-bedded sandstones with minor conglomerate units.

Field sites were chosen based on work by Barrett and Webb (1973), Plume (1976, 1978, 1982) and Isaac *et al* (1995). Proximity to the Heimdall Erosion Surface was also important. The inset maps below show campsites, field sites, routes and locations of measured sections. The key for the inset maps can be seen in Fig 1-2B. Campsites were located at (Fig 1-1):

- Mt Jason (S 77º 29.059', E 161º 36.130')
- Mt Boreas (S 77º 29.782, E 161º 13.769)
- Mt Electra (S 77º 30.697', E 160º 51.374')
- The valley floor west of Lake Vashka (S 77º 21.237', E 161º 03.794')
- A snowfield west of Sponsors Peak (S 77º 18.027', E 161º 17.503')

The field party in January 2007 included Dr Margaret Bradshaw, Dr John Bradshaw, Dr Robert Bolhar and the author. In January 2008, MSc student Timothy O'Toole was the fourth member of the party.

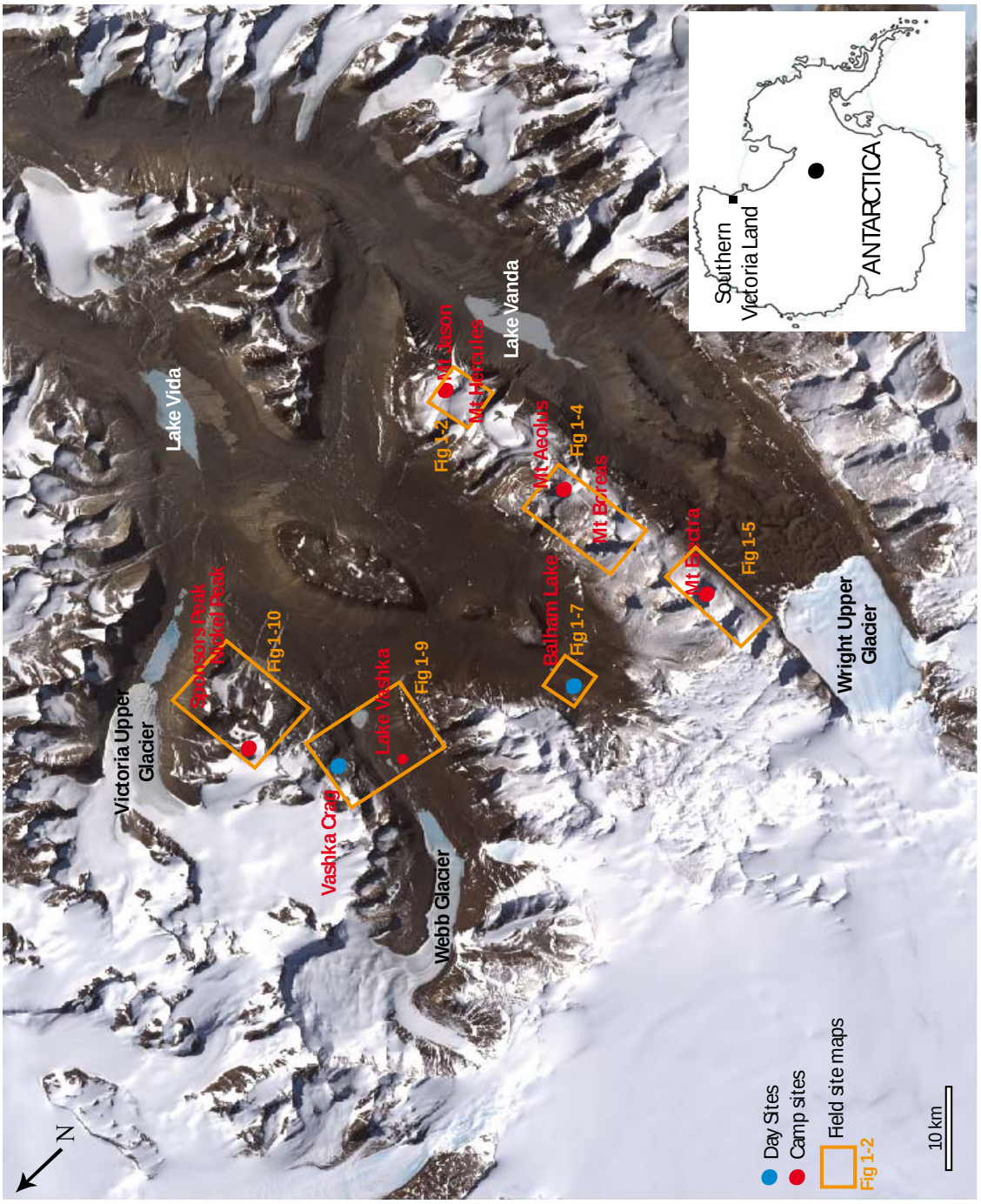

Figure 1-1: Overall location of field area and field sites. Satellite image (NASA, 2008) and inset map (1-World Maps Online, 2008)

Fieldwork at Mt Jason (Fig 1-2A) was focused on the north and east face (Fig 1-3A, B) and the col between Mt Jason and Mt Hercules. At Mt Hercules, sediments were observed on the eastern face. The base of the measured sections occur at: Mt Jason, S 77º 28.918', Eº 161 36.006' and Mt Hercules, S 77º 29.117', E 161º 26.854' (Fig 1-2A).

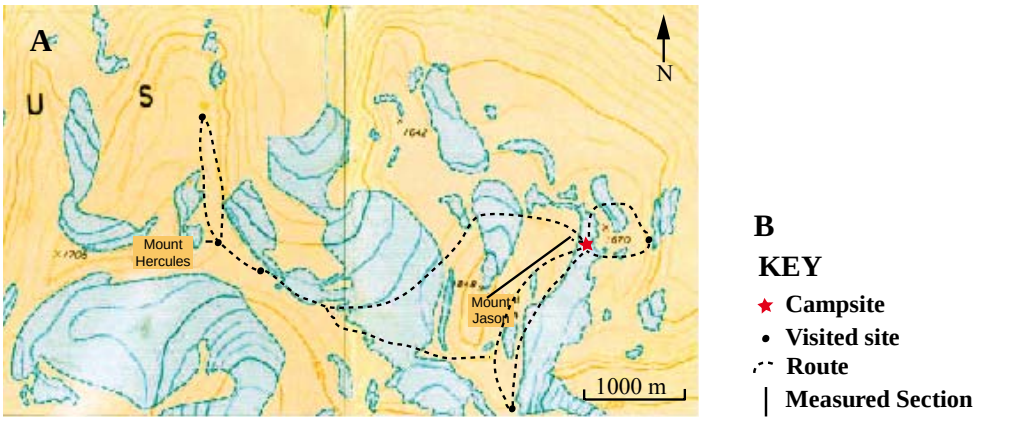

Figure 1-2: A) Fieldwork locations at Mt Jason and Mt Hercules. (USGS, 1977c) **B)** Key for all inset maps.

Figure 1-3: A) Eastern slope (NB figures at bottom left) and **B)** Northern face of Mt Jason

Fieldwork at Mt Aeolus was restricted to one extensive stratigraphic section from the basement through a large portion of the Taylor Group. The section begins at S 77º 30.319', E 161º 18.205' (Fig 1-4). Two sites were investigated at Mt Boreas, one northeast of Mt Boreas and the other to the southeast (Fig 1-4). One stratigraphic column was measured to the southeast of the camp beginning at S 77º 30.585', E 161º 10.562'.

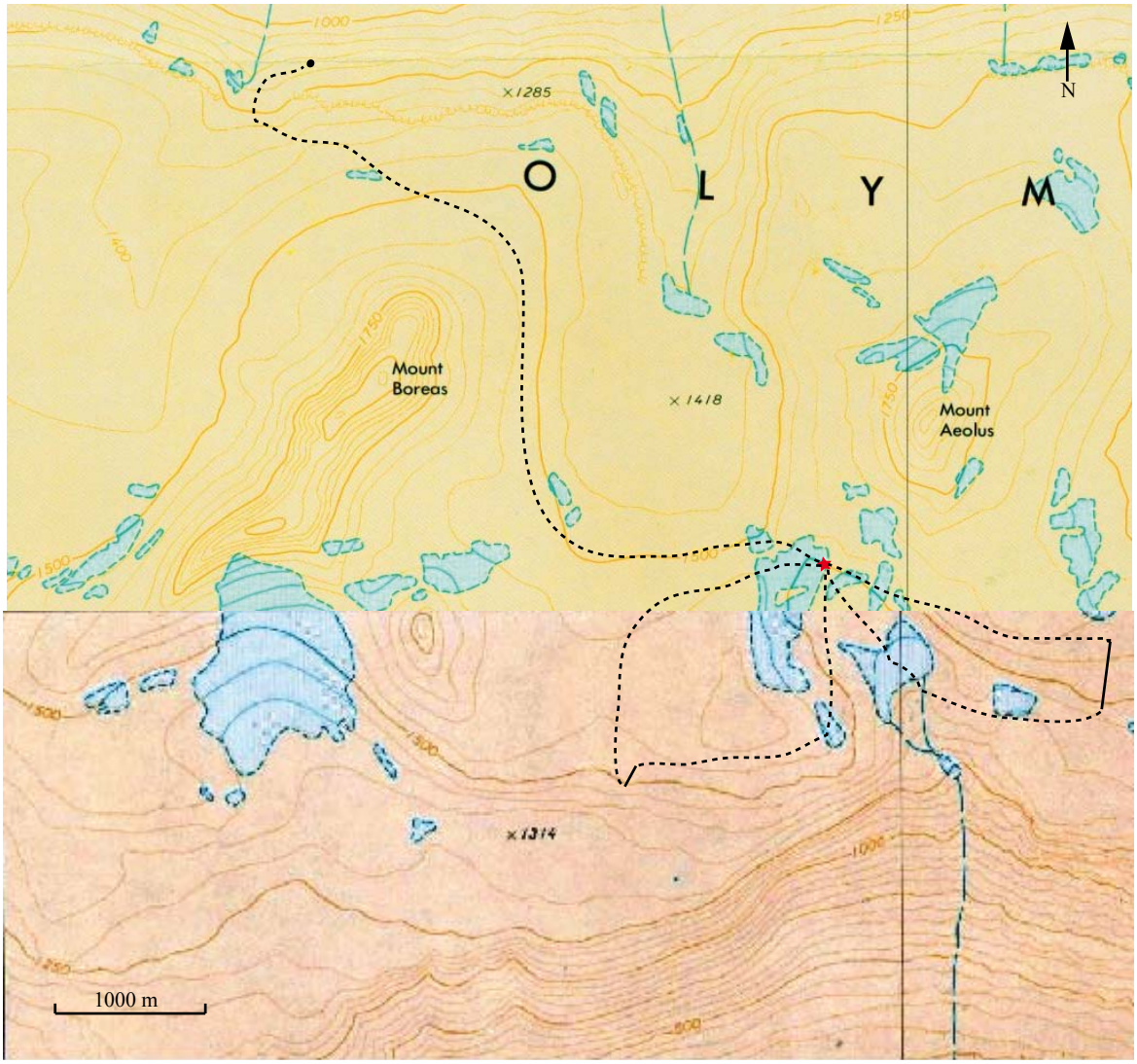

Figure 1-4: Fieldwork locations at Mt Aeolus and Mt Boreas. (USGS, 1977 & 1977c)

Fieldwork at Mt Electra (Fig 1-5) was undertaken east below Mt Dido (1-6B), directly below camp and to the west near the terminus of the Upper Wright Glacier (Fig 1-6A)(Fig 1-5). A stratigraphic column was measured below camp, S 77º 30.941', E 160º 51.559' (Fig 1-5).

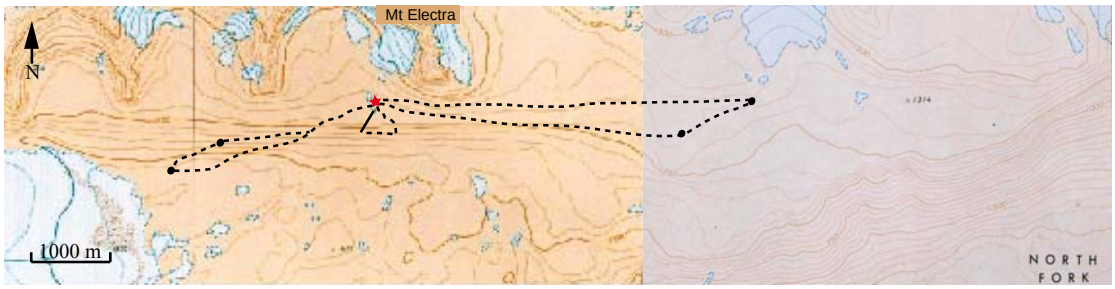

Figure 1-5: Fieldwork locations at Mt Electra (USGS 1997 & 1977b)

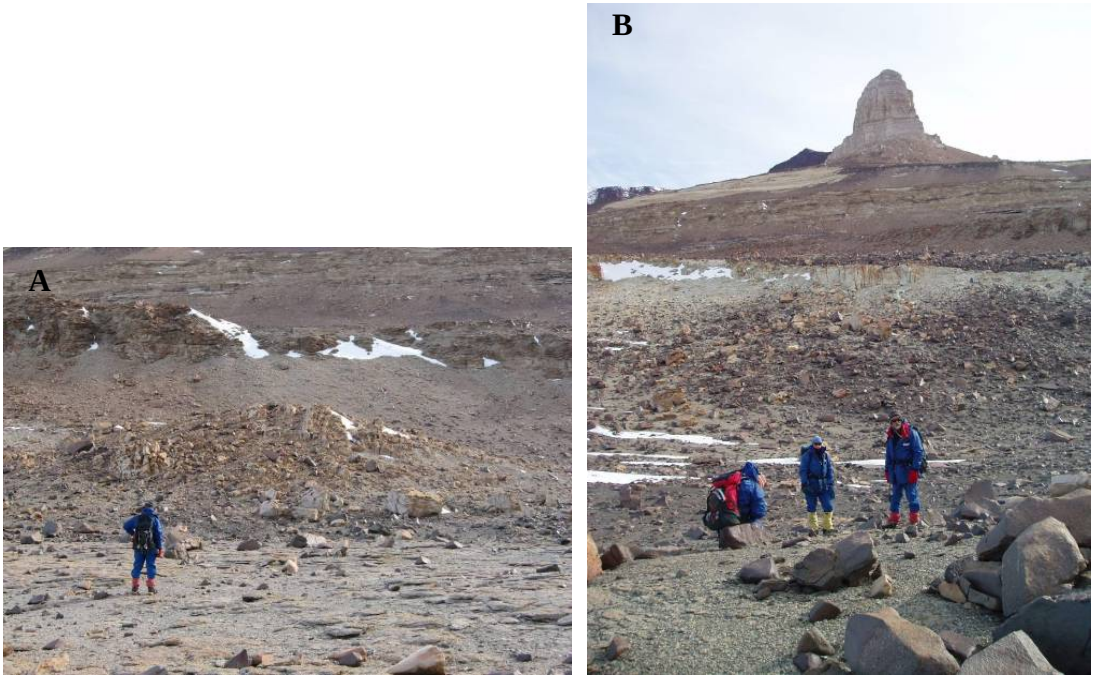

Figure 1-6: A) Valley side west of Mt Electra. **B)** Valley side east of Mt Electra. People are standing on basement rocks near base of Boreas Subgreywacke Member, Mt Dido in background

Balham Lake was a helicopter supported day trip from Sponsors Peak camp. Fieldwork was concentrated on examining the section measured by Barrett and Webb (1973). A stratigraphic column was measured beginning at S 77º 25.823', E 160º 53.733' (Fig 1-6). Permission was granted by Antarctica New Zealand to work in Antarctic Special Protected Area (ASPA) 123 (Barwick Valley, Victoria Land). An ASPA is an area protected by the Protocol on Environmental Protection to the Antarctic Treaty. ASPA 123 is protected because it has had a low amount of disruption by humans and is being used as a reference site to measure changes in more heavily used areas in the McMurdo Dry Valleys.

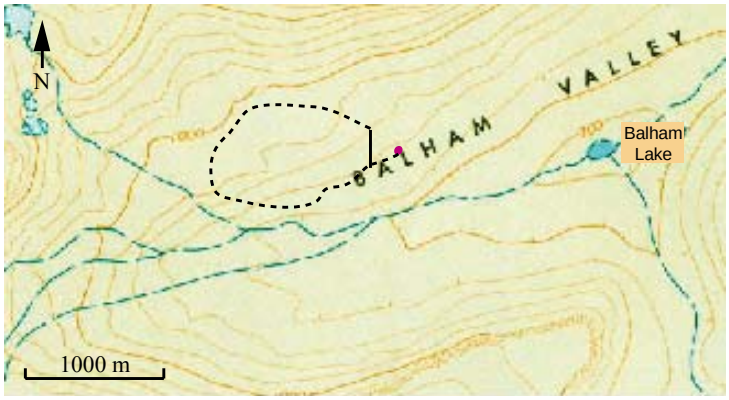

Figure 1-7: Fieldwork locations at Balham Lake. (USGS, 1977a)

Outcrops at Lake Vashka were in three crags along the southern side of the Barwick Valley (Fig 1-8). Crags are numbered from west to east: 1) S 77º 21.600', E 161º 05.612'. 2) S 77º 21.660', E 161º 06.071'. 3) 77º 21.740', E 161º 06.825' (Fig 1-8, 1-9). A section was measured on each crag. Permission was granted to camp and work in ASPA 123 where impact on the environment was kept to a minimum.

Vashka Crag was a helicopter supported day trip from Sponsors Peak. No sections were measured but outcrops were observed and recorded (Fig 1-9). Permission was granted to work for one day in ASPA 123.

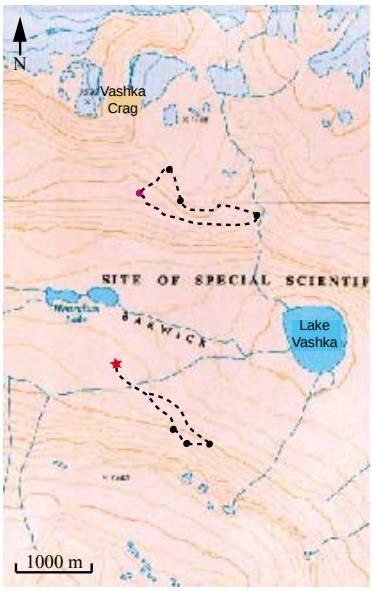

Figure 1-8: Fieldwork locations at Lake Vashka and Vashka Crag. (USGS, 1977c)

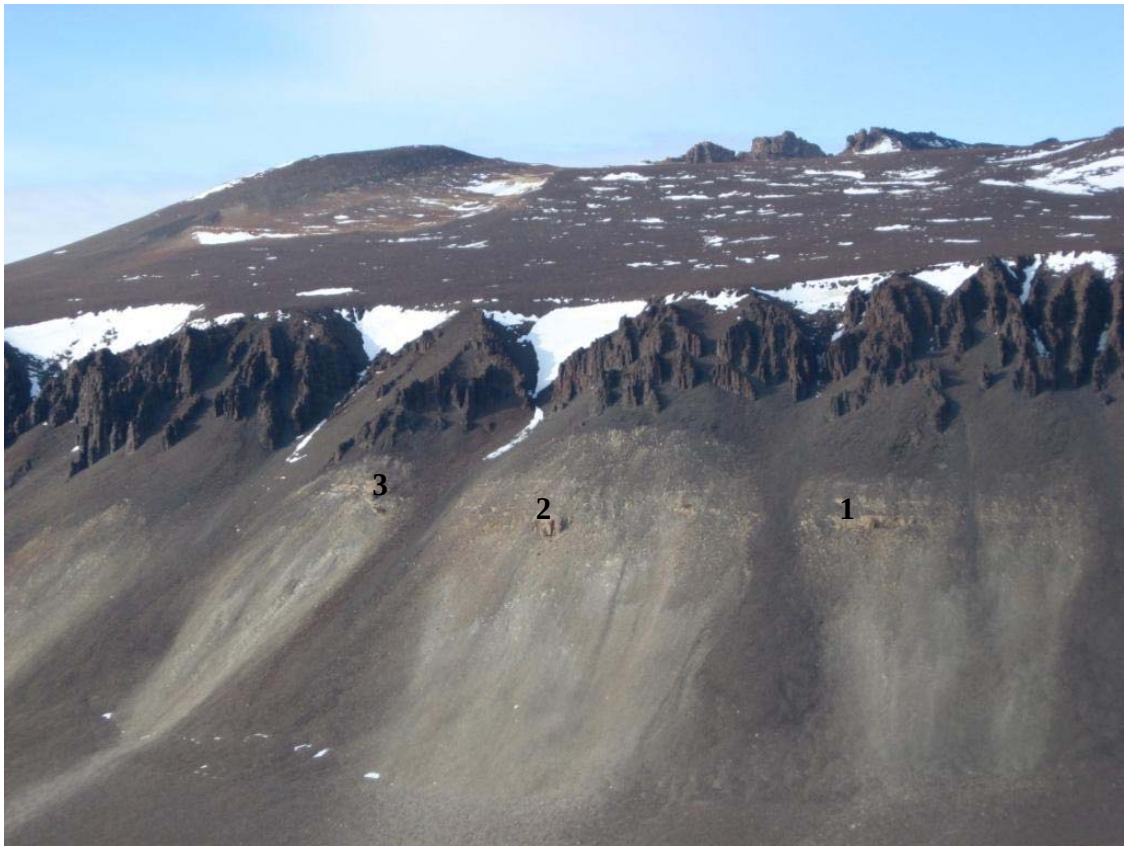

Figure 1-9: Location of crags on southern side of Barwick Valley. Dolerite cliffs are approximately 100 to 150 m high.

No stratigraphic column was measured at Sponsors Peak, although several outcrops were observed (Fig 1-10). Outcrops were observed directly behind camp, on the col between Sponsors and Nickel Peaks and southwest of camp. The Sponsors Peak camp was located just outside the boundary of ASPA 123. Day trips were taken from here to Vashka Crag and Balham Lake as these sites are inside ASPA 123.

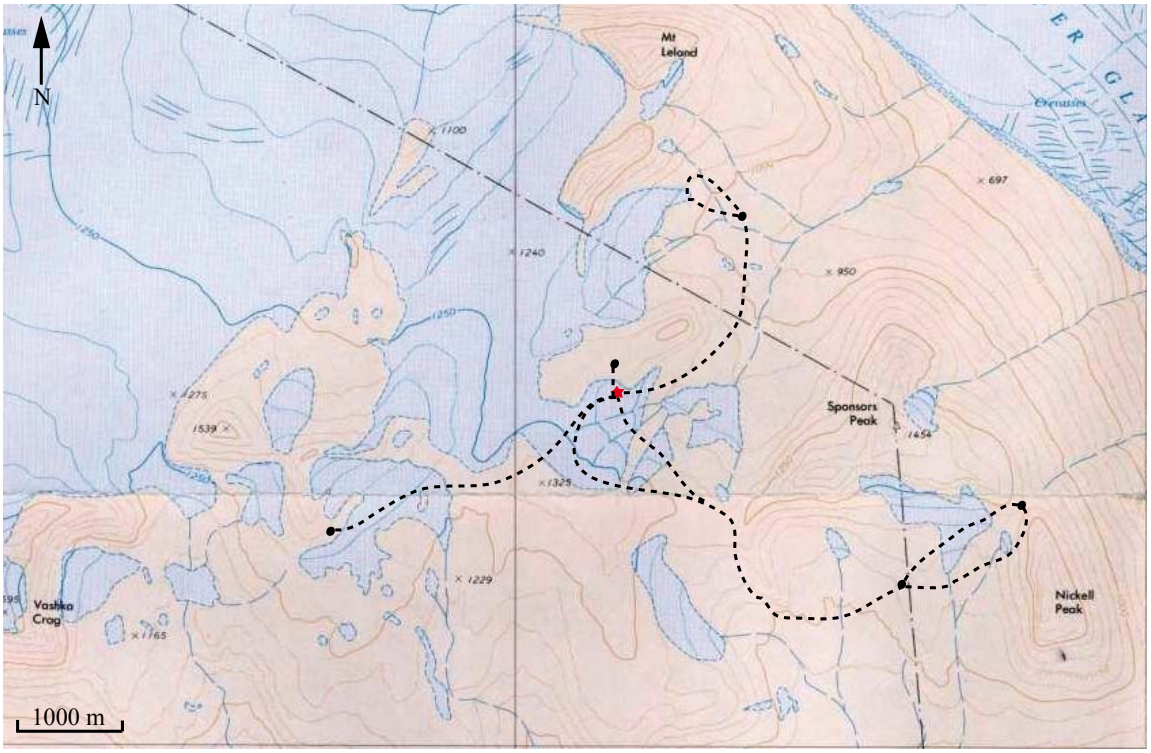

Figure 1-10: Fieldwork locations at Sponsors Peak. (USGS, 1977c)

1.3 Methodology

At each field site we did an initial reconnaissance to determine if enough outcrop existed to measure a stratigraphic column and the optimal place to measure the section. Paleocurrent measurements, clast counts, rock samples and general notes were made whenever possible. Laboratory analysis was done at the University of Canterbury (UC) and the Research School of Earth Sciences, Australian National University (ANU) in collaboration with Dr Mike Palin of the Department of Geology, University of Otago.

1.3.1 Stratigraphic Columns

Stratigraphic columns were measured in the field in areas with the most continuous and accessible exposure. The columns are concentrated on sections that include the Heimdall Erosion Surface and could incorporate one or more of the New Mountain Sandstone, Altar Mountain Formation and Odin Arkose Member. It was important to include the Heimdall Erosion Surface to allow correlations between sites and because this was the primary focus of the research. Measurements were rounded to the

nearest 10 cm and beds less than 10 cm were lumped together. The sections were measured using a ruler and Abney level. The data was then drawn into stratigraphic columns using Adobe Illustrator CS2. The completed stratigraphic columns can be seen in Appendix A1.

1.3.2 Paleocurrent Directions

Paleocurrent data was obtained from measurements made of ripple, cross bed and trough orientations. Most were from cross beds foresets as these were the most common feature. Paleocurrents are limited to the New Mountain Sandstone Formation and Odin Arkose Member of the Altar Mountain Formation. These were made in the field using a Suunto or Brunton compass. Readings from the Suunto compasses were corrected for New Zealand declination of 21°. All data was corrected for the Antarctic magnetic variation, which was obtained from www.ngdc.noaa.gov/seg/geomag/redirect.shtml. Data can be seen in Appendix A2. Flow directions were converted to rose diagrams using Grapher5.

1.3.3 Thin Sections and Point Counts

Thin sections were made for point counts and description of representative samples of each unit. The thin sections were cut and mounted on glass slides using Epotec 301 epoxy resin and ground to 0.03 mm thick. Unpolished slides were etched with hydrofluoric acid and stained with sodium cobalt nitrite for alkali feldspar (turns yellow) and rhodizonic acid for plagioclase feldspar (turns red) following techniques outlined in Lewis (1984). Often alteration products of the feldspar take up the stain. Point counts of the stained slides were done using the automated Prior Swift James point counter and recorded in spreadsheets (Appendix B1). These were used to create QFL diagrams and aid in the provenance interpretation of the samples. Photos of the thin sections were taken using a Leica DMXRP with Leica Digital DC300 or Moticam 2300 camera. Photos and QFL diagrams can be seen in the following chapters.

1.3.4 Rock Samples and Clast/Pebble Counts

Hand specimens of sandstones, siltstones and granule sandstones were collected at pertinent places in the measured sections for thin section analysis and comparison. Representative samples of conglomerate pebbles, especially possible rhyolites and exotic

sandstone clasts, were taken at each site and at semi regular intervals. Sandstone clasts from conglomerate units were taken for thin section analysis. Where basement rocks were observed representative material was collected. The samples are numbered using the first letter of the field site where they were collected followed by a number (i.e. Sample 5 from Mt Jason = J5). All the samples taken in the field are recorded in Appendix C.

Pebbles deposited on the Heimdall Erosion Surface were counted *in situ* where a significant conglomerate existed. This was to determine how the composition of the conglomerate varied across the field area. 100 pebbles in total were counted within a defined area. Graphs of pebble/clast counts can be seen in the following chapters.

1.3.5 Geochronology

Rocks collected by Dr Robert Bolhar from below, on and above the Heimdall Erosion Surface at Mt Electra were dated using Laser Ablation Inductively Coupled Plasma Mass Spectrometry (LA-ICP-MS) at ANU. The zircon mounts were made at the University of Canterbury. Rock samples were crushed twice and sieved so that grains no bigger than 125μm were included. The material was then separated using Sodium Polytungstate and Lithium Polytungstate with a specific gravity of approximately 2.91. Once the heavier material was separated and washed, the zircons were picked out using a stereomicroscope. 120 zircons were picked from each sample, in the hope of obtaining 100 spots. The zircons were mounted in Epotec 301 epoxy resin and polished to expose the grains. Results and an explanation of the instrument, process and data analysis (described by Palin (2008)) are found Appendix B2.

1.3.6 Cathodoluminescence (SEM-CL)

To support the LA-ICP-MS, Scanning Electron Microscopy-Cathodoluminescence (SEM-CL) images were taken of the zircons to determine whether the core or rim had been sampled and to see what condition the zircons were in. Samples were coated in gold using the Emitech K550x for 20 mA at 1.2kV, which gave a coating approximately 50 Å. A Leica S440 scanning electron microscope with a Gatan Oxford miniCL attached was used to analyse the samples.

SEM-CL was also used to look at quartz from the same samples as the LA-ICP-MS. The samples were also coated in gold using the technique described above. It was difficult to obtain good images. The best images were obtained when using a working distance of 20 mm, EHT of 20 to 25 kV and beam current between 500pA to 1.0 nA. The purpose was to find fabrics that would be diagnostic of quartz from volcanic, plutonic, hydrothermal or metamorphic rocks as outlined in Bernet and Basset (2005) and Boggs and Krinsley (2006) and therefore determine where the quartz grains are sourced from.

1.4 Thesis Structure

An introduction to the field area, field sites and methodology are covered in this chapter (Chapter 1). Previous work and interpretations on the formations within the Taylor Group are detailed in Chapter 2 and highlight controversy over interpretation of the depositional setting of the New Mountain Sandstone.

The New Mountain Sandstone and Altar Mountain Formation are examined in separate chapters. Each includes paleocurrents, trace fossils and descriptions from each field site were the formations where observed. For example, in Chapter 3 the New Mountain Sandstone is divided into lithofacies and described at each field site to determine lateral patterns and variations. The composition of the each lithofacies is analysed and compared. All the data is then combined to determine the depositional environment. This is repeated for the Altar Mountain Formation with its Odin Arkose Member in Chapter 5.

The Heimdall Erosion Surface and conglomerate immediately overlying it are described in Chapter 4 to establish the paleogeography of the surface and if it changes over the field area. The mechanisms that formed the erosion surface, processes that occurred during erosion and the depositional setting of the conglomerate lag are included.

The provenance of New Mountain Sandstone and Odin Arkose Member of the Altar Mountain Formation are established in Chapter 6 to ascertain if the sediment source

changes across the Heimdall Erosion Surface. This combines LA-ICP-MS and SEM-CL data.

The final chapter includes discussions of previous interpretations of the depositional environment across the Olympus Range and Bull Pass-St Johns Range area, suggested revisions of nomenclature and final conclusions.

Chapter Two: Geological Background

2.1 Introduction

In southern Victoria Land (SVL) the sedimentary Beacon Supergroup overlies plutonic and metasedimentary basement (Koettlitz Group and Granite Harbour Intrusives) and is intruded by the Ferrar Dolerite. The Beacon Supergroup in this area has been investigated since Scott's expedition in 1901 (Ferrar, 1907). Debenham (1921) did further mapping as part of the Terra Nova expedition in 1910. The area was not visited again until the International Geophysical Year (IPY) in 1957-1958 when major work done in the Dry Valleys by researchers at Victoria University (McKelvey and Webb, 1959, 1962; Webb and McKelvey, 1959; Allen and Gibson, 1962; Webb, 1963).

This chapter outlines research to date particularly in relation to paleoenvironment interpretations of the lower Beacon Supergroup (McKelvey and Webb, 1959, 1962; Webb and McKelvey, 1959; Allen and Gibson, 1962; Vialov, 1962; Harrington and Speden, 1962; Webb, 1963; Webby, 1968; Barrett, 1971, 1977; Barrett and Webb, 1973; Barrett and Kohn, 1975; Plume, 1978, 1982; Bradshaw, 1981; Turnbull *et al*, 1994; Isaac *et al*, 1995). The focus is on the formations with conflicting interpretations that have lead to this current research. Facies, sedimentary structures, trace fossils, and proposed depositional environments for each formation from previous research are presented here.

Stratigraphic columns by Barrett and Webb (1973), sedimentological work by Plume (1978) and recent geological mapping by Turnbull *et al* (1994) and Isaac *et al* (1995) have provided the basis for this study. Previous work on the contact of the basement with the overlying sediments is important and outlined briefly (Allibone *et al*, 1993 and 1993a; Allibone and Wysoczanski, 2002).

2.2 Basement

The basement in southern Victoria Land is composed of Proterozoic Koettlitz Group and early Paleozoic Granite Harbour Intrusives (Isaac *et al*, 1995 and references therein). The Koettlitz Group is the oldest basement rocks (Proterozoic) in SVL and is comprised of deformed metasediment, of upper amphibolite facies (Allibone *et al,* 1993). The Koettlitz Group is made up of the Hobbs Formation and Salmon Marble in the Olympus Range map area (Isaac *et al,* 1995). The Hobbs Formation includes politic and psammitic schists, minor marble and calc-silicate rocks (Isaac *et al*, 1995 and references therein). The Salmon Marble is a dominantly white marble with leucocratic, quartzofeldspathic gneiss and orange to buff layers of schist and gneiss (Isaac *et al*, 1995 and references therein).

The Granite Harbour Intrusives are divided into suites based on composition and date of emplacement, as outlined by Allibone *et al* (1993). The DV1a suite is comprised of the monzodiorite to granodiorite plutons and hornblende-biotite orthogneisses (Allibone *et al* 1993, 1993a). The plutons were emplaced between 589 and 490 Ma and the older plutons were emplaced during the later stages of the Koettlitz Group deformation (Allibone *et al*, 1993, 1993a). The DV1b suite was emplaced at a relatively higher crustal level and is comprised of biotite granitoid dikes and biotite orthogneisses. The plutons were emplaced around 490 Ma (Allibone et al 1993, 1993a). The DV2 suite was emplaced between 480 and 455 Ma. The emplacement of the DV2 suite postdates emplacement of the Vanda dikes (Allibone *et al*, 1993, 1993a).

2.3 Ferrar Dolerite Group

The Ferrar Dolerite Group of sills and dikes intrude the Koettlitz Group, Granite Harbour Intrusives and Beacon Supergroup sediments (Isaac *et al,* 1995). The sills are 70 to 500 m thick, with the thicker sills intruding into the basement (basement sill of Gunn and Warren, 1962) or the Kukri Erosion Surface contact (peneplain sill of Gunn and Warren, 1962). Smaller sills are typically found higher up in the Beacon Supergroup

(Isaac *et al*, 1995). Dikes are smaller in scale (metre scale) and can often be traced for several kilometres (Isaac *et al*, 1995).

2.4 Beacon Supergroup

The Beacon Supergroup is a sequence of Devonian or older to Triassic sediments unconformably deposited on basement throughout SVL and the Dry Valleys (Barrett, 1971; Bradshaw, 1981). Harrington (1965) divided the Beacon Supergroup into the older Taylor Group of mainly Devonian age or younger and the Victoria Group of Permian and Triassic age, which are separated by the Maya Erosion Surface (Fig 2-1). The lower units of the Taylor Group from New Mountain Sandstone Formation to Altar Mountain Formation (Fig 2-1) are of main interest in this thesis. The Beacon Supergroup contains three intraformational unconformities (excluding the basement contact); only the Heimdall Erosion Surface (between the New Mountain Sandstone and Altar Mountain Formation) and the basal nonconformity (Kukri Erosion Surface) are pertinent to this research. Paleoenvironment interpretations for each of the formations and erosion surfaces in the Taylor Group are described below. This chapter aims to show the issues relating to interpretations of depositional environments within the lower Taylor Group. Work by Harrington and Speden (1962) at the type section of the Beacon Supergroup at West Beacon suggested that the entire Taylor Group is predominantly marine in origin with some estuarine or non-marine units in the lower part of the sequence. Barrett and Kohn (1975) however, infer that the entire Taylor Group was deposited in a northeast sloping floodplain and Woolfe (1990) supports a non-marine origin for the Taylor Group.

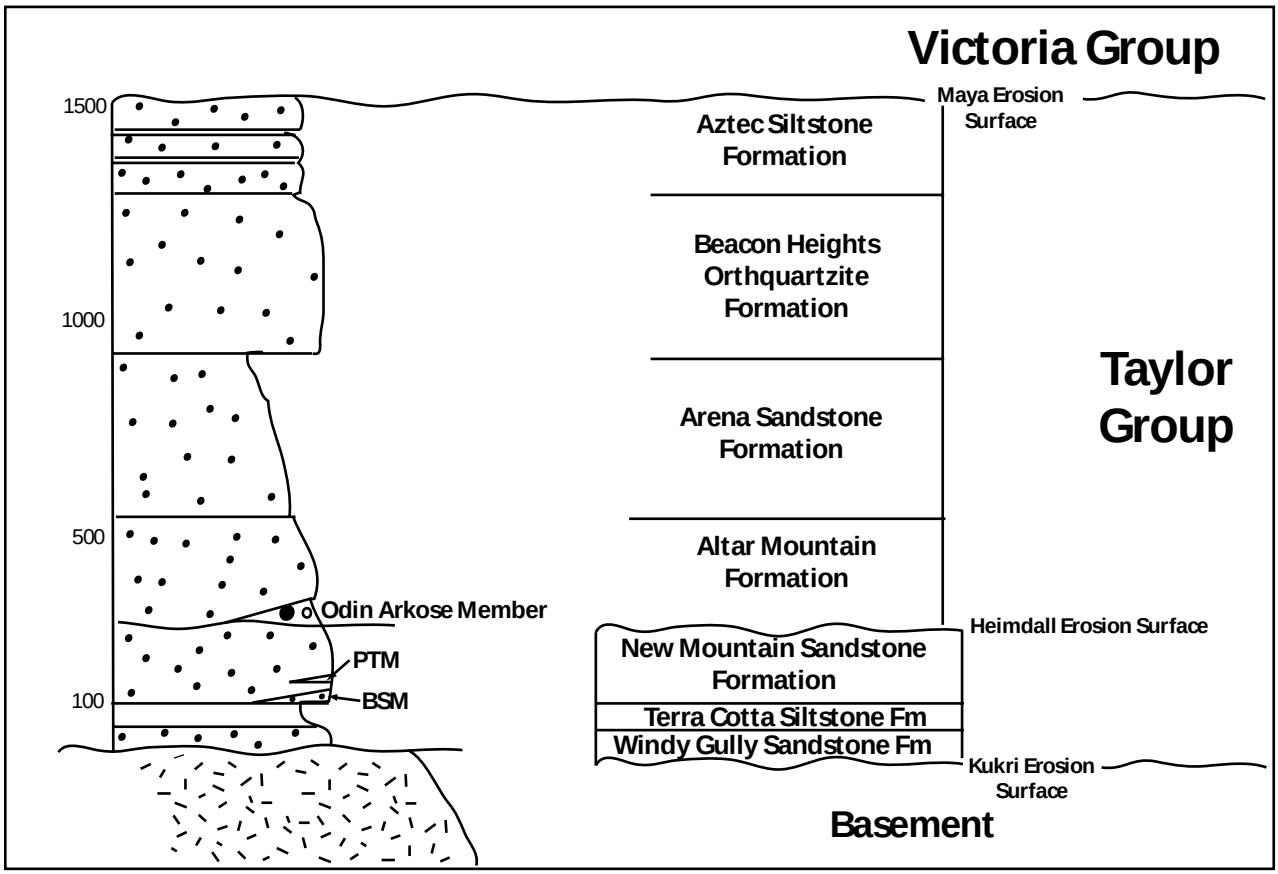

Figure 2-1: Stratigraphy of the Taylor Group (lower Beacon Supergroup) in southern Victoria Land. PTM = Plane Table Member. BSM = Boreas Subgreywacke Member. Adapted from Bradshaw (1981).

2.4.1 Kukri Erosion Surface (KES)

The nonconformity between the basement and the overlying Beacon Supergroup sediments throughout SVL is the Kukri Erosion Surface (KES). Basement rocks beneath the KES are weathered very little (Barrett, 1971). The erosion surface overall dips to the northwest and has a large amount of relief (Isaac *et al*, 1995). Basement highs can be inferred from several situations 1) where the younger Heimdall Erosion Surface has removed the Kukri Erosion Surface, 2) where the lower formations of the Beacon Supergroup are absent or 3) where sediments seem to onlap onto the basement (McKelvey *et al*, 1977; Isaac *et al*, 1995). The relief is also affected by intrusions of Ferrar Dolerite, which makes recognition of the paleo-relief difficult to assess.

2.4.2 Windy Gully Sandstone Formation

The Windy Gully Sandstone (Fig 2-1) occurs from Mt Jason in the north, where it is thickest, thinning to Mt Kempe in the south (Plume, 1978) (Fig 2-2). The sandstone rests unconformably on the Kukri Erosion Surface. There is a discontinuous basal conglomerate up to 3 m thick, which contains vein quartz, schist and granite clasts ranging in size from granules to boulders up to 2 m in diameter (Plume, 1978). Overall, the formation is a light tan or white, medium to coarse-grained, massive to blocky, well-bedded quartzose sandstone (Plume, 1978). Sedimentary structures include cross-beds, desiccation cracks, and symmetrical ripple marks (Plume, 1978). Plume (1982) proposes deposition was by large braided fluvial streams and cites possible aeolian origin for some of the cross beds. The cross-beds are up to 3 m thick and alternate with thin (10 cm thick) bioturbated horizons rich in *Heimdallia* (Bradshaw, 1981). Other trace fossils include *Diplichnites gouldi* trackways on cross-bed foresets and *Didymaulichnus nankervisi* on the bottom of bioturbated beds (Bradshaw, 1981). Bradshaw (1981) suggests that the Windy Gully Sandstone was deposited in a tidally active marine environment, predominantly in active channels and on the surrounding tidally emergent bioturbated sand flats.

2.4.3 Terra Cotta Siltstone Formation

The lower contact of the Terra Cotta Siltstone (Fig 2-1) with the Windy Gully Sandstone is gradational or interfingering over about 1 m with the Terra Cotta Siltstone (Plume, 1978). The Terra Cotta Siltstone varies in thickness and lithology across southern Victoria Land. It is at its thickest at Mt Kempe (82 m) and thins to 8 m at Mt Jason in the Olympus Range (Plume, 1978; Bradshaw, 1981) (Fig 2-2). The Terra Cotta Siltstone is composed of dark purple, brown and dark red siltstone, shales and minor sandstone (Plume, 1978). The numerous sedimentary structures include straight crested, symmetrical ripple marks, mudstone clast conglomerates, trace fossils, mud cracks and loading features. There are also carbonate concretions (Plume, 1978). The sedimentary structures alone do not point to any particular depositional environment and Plume (1982) cites ^{13}C values from carbonate concretions, siltstone lithofacies and lack of body fossils in support of a lacustrine paleoenvironment. On the other hand, Bradshaw (1981),

reports *Cruziana* and *Rusophycus* trace fossils that provide strong evidence for marine origin of the siltstones. Bradshaw (1981) suggests a coastal lagoon cut off from major marine influence by a barrier beach. Northwards the lagoon facies interfinger with barrier beach facies. *Diplichnites* and *Didymaulichnus* found on other surfaces indicate arthropod movement in channels linking the lagoon to the sea. Mud cracks observed in the unit could either be formed at extreme low tides or with abrupt changes in salinity, related to dynamic connection with the sea (Bradshaw, 1981).

2.4.4 New Mountain Sandstone Formation

The New Mountain Formation (Fig 2-1) is a medium to coarse-grained light tan sandstone that rests conformably on the Terra Cotta Siltstone (Plume, 1978). The sandstone is thickest (295 m) at Miller Glacier (McKelvey *et al*, 1977) and is found from Mt Leland in the north and as far south as Rotunda (Plume, 1978; Isaac *et al*, 1995) (Fig 2-2). The thickness of the New Mountain Sandstone Formation decreases to the north and the west (Isaac *et al*, 1995). The unit is dominated by trough cross-beds, which are 0.5 to 2 m thick in the lower part of the unit but up to 8 m thick nearer the top, alternating with intensely bioturbated layers (Bradshaw, 1981). Other sedimentary structures include desiccation cracks, primary current lineation, red-beds, trace fossils, ripples and scour and fill channels (Plume, 1978). Trace fossils include *Heimdallia* (which makes up the bioturbated layers) and *Diplichnites* trackways found on cross-bed foresets, which suggest sub-aqueous origin (Bradshaw, 1981). In the north the Heimdall Erosion Surface truncates the New Mountain Sandstone and *Skolithos* trace fossils only appear above the erosion surface (Bradshaw, 1981). In the Ferrar and Taylor Glacier region to the south, *Skolithos* trace fossils dominate the top of the New Mountain Sandstone where there is no truncation by the Heimdall Erosion Surface (Bradshaw, 1981). Bradshaw (1981) drew attention to the similarity with the Windy Gully Sandstone and therefore proposed a tidally active environment with channels, similar to the Windy Gully. Plume (1982) interprets the New Mountain Sandstone as a non-marine deposit similar to the deposits of the Brahmaputra River, India, due to the form of the cross bedding, scour and fill channels and interbedded thin siltstone beds. Plume (1982) also suggests that the upper part of the New Mountain Formation could be aeolian due to paleocurrents from the cross beds trending in a direction independent from paleoslope. Wizevich (1997) interprets the

New Mountain Sandstone at Table Mountain to be fluvial and aeolian in origin. Paleocurrent data from Barrett and Kohn (1975) show that in the north the New Mountain Sandstone was deposited by predominantly west flowing currents and they suggest it was deposited in a shallow marine environment with the large scale cross beds being formed by migration of large sand waves in shallow seas. In the south, the sediments became finer and deposition was from southwest flow of low sinuosity streams (Barrett and Kohn, 1975). Deposition ended due to uplift in the north (Barrett and Kohn, 1975) and erosion by the Heimdall Erosion Surface.

2.4.4a Boreas Subgreywacke Member

The Boreas Subgreywacke Member occurs at the base of the New Mountain Sandstone Formation in the north of the Dry Valleys and is at its maximum thickness of 16 to 17 m at Mt Boreas (Plume, 1978; Bradshaw, 1981) (Fig 2-1). The lateral extent of the unit is questionable due to the lack of exposure and clear definition. The type section at Mt Boreas, consists of alternating beds of argillite and poorly sorted coarse sandstone and conglomerate beds, which contain granite, quartz and feldspar pebbles (Plume, 1978). Angularity of the clasts indicates that it was deposited close to its source (Plume, 1982). At Plane Table, the unit consists of fining upwards cycles from reddish-brown, coarse-grained sandstone to well sorted massive white sandstone (Plume, 1978). The unit is very different at the two locations. At both locations, however the unit is overlain by the more quartzose New Mountain Sandstone and therefore has the same stratigraphic position. The Boreas Subgreywacke Member is interpreted as a debris flow from a granitic source (Bradshaw, 1981) or an alluvial fan (Plume, 1982).

2.4.4b Plane Table Member

The Plane Table Member occurs within the New Mountain Sandstone and is a dark purple and dark olive green siltstone (Fig 2-1). The unit has a thickness of 5 to 9 m and lateral extent of 1 km within the New Mountain Sandstone at Plane Table in the Asgard Range (Plume, 1978) (Fig 2-2). The upper and lower contacts are gradational. Plume (1982) uses comparison to the Terra Cotta Siltstone to interpret it as a lacustrine deposit.

2.4.5 Heimdall Erosion Surface (HES)

The Heimdall Erosion Surface is a disconformity/paraconformity that is restricted to southern Victoria Land and separates the New Mountain Sandstone from the overlying Odin Arkose Member of the Altar Mountain Formations (McKelvey *et al*, 1970, 1977). The erosion surface varies in character regionally across SVL. In the north, the Heimdall Erosion Surface truncates the New Mountain Sandstone and in some areas has cut down to basement plutons leaving no evidence of the lower part of the Taylor Group (McKelvey *et al*, 1977). The Heimdall Erosion Surface converges with the older basal Kukri Erosion Surface at several locations throughout SVL (Wheeler and Balham Valleys, and at Packhard Glacier) (McKelvey *et al*, 1977) (Fig 2-2). Towards the south, the unconformity begins to die out with apparent continuous sedimentation between the New Mountain Sandstone and Altar Mountain Formation (McKelvey *et al*, 1977; Plume, 1978).

2.4.6 Altar Mountain Formation

The Altar Mountain Formation has a maximum thickness of 235 m recorded at West Beacon and is found from Mt Suess in the north to Rotunda (McKelvey *et al*, 1977; Bradshaw, 1981) (Fig 2-1, 2-2). The formation is the lowest in the Victoria Group and commonly overlies the New Mountain Sandstone but in the north is deposited directly on the basement (Barrett and Kohn, 1975; Savage, 2005). The Altar Mountain Formation is composed of quartzose white or brown medium sandstone and dark green, brown or red fine sandstone (McKelvey *et al*, 1977; Isaac *et al*, 1995). It is described as a series of stacked fining up cycles; the cycles have erosive basal contacts and basal conglomerates, composed of rip up clasts and quartz granules and pebbles (Isaac *et al*, 1995). The sandstones contain ferruginous concretions, pyrite cubes and ferruginous speckles (McKelvey *et al*, 1977; Isaac *et al*, 1995). Sedimentary structures include trough and planar cross beds, ripples, mud cracks, millimetre scale laminations and dewatering structures (McKelvey *et at*, 1977; Isaac *et al*, 1995). Trace fossils include *Tigillites-Diplocraterion*, *Skolithos* and *Beaconites antarcticus* (Barrett and Webb, 1973; Bradshaw, 1981; Isaac *et al*, 1995). Cross bed measurements indicate flow towards the northwest (Barrett and Kohn, 1975). Bradshaw (1981) suggests that the Altar Mountain

Formation is shallow marine due to trace fossil assemblages and that the formation marks the maximum marine transgression. Barrett and Kohn (1975) suggest the Altar Mountain Formation was deposited in a coastal non-marine environment due to the presence of siltstone with mud cracks.

2.4.6a Odin Arkose Member

The Odin Arkose Member is coarse feldspathic sandstone, which disconformably overlies the New Mountain Sandstone on the Heimdall Erosion Surface (McKelvey *et al*, 1977; Isaac *et at,* 1995) or rests nonconformably on basement rocks (McKelvey *et al*, 1977) (Fig 2-1). The thickness is difficult to determine because the upper contact with the rest of the Altar Mountain Formation is gradational but is between 10 and 61 m (Barrett and Webb, 1973; McKelvey *et al*, 1977), with a maximum thickness of 61 m between Mt Baldr and Thor (McKelvey *et al,* 1977). The Odin Arkose is found as far north as Mt Suess where is it known as the Sperm Bluff Formation (Savage, 2005) but becomes hard to distinguish from the overlying Altar Mountain Formation south of the Asgard Range (McKelvey *et al,* 1977) (Fig 2-2). The Member is composed of a thin basal conglomerate containing rounded quartz pebbles and other lithologies, overlain by trough and planar cross-bedded medium arkosic sandstone (Barrett and Webb, 1973; McKelvey *et al,* 1977; Bradshaw, 1981; Isaac *et al*, 1995). Current flow within the Odin Arkose is from the west to the southwest (Barrett and Kohn, 1975; Isaac *et al,* 1995). Barrett and Kohn (1975) suggest this reflects uplift in the area around Mt Suess in the north. *Skolithos* trace fossils are present within the Odin Arkose Member (Bradshaw, 1981). The trace fossils and association with the overlying Altar Mountain Formation suggests a shallow marine environment (Bradshaw, 1981). Though Barrett and Kohn (1975) suggest deposition by low sinuosity streams flowing to the southwest.

2.4.7 Arena Sandstone Formation

The lower boundary of the Arena Sandstone is gradational with the underlying Altar Mountain Sandstone (Bradshaw, 1981) (Fig 2-1). The formation is widespread throughout SVL with a maximum thickness of 355m at West Beacon (McKelvey *et al*, 1977; Bradshaw, 1981) (Fig 2-2). The formation is a medium to fine-grained sandstone with clay cement (Bradshaw, 1981), and minor coarse and very fine-grained sandstone

and thin shaley siltstones (Isaac *et al*, 1995). Limonite speckles, ferruginous concretions and trace fossils (*Beaconites barreti, Beaconites antarcticus* and *Skolithos*) occur (Bradshaw, 1981; Isaac *et al*, 1995). Planar and trough cross beds are the dominant sedimentary structure and are 0.5 to 1.8 m thick (Isaac *et al*, 1995). Paleocurrents show flow to the north and southeast (Barrett and Kohn, 1975; Isaac *et al*, 1995). Bradshaw (1981) interprets the Arena Sandstone as deposition on a low gradient sand plain with periodic flooding but recognizes the lack of channels, pebble lags and mudstone horizons. Barrett and Kohn (1975) suggest the formation is an alluvial plain deposit.

2.4.8 Beacon Heights Orthoquartzite Formation

The Beacon Heights Formation is a medium grained quartzarenite with quartz cement (Bradshaw, 1981) with a gradational lower contact with the Arena Sandstone (Fig 2-1). The formation is widespread throughout SVL and a maximum thickness of 219 m is recorded at West Beacon (McKelvey *et* al, 1977; Bradshaw, 1981) (Fig 2-2). Sedimentary structures include trough and planar cross-beds and horizontal laminations (Bradshaw, 1981; Isaac *et al*, 1995). Paleocurrents show flow to the northwest and southeast (Isaac *et al*, 1995). Trace fossils include *Skolithos, Beaconites sp. Didymaulyponomos rowei,* fossil fish remains and lycopod stems (Bradshaw, 1981; Isaac *et al*, 1995). The lycopod stems and fossil fish indicate a Middle Devonian age (McKelvey *et al*, 1977; Isaac *et al*, 1995). Barret and Kohn (1975) suggest that low sinuosity braided streams deposited the Beacon Heights Formation, which is supported by Bradshaw (1981).

2.4.9 Aztec Siltstone Formation

The Aztec Siltstone is up to 114 m thick (Barrett and Webb, 1973) and is composed of interbedded sandstone, siltstone and mudstone (Fig 2-1). The sandstones are trough cross-bedded, parallel and ripple laminated (Isaac *et* al, 1995). Sedimentary structures include desiccation cracks, root structures, ripples, intraformational conglomerates and paleosols (Bradshaw, 1981; Isaac *et* al, 1995). Paleocurrent directions are from the northeast (Barrett and Kohn, 1975). *Thalassinoides, Beaconites* (Barrett, 1971; Bradshaw, 1981) and fossil fish remains have been found in the Aztec Siltstone (Isaac *et al*, 1995 and references therein). The fossil fish remains indicate a Middle to

Lower Devonian age for the Aztec Siltstone (Isaac *et al*, 1995 and references therein). The Aztec Siltstone is interpreted as an alluvial plain red bed sequence (Bradshaw, 1981 and references therein).

2.4.10 Summary of Depositional Settings

Table 2-1 summarises depositional environments proposed by previous authors and highlights the contention over the depositional environment for the New Mountain Sandstone Formation.

Table 2-1: Summary of depositional settings for formations and members within the Taylor Group, lower Beacon Supergroup.

Author	Windy Gully Formation	Terra Cotta Formation	New Mountain Formation	Boreas Subgreywacke Member	Plane Table Member	Altar Mountian Formation	Odin Arkose Member	Arena Formation	Beacon Heights Formation	Aztec Formation
Harrington and Speden (1962)	Mostly marine with some lower beds maybe estuarine or non-marine.									
Barrett and Kohn (1975)	-	-	Shallow marine. Large sand waves.	-	-	Non-marine, possible coastal environment	Low sinuosity streams	Alluvial plain deposit	Low sinuosity braided streams	-
Barrett (1979)	-	Lacustrine	Aeolian	-	-	-	-	-	-	-
Bradshaw (1981)	Tidally active marine environment. Shallow marine	Coastal lagoon	Shallow marine	Debris flow	-	Shallow marine	Shallow Marine	Low gradient sand plain with periodic flooding	Low sinuosity braided streams	Low-lying muddy alluvail plain
Plume (1982)	Large braided fluvial streams, aeolian origin for some cross beds	Lacustrine	Non-marine. Aeolian and/or sandy braided river.	Alluvial fan	Lacustrine	-	-	-	-	-
Woolfe (1990)	Non-marine based on trace fossils.									
Turnbull *et al* (1994)	-	-	Fluvial	-	-	-	-	-	-	-
Wizevich (1997)	-	-	Fluvial-Aeolian	-	-	-	-	-	-	-

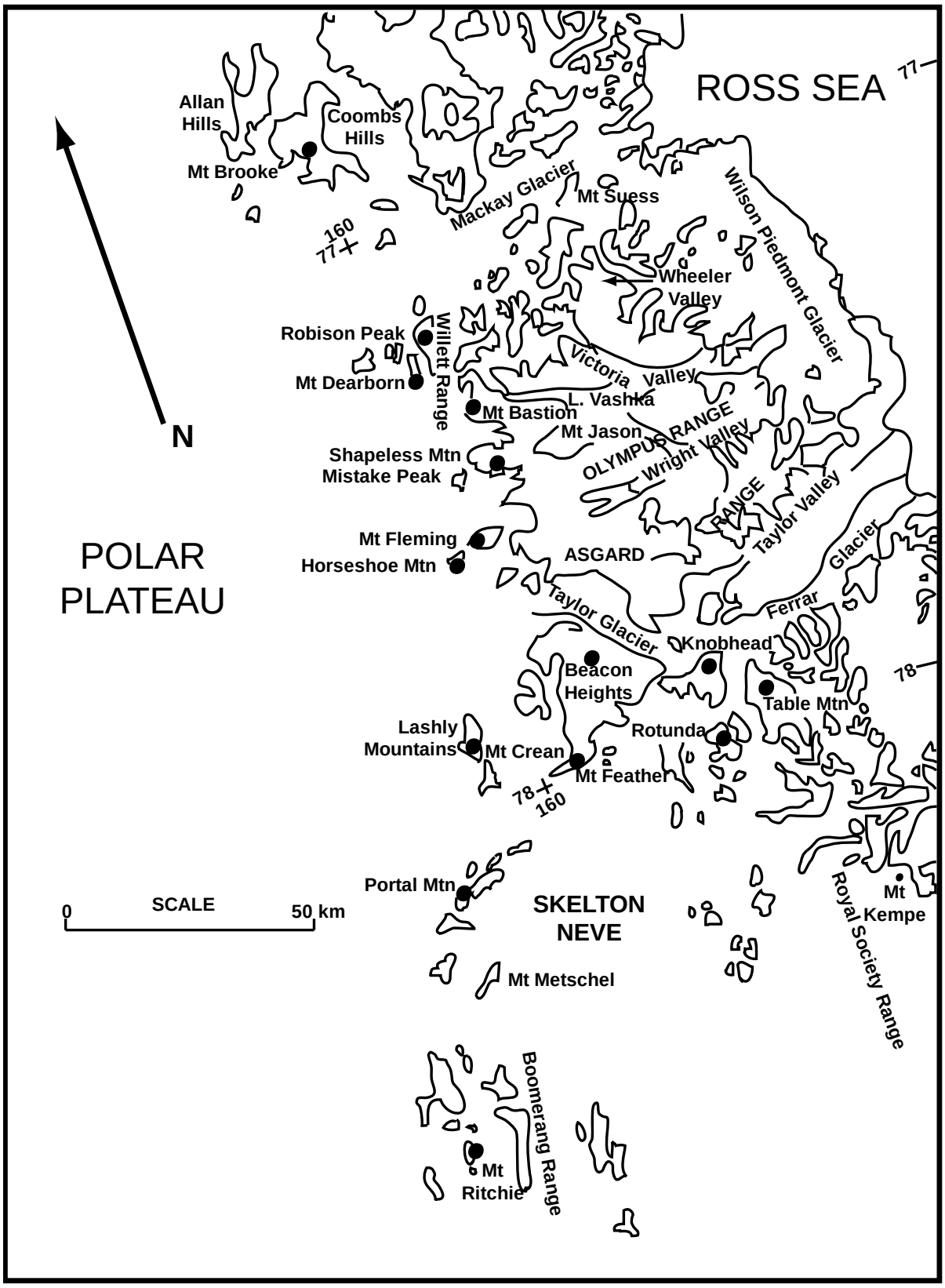

Figure 2-2: Skelton –Mackay Glacier Area. Adapted from Barrett and Webb (1973)

2.5 Summary

The basement rocks of the Olympus Range area are composed of Proterozoic Koettlitz Group and early Paleozoic Granite Harbour Intrusives. The regional Kukri Erosion Surface truncates the basement with a large amount of relief.

Deposited on the Kukri Erosion Surface are the Devonian to Triassic rocks of the Beacon Supergroup, including the New Mountain Sandstone and Altar Mountain Sandstone with its Odin Arkose Member. Several depositional environments have been proposed for the New Mountain Sandstone. The Heimdall Erosion Surface is an intra-group unconformity that truncates the New Mountain Sandstone.

Sills and dikes of the Ferrar Dolerite intrude the basement and Beacon Supergroup sediments.

Chapter Three: New Mountain Sandstone Formation

3.1 Introduction

The New Mountain Sandstone Formation is in the lower Taylor Group. It overlies the Windy Gully Sandstone and Terra Cotta Siltstone or basement rocks, and directly underlies the Heimdall Erosion Surface. This chapter describes the different lithofacies into which the New Mountain Sandstone Formation has been divided up into, including sedimentary structures, trace fossils, paleocurrent indicators and composition. Different depositional patterns at each field site are described from east to west along the Olympus Range and from south to north. Stratigraphic columns for field sites can be found in Appendix A1. Field sites where the New Mountain Sandstone was not observed or examined extensively are omitted from this chapter.

3.2 Lithofacies

The lithofacies of the New Mountain Sandstone Formation are described from the stratigraphically lowest observed outcrop unit to the upper units, which are truncated by the Heimdall Erosion Surface. Overall the New Mountain Sandstone is quartzose sandstone. Fine sand to granule quartz are common throughout the formation, therefore the lithofacies divisions are based on sedimentary structures, trace fossils and the relative abundance of pebbles within the sandstone. Feldspar is also abundant in the lower part of the formation.

3.2.1 Basal Conglomerate Lithofacies (BCL)

The Basal Conglomerate Lithofacies is deposited directly on the Kukri Erosion Surface. It is a pebble to boulder conglomerate composed of granite, milky quartz (often angular), rhyolite and pegmatite. The largest recorded boulder is 90 cm across (Fig 3-15). The conglomerate is predominantly matrix supported but becomes clast supported in areas with larger clast sizes. The matrix is composed of fine sand, which is dark green, yellow or red coloured. The lithofacies can be found at the base of the New Mountain Sandstone only where the Windy Gully Sandstone and Terra Cotta Siltstone are not present.

3.2.2 Pebbly Sandstone Lithofacies (PSL)

The Pebbly Sandstone Lithofacies is composed of predominantly very coarse sand to granule quartz and feldspar, with dispersed pebbles. This alternates with more quartzose fine to medium sandstone with granules of quartz and feldspar. The coarser facies is more dominant. Granule to coarse sand lenses and granule to medium pebble layers also occur. Both sandstones have trough cross beds (20 to 30 cm thick). Coarser material often lines foreset traces and increases from the top of foreset to the bottom (Fig 3.1A). Small scale slumping is seen rarely in the unit at the same scale as the cross beds.

Figure 3-1: **A)** Granules lining foreset traces in the PSL. Photo by: Margaret Bradshaw. **B)** Brown fine sandstone and **C)** pale fine laminated sandstone within PSL at Mt Jason (Appendix A1/1)

Fine to very coarse pebbles consist of: 1) Sub-angular to sub-rounded smokey, vein and pink stained quartz. 2) Quartzite. 3) Angular to rounded alkali feldspar. 4) Angular to sub-rounded brownish-red fine sandstone, irregularly shaped (Fig 3-1B). 5) Pale coloured laminated fine sandstone (Fig 3-1C). 6) White siltstone.

A coarser variation of the PSL with abundant angular quartz granules in medium to fine sandstone, concentrated in small trough cross beds (Fig 3-2B) and on bounding surfaces

(Fig 3-2A) was observed only at Lake Vashka. The unit also contains rare ripples, *Thalassinoides* and mudstone layers.

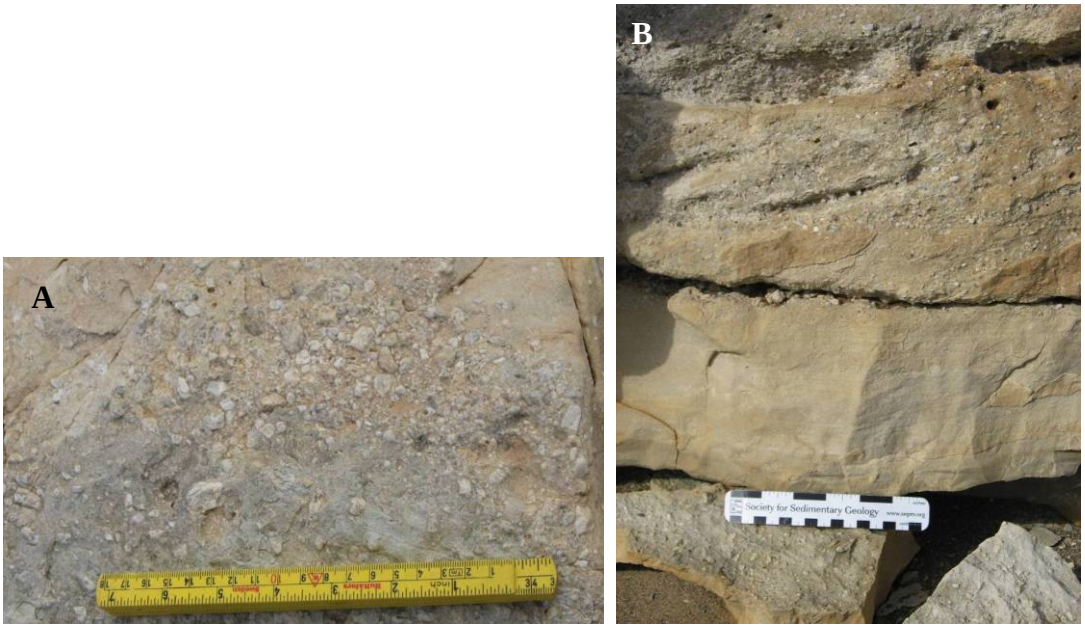

Figure 3-2: A) Granule and pebble layer on bounding surface. **B)** Cross bed with angular quartz lining foresets and fine sandstone cross beds. Lake Vashka (Appendix A1/7a)

The Pebbly Sandstone Lithofacies is characterised by trough cross-bedded, very coarse feldspathic sandstone with granules alternating with more quartzose medium sandstone. There are scattered and grouped pebbles and high feldspar occurrence. The lithofacies also contains parallel thinly bedded or stratified sandstone with granules concentrated in layers.

3.2.3 Granule Cross-bedded Lithofacies (GCL)

The Granule Cross-bedded Lithofacies consists of trough cross-bedded medium sandstone with granules and rare pebbles (brown fine sandstone, quartz) found on the foresets. Trough cross beds are 20 to 40 cm thick. Lenses of coarse to very coarse sand with feldspar occur within and between the finer beds. Within the GCL *Heimdallia* occur in beds 20 to 30 cm thick (Fig 3-3) and as singular burrows across the top of the foresets. Some *Heimdallia* beds have a smoothed upper contact. Beds containing *Heimdallia* burrows are composed of poorly sorted medium sandstone with occasional granules.

The GCL differs from the PSL in that it is composed of overall finer sediment, granules and pebbles are more rare and it contains *Heimdallia.*

Figure 3-3: *Heimdallia* beds within the GCL, east face of Mt Jason. Photo by: Margaret Bradshaw

3.2.4 Pinstripe Cross-bedded Lithofacies (PCL)

The Pinstripe Cross-bedded Lithofacies is composed of very well sorted, cross-bedded, medium quartzose sandstone. Pinstriping is caused by millimetre scale lamination of the foresets due to alternating fine and very fine sand or concentration of darker material (Fig 3-4A). The cross beds are 3 to 4 m thick. It is unknown how far they extend laterally due to outcrop restrictions. The Heimdall Erosion Surface truncates the PCL.

There is slumping of cross bed sets into a slurry, which is mainly amorphous but contains pieces of the original layered cross bed set (Fig 3-4B). Slumping only affects singular cross bed sets and over or underlying sets remain intact (Fig 3-4C). The lithofacies also weathers cavernously and is a cream orange colour.

Figure 3-4: **A)** Pinstripe Cross-bedded Lithofacies. **B)** Slumping within the Pinstripe Lithofacies. Note blocks showing original laminations. **C)** Upper contact of slumped bed shows that the overlying cross bed is not affected. Lake Vashka.

3.2.5 Cross-bedded Sandstone Lithofacies (CSL)

The Cross-bedded Sandstone Lithofacies consists of tangential cross-bedded, well sorted, medium to fine quartzose sandstone. The cross beds range from 1 to 3 m thick and can extend for up to 8 m laterally. The individual foreset beds are 1 to 3.5 cm thick and fine upwards from coarse to medium sand or medium to fine sand. Cross bed sets are wedge-like or tabular in shape and are composed of medium to low angle, concave up beds that curve asymptotically downwards to a flat lower boundary. The cross beds sets commonly weather to a flaggy outcrop.

Slumping is observed rarely throughout the lithofacies. Original layering of the cross bedding is contorted with beds changing in thickness but remaining unbroken. The slumping is stratigraphically confined to single beds, is laterally continuous for up to 200 m and local and does not affect the over or underlying beds. Beds with slumping are not commonly associated with *Heimdallia* layers. Slumping also shows a soupy texture, flame structures and ball and pillow structures.

Ripples occur higher within the CSL and are not associated with intense *Heimdallia* bioturbation. Both symmetric and asymmetric forms are observed. The ripples are found on the foresets and vary in size and shapes but are generally flat and sinuous crested with broad troughs and crests.

Heimdallia are very abundant in the Cross-bedded Sandstone Lithofacies and occur both on bounding surfaces between the cross beds (10 to 50 cm thick) and as layers within and parallel to the foresets (5 to 20 cm thick). In some cases singular *Heimdallia* burrow down into the cross bed below or almost destroy a cross bed leaving only small foreset pieces. In most cases, however, the *Heimdallia* trace fossils do not appear to penetrate from the bioturbated beds into the cross beds below and are bound by smooth upper and lower contacts.

Other trace fossils found within the Cross-bedded Sandstone Lithofacies include *Diplichnites gouldi* trackways on the top of foreset beds (Fig 3-5A), *Didymaulyponomos*, *?Siskemia elegans* (Walker, 1985) collared burrows (Fig 3-5C), scoop-like burrows (Fig 3-5C) and nestling structures (?*metaichna*) (Fig 3-5B).

The Cross-bedded Sandstone Lithofacies is distinguished from the Pinstripe Cross-bedded Lithofacies due to trace fossils, different of slump morphology, cross bed size, grainsize and degree of sorting.

A rare variation of the Cross-bedded Sandstone Lithofacies is observed at Mt Jason. The facies is cream and green coloured very fine sandstone to siltstone alternating with massive medium sand (up to 40 cm thick). The contacts between the two lithologies are very sharp and irregular. The siltstone has many sedimentary structures including laminar and lenticular bedding, flame structures and ball and pillow structures (Fig 3-6A, B). At the top of the lithofacies is a mud crack horizon (Fig 3-6C). The outcrop of this facies is 1.5 m thick and 2 m wide.

Figure 3-5: A) *?Siskemia elegans*. **B)** Nestling structure (?*metaichna*). **C)** Collared and scoop-like burrows **D)** *Diplichnites gouldi* trackways. Photos by: Margaret Bradshaw

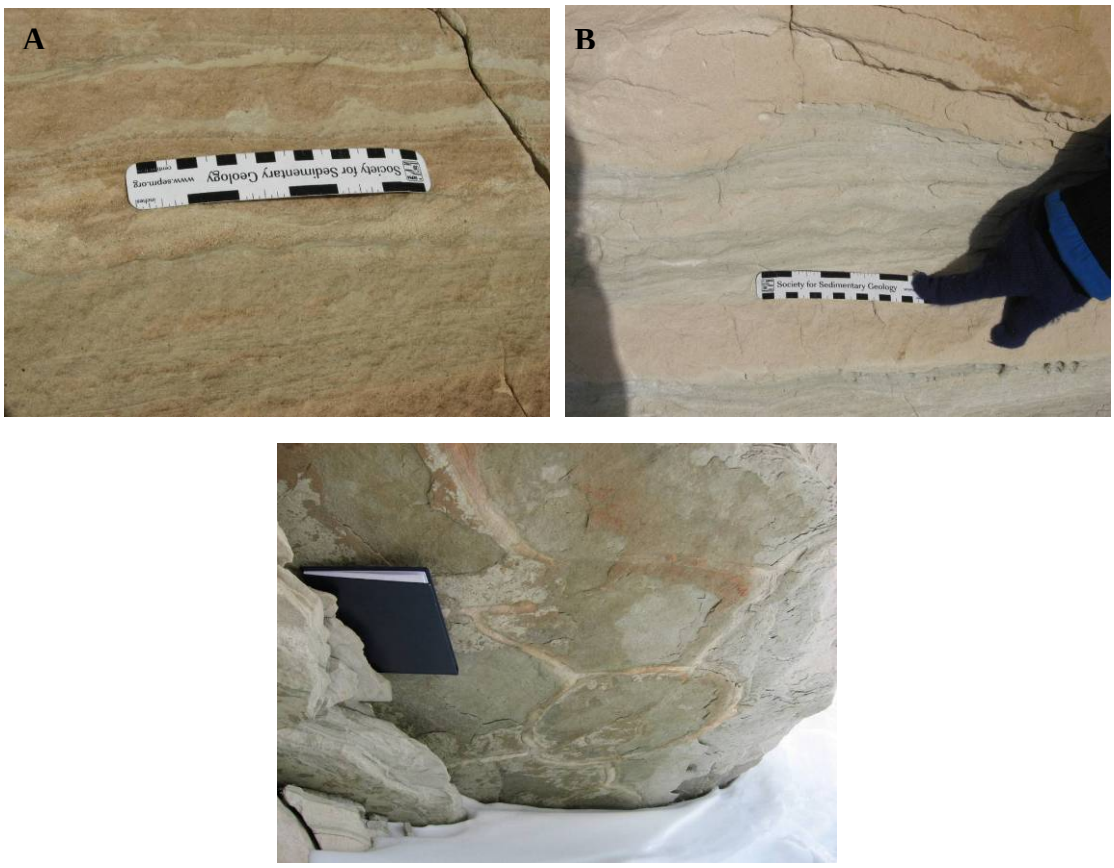

Figure 3-6: **A)** Alternating medium sandstone and fine sandstone with flame structures. **B)** Ripple laminated fine sandstone. **C)** Mud cracks. Mt Jason.

3.3 Overview

The sedimentary sequence within the New Mountain Sandstone Formation, where it overlies the Terra Cotta Siltstone or Windy Gully Sandstone, starts with Pebbly Sandstone Lithofacies and/or the Granule Cross-bedded Lithofacies followed by the Cross-bedded Sandstone Lithofacies, which is truncated by the Heimdall Erosion Surface. Where the New Mountain Sandstone directly overlies the Kukri Erosion Surface the basal unit is typically Basal Conglomerate Lithofacies followed by the other lithofacies. The Cross-bedded Sandstone Lithofacies is the most abundant lithofacies and is found at all places where the New Mountain Sandstone is observed. The lithofacies varies from 30 to 100 m thick with no discernable pattern to changes in thickness throughout the field area. PSL is found at Mt Jason, Mt Electra and Lake Vashka and the GCL is found at most other sites. The Pebbly Sandstone Lithofacies varies in thickness from 1 to 10 m and the Granule Cross-bedded Lithofacies from 7 to 23 m thick. As with the Cross-bedded Sandstone Lithofacies there does not seem to be a pattern in the thickness of deposition of the Pebbly Sandstone or Granule Cross-bedded Lithofacies where it is observed. There is only one occurrence of the fine facies within the Cross-bedded Sandstone Lithofacies and this is at Mt Jason. The Pinstripe Cross-bedded Lithofacies is only found at Lake Vashka, where it stratigraphically overlies the Pebbly Sandstone Lithofacies or sits directly in the Kukri Erosion Surface, and is truncated by the Heimdall Erosion Surface. The New Mountain Sandstone is much thinner, relative to other locations, at Lake Vashka.

3.4 Facies Distribution and Relationships in Observed Sections

The pattern of deposition, in terms of the lithofacies described above, is outlined for each field site where the New Mountain Sandstone was observed and recorded. Descriptions start at the bottom contact and continue until the upper limit at that site, either where the Heimdall Erosion Surface truncates it or the rocks are obscured.

3.4.1 Mt Jason

The total thickness of the New Mountain Sandstone measured at Mt Jason is 69.2 m (Appendix A1/1). The stratigraphic section at Mt Jason begins with scree at the lowest outcrop. The lower 2.6 m is Pebbly Sandstone Lithofacies composed of alternating beds of trough cross-bedded medium sandstone and granule sandstone with pebbles of quartz, quartzite and red and pale laminated sandstone. Paleocurrents within the Pebbly Sandstone

Lithofacies suggest flow to the east (Fig 3-7A). Overlying PSL is the Granule Cross-bedded Lithofacies, which is 19.5 m thick. The first evidence of *Heimdallia* bioturbation occurs at the base of the GCL however a lot of the lithofacies is obscured by snow and scree (Appendix A1/1). The GCL is composed of trough cross-bedded medium sandstone with scattered granules and pebbles and rare granule to coarse sandstone lenses. The number of pebbles in GCL is less than that observed in PSL. Cross beds within the GCL do not show a uniform paleocurrent direction but are widely spread (Fig 3-7B)

The contact between the Granule Cross-bedded Lithofacies and the Cross-bedded Sandstone Lithofacies is obscured by a dike but is identified by a change from arkosic cross-bedded medium sandstone with granules to cross-bedded quartzose well sorted medium to fine sandstone (Appendix A1/1). The CSL is 45 m thick and is truncated by the Heimdall Erosion Surface. The lower 7 m of the Cross-bedded Sandstone Lithofacies has very coarse sand and granules lining separate foreset beds. The CSL is very prominent and extensive at Mt Jason, observed on the eastern and western faces and on the col between Mt Jason and Mt Hercules. On the col the thickness of the CSL is unknown because the base was not observed. Extensive exposure of ripples on the col was the main feature of interest. Paleocurrent data indicates flow towards the southwest (Fig 3-7C).

Within the upper CSL is one example of the fine facies described in Chapter 3.2.5, which occurs 5 m below the Heimdall Erosion Surface. The unit is 1.5 m thick and 2 m wide and surrounded by snow and rubble. The layering of the facies is horizontal but in cross section beds can be seen rising at an angle into the Cross-bedded Sandstone Lithofacies (Fig 3-8).

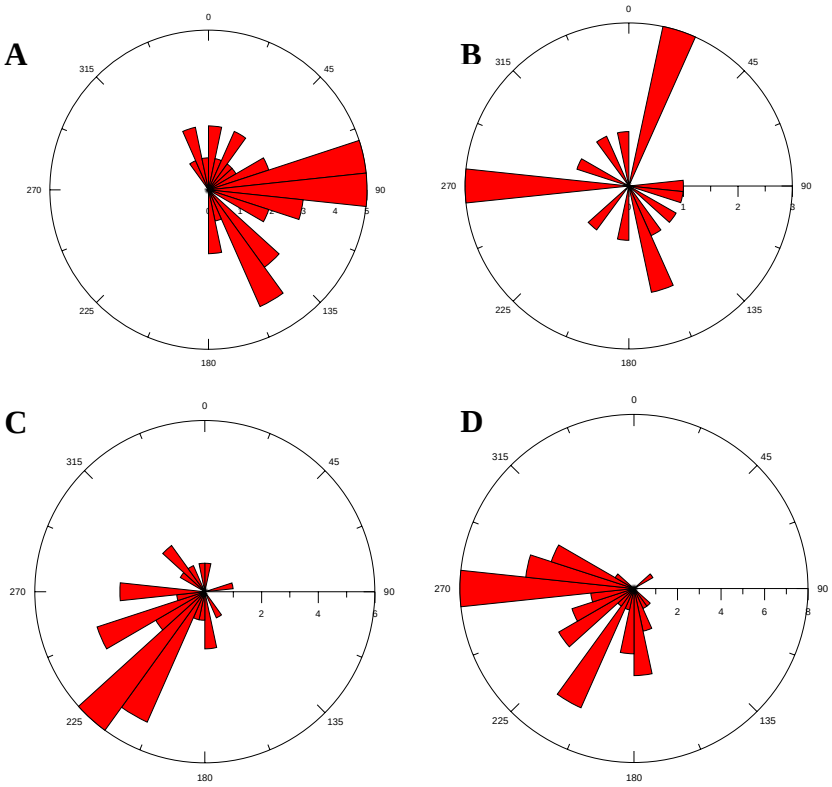

Figure 3-7: **A)** Paleocurrent directions within the Pebbly Sandstone Lithofacies (n=38), **B)** Granule Cross-bedded Lithofacies (n=17) **C)** Cross-bedded Sandstone Lithofacies (n=101) **D)** Ripple trends within the Cross-bedded Sandstone Lithofacies (n=48). Mt Jason

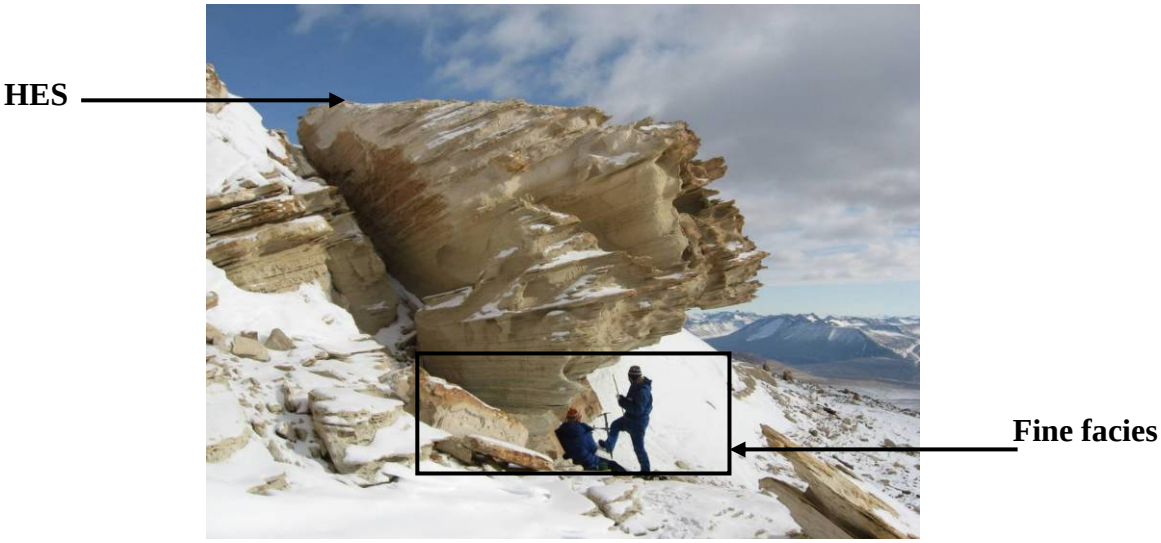

Figure 3-8: Horizontally bedded very fine sandstone at the base (in box) changing into Cross-bedded Sandstone Lithofacies upwards. The CSL is truncated by the Heimdall Erosion Surface.

The relationship between cross beds and *Heimdallia* in the CSL is seen in Fig 3-9. The cross beds are predominantly low angle and the *Heimdallia* beds are flat or nearly so. *Heimdallia* beds are can be followed laterally for tens of metres (J Bradshaw, pers comms,

2008) and are flat or gently dipping. They either follow the dip direction of the underlying foreset or cut across foresets. The beds can be tabular or wedge shape. Typically, *Heimdallia* beds are 5 to 50 cm thick and the traces are normally 1 cm wide. Thicker *Heimdallia* traces (1.7 cm) also occur along the top of foresets. Higher in the section, *Heimdallia* beds become thinner and less prominent and ripples begin to appear. *Diplichnites gouldi*, nestling structures (?*Metaichna*), collared burrows, scoops, *Didymaulyponomos* and *?Siskemia elegans* are also found within the Cross-bedded Sandstone Lithofacies (Fig 3-5). The scoops and collared burrows are commonly associated and are widely exposed on the col between Mt Jason and Mt Hercules.

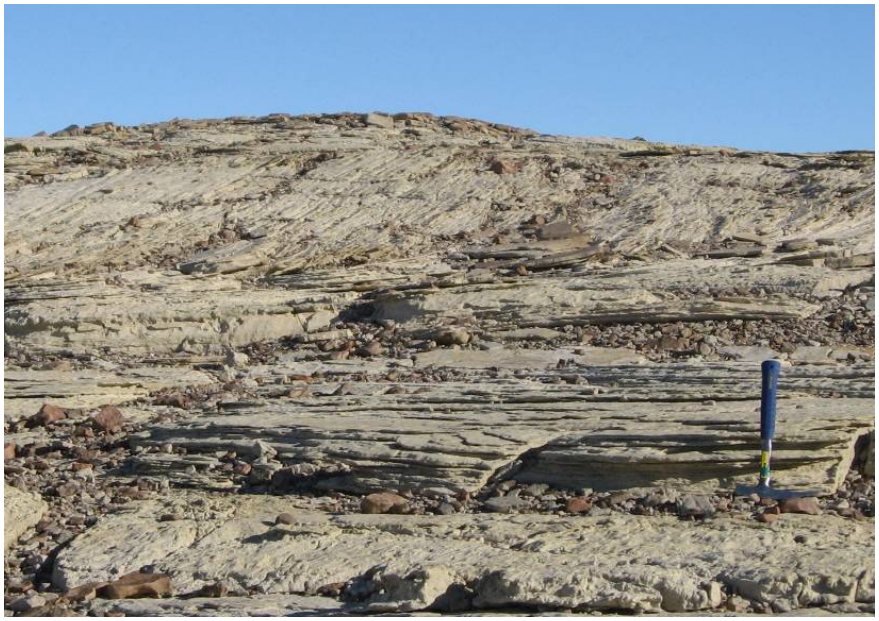

Figure 3-9: Relationship between *Heimdallia* and cross bed sets. Mt Jason.

Ripples are widely observed in the Cross-bedded Sandstone Lithofacies, and are typically flattened sinuous crested types with broad troughs and crests. There are some examples of narrow crest and trough types. The samples are nearly equally split between asymmetric and symmetric ripples. Ripple crest trends suggest currents to the southwest and west (Fig 3-7D). This is consistent with the data from the cross bed measurements within the Cross-bedded Sandstone Lithofacies (Fig 3-7B). However, both are very different from the paleocurrents from the Pebbly Sandstone and Granule Cross-bedded Lithofacies.

Slumping is observed midway up the Cross-bedded Sandstone Lithofacies, generally above the section with high concentrations of *Heimdallia*. Slumping is characterised by folding of the foresets (Fig 3-10B) while retaining the foreset bedding structure, creating

flame and ball and pillow structures (Fig 3-10C), and changing the thickness of the foreset beds. The slumps extend laterally for over 200 m (J. Bradshaw, pers comms, 2008). Fig 3-10A and 3-10B and C, are the same slump horizon but are about 200 m or more apart.

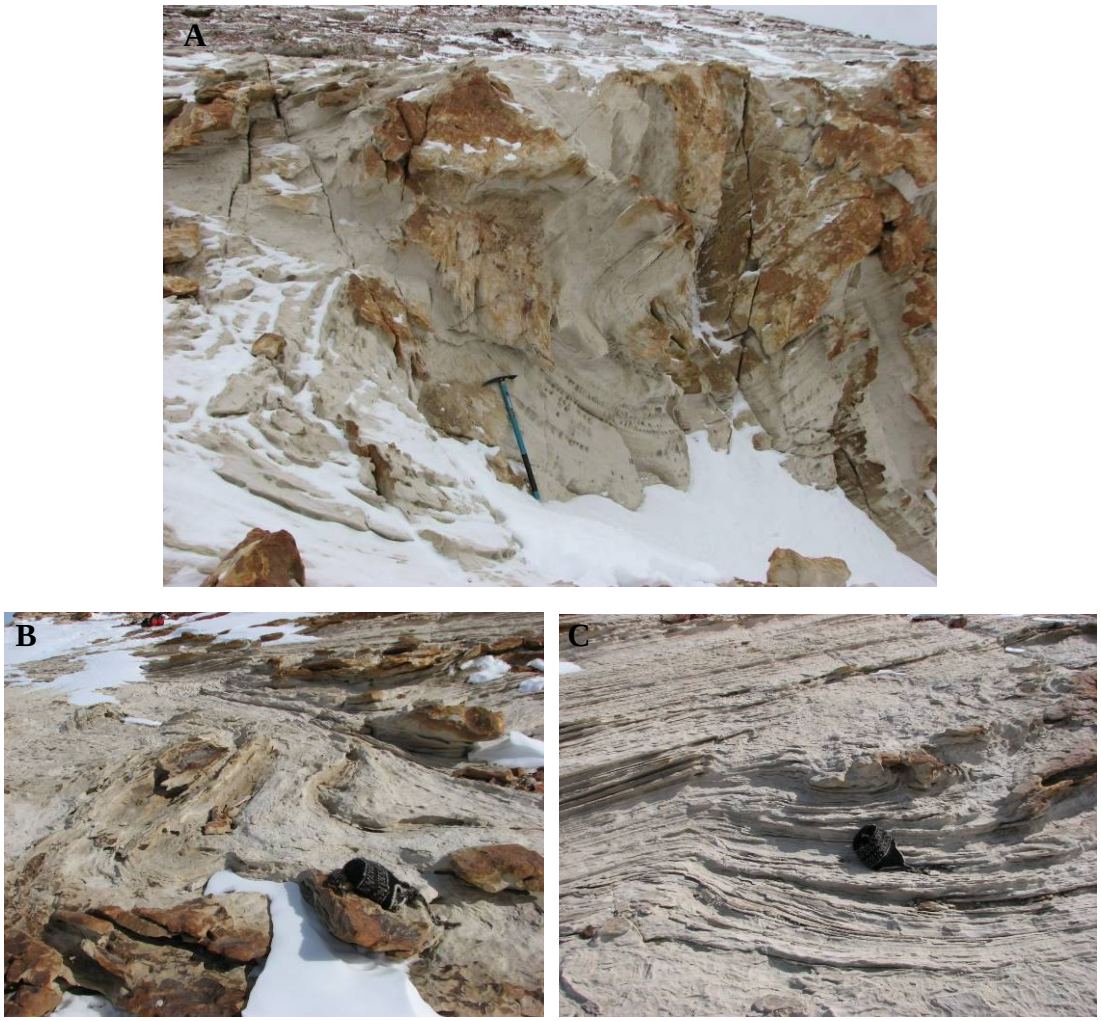

Figure 3-10: Slumping of cross beds in Cross-bedded Sandstone Lithofacies. Mt Jason.
Photos by: John Bradshaw

Overall, the sequence at Mt Jason begins with the Pebbly Sandstone Lithofacies overlain by Granule Cross-bedded Lithofacies, which is then overlain by the Cross-bedded Sandstone Lithofacies. At the base of CSL there are granules and coarse sand on the foresets and the cross beds are interbedded with *Heimdallia*. *Heimdallia* bed occurrence decreases up section and ripples and slumps are found and are laterally correlative with the outcrops on the col between Mt Jason and Mt Hercules. Above the ripples, one outcrop of the fine subfacies is observed. The Heimdall Erosion Surface cuts the Cross-bedded Sandstone Lithofacies.

3.4.2 Mt Aeolus

Much of the outcrop at Mt Aeolus was obscured by snow. The succession at the field site is observed from the Windy Gully Sandstone Formation up through the New Mountain Sandstone to the Heimdall Erosion Surface.

The Windy Gully Sandstone Formation sits directly on the Kukri Erosion Surface and is 35 m thick. There is a basal conglomerate that is 50 cm thick and composed of granite and quartz (with rod-like crystals) pebbles and cobbles. It occurs in isolated very small outcrops. An obscured 4 m section occurs between the conglomerate and overlying sandstone (Appendix A1/3). The Windy Gully Sandstone differs from the New Mountain Sandstone in that it contains mainly massive (0.2 to 4 m thick) and horizontally laminated beds (0.2 to 3 m thick) of medium and coarse sandstone. The cross beds are much smaller overall, 10 to 30 cm thick, but large scale cross beds exist at the top of the section (up to 1 m thick). The presence of dark fissile sandstone on a gentle slope at 33 m could indicate the location of the Terra Cotta Siltstone. The Terra Cotta Siltstone separates the Windy Gully and New Mountain Sandstones (Fig 2-1).

The contact between the Terra Cotta Siltstone and New Mountain Sandstone is not observed but is taken at around 35 m. The lower unit of the New Mountain Sandstone at Mt Aeolus is Granule Cross-bedded Lithofacies and is a minimum 7.7 m thick (Appendix A1/3). The overall unit is medium sandstone and pebble material is not abundant, sandstone pebbles are especially lacking. The lithofacies is composed of alternating beds of poorly sorted very coarse quartz and feldspathic sandstone and very well sorted medium sandstone. Both units are trough cross-bedded on a 10 to 40 cm scale. The lower beds contain scattered coarse quartz pebbles. There are also *Heimdallia* and unidentified vertical and horizontal burrows (Appendix A1/3).

The contact between GCL and the overlying Cross-bedded Sandstone Lithofacies is obscured by scree. The CSL is 38.5 m thick (Appendix A1/3). The lithofacies is composed of cross-bedded (0.5 to 1.5 m thick), poorly sorted, very coarse sandstone and very well sorted fine and medium sandstone. The lithofacies also contains massive beds of well-sorted fine or medium sandstone, 1.5 to 3 m thick, and *Heimdallia* trace fossils. The *Heimdallia* are associated with cross bedding and are observed in only two layers within the lithofacies (Appendix A1/3). This is interpreted as CSL, though the lithofacies is relatively coarser grained than other examples and contains massive beds. The cross beds are a similar size to

other outcrops of CSL across the field area. Massive sand units are not observed at other field sites. The Heimdall Erosion Surface truncates the CSL.

In summary, the sequence at Mt Aeolus begins with the Windy Gully Sandstone and Terra Cotta Siltstone. The New Mountain Sandstone is comprised of Granule Sandstone Lithofacies overlain by the Cross-bedded Sandstone Lithofacies. The Heimdall Erosion Surface truncates the Cross-bedded Sandstone Lithofacies.

3.4.3 Mt Electra

The New Mountain Sandstone Formation is recorded in the east below Mt Dido and west above the Wright Upper Glacier.

Below Mt Dido (Fig 1-5, 1-6B), the sequence rests directly on the basement (Granite Harbour Intrusives) beginning with the Boreas Subgreywacke Member. The outcrop is inferred to be the Boreas Subgreywacke Member due to similarities to descriptions in Plume (1982) and Isaac *et al* (1995). The member is composed of a reddish medium sand matrix in which 'float' milky quartz (angular coarse pebble to cobble), jasper, pebbles of very dark angular mudstone and rare, discontinuous mud layers (Fig 3-11A). Very small outcrops are scattered over a large area and about 3 m of the Boreas Subgreywacke Member was observed. However, the limited and poor outcrop and the large gap (140 m) between the member and overlying New Mountain Sandstone outcrop implies that Boreas Subgreywacke Member does not occur at the base of the New Mountain Sandstone, and that the Windy Gully Sandstone probably intervenes. Outcrops of the member occur at different heights (2 to 4 m apart vertically) suggesting that the Kukri Erosion Surface is irregular.

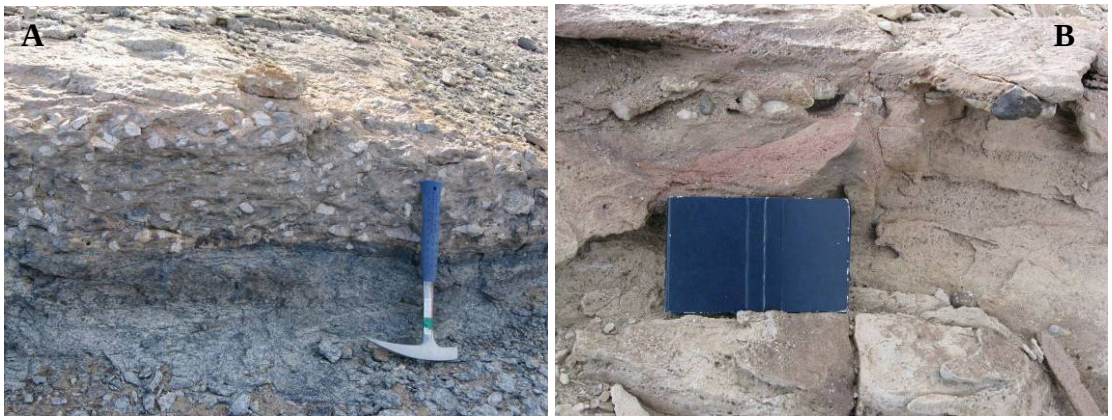

Figure 3-11: **A)** Boreas Subgreywacke Member. **B)** Pebble layer within Pebbly Sandstone Lithofacies. Mt Dido section east of Mt Electra.

Above the 140 m gap between the Boreas Subgreywacke Member and the next outcrop, the rocks have been assigned to New Mountain Sandstone. It is the Pebbly Sandstone Lithofacies and is composed of coarse to very coarse sandstone with granules along the foresets and pebble lags on bounding surfaces (Fig 3-12B). The pebbles are composed of quartz (angular to sub-angular), quartzite and lithic clasts. Pebbles are also scattered throughout the foresets and sometimes aligned along the foreset traces. The cross beds appear to be up to 1 m thick but are hard to measure. Cross bed sets containing the pebbles can be traced for over 100 m laterally and 9 to 10 m vertically. Overlying them is a medium sandstone with small scale cross beds (40 cm thick). The entire Pebbly Sandstone Lithofacies unit is about 30 m thick. The cross beds within PSL indicate flow directions predominantly to the east (Fig 3-12A).

Overlying the Pebbly Sandstone Lithofacies is the Cross-bedded Sandstone Lithofacies. The contact between the lithofacies occurs at the first evidence of *Heimdallia* trace fossils. The CSL is typical flaggy cross-bedded medium sandstone. Outcrop is limited due to the unit being slope forming and covered in scree. A large bench tops this unit, which is where the Heimdall Erosion Surface truncates the New Mountain Sandstone. The CSL is about 30 m thick. Measurements of cross beds within the CSL indicate a predominant paleocurrent direction to the northwest (Fig 3-12B), which is remarkably different from the underlying Pebbly Sandstone Lithofacies.

In summary, though much of the exposure below Mt Dido is covered in scree the succession can be seen to go from Boreas Subgreywacke Member, probably Windy Gully Sandstone to New Mountain Sandstone, which is composed of the Pebbly Sandstone Lithofacies overlain by Cross-bedded Sandstone Lithofacies.

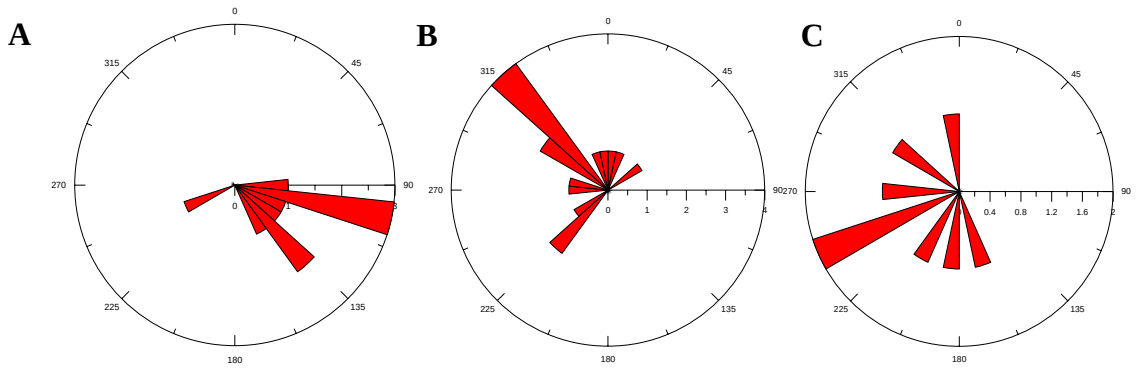

Figure 3-12: **A)** Paleocurrent directions from Pebbly Sandstone Lithofacies (n=10) and **B)** Cross-bedded Sandstone Lithofacies (n=15), east of Mt Electra. **C)** Cross-bedded Sandstone Lithofacies near the Upper Wright Glacier (n=8).

In the west near the Upper Wright Glacier, the New Mountain Sandstone is deposited directly on the basement of Granite Harbour Intrusives. No Basal Conglomerate Lithofacies is observed; instead, the Cross-bedded Sandstone Lithofacies sits directly on the basement. The CSL is composed of large-scale cross beds (up to 3 m thick) that lack *Heimdallia*. The foreset beds are 3 to 3.5 cm thick and each fine up from coarse to medium sand. One channel (2 m deep and 7 m across) with a jagged edge cuts into the cross beds and is filled with massive medium to fine sandstone (Fig 3-13). Above the channel granules begin to appear on the foresets but only in a zone 1.5 m thick. The CSL lithofacies is 100 m thick and is truncated by the Heimdall Erosion Surface. Cross beds within the Cross-bedded Sandstone Lithofacies near the Upper Wright Glacier indicate flow toward to southwest, however there is a large spread of flow directions (Fig 3-12C)

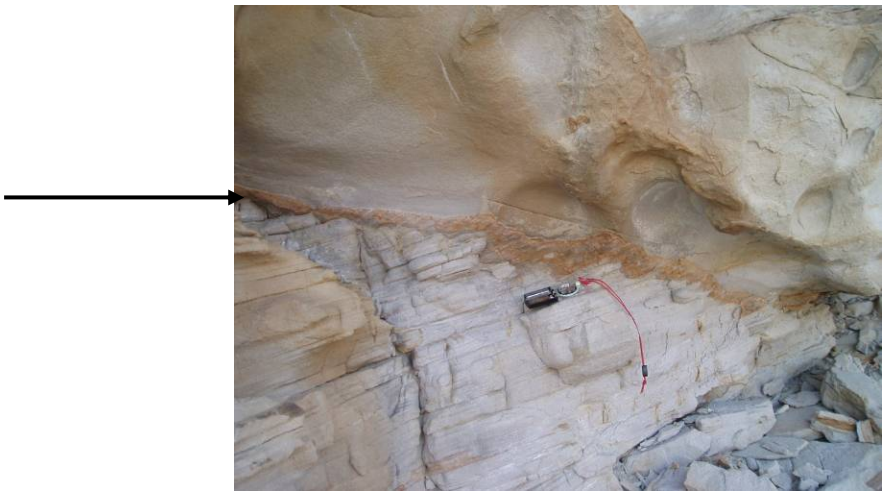

Figure 3-13: Channel and fill within the Cross-bedded Sandstone Lithofacies west of Mt Electra. Note the jagged edge shown by the arrow. Photo by: Margaret Bradshaw.

3.4.4 Lake Vashka

The New Mountain Sandstone Formation outcrops on three crags on the southern side of the Barwick Valley; they are described from west to east. The crags are surrounded by extensive scree, which obscures a lot of exposure. The distance between the western and middle crag is 300 m and between the middle and eastern crag is 600 m (Fig 1-8, 1-9).

The basal contact is not exposed on the most westerly crag. The lowest lithofacies present is the Pebbly Sandstone Lithofacies, which is 5.2 m thick. The base of the measured section (Appendix A1/7a) is probably very close to the Kukri Erosion Surface because boulders with rhyolite, quartz and green very fine sandstone pebbles were found in the slope

beneath the measured section. The lithofacies is composed of small trough cross beds or horizontal thick or thinly bedded sandstone with abundant angular quartz granules in medium to fine sandstone. Thick and thinly bedded units are up to 1 m thick and beds range from 1 to 5 cm thick. The cross beds are up to 30 cm thick. The unit also contains rare ripples, *Thalassinoides* (Fig 3-14A) and mudstone layers. Overlying the Pebbly Sandstone Lithofacies is the Pinstripe Cross-bedded Lithofacies, however there is a transitional unit between the two. The unit is composed of 1.2 m of bioturbated medium sandstone with remnant laminations and a granule to pebble layer at the base. The Pinstripe Cross-bedded Lithofacies is an estimated 35 m thick (J. Bradshaw, pers comms, 2007) and is composed of 3 to 4 m thick cross-bedded medium sandstone with millimetre scale laminations. There is no top contact at the western crag.

At the middle crag, the Pinstripe Cross-bedded Lithofacies is also exposed, and is truncated by the Heimdall Erosion Surface. However, the thickness of the lithofacies was not measured. Paleocurrent data from this crag indicate flow to the north (Fig 3-14B).

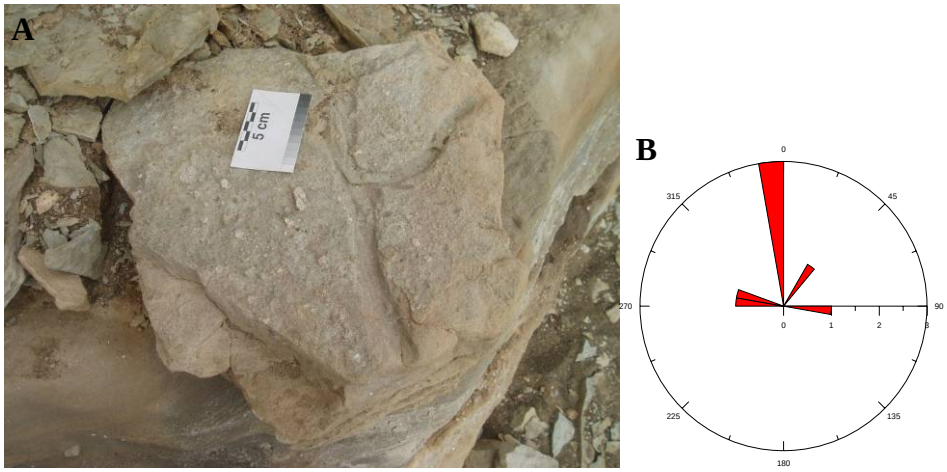

Figure 3-14: **A)** *Thalassinoides* trace fossils within the Pebbly Sandstone Lithofacies, Lake Vashka. Photo by: Margaret Bradshaw **B)** Paleocurrent directions from the Pinstripe Cross-bedded Lithofacies, middle crag, Lake Vashka (n=7).

At the most easterly crag, both the Heimdall and Kukri Erosion Surfaces are observed. The Basal Conglomerate Lithofacies is deposited on Koettlitz Group basement (Isaac *et al*, 1995). At this location huge granite boulders occur (Fig 3-15), as do milky quartz, rhyolite and pegmatite. The clasts of the Basal Conglomerate Lithofacies are deposited on the basement or supported in the overlying PCL.

The Pinstripe Cross-bedded Lithofacies overlies the BCL. The Heimdall Erosion Surface truncates the Pinstripe Cross-bedded Lithofacies, though is not observed in direct contact with the lithofacies as a thin sill runs along the contact (Appendix A1/7c). The lithofacies is a maximum 37.5 m thick but pinches to the east as the KES and HES appear to converge. Convergence is due to the large amount of relief on the Kukri Erosion Surface and the relative flatness of the Heimdall Erosion Surface. Observations made at the eastern crag indicate a relief of at least 40 m and slope of maybe 40 to 50º on the KES.

Figure 3-15: Granite boulder (90 cm) above Kukri Erosion Surface at Vashka Lake. Ruler is 50 cm.

3.4.5 Vashka Crag

The outcrop at Vashka Crag is very scattered and discontinuous making observation and interpretation difficult. The basement is observed and is capped by the Basal Conglomerate Lithofacies (Fig 3-16). The lithofacies is 9 cm thick and is composed of a fine sand matrix supporting angular milky quartz pebbles, overlain by a fine to medium quartzose sand.

Stratigraphically higher, there are scattered outcrops of Granule Cross-bedded Lithofacies. The lithofacies is composed of alternating cross beds (10 to 30 cm thick) of poorly sorted medium sand to granule quartz and feldspathic sandstone and moderately sorted medium to coarse quartz sandstone. *Heimdallia* beds are also in evidence. No large-scale flaggy cross beds of the Cross-bedded Sandstone Lithofacies were seen.

Figure 3-16: Basal Conglomerate Lithofacies deposited on basement at Vashka Crag. Arrow indicates the Kukri Erosion Surface.

3.4.6 Sponsors Peak

In the basin to the south of Sponsors Peak (Fig 1-10) a section was observed up to the col between Sponsors and Nickel Peaks. At the base of the section isolated blocks of Basal Conglomerate Lithofacies and overlying sandstone where found within 1 m of each other, but the lithofacies was not found in contact with the basement. The Basal Conglomerate Lithofacies is composed of green breccia containing angular milky quartz pebbles (similar to Vashka Crag).

Overlying the Basal Conglomerate Lithofacies is 100 m of Cross-bedded Sandstone Lithofacies. It is a flaggy cross-bedded medium sandstone with occasional granule to medium sand quartz scattered throughout. The cross beds also have *Heimdallia* layers and trackways. The flaggy cross beds continue until truncation by the Heimdall Erosion Surface on the col between Sponsors and Nickel Peaks. Measurements from the Cross-bedded Sandstone Lithofacies indicate paleocurrents in directions towards an area between southwest and west (Fig 3-17A) though this is from a small sample number.

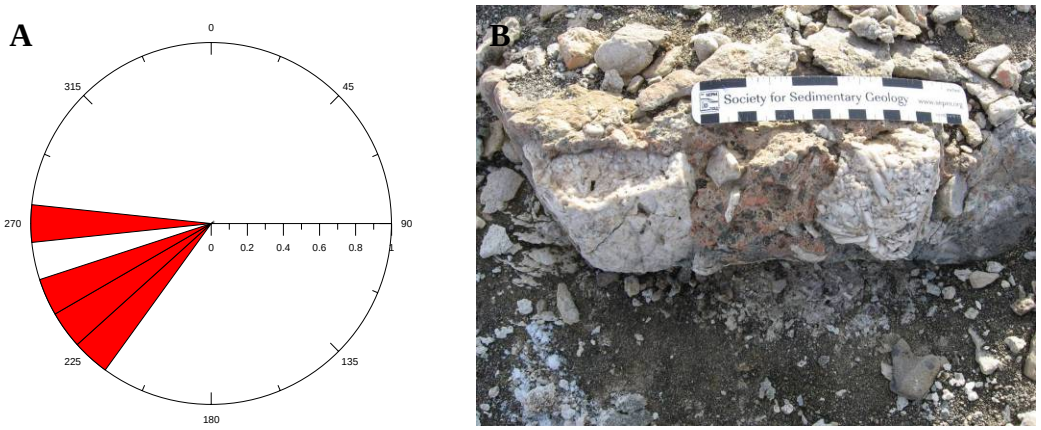

Figure 3-17: **A)** Paleocurrents from the Cross-bedded Sandstone Lithofacies at Sponsors Peak (n=4). **B)** Basal Conglomerate Lithofacies behind Sponsors Peak camp.

This succession is also observed directly behind the Sponsors Peak campsite (Fig 1-10). The Basal Conglomerate Lithofacies is observed resting directly on the Granite Harbour Intrusives and contains cobbles of granitoid and milky quartz with rod like crystals (Fig 3-17B) supported by a matrix of fine sand. The lithofacies is 40 cm thick. The overlying Cross-bedded Sandstone Lithofacies cross beds are draped over the conglomerate and have continuous deposition up to the ridge behind Sponsors Peak camp (Fig 1-10). The thickness of the Cross-bedded Sandstone Lithofacies at this site is unknown, as it is not seen to be truncated by the Heimdall Erosion Surface, but it must be at least 20 m.

3.5 Composition

Point counts of samples throughout the field area are analysed to determine the composition and provenance of the New Mountain Sandstone. Photos of the thin sections are also included to show differences in composition, grain size and particular or peculiar depositional fabrics or types. For point count data refer to Appendix B1.

The QFL diagram below (Fig 3-18) shows the grouping of samples in relation to each lithofacies. The diagram also shows the evolution in sediment composition of the New Mountain Sandstone up section in the most prominent lithofacies types (Pebbly Sandstone, Granule Cross-bedded and Cross-bedded Sandstone Lithofacies).

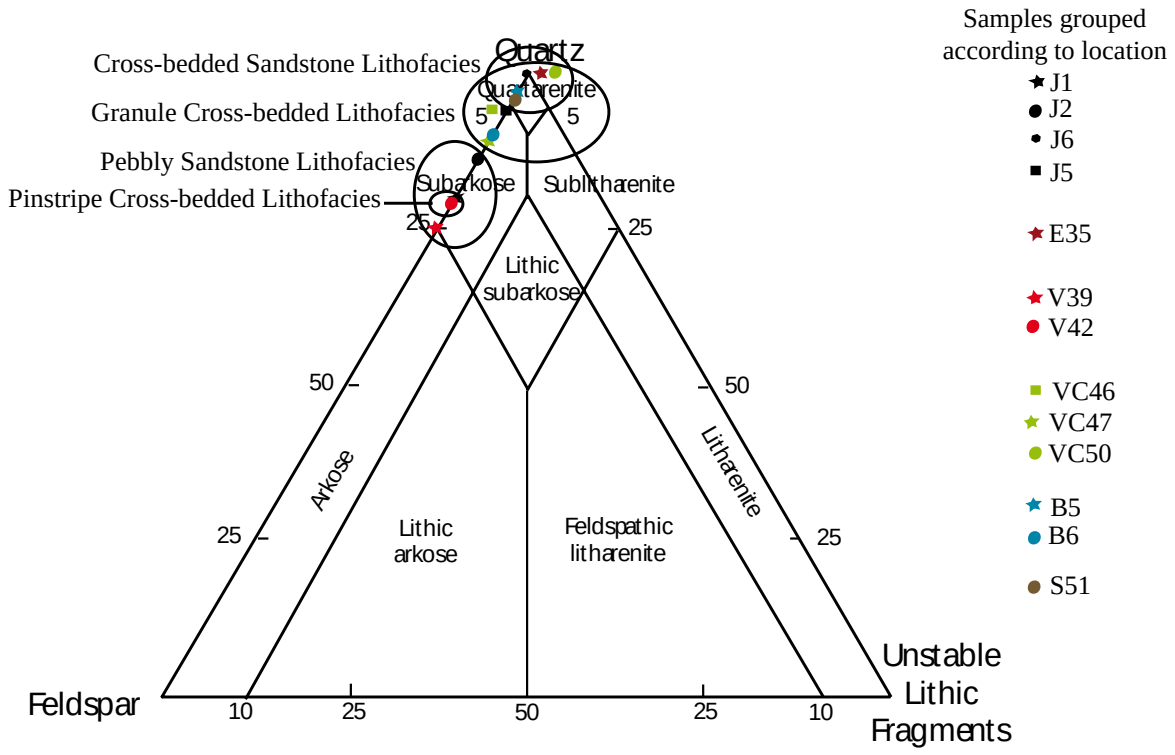

Figure 3-18: QFL plot of the New Mountain Sandstone. (Adapted from Blatt and Tracey, 1996)

3.5.1 Basal Conglomerate Lithofacies

The Basal Conglomerate Lithofacies is composed of pebble to boulder milky quartz, quartzite, granite, rhyolite and altered pegmatite. The matrix is composed of medium to fine sand and is similar to the lithofacies of the New Mountain Sandstone that are immediately overlying it. Milky quartz boulders showing rod-like crystals were found above Sponsors Peak camp, milky quartz found at other localities (Vashka Crag and other Sponsors Peak section) could be of the same type but the pebble size is smaller so the rod-like crystals are not apparent.

3.5.2 Pebbly Sandstone Lithofacies

The Pebbly Sandstone Lithofacies is composed of 14 to 25% feldspar and mono and polycrystalline quartz (80 to 85%). The lithofacies is an arkose to subarkose (Fig 3-18). Alkali feldspar is the most common, though plagioclase is also present (Appendix B1). The figures show the wide spread in grain sizes from fine sand (Fig 3-19C, D) to very coarse sand (Fig 3-19A, B). Feldspar can be seen in Fig 3-19D and C. Quartz overgrowths are seen rarely (Fig 3-19A, B). Pebbles within the lithofacies are composed of red sandstone, quartz, quartzite, white siltstone, feldspar and fine laminated sandstone.

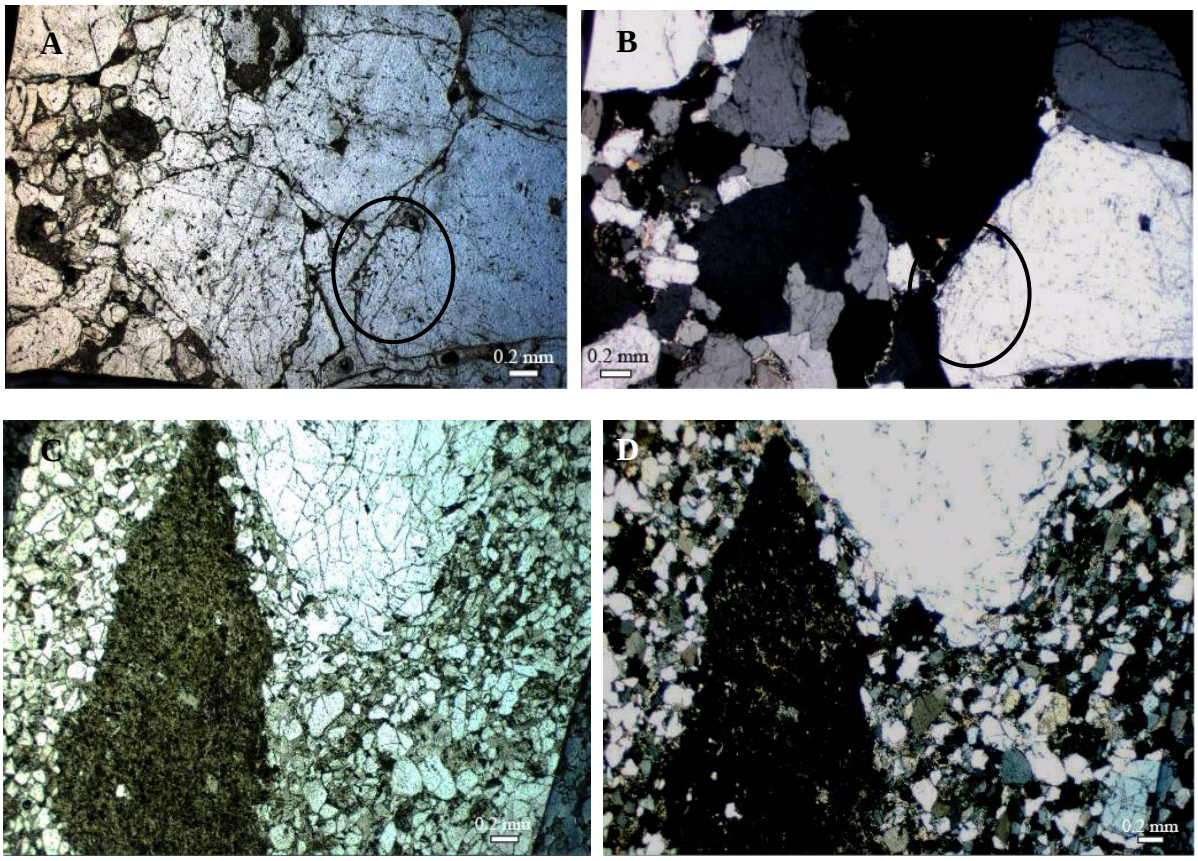

Figure 3-19: Representative samples of Pebbly Sandstone Lithofacies from Mt Jason. Monocrystalline quartz and circled quartz overgrowths. **A)** Plain polarised light**. B)** Cross-polarised light. Altered feldspar and quartz (showing variation in grain size) **C)** Plain polarised light. **D)** Cross-polarised light. Note 0.2 mm scale.

3.5.3 Granule Cross-bedded Lithofacies

The Granule Cross-bedded Lithofacies is composed of feldspar (6 to 11%) and quartz (75 to 94%). The lithofacies is a subarkose (Fig 3-18), though has less feldspar than the Pebbly Sandstone Lithofacies. Quartz is both mono and polycrystalline (Fig 3-20D), though polycrystalline quartz is less common than in the Pebbly Sandstone Lithofacies. The feldspar is mainly alkali feldspar (Fig 3-20C) with little or no plagioclase feldspar; except at Mt Jason (J5), where there is more plagioclase feldspar than alkali feldspar. Quartz overgrowths are observed rarely throughout the lithofacies (Fig 3-20A, B).

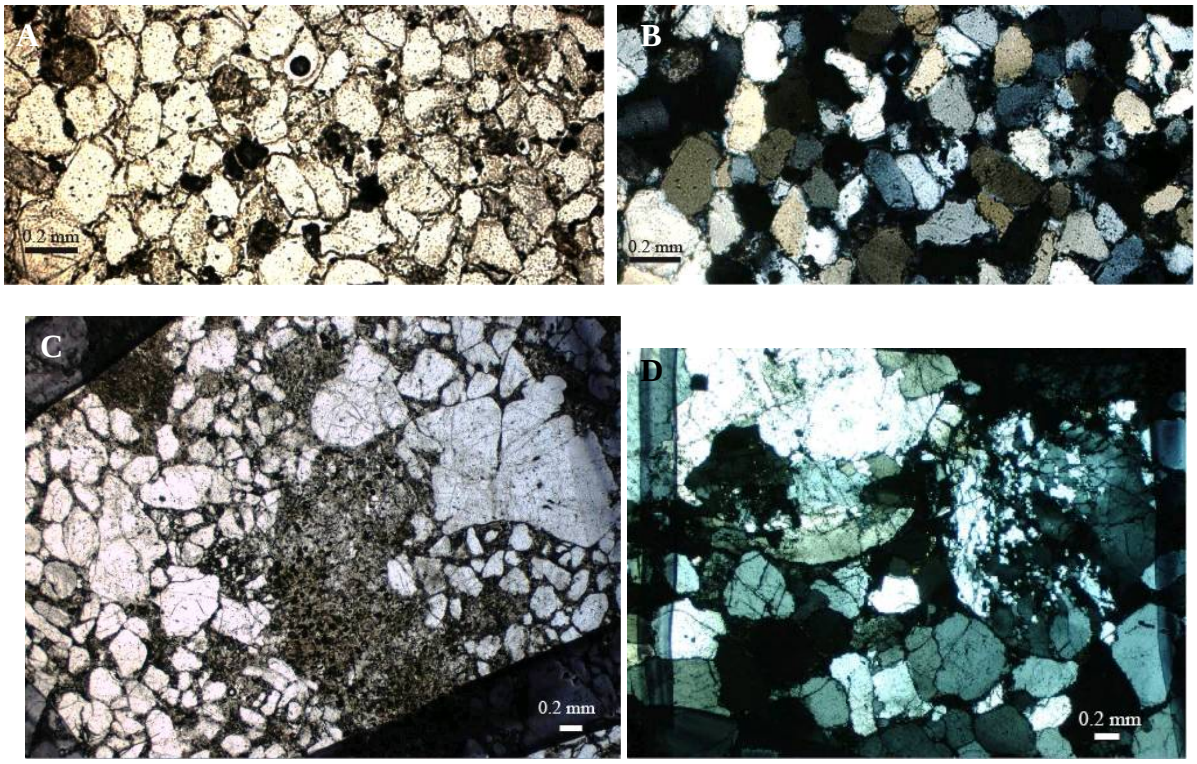

Figure 3-20: Representative samples of Granule Cross-bedded Sandstone from Vashka Crag and Mt Aeolus. Quartz overgrowths and monocrystalline quartz, Mt Aeolus. **A)** Plain polarised light. **B)** Cross-polarised light. **C)** Quartz and altered feldspar, Vashka Crag **D)** Mono and polycrystalline quartz, Vashka Crag (cross-polarised light).

3.5.4 Pinstripe Cross-bedded Lithofacies

The Pinstripe Cross-bedded Lithofacies is composed of 79% quartz and 21% feldspar. The lithofacies is a subarkose (Fig 3-18) and is similar to the Pebbly Sandstone Lithofacies. It is composed of predominantly alkali feldspar and monocrystalline quartz. The thin sections show the change in colour that is expressed as a pinstripe texture (Fig 3-21A, B).

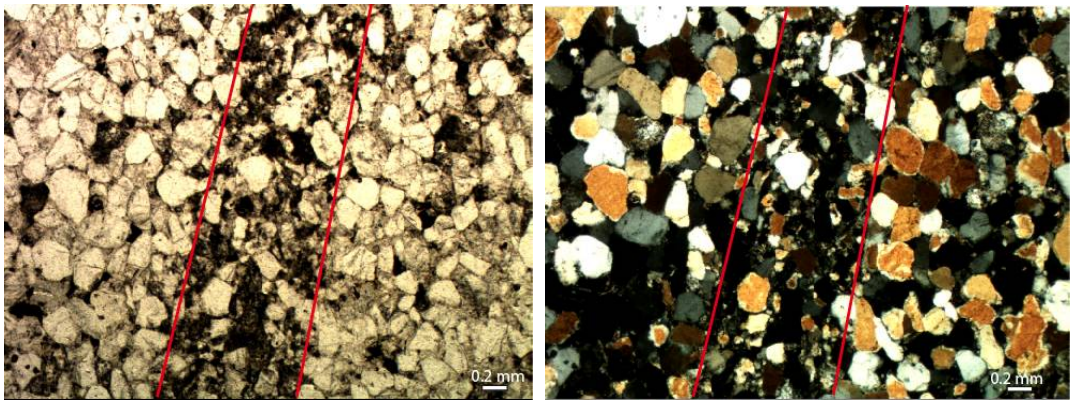

Figure 3-21: Representative sample of the Pinstripe Cross-bedded Lithofacies, Lake Vashka. Pinstripe texture shown by alternating medium and fine sand. Left image taken under plain polarised light and right image under cross-polarised light.

3.5.5 Cross-bedded Sandstone Lithofacies.

Cross-bedded Sandstone Lithofacies is a quartzarenite (>95% quartz) (Fig 3-18). Thin sections of the Cross-bedded Sandstone Lithofacies shows that the lithofacies is entirely made of quartz and overgrowths occur throughout the lithofacies, creating the cement. Dust rims are seen rarely (Fig 3-23A, B). Most quartz is monocrystalline but polycrystalline quartz grains are seen in samples from Vashka Crag (3-22A, B). These samples also contain zeolite matrix that can be attributed to the proximity of the outcrop to intrusions of the Jurassic Ferrar Dolerite (Fig 3-22C, D).

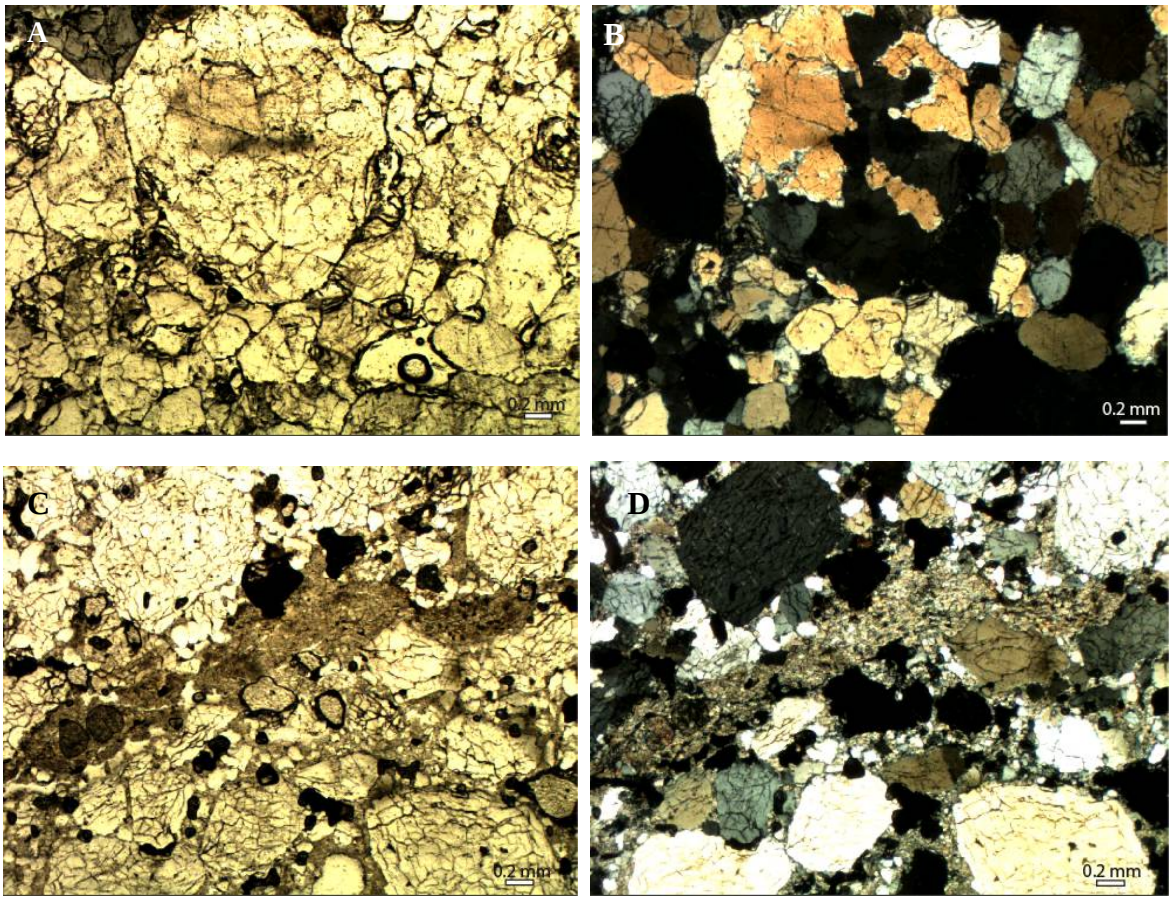

Figure 3-22: A) and **B)** polycrystalline quartz and monocrystalline quartz within the Cross-bedded Sandstone Lithofacies, Vashka Crag. **C)** and **D)** Zeolite matrix and quartz in Cross-bedded Sandstone Lithofacies, Vashka Crag.

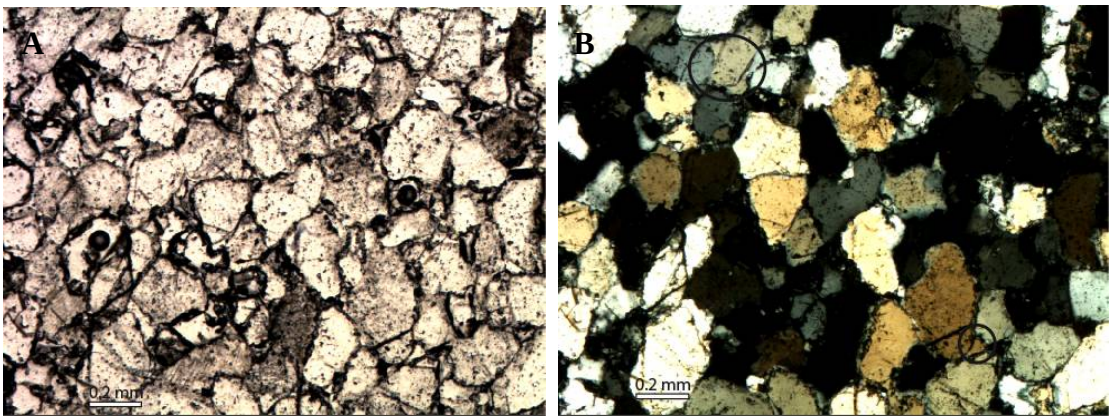

Figure 3-23: Cross-bedded Sandstone Lithofacies at Mt Jason showing common quartz overgrowths and rare dust rims (circled). **A)** Plain light and **B)** cross-polarised light.

3.6 Interpretation

The lithofacies within the New Mountain Sandstone have previously been interpreted as fluvial (braided river), aeolian and marine deposits (Barrett and Kohn, 1975; Barret, 1977; Bradshaw, 1981; Plume, 1982; Woolfe, 1990; Wizevich, 1997). As outlined in Chapter 2.4.4 the depositional environment of the New Mountain Sandstone is contentious and using different data sets gives rise to different interpretations. This chapter integrates a variety of data types that includes sedimentary structures and trace fossils and assesses the depositional environment for each lithofacies. Important in interpretation are the adjacent deposits and the bounding units. In accordance with Walthers Law, in an unbroken succession the depositional environments of the adjacent lithofacies, both vertically and horizontally, must be compatible.

The widely different depositional environments cited above are the result of similarity between the deposits of the fluvial, marine and aeolian environments. Well rounded, well sorted and commonly clay poor deposits are often seen as aeolian but can arise as the result of the reworking of aeolian deposits in marine or fluvial environments (Collinson, 1986a). The Cross-bedded Sandstone Lithofacies is the most distinctive facies within the New Mountain Sandstone and the most difficult to interpret in terms of depositional environment as medium to fine cross-bedded sandstones are found in aeolian, marine and fluvial settings. The Pebbly Sandstone and Granule Cross-bedded Lithofacies could occur in both fluvial and marine deposits, and the Pinstripe Cross-bedded Lithofacies is only an aeolian deposit.

The facies of braided rivers are either gravel or sand dominated, and mud is a common secondary deposit (Boggs, 2001). Migration of channels within the river system creates coarse trough cross-bedded channel deposits overlain by finer deposits with planar cross lamination, planar and ripple cross lamination and massive sandstones (Blatt *et al*, 1980; Hjellbakk, 1997; Bridge and Lunt, 2006). Collinson (1986) states that braided rivers create concave-upwards based, lenticular channel bodies. Typical deposits of coarse braided rivers commonly contain massive, horizontal or cross-bedded gravels with reactivation surfaces, wedges of sand between gravel foresets, and channels lined with coarse material draped with finer sediment (Collinson, 1986). Sandy braided rivers are gradational with coarse braided types and commonly have trough and tabular cross beds, reactivation surfaces and mud drapes (Collinson, 1986). A typical feature of sandy braided rivers is transverse bars (Blatt *et al*, 1980). The migration of transverse bars produces deposits with trough and tabular cross beds with scour surfaces and gravel lags at the base (Blatt *et al*, 1980). Hjellbakk (1997) describes irregular and lenticular shaped trough cross bed sets that are the result of dune migration. Study of the Brahmaputra River in India by Coleman (1969) provides ample information on the facies and structures found in large sandy braided rivers. Sediments within the Brahmaputra River are composed of trough cross-bedded fine sand and trough fill of poorly sorted clayey silts and silty clays, with occasional lenticular cross-stratified silts (Coleman, 1969). Organic debris is often trapped along foresets or at the base of scours and burrows, soil horizons or roots have formed where the cross beds are exposed (Coleman, 1969; Bridge and Lunt, 2006). Mud cracks can also be found in sandy braided river deposits (Bridge and Lunt, 2006). Distorted stratification is also observed by Coleman (1969) in the deposits and he proposes that the distortion is due to one or a combination of the following: rapid rise and fall of the river, heavily sediment laden currents, fine grained nature of the deposits or intensive scouring and slope steepening.

The lithofacies within the New Mountain Sandstone Formation have few similarities to the fluvial deposits described above. The cross beds within the Pebbly Sandstone and Granule Cross-bedded Lithofacies are similar in morphology to those in fluvial systems, when looking down the direction of flow. However they do not contain mud, fine sand drapes or coarse material lining the lower bounding surface of trough cross beds or foreset beds. There is also a lack of organic detritus within and between the cross bed sets and no evidence of formation of soil horizons or roots. Pebbles within the Pebbly Sandstone Lithofacies rarely occur in groups big enough to be called a lag and are often scattered throughout the foresets.

In sandy fluvial deposits pebbles should be more common and would be deposited as lags lining the base of cross bed sets. The Cross-bedded Sandstone Lithofacies also has no similarities to fluvial deposits. The cross beds are tangential and tabular in form and the lithofacies contains no fine material draping or lining foreset beds or bounding cross bed sets. The base of the cross bed sets is flat in comparison to concave-up types found in fluvial settings. None of the lithofacies within the New Mountain Sandstone contain planar lamination, ripple cross lamination or scoured surfaces. Overall deposition of the New Mountain Sandstone Formation is very uniform and there is little variation in sedimentary structures and sediment size, which would be expected in a sandy braided river system.

Therefore, none of the lithofacies of the New Mountain Sandstone Formation are deposited in a fluvial environment. All the things that are signatures of fluvial systems, pebble lags, scour surfaces, reactivation surfaces, mud drapes along the foresets, obvious concave channel boundaries and organic detritus, are lacking in the New Mountain Sandstone. Therefore, it is reasonable to conclude that they are not fluvial deposits.

The Pebbly Sandstone and Granule Cross-bedded Lithofacies have many similarities to marine, especially shallow marine, deposits. The shallow marine depositional environments associated with beaches include the shoreface, offshore transition and offshore zones (inner shelf) (Boggs, 2001) (Fig 3-24), which are affected by waves and longshore currents (Boggs, 2001; Howell and Flint, 2003). Sediments within the upper shoreface zone range in size from fine sand to gravel and sedimentary structures include multidirectional trough cross beds formed by migration of dunes or ripples, sub horizontal plane beds, low angle bidirectional trough cross beds (Boggs, 2001; Bezerra *et al*, 1998) and a lack of trace fossils (Blatt *et al*, 1980). Upper shoreface deposits are influenced by translational waves and longshore currents (Bezerra *et al*, 1998; Boggs, 2001). Middle-shoreface deposits are composed of fine to medium sand with minor silt and shell material. Gravels can also be found here. Boggs (2001) states that the structures found in this zone can be very complex and can include low-angle planar bedding, ripple cross-lamination, trough cross beds and commonly *Skolithos* trace fossils. Equivalent of the Boggs (2001) middle shoreface are lower shoreface deposits described by Blatt *et al* (1980) that are composed of fine to medium fine cross-bedded sandstone in sets 30 to 40 cm thick and include trace fossils. Middle shoreface sediments are deposited under high-energy conditions due to interaction with waves, rip currents and longshore currents (Boggs, 2001).

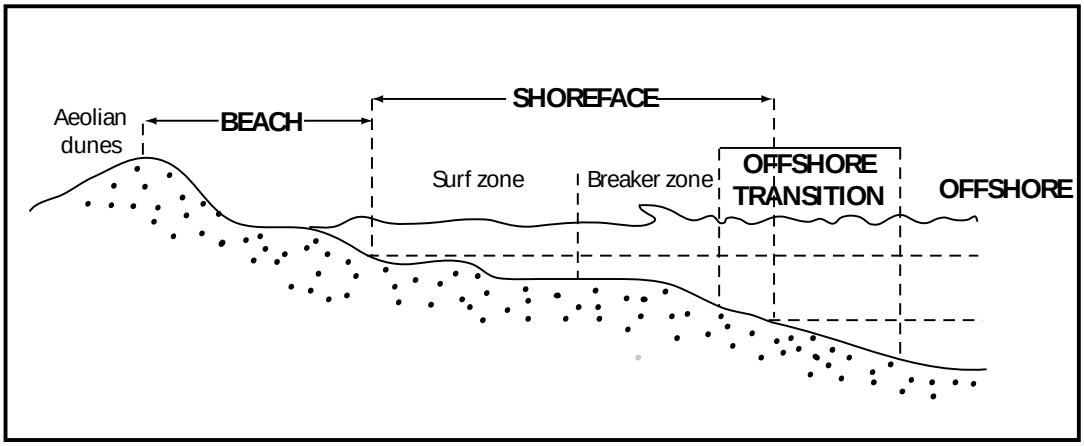

Figure 3-24: Beach and nearshore deposit zones. Adapted from Boggs (2001)

The Pebbly Sandstone Lithofacies has many similarities to the deposits of the upper-shoreface environment. The sediment size of the Pebbly Sandstone Lithofacies is typical of upper-shoreface deposits (fine sand to granule), contains pebbles and coarse sand to granule lenses and layers. Paleocurrent directions from both Mt Jason and Mt Electra are moderately bidirectional; there are characteristics of multidirectional flow that could be due to the small sample size. The trough cross beds result from migration of sub-aqueous dunes or ripples. The pebbles within the lithofacies are composed of quartz, quartzite, fine laminated sandstone and brown sandstone. The quartz and quartzite pebbles could be from basement sources and the sandstones from exotic sources outside the field area or underlying formations in the Taylor Group.

The Granule Cross-bedded Lithofacies is also similar to shoreface deposits and was probably deposited in the middle shoreface. The lack of extensive pebbles, relatively finer grainsize and *Heimdallia* trace fossils indicate that the lithofacies was deposited in slightly deeper water than the Pebbly Sandstone Lithofacies. Paleocurrents from the Granule Cross-bedded Lithofacies are inconclusive due to small sample size. However, it can be seen that the currents have a wide spread which could be due to the interaction between longshore currents, waves and rip currents in the depositional area. *Heimdallia* bioturbation occurred at times or in areas of relatively lower energy that left the animals time to move through the substrate before deposition of the next cross bed.

The Pebbly Sandstone and Granule Cross-bedded Lithofacies are similar to a marine facies of the Hardyston Formation, Eastern Pennsylvania USA (Simpson *et al*, 2002), which is a shoreface deposit. The Pebbly Sandstone Lithofacies has many similarities to facies 6 of

Facies Association C (FA C) of the Hardyston Formation (Simpson *et al,* 2002). Facies 6 contains trough cross beds of medium to coarse-grained pebbly sandstone with abundant feldspar (Simpson *et al,* 2002). The beds of facies 6 also display a decrease in the number of pebbles vertically and are bioturbated at the top by *Skolithos* (Simpson *et al,* 2002). No comparison can be made between the cross beds of facies 6 and PSL and GCL because cross bed thickness was not included in Simpson *et al* (2002). *Skolithos* are not found in the Pebbly Sandstone or Granule Cross-bedded Lithofacies but *Heimdallia* are present. Simpson *et al* (2002) interpret FA C as a lower shoreface to foreshore environment and suggests the cross beds are due to migration of ripples. Simpson *et al,* (2002) interpret the spread of paleocurrents to be due to a combination of shore-parallel (deposition by longshore currents) and offshore-directed currents (reworking of sand sheets by wave or rip action).

The Pebbly Sandstone Lithofacies is therefore interpreted as deposited in an upper shoreface environment with long shore currents from the west during fair weather systems creating the main paleocurrent direction and reworking by waves, tides or rip currents creating variations in paleocurrent direction. The cross beds were deposited as sub-aqueous dunes and ripples and migrated across the shoreface. The sediment of the Pebbly Sandstone Lithofacies is immature and feldspathic. Feldspar has the tendency to weather more easily than quartz so the presence of feldspar indicates the source for the sediment is not far away and this is the first cycle of sediment weathering. The pebbles found within the unit are from both exotic and basement sources. The exotic pebbles are from deposits on the exposed plain that feeds the marine system or have been carried along shore by longshore currents. Fine laminated sandstone clasts could have been sourced from deeper water or from aeolian deposits on the beach dunes.

The Granule Cross-bedded Lithofacies was deposited in a similar environment to the Pebbly Sandstone Lithofacies but in the middle shoreface, with less pebble influx due to deeper water and periods of lower energy leading to *Heimdallia* bioturbation.

Differentiation of shallow marine from aeolian deposits is difficult due to the similarity of the deposit types. Deposits of aeolian origin are characterised by large scale cross bedding, high index ripples, wind ripple and grainfall laminae, pinstripe texture, high degree of sorting, ‘frosted’ grain surfaces and lack of mica or clay minerals (Collinson, 1986a; Mazzullo *et al,* 1991; Trevena and Cole, 1999; Loope, 2004). Trough or tabular cross beds can be 0.1 to 100 m high with foreset beds deposited at angles between 24 and 34º (Blatt

et al, 1980) and up to 40º (Collinson, 1986a). This is very similar to shallow marine deposits except for the 'frosted' grains, and lesser degree of sorting and scale of cross beds were exceptionally larger. No one factor will determine whether the deposits are aeolian or shallow marine, rather a combination of features will lead to the most likely depositional environment.

The Pinstripe Cross-bedded Lithofacies fits the criteria for an aeolian deposit. This is due to the pinstripe texture of the lithofacies, different slumping type and overall size of cross beds (up to 4 m thick). The lithofacies is very localised and was deposited on the basement in a dune field adjacent to the coastline at the same time as the Pebbly Sandstone and Granule Cross-bedded Lithofacies. The transitional unit at the base of the Pinstripe Cross-bedded Sandstone Lithofacies observed at the eastern crag at Lake Vashka is a beach deposit. It was deposited during the lateral change from a shallow marine (Pebbly Sandstone Lithofacies) to aeolian environment at Lake Vashka.

The cross bed sets of the Cross-bedded Sandstone Lithofacies are planar to tangential in shape and are predominantly low angle. This is diagnostic of both marine and aeolian cross beds. The Cross-bedded Sandstone Lithofacies is moderately to well sorted, with fining up cycles on each foreset bed. The sorting of the foresets suggests the beds are of marine origin because aeolian cross beds should be extremely well sorted (Blatt *et al*, 1980; Collinson, 1986a) and foresets coarsen up to form a pinstripe texture. Frosting indicates that the grains have been abraded as they are blown around by the wind. Sand within the Cross-bedded Sandstone Lithofacies does not show frosting in hand specimen and only show rare dust rims with overgrowths in thin section (Fig 3-22). The base of the cross bed sets in the Cross-bedded Sandstone Lithofacies are more flat than curved and commonly have a slight dip depending on the underlying morphology.

The large cross beds of the Cross-bedded Sandstone Lithofacies are similar to those found within the Arno Limestone, Oamaru (Ward and Lewis, 1975). These cross beds are between 0.5 and 2 m thick, planar or concave up (trough cross beds) and commonly wedge shaped (Ward and Lewis, 1975). Planar erosion surfaces, often obscured by bioturbation, bound the cross bed sets (Ward and Lewis, 1975). The paleoenvironment of the cross-bedded unit of the Arno Limestone is interpreted as marine dune bedforms analogous to those in the North Sea (Ward and Lewis, 1975). Cross beds within Facies Association 2 of the Muth Formation, Northern India (Draganits *et al*, 2001) are similar to the cross beds in the Cross-

bedded Sandstone Lithofacies. Facies Association 2 is interpreted as a shallowest foreshore, backshore and coastal dune sediments (Draganits *et al,* 2001). The cross beds also contain *Diplichnites* trackways and slumping.

Heimdallia are found both between cross bed sets and within cross beds. Between the cross bed set they are associated with more than one set, and act as a bounding surface for more than one overlying cross bed set. This infers that the *Heimdallia* did not occur in restricted areas such as ponds, which would have led to lensoidal rather than wedge or tabular shaped beds. *Heimdallia* also burrow into the top of underlying cross beds.

Slumping is very important in helping determine the depositional environment because it can give insights into whether the cross beds were underwater or not. Slumping in the Cross-bedded Sandstone Lithofacies exhibits characteristics of waterlain sediments. These include folding of the beds and mixture of them into a soupy texture. Individual foreset beds retain original bedding shape but change in thickness occur throughout the slump and are deformed into flame and ball and pillow structures. The type of deformation and lack of bed cohesion indicate that the cross set was waterlogged when deformation occurred. At Mt Jason, slumping occurs on a large lateral scale, meaning cross beds at the same topographic height are slumped. This suggests large-scale sedimentary liquefaction due to the water saturated nature of the cross beds. Localised slumping was due to oversteepening or removal of support. If it were an aeolian environment, slumping would be confined to single cross bed sets and would not affect adjacent cross bed sets, as seen at Mt Jason.

Slumping, cross bed shape, grainsize, sorting and similarities to other shallow marine deposits suggest that the Cross-bedded Sandstone Lithofacies was deposited in a shallow marine environment. It was probably on the lower shoreface with longshore currents flowing towards the northwest and southwest leading to the migration of dunes and the formation of cross beds. Ripples were formed by local current changes brought about by waning flow, rip currents or eddy currents over the crest of dunes. Slumping was probably due to post depositional shaking events. *Heimdallia* bioturbation occurred due to lower energy conditions with little or no sediment deposition; this could be on foreset beds or across dunes.

The Basal Conglomerate Lithofacies is a coarse matrix supported conglomerate composed of granite, milky quartz, rhyolite and pegmatite. The matrix material is commonly medium to fine sand, which is often similar to the grainsize of the overlying lithofacies

(either Granule Cross-bedded or Cross-bedded Sandstone Lithofacies). The similarity shows that the BCL was formed when deposition of the overlying lithofacies was initiated. This could have occurred as loose material fell off highs in the Kukri Erosion Surface and was reworked in the marine environment immediately prior to deposition of the GCL or CSL or coeval with deposition of the lowest part of the lithofacies.

The composition of the lithofacies of the New Mountain Sandstone Formation is dominated by quartz, with feldspar found in the lower lithofacies. The formation is entirely devoid of lithics in the sandstones but contains pebbles. Overall, the New Mountain Sandstone begins with an arkosic pebbly unit at the base, followed by a less arkosic granule unit and overlain by an entirely quartzose medium sandstone. This pattern varies at each field site. The grainsize of the New Mountain Sandstone fines upwards and is also associated with a decrease in feldspar upwards. The maturing of the sediment up section could be a result of reworking of older sediment, changing sediment source or change in environment. Contacts between all the lithofacies are gradational showing that the environment and/or sediment source changed over time. The lack of feldspar, sorting and rounding of sand grains in the Cross-bedded Sandstone Lithofacies could indicate reworking of the underlying sediment weathering away feldspars or a change in environment meaning coarser material was not deposited.

The New Mountain Sandstone Formation is a shallow marine deposit that changes up section due to relative rise in sea level. The change is from the Pebbly Sandstone Lithofacies, which is an upper shoreface deposit and changes up section to a middle (Granule Cross-bedded Lithofacies) and lower shoreface deposit (Cross-bedded Sandstone Lithofacies). The environment that deposited the Pebbly Sandstone and Granule Cross-bedded Lithofacies existed from Mt Jason to the eastern section of Mt Electra and north to Lake Vashka and Vashka Crag. The Pinstripe Cross-bedded Lithofacies was deposited at the same time in aeolian dunes adjacent to the shoreline. During deposition of the Cross-bedded Sandstone Lithofacies the coastline advanced to the north and encompassed Sponsors Peak. The finer deposits (very fine sandstone, flame structures, ripple laminae, mud cracks) at the top of the CSL at Mt Jason may indicate the beginning of relative sea level fall. This led to an estuarine intertidal environment and ultimately led to the exposure of the whole area. A further fall in relative sea level led to truncation of the New Mountain Sandstone and underlying basement and the formation of the Heimdall Erosion Surface.

The Boreas Subgreywacke Member was only observed at Mt Electra (Chapter 3.4.3). The member has previously been interpreted as occurring at the base of the New Mountain Sandstone (Plume, 1978; Isaac *et al*, 1996). The outcrop at Mt Electra was not observed in contact with any of the overlying formations. The lack of upper contact and the distance to the next sandstone outcrop (140 m), which is New Mountain Sandstone, suggests that the Boreas Subgreywacke Member could be deposited at the base of the Windy Gully or New Mountain Sandstone. The Boreas Subgreywacke is interpreted to be at the base of the Windy Gully Sandstone (Fig 7-3) due the limited and poor nature of the outcrop and the ambiguity over the upper contact.

3.7 Summary

- The New Mountain Sandstone Formation comprises five lithofacies: Basal Conglomerate Lithofacies, Pebbly Sandstone Lithofacies, Granule Cross-bedded Lithofacies, Cross-bedded Sandstone Lithofacies and Pinstripe Cross-bedded Lithofacies.
- The New Mountain Sandstone Formation was deposited in a shallow marine environment and shows deepening water over time followed by shallowing prior to the Heimdall Erosion Surface
- Basal Conglomerate Lithofacies was deposited as a debris flow or basal lag on the Kukri Erosion Surface
- Pebbly Sandstone Lithofacies is an upper shoreface deposit.
- The Granule Cross-bedded Lithofacies was deposited in a middle shore face environment.
- Cross-bedded Sandstone Lithofacies was deposited in a lower shoreface environment with shallowing upward towards the end of deposition at Mt Jason.
- Pinstripe Cross-bedded Lithofacies is an aeolian deposit.

- The sediments of the New Mountain Sandstone become more quartzose and finer up section showing a change in sedimentary source and depositional environment over time.
- The pebbles within the New Mountain Sandstone were sourced from exotic and basement sources.

Chapter Four: Heimdall Erosion Surface

4.1 Introduction

This chapter focuses on the Heimdall Erosion Surface and the conglomerate immediately overlying it. The conglomerate makes up the lowest part of the Odin Arkose Member of the Altar Mountain Formation. The Heimdall Erosion Surface is described in terms of its relief and morphology and inferences are made as to the mechanisms that led to the formation of the surface. The erosion surface and conglomerate are described at each field location east to west along the Olympus Range and then to the field sites in the north of the Dry Valleys.

4.2 Heimdall Erosion Surface (HES)

4.2.1 Relief and Morphology

The Heimdall Erosion Surface is a sharp erosive contact that typically has a relief of 10 to 50 cm. The surface has eroded the large cross beds of the Cross-bedded Sandstone or Pinstripe Cross-bedded Lithofacies at the top of the New Mountain Sandstone Formation. At many locations, erosion is controlled by the foresets creating an irregular saw tooth pattern (Fig 4-1). In areas where the dip of the cross beds at the top of the New Mountain Sandstone appear to be low angle, the relief on the erosion surface is much smaller. This is often the apparent dip because the outcrop face may not be at right angles to the cross bed set nor the top surface exposed. The dip could also appear low angle due to the tangential shape of the cross beds or the location in the cross bed set where the erosion surface has cut (i.e. if it were nearer the top, the foresets would be steeper). This morphology is typical and observed throughout the field area, although the scale varies. At many of the field sites relief on the erosion surface was difficult to discern due to the flat nature of the outcrop. At all locations, the rock underlying the erosion surface is very fresh and appears unweathered. The Heimdall Erosion Surface is essentially flat lying but may show a small dip due to differential uplift by the intrusion of Jurassic Ferrar Dolerite post formation (Chapter 2.4) and uplift of the Transantarctic Mountains.

Figure 4-1: Saw tooth pattern created by erosion of the New Mountain Sandstone Formation, west face of Mt Jason.

4.3 Odin Arkose Member of the Altar Mountain Formation

4.3.1 Conglomerate Lithofacies

The Conglomerate Lithofacies immediately overlies the Heimdall Erosion Surface and varies in composition, position relative to the HES and thickness laterally. The lithofacies is composed of pebbles (described below) and massive sandstone layers similar to the conglomerate matrix material. The lithofacies is typically matrix supported, though rarely clast supported in pockets (see Chapter 4.5.1, Fig 4.2C). The matrix is composed of poorly sorted, fine sand to granule, mainly medium sand, quartz (milky, smokey and clear) and feldspar. Quartz grains are sub-rounded to well-rounded and feldspars are sub-angular to sub-rounded. The lithofacies is deposited directly on the erosion surface. In many places only sandstone without pebbles rests on the erosion surface. Only at Mt Hercules were *Skolithos* traces found in the Conglomerate Lithofacies.

Listed below are the all the pebble types in the Conglomerate Lithofacies. Not all types are found at each field site, so pebble types observed at different field sites are stated in the respective sections.

1) Quartz (milky, smokey, clear and pink stained).
2) Plagioclase and alkali feldspar.

3) Quartzite (Dark grey, light grey and white)
4) Pink sandstone.
5) Light grey-pink poorly sorted sandstone.
6) Dark grey coarse sandstone.
7) Green very fine sandstone.
8) White siltstone.
9) Red medium sandstone.
10) Grey sandstone.
11) Jasper.
12) Rhyolite

4.4 Overview

The Heimdall Erosion Surface is observed throughout the field area. In the Olympus Range and at Sponsors Peak the HES truncates the top of the Cross-bedded Sandstone Lithofacies. At Lake Vashka the HES truncates the Pinstripe Cross-bedded Lithofacies and appears to converge with the underlying Kukri Erosion Surface. At Balham Lake, the Heimdall Erosion Surface converges with the Kukri Erosion Surface and cuts into basement; the underlying New Mountain Sandstone is not present. The HES was not observed at Vashka Crag. Typically, the relief on the erosion surface is 10 to 50 cm and the surface cuts down the foresets of the underlying lithofacies of the New Mountain Sandstone creating a jagged pattern.

The Conglomerate Lithofacies is observed at all locations in association with the Heimdall Erosion Surface. There is a large lateral variation in the composition of the lithofacies. Thickness ranges from 2 to 60 cm.

4.5 Facies Distribution and Relationships in Observed Sections

4.5.1 Mt Jason

At Mt Jason, the erosion surface has a relief of 50 cm and has a pronounced jagged saw tooth pattern (Fig 4-1). The foresets of the underlying New Mountain Sandstone have

retained their integrity indicating they were fully lithified before erosion took place. The saw tooth pattern is most pronounced on the west face of Mt Jason. On the eastern face of Mt Jason the pattern is less pronounced and the scale of erosion varies from nearly flat to 50 cm (Fig 4-2A, B). The surface is visible due to the colour change between the New Mountain Sandstone and overlying Odin Arkose Member and truncation of the cross beds.

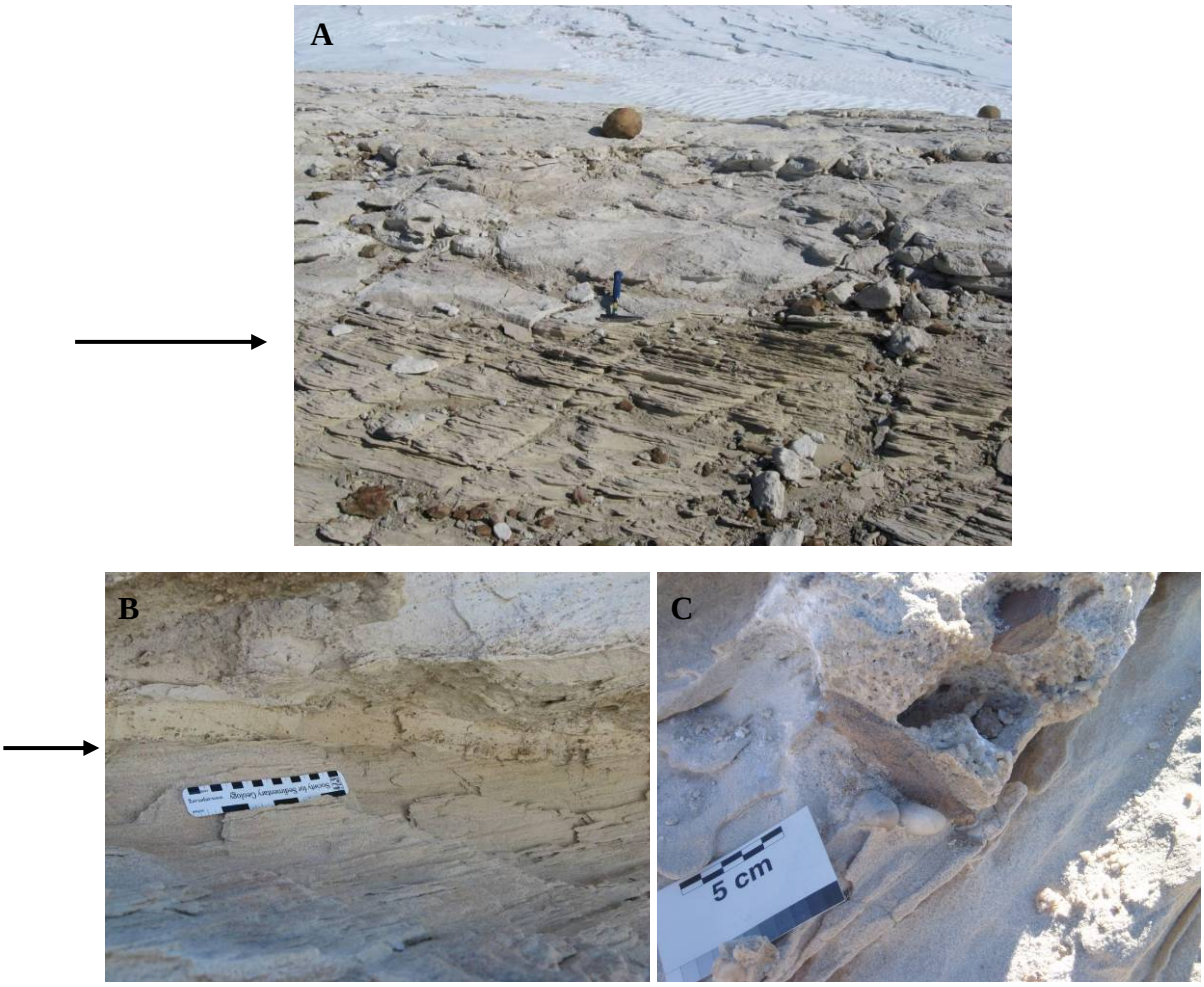

Figure 4-2: Exposure of the Heimdall Erosion Surface (shown by arrow), east face of Mt Jason. **A)** HES shown by change in sediment colour and depositional type. **B)** Small-scale erosion of Cross-bedded Sandstone Lithofacies. **C)** Pocket in HES filled by Conglomerate Lithofacies pebbles, east face of Mt Jason. Photo by: Margaret Bradshaw

At Mt Jason, the Conglomerate Lithofacies sits directly on the Heimdall Erosion Surface. The conglomerate varies from 10 to 60 cm thick, controlled by the slope of the underlying surface and the size of the pebbles (larger pebbles = thicker conglomerate). On the eastern face, it fills depressions or pits in the erosion surface and is both clast and matrix supported. The pits in the erosion surface are jagged and not rounded (Fig 4-2C). The east face of Mt Jason is the only locality where red sandstone (coarse pebble) clasts are found.

Table 4-1 shows pebble types and sizes found at Mt Jason. On the western face of Mt Jason, approximately 1 km away, the sediment overlying the HES is mainly matrix material (poorly sorted, fine sand to granule quartz and feldspar) with few pebbles.

Table 4-1: Pebbles within the Conglomerate Lithofacies, east face of Mt Jason

Type	Size	Roundness
Smoky and milky quartz	Granule to very coarse pebble	Sub rounded
Plagioclase feldspar		
White siltstone		
Dark grey sandstone	Medium to very coarse pebble	Sub rounded
Dark and light grey quartzite	Granule to very coarse pebble	Sub rounded to rounded
Pink sandstone	Medium pebble to cobble	Sub angular to sub rounded
Light grey-pink sandstone	Coarse to very coarse pebble	Sub rounded
Grey sandstone	20 to 30 cm across, 3 to 9 cm thick	Sub angular
Green very fine sandstone	medium to coarse pebble	
Red sandstone	coarse pebbles	

4.5.2 Mt Hercules

The erosion surface at Mt Hercules has a relief of about 10 cm. Erosion appears nearly parallel to the underlying cross beds of the New Mountain Sandstone because the beds are at a low angle (unknown what part of the cross bed set is in view). The erosion surface and the underlying New Mountain Sandstone are burrowed by *Skolithos. Skolithos* burrows, containing quartz pebbles, extend 15 cm downward from Heimdall Erosion Surface into the underlying New Mountain Sandstone Formation (Fig 4-3), indicating that the bioturbation took place post-erosion and that the New Mountain Sandstone was not fully lithified at this site.

Overlying the HES is 25 cm of fine to coarse sandstone (similar to matrix material) between the erosion surface and the base of Conglomerate Lithofacies, which is 3 to 8 cm thick (Fig 4-3).

Figure 4-3: Skolithos burrows extending down into the New Mountain Sandstone (black arrow) and Conglomerate Lithofacies pebbles (red arrow), Mt Hercules.

The Conglomerate Lithofacies contains: 1) pink sandstone (granule to cobble, sub-rounded) clasts that are slabby in character and lie either flat or dipping to south and southwest. 2) Milky, pink stained and smokey quartz (coarse pebble, sub-angular to rounded). 3) 20-25% feldspar (fine sand to fine pebble, sub-rounded). 4) White and light grey quartzite (granule to very coarse pebble, sub-rounded).

Several hundred metres north of the measured section grey sandstone boulders (10 to 30 cm across) are found directly on the erosion surface. The boulders form a type of pavement and appear to have been broken *in situ* (Fig 4-4). Grey sandstone boulders are observed elsewhere on the Heimdall Erosion Surface at Mt Hercules, however there are usually only 1 to 3 boulders in any one place and do not form pavements.

Figure 4-4: Grey sandstone cobbles forming an *in situ* pavement, Mt Hercules.

4.5.3 Mt Aeolus

At Mt Aeolus, the Heimdall Erosion Surface cuts into the New Mountain Sandstone and has a relief of 30 cm, which is less pronounced and smoother than at other localities. This could be due to the cross beds being low angle and the foresets thinner (1 cm) directly below the erosion surface (Fig 4-5).

Figure 4-5: Heimdall Erosion Surface (head of hammer placed on the surface), Mt Aeolus.

At Mt Aeolus, the Conglomerate Lithofacies varies between 5 and 20 cm thick across an 80 m length of outcrop. Locally, typical Conglomerate Lithofacies is deposited directly in the erosion surface at the section line. Laterally however, either well-sorted medium to coarse

sandstone or poorly sorted medium sand to granule sandstone with fine to coarse quartz pebbles, typical of matrix material, is found on the surface. There is no pattern to the lateral variation in deposition of the conglomerate lithofacies.

Pebbles found in the Conglomerate Lithofacies (Fig 4-6) are listed below. Fig 4-7 shows that quartz and grey sandstone are the most common pebbles in the Conglomerate Lithofacies at Mt Aeolus.

- Pink sandstone. Largest piece 13 cm across and 1 cm thick
- Grey sandstone. Medium pebble to cobble.
- Milky, smoky and pink stained quartz. Sub-angular to very well rounded. Granule to coarse pebble.
- White siltstone. Medium pebble.
- Dark grey coarse sandstone.
- Light grey quartzite.

Figure 4-6: Conglomerate Lithofacies at Mt Aeolus (plan view).

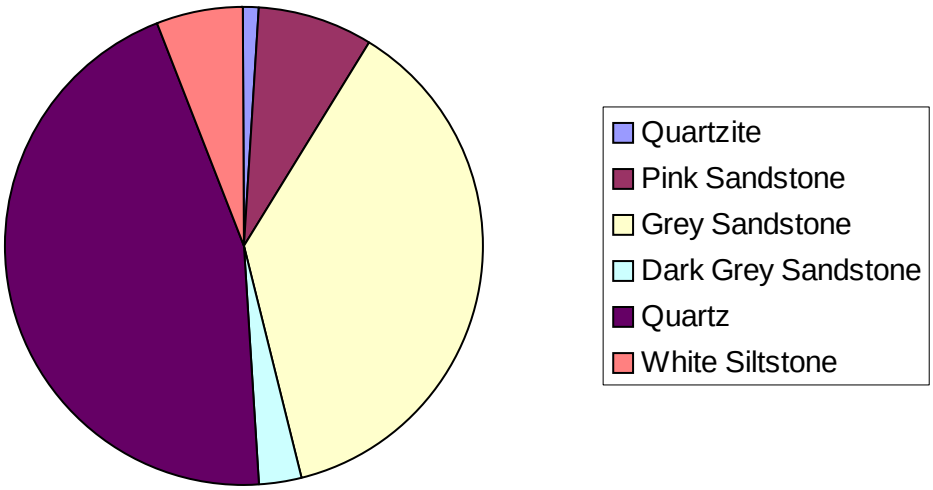

Figure 4-7: Pebble count from Conglomerate Lithofacies at Mt Aeolus

4.5.4 Mt Boreas

Exposure of the Heimdall Erosion Surface north of Mt Boreas (Fig 1-4) is restricted and forms a bench; the relief on the surface is approximately 50 cm. This morphology is repeated to the southeast of Mt Boreas (Fig 1-4, Appendix A1/4). The surface erodes along the foresets of the underlying New Mountain Sandstone but is not very jagged.

Exposure at Mt Boreas was poor due to extensive snow cover. The Conglomerate Lithofacies outcrops on the southern flanks of Mt Boreas and in a shallow valley between Mt Boreas and Mt Aeolus (Fig 1-4). Both the outcrops contain typical Conglomerate Lithofacies, which is up to 20 cm thick. However, similar to Mt Aeolus and Mt Jason, a medium sand to granule unit is deposited on the surface in where the Conglomerate Lithofacies is absent. Pink sandstone slabs are prominent and range in size from granule to cobble but are mostly coarse pebble. Biscuit shaped pebbles of pink sandstone in the Conglomerate Lithofacies to the southeast of Mt Boreas do not lie flat along the surface as in other field areas but at random orientations within the conglomerate (Fig 4-8). The conglomerate also contains quartzite (dark and light grey, granule to very coarse pebble), plagioclase feldspar (very coarse sand to medium pebble) and milky and smoky quartz (coarse sand to granule).

Figure 4-8: Randomly orientated pink sandstone clasts in the Conglomerate Lithofacies southeast of Mt Boreas.

4.5.5 Mt Electra

The Heimdall Erosion Surface appears to dip on a local scale from below Mt Dido west to the Wright Upper Glacier. Below Mt Dido (Fig 1-5) the pattern of outcrop made it difficult to see the relief on the HES. The Conglomerate Lithofacies is 2 to 3 cm thick (Fig 4-9A) and sits directly on the Heimdall Erosion Surface. The lithofacies contains clasts of mainly quartz, quartzite (granule to medium pebble) and rare jasper (medium pebble), which is not found at any other locality.

At the base of the measured section (Appendix A1/5a) the Heimdall Erosion Surface is not exposed. However, the Cross-bedded Sandstone Lithofacies of the New Mountain Sandstone and the overlying Odin Arkose Member were observed within 0.5 m of each other. Pebbles were dug from where the surface was expected to be found and are predominantly composed of quartz and quartzite pebbles ranging from granule to very coarse pebble.

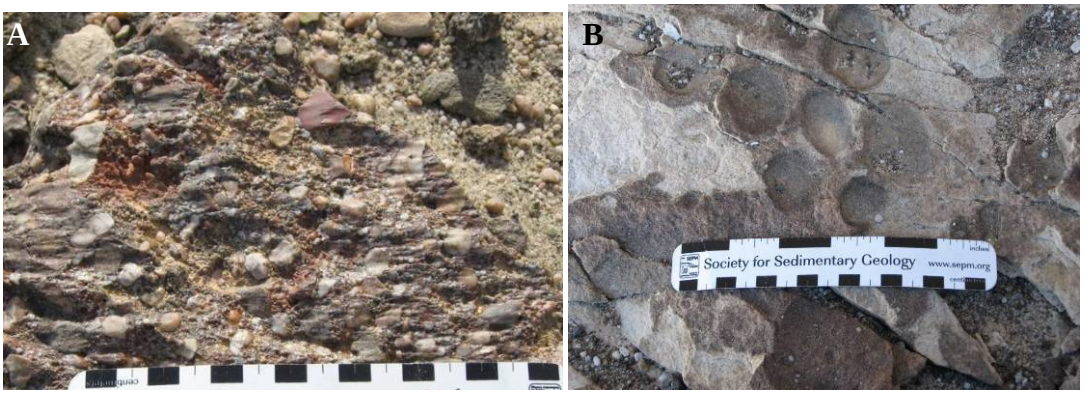

Figure 4-9: A) Conglomerate Lithofacies, east of Mt Electra. **B)** Cavities left by sandstone pebbles on the Heimdall Erosion Surface, west of Mt Electra.

Deposition to the west of Mt Electra, above the Wright Upper Glacier (Fig 1-5), is different again. The relief on the HES is 20 cm and the surface is smoother. This is due to erosion not being concentrated along the individual foresets, which commonly leads to a jagged pattern. Directly on the Heimdall Erosion Surface are rounded cavities (1 to 4 cm across) where green sandstone pebbles have weathered out (Fig 4-9B). Overlying the pebble cavity layer is 20 cm of fine sand to granule sandstone and 50 cm of very poorly sorted fine sand to medium pebble sandstone (Appendix A1/5b), topped by thin green mud with vertical burrows. There are two more pebble layers at this locality; the first is 3 to 4 cm thick and directly overlies the green mud (Fig 4-10A). The first conglomerate layer contains typical Conglomerate Lithofacies and is a poorly sorted, sub-rounded, granule to coarse pebble matrix supported conglomerate. The second conglomerate layer is thicker and occurs 1.4 m above the erosion surface and 0.7 m above the first conglomerate layer. The layer is typical Conglomerate Lithofacies, containing quartz, pink sandstone, grey sandstone and quartzite (Fig 4-10B). Within the second conglomerate layer the pink sandstone pebbles are long and thin, up to 22 cm across and 5 to 8 mm thick; this suggests that the sandstone clasts have not been transported a long distance. Quartz and quartzite pebbles are sub-angular to sub-rounded and granule to cobble size. This conglomerate layer varies greatly in composition, height (varies within 30 cm) and thickness laterally.

Figure 4-10: A) Green mudstone and overlying first conglomerate layer and **B)** second conglomerate layer (Chapter 5), west of Mt Electra.

8 to 10 m east of this outcrop the Heimdall Erosion Surface is barely discernible and is only seen due to truncation of the New Mountain Sandstone foresets and a change in colour (Fig 4-11). Overlying the Heimdall Erosion Surface is a structureless medium to coarse

sandstone with granules. Conglomerate Lithofacies containing pink sandstone, quartz and quartzite, occurs at 1.4 m above the HES.

Figure 4-11: Heimdall Erosion Surface shown by colour change and cutting of the cross beds (at arrow), west of Mt Electra.

As shown by the outcrops at Mt Electra the Conglomerate Lithofacies varies regionally and locally. In the east (below Mt Dido), the lithofacies is deposited directly in the Heimdall Erosion Surface. Below camp (measured section), the lithofacies is also deposited directly in the HES. However, in the west (near the Wright Upper Glacier), the conglomerate is not deposited directly on the HES, there are two pebble layers and 10 m laterally there is no conglomerate deposited on the surface.

4.5.6 Balham Lake

In the Balham Valley the New Mountain Sandstone is absent and the Heimdall Erosion Surface cuts directly into the Koettlitz Group. The actual surface does not crop out due to scree cover, however sedimentary rocks of the Odin Arkose Member are observed 1 to 2 m above basement. Due to this there is no idea of the geometry of the erosion surface but it joins the Kukri Erosion Surface and may show similar relief. Possible Conglomerate Lithofacies was observed in patches and is composed angular granule to pebble milky quartz and sandstone clasts in a very fine sand matrix. The matrix and sandstone clasts are very altered due to proximity to dolerite intrusives.

4.5.7 Lake Vashka

The Heimdall Erosion Surface is observed on the middle and eastern crags at Lake Vashka (Chapter 1.5.5). The HES truncates the Pinstripe Cross-bedded Lithofacies of the New Mountain Sandstone and shows erosion down the foresets as seen in other localities (Fig 4-12A). The relief is hard to determine due to the restricted nature of the outcrops but could be up to 10 cm.

At the most easterly crag the Heimdall Erosion Surface cuts into the PCL but is separated from the sandstone by a thin intrusion (Appendix A1/6c). The HES appears to converge with the basal Kukri Erosion Surface. Due to the large amount of relief on the Kukri Erosion Surface (Chapter 2.3.1) and the relative flatness of the Heimdall Erosion Surface it can be inferred that the two eventually converge, though this was not observed, as the surfaces were lost under scree cover.

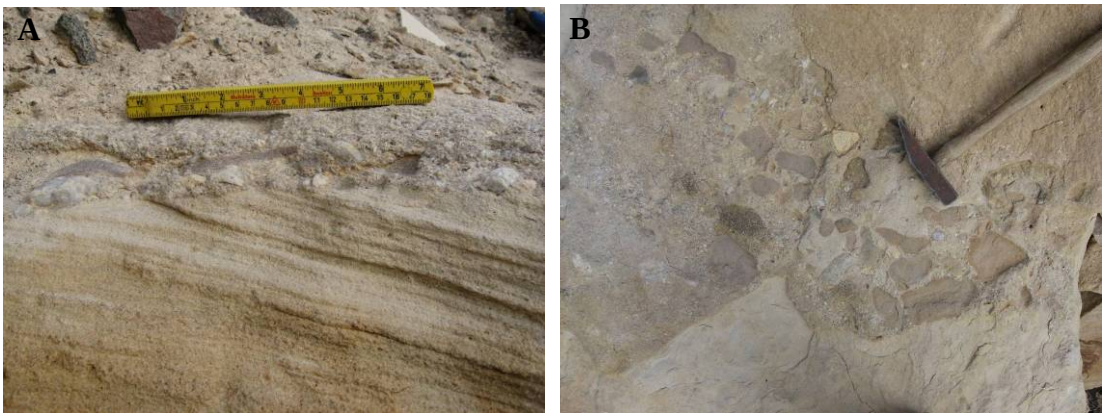

Figure 4-12: A) Heimdall Erosion Surface cutting Pinstripe Cross-bedded Lithofacies and **B)** Conglomerate Lithofacies, middle crag Lake Vashka

There is limited exposure of the Conglomerate Lithofacies at Lake Vashka (Fig 4-12A, B), confined to the middle and eastern crags on the southern side of the Barwick Valley (Appendix A1/6b, 6c). The conglomerate is 5 to 10 cm thick and is deposited directly on the HES. Pink sandstone clasts are once again thin and slabby (8 to 20 cm across and up to 3 cm thick). A clast count (Figure 4-13) shows that pink sandstone is the most prominent clast followed by quartz. Other clasts included quartzite, feldspar, white siltstone, rhyolite and granitoid.

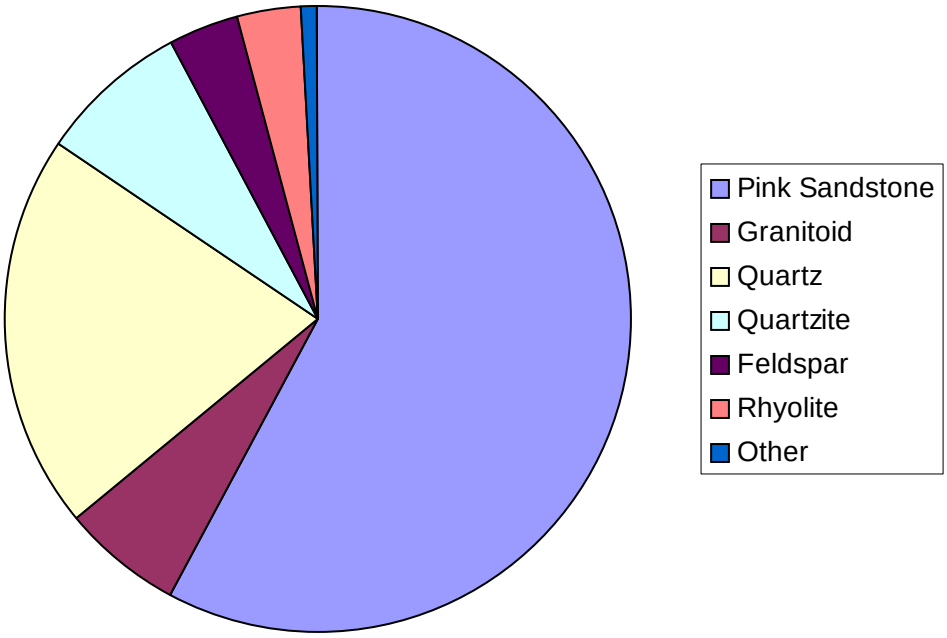

Figure 4-13: Pebble count from Conglomerate Lithofacies, middle crag at Lake Vashka. Source: Dr Margaret Bradshaw.

4.5.8 Sponsors Peak

At Sponsors Peak, the Heimdall Erosion Surface forms the col between Nickel and Sponsors Peaks (Fig 1-10) and truncates the Cross-bedded Sandstone Lithofacies. The HES had a shallow dip (4º) to the southwest. There was not sufficient enough exposure to determine the relief on the surface.

Small patches of Conglomerate Lithofacies were found on the col. The conglomerate is up to 5 cm thick and the pebbles are very spread out across the surface (Fig 4-14) but not infilling pits. The conglomerate is composed of pink sandstone (up to 10 cm across, sub-angular to sub-rounded), white and smoky quartz (sub-rounded to rounded, granule to coarse pebble); light and dark grey quartzite (sub-rounded, fine to coarse pebble) and white siltstone (fine to medium pebble, sub-angular to sub-rounded). Two pebble counts show that pink sandstone and quartz are the most predominant lithologies in the conglomerate (Figure 4-15).

Figure 4-14: Conglomerate Lithofacies at Sponsors Peak.

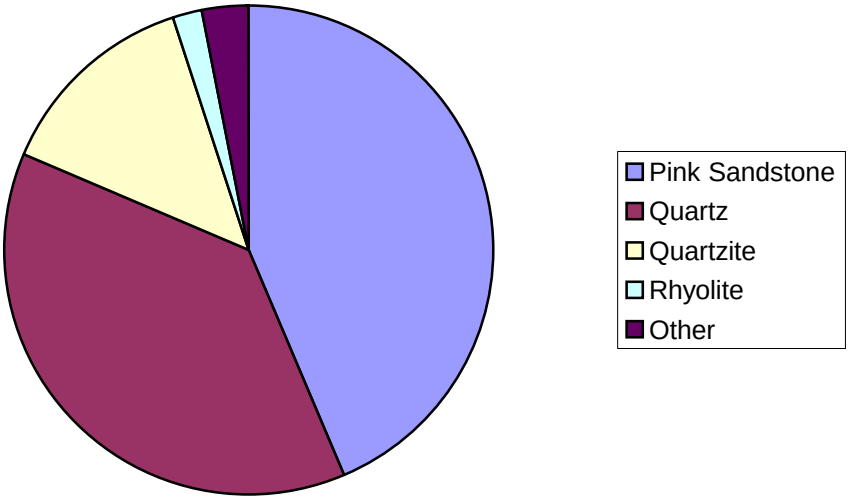

Figure 4-15: Pebble counts from Conglomerate Lithofacies, Sponsor Peak. Source: Greer Gilmer and Margaret Bradshaw

The Heimdall Erosion Surface was also observed to the southwest of Sponsors Peak camp cutting the New Mountain Sandstone, on an outcrop mapped by Isaac *et al* (1995) as Arena Sandstone. The relief on the erosion surface was not observed due to small outcrop size. The Conglomerate Lithofacies is composed of pink sandstone (up to 13 cm by 10 cm)

(Fig 4-16A), quartz and quartzite (fine to very coarse pebble). Green very fine sandstone clasts are also observed and are 5.5 by 11 cm (Fig 4-16B). The lithofacies is up to 10 cm thick.

Figure 4-16: A) Pink sandstone and **B)** Green very fine sandstone in Conglomerate Lithofacies southwest of Sponsors Peak camp.

4.6 Composition

Sandstone pebbles within the Conglomerate Lithofacies from Mt Jason, Mt Electra and Mt Boreas were analysed to determine if there were similarities in composition across the field area within same coloured pebble types or if any pebbles were similar in composition to the underlying New Mountain Sandstone. Conglomerate Lithofacies matrix was not analysed extensively. Point count data can be found in Appendix B1.

4.6.1 Conglomerate Lithofacies

Listed below are compositions of pebbles and found in the Conglomerate Lithofacies.

1. Milky, smoky, clear and pink stained quartz. Sub-rounded to well-rounded
2. Plagioclase and alkali feldspar. Granule to medium pebble. Angular to sub rounded.
3. Quartzite
    a. Dark Grey Quartzite. Medium sand, well sorted dark grains with lighter cement.
    b. Light Grey Quartzite. Medium to very coarse sand. Well sorted.
    c. White Quartzite. Fine sand.
4. Pink slabby or biscuit-like sandstone. Very well sorted, rounded, medium to fine sandstone. The sandstone is generally pink in colour but can also be light tan or brown, the pink colour is often restricted to outer rind of the clast. The samples from

Mt Aeolus and Mt Boreas are quartzarenite (Fig 4-17). Sample V43A from Lake Vashka is subarkose.

5. Light grey-pink poorly sorted sandstone. Poorly sorted, very coarse to medium sandstone composed of sub angular to sub rounded smoky, milky and clear quartz. Pinkish stained material (possible cement) filling in gaps between grains.

6. Dark grey coarse sandstone. Poorly sorted, fine to coarse sand but mainly medium sandstone composed of sub-angular to sub-rounded, clear and smoky quartz and angular white flecks. Rare rounded, very coarse sand quartz grains. The colour can vary between dark and light grey but the composition remains the same.

7. Green very fine sandstone with rare medium and fine quartz sand.

8. White siltstone with medium quartz sand grains.

9. Red medium sandstone. Moderately sorted, medium to coarse quartz sandstone. Possible red coloured cement. Grains are sub-rounded to rounded. Samples from Mt Jason show that the red sandstone is a subarkose (Fig 4-17).

10. Grey sandstone. Very well sorted fine sandstone. The sample from Mt Jason is a subarkose (Fig 4-17).

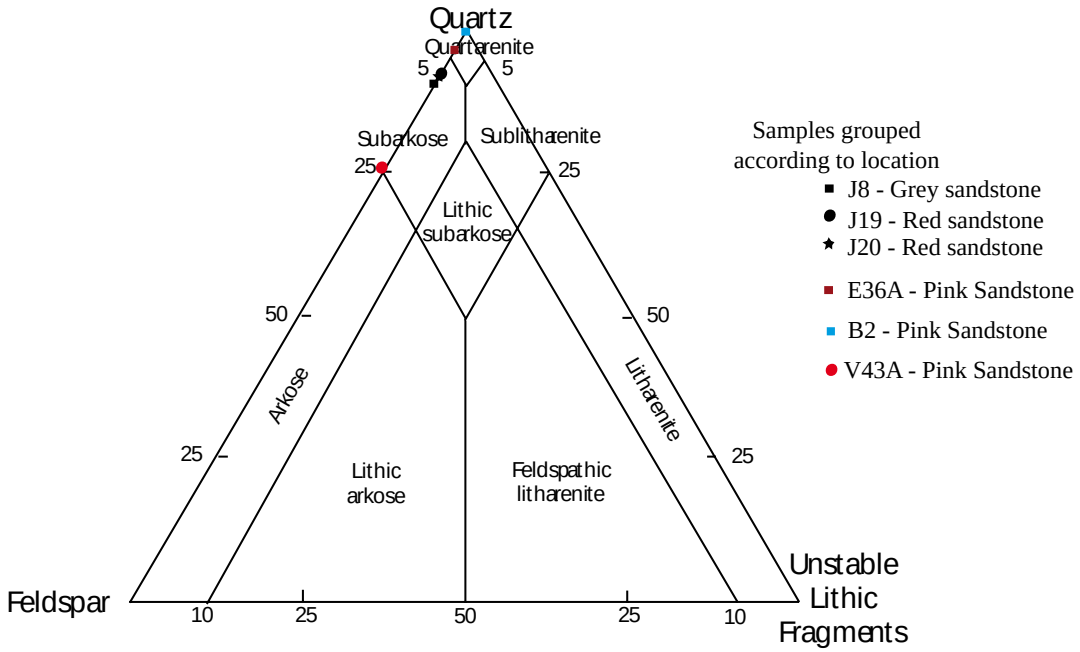

Figure 4-17: QFL plot of Conglomerate Lithofacies pebbles. Adapted from Blatt and Tracey (1996)

Pink sandstone from Mt Electra and Mt Boreas is similar to the composition of the underlying Cross-bedded Sandstone Lithofacies in the New Mountain Sandstone. However, sample V43A is a subarkose. This could show that this is different sandstone or, more likely that the pink sandstone covers a wide range of compositions. Figures 5-18A and B show that although the composition of the pink sandstone is similar to the Cross-bedded Sandstone

Lithofacies, the texture of the clasts is different. The thin sections of the pebbles show that the pink sandstone is composed of rounded and irregularly shaped quartz sand. The quartz is always monocrystalline and a fine matrix separates the grains. No overgrowths or pressure solution boundaries are evident. Sample V43A shows that the feldspar is altered and grey (Fig 5-19A). It also shows fragmented quartz grains with some rounding (Fig 5-19A, B).

The red sandstone clasts (Fig 5-20A, 5-21A, B) are similar to the pink sandstone except both the samples contain feldspar and the amount of fine matrix material seems to be greater. Polycrystalline quartz is also present in the sandstone as seen in Fig 5-21B. The matrix is too fine to determine what the cause of the red colour is.

Grey sandstone clast is composed of quartz and feldspar (Fig 5-20B). The feldspar is grey, compared to the quartz grains, due to alteration. The sand grains float in cement, which indicates there was a matrix that has been recrystallised.

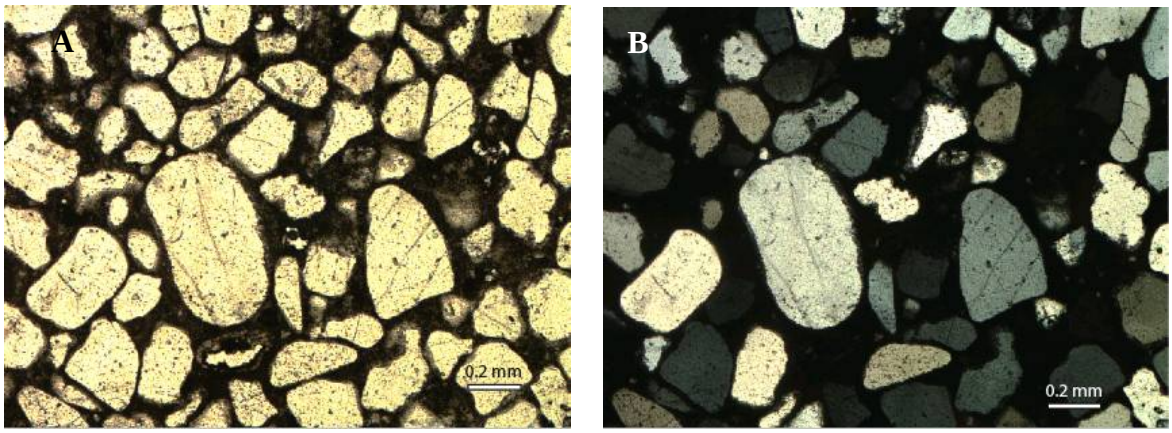

Figure 4-18: Pink sandstone (B2) from Conglomerate Lithofacies, Mt Boreas. **A)** Plain polarised light and **B)** cross-polarised light.

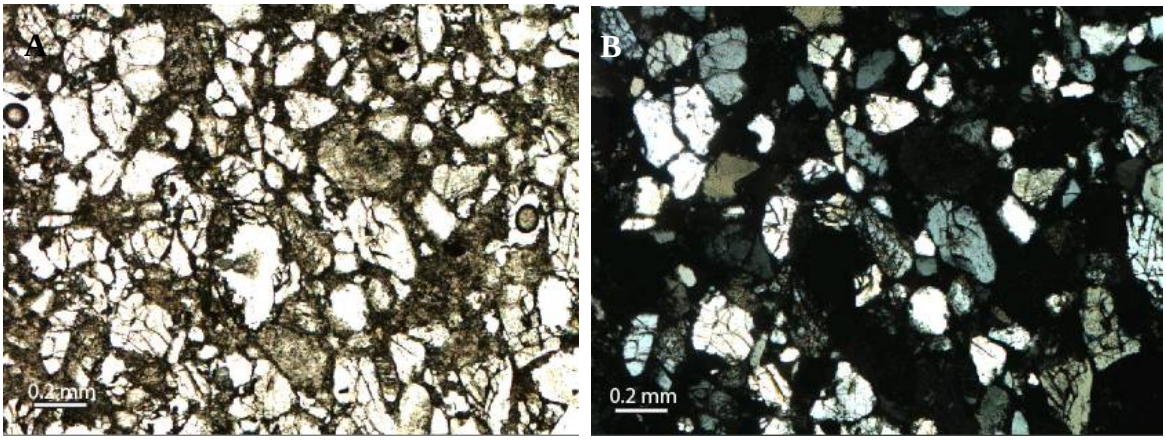

Figure 4-19: Pink sandstone (V34A) from Conglomerate Lithofacies. Lake Vashka. **A)** Plain polarised light and **B)** cross-polarised light.

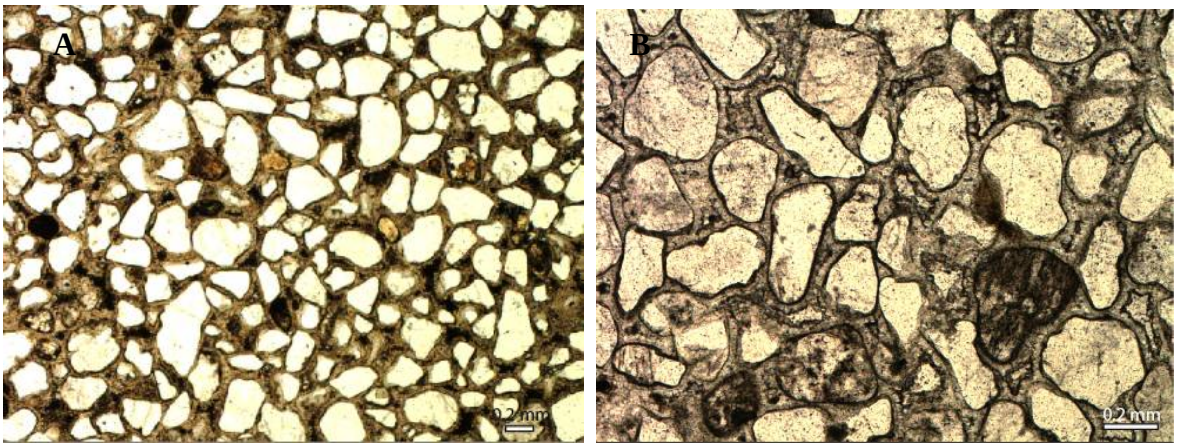

Figure 4-20:A) Red sandstone (J19) from the Conglomerate Lithofacies, Mt Jason. **B)** Grey Sandstone (J8) from Conglomerate Lithofacies, Mt Jason.

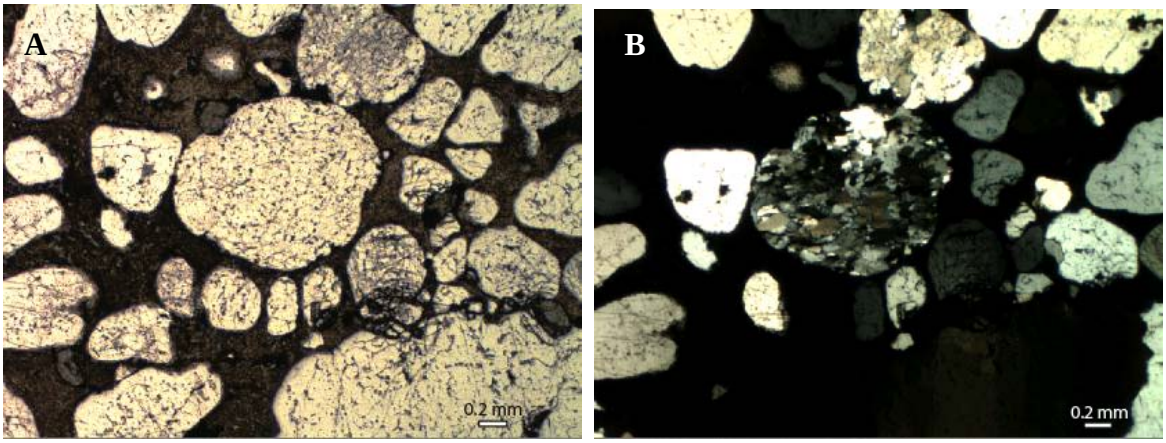

Figure 4-21: Red sandstone (J20) from Conglomerate Lithofacies, Mt Jason. **A)** Plain polarised light. **B)** Cross-polarised light.

The composition of the sandstone clasts show that they are from unknown sources and none are derived from the directly underlying New Mountain Sandstone. The pink sandstone clasts are similar in composition to the Cross-bedded Sandstone Lithofacies and it was briefly thought that the CSL could be the source for the pink sandstone. However, comparison of the thin sections of the CSL and pink sandstone shows that the two have different cement textures. Red and grey sandstone clasts are similar in composition to each other and also look similar in thin section but are different from the pink sandstone. Other sandstone clasts vary in grainsize from others but where not examined in thin section so compositional variations are unknown.

The matrix of the Conglomerate Lithofacies was not extensively sampled for point count analysis. The matrix material contains both quartz and feldspar (though this did not show up in the point counts). There is only one sample from Mt Jason and it shows the matrix

to be a quartzarenite (Fig 5-12). The quartz is mono and polycrystalline (Fig 4-22C). The Mt Jason sample shows that the contacts between the grains are very close and some are stylolitic (Fig 4-22B, C). Sample J7 also contains polycrystalline quartz and altered feldspar (Fig 4-22). It is unusual that the matrix of the Conglomerate Lithofacies is a quartzarenite when the overlying Odin Arkose Member is an arkose to subarkose (see Chapter 6.4.1). This could be due to the small sample that is seen in a thin section in comparison to the lithofacies in general. In addition, the feldspars are often large and the thin section may have fallen between two pebbles and therefore appeared not to contain any feldspar.

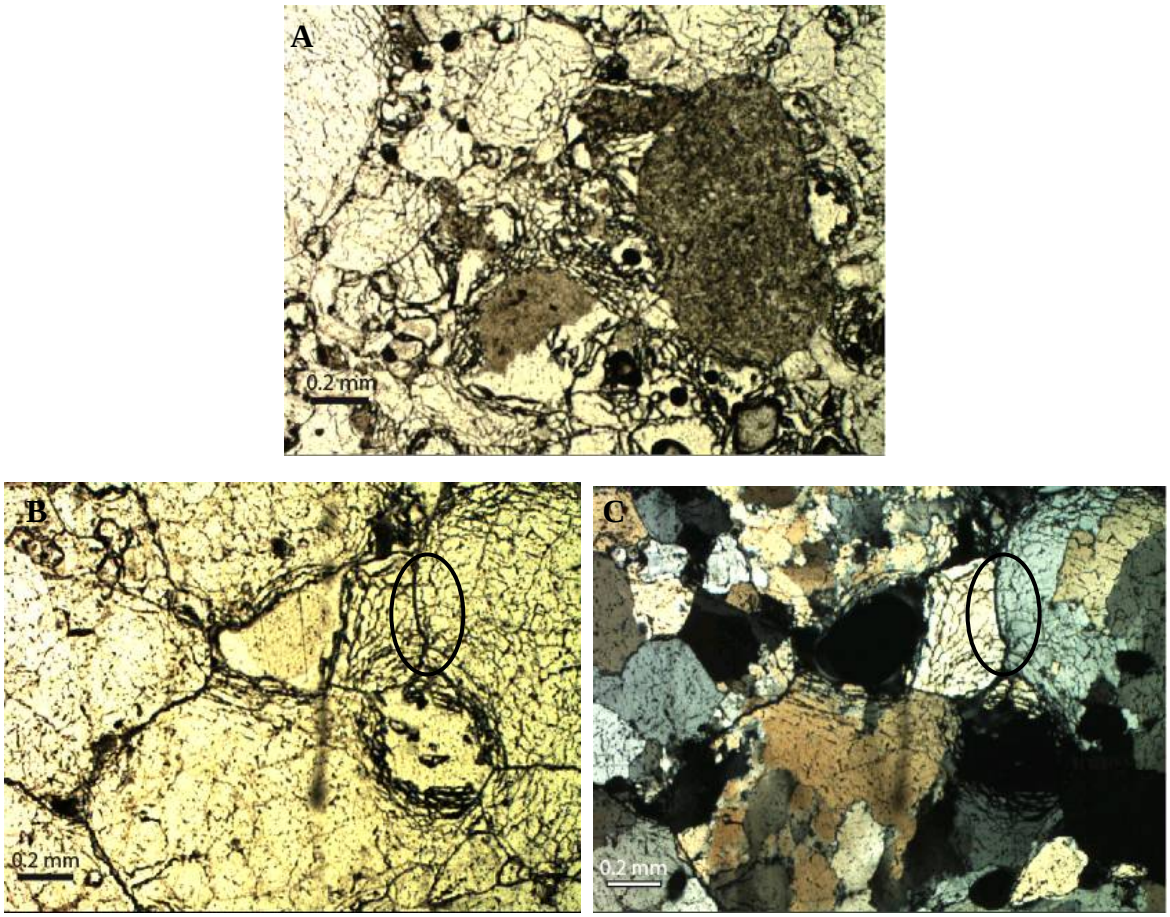

Figure 4-22: Conglomerate Lithofacies matrix, Mt Jason. **A)** Altered feldspar. Plain polarised light. Stylolitic contacts (circled) and polycrystalline quartz. **B)** Plain polarised light and **C)** cross-polarised light.

4.7 Interpretation

The amount of relief on the Heimdall Erosion Surface (zero to 50 cm) varies throughout the field area, as does the morphology of the surface. The morphology depends on the degree of lithification of the underlying New Mountain Sandstone. From the pronounced

jagged pattern observed on the western flank of Mt Jason, to more minor erosion down the foresets (observed at Mt Aeolus, Mt Electra east and Sponsors Peak) or a smooth surface with negligible selective erosion of the underlying foresets of the New Mountain Sandstone (Mt Electra west). At Mt Hercules *Skolithos* burrows pass through the underlying CSL indicating that the sandstone was not lithified. At Lake Vashka the HES truncates the Pinstripe Cross-bedded Lithofacies of the New Mountain Sandstone and converges with the Kukri Erosion Surface at the eastern end of the outcrop. The underlying Pinstripe Cross-bedded Lithofacies was lithified prior to erosion as the HES has cut down into the cross-bed foresets. At Balham Lake the HES cuts down into Koettlitz Group and the New Mountain Sandstone is absent.

The morphology of the erosion surface suggests that the New Mountain Sandstone was partially or totally lithified prior to erosion throughout most of the field area. It would need to be well lithified to produce the jagged form, as individual foresets were pried off as coherent pieces. The jagged pattern is analogous to that seen on the shore platform a Waipouri's Mark, Wairarapa. New Zealand (Field, 2005). The pockets observed at Mt Jason are jagged showing that the underlying sandstone was lithified and pebbles were deposited in already formed pits. This raises the question as to when and how the New Mountain Sandstone was lithified. It could have been immediately post deposition on the sea floor, by deep burial after deposition, by cement just prior to erosion or during sub-aerial exposure. This is important in estimating the amount of time between deposition and subsequent erosion of the New Mountain Sandstone. If cementation was from burial it would mean a large break between deposition and erosion but if it was due to cementation processes immediately post deposition or during exposure then the break could have been shorter.

A particular feature of the HES is the lack of highly weathered material underlying it. This could indicate erosion occurred in a high-energy environment and that all the weathered material has been removed. Alternatively, clearing of the surface could have been a secondary process long after erosion and just prior to deposition of the Odin Arkose Member. Burrowing by *Skolithos sp.* on the surface at Mt Hercules shows that the erosion surface was underwater and in a high-energy environment especially at that locality (see Chapter 4.5.2 and 6.5). It is possible that in later stages the HES was similar to a modern day shore platform prior to deposition of the Conglomerate Lithofacies and was exposed to fluvial currents, wave action and marine currents. The saw tooth pattern is due to water flowing preferentially along the partially or totally lithified foreset beds of the Cross-bedded Sandstone and Pinstripe Cross-bedded Lithofacies of the New Mountain Sandstone leading to erosion of the foreset

beds. In other areas the underlying New Mountain Sandstone was not well lithified and this led to a smooth surface and local burrowing.

Initially, the Heimdall Erosion Surface was formed due to marine regression across the field area, caused by fall in relative sea level (to the south) either eustatic or tectonic uplift in the north. This led to exposure and erosion of the underlying sandstones and basement rocks. After an unknown amount of time relative sea level rose and the sea transgressed across the field area and the HES became a shore platform that was exposed to wave and current action. This caused further erosion of the surface, and probably created the saw tooth pattern, and removal of weathered material. The jagged pattern was most likely formed at this time because the pronounced jaggedness would not have survived very long and deposition of the Conglomerate Lithofacies across the surface meant it was preserved. At places where the erosion surface was not lithified a smoother pattern of erosion resulted.

The Heimdall Erosion Surface is observed from the Olympus Range to Sponsors Peak in the north but Plume (1978) and McKelvey *et al* (1977) suggest that the erosion surface dies out to the south with continuous sedimentation between the New Mountain Sandstone and overlying Altar Mountain Formation. This indicates that exposure of the HES extended from the Olympus Range and north but sedimentation continued in a sedimentary basin centred on the Asgard Range or further south (Fig 2-2). The large-scale concordant nature of the erosion surface suggests that exposure occurred over a wide area at approximately the same time. The appearance of erosion at different levels within the New Mountain Sandstone could be due to differences in the thickness of the Windy Gully Sandstone, Terra Cotta Siltstone and New Mountain Sandstone at each site, and basement highs on the Kukri Erosion Surface across the field area. Therefore, when the formations were eroded it led to the illusion of erosion at different levels.

The Conglomerate Lithofacies was deposited on the Heimdall Erosion Surface by currents flowing over the shore platform. Deposition of the Conglomerate Lithofacies on to the Heimdall Erosion Surface varies across the field area. For example, at Mt Electra west a mud layer occurs beneath the conglomerate, which could indicate low-energy, waning flow or an estuarine/tidal environment. Whereas at most other field sites (Mt Jason, Mt Electra east and middle, Mt Aeolus, Mt Boreas, Lake Vashka and Sponsors Peak) the conglomerate is deposited directly on the surface. If the Heimdall Erosion Surface was a shore platform during deposition of the Conglomerate Lithofacies, this variation in lithofacies is consistent

with modern shore platforms that can be very variable within a small area. Different processes would operate on different parts of the shore platform as the shoreline moved across the platform over time. The Conglomerate Lithofacies was probably deposited as the sea transgressed the Heimdall Erosion Surface.

The sandstone clasts found in the Conglomerate Lithofacies may have been sourced from sandstones formed on the shore platform (Heimdall Erosion Surface) and were transported across the platform by currents or are from exotic sources outside the field area and were transported by longshore currents into the field area. Alternatively, the sandstone clasts could also have been sourced from older formations in the Taylor Group (Terra Cotta Siltstone and Windy Gully Sandstone). With no thin sections of the Terra Cotta or Windy Gully it is difficult to determine how similar in composition the clasts are. The Windy Gully Sandstone is a medium to coarse sandstone (Chapter 2.4.2) and could have been the source for any of the sandstone pebbles. The Terra Cotta Siltstone could also be a source because it contains sandstone layers (Chapter 2.4.3). The New Mountain Sandstone in the field area is not considered a source due to differences in cement texture when compared to the sandstone clasts. There are no other sandstones underlying the Heimdall Erosion Surface within the Olympus Range or Bull Pass-St Johns Range areas that could be a source for the sandstone pebbles. It is likely that the some of the sandstone pebbles were not transported very far due to their size, especially the pink sandstone, which is commonly very thin and large and so could not have travelled far or would be broken up more. It is possible the pink sandstones represent thin local sandstone deposits on the Heimdall Erosion Surface that were eroded and broken during marine transgression. The grey sandstone clasts at Mt Hercules also appear to not have been transported far because they form a pavement and appear to have broken *in situ*. The quartz, feldspar and quartzite pebbles are sourced from the Granite Harbour Intrusives and Koettlitz Group. The Conglomerate Lithofacies matrix was deposited by the same processes and at the same time as the pebbles.

4.8 Summary

- The Heimdall Erosion Surface is observed throughout field area and has a relief of zero to 50 cm.

- The Heimdall Erosion Surface was formed from marine regression and exposure, followed by marine transgression. It is interpreted as a shore platform during deposition of the Conglomerate Lithofacies.

- The Conglomerate Lithofacies is deposited directly on or close to the HES. It is composed of sandstone pebbles sourced from exotic or distal underlying Taylor Group sources and feldspar, quartz and quartzite sourced from the underlying basement rocks.

- Marine processes deposited the Conglomerate Lithofacies as the sea progressively flooded the shore platform (HES) as a result of relative sea level rise.

Chapter Five: Altar Mountain Formation and Odin Arkose Member

5.1 Introduction

The Altar Mountain Formation overlies the Heimdall Erosion Surface (Fig 2-1) throughout the field area. The Odin Arkose Member of the Altar Mountain Formation makes up the lower part of the formation and is deposited directly on the Heimdall Erosion Surface as a conglomerate fining up to arkosic sandstone. The Odin Arkose Member was observed at most field sites but the Altar Mountain Formation was only observed at five field locations, though it is known to exist across the entire field area.

5.2 Lithofacies

The Altar Mountain Formation and Odin Arkose Member are divided into different lithofacies based on composition, grainsize and sedimentary structures. The Odin Arkose Member is divided into two lithofacies, one of which is covered in Chapter 4 and the remaining Altar Mountain Formation is divided into two lithofacies. Overall, the sequence fines upwards from the coarser feldspathic Odin Arkose Member to the finer more quartzose Altar Mountain Formation.

5.2.1 Conglomerate Lithofacies (CL)

Briefly, the Conglomerate Lithofacies is composed of sandstone, quartz, feldspar and quartzite clasts in a poorly sorted, fine sands to granule quartzose and feldspathic matrix. The lithofacies is very variable across the field area. This lithofacies is described in detail in Chapter 4. The lithofacies is included to show that it is part of the Odin Arkose Member and that the two lithofacies are gradational.

5.2.2 Trough Cross-bedded Lithofacies (TCL)

The Trough Cross-bedded Lithofacies is composed of two different types of trough cross-bedded sandstone: 1) coarse sand to granule feldspathic sandstone, with generally higher visible feldspar percentage and 2) fine to medium feldspathic sandstone, often with coarse to granule quartz and less visible feldspar picking out the foreset traces. There are also rare thin green-brown mud horizons that drape the bounding surfaces of cross bed sets

and are broken into clasts down foresets (Fig 5-1). Cavities within cross beds indicate the presence of weathered out mud clasts. Quartz, pink and grey sandstone (similar to those found in the Conglomerate Lithofacies) and mud pebbles are scattered throughout the cross beds and in local layers or lenses, becoming more rare towards the top of the lithofacies. The upper contact is gradational with the rest of the Altar Mountain Formation and is best drawn where feldspar becomes less visible.

Figure 5-1: Mudstone draping and broken into clasts down a cross bed set in the Trough Cross-bedded Lithofacies, Mt Jason.

Skolithos linearis and *Skolithos sp.* trace fossils are common within the Trough Cross-bedded Lithofacies and occur at various levels and concentrations within the lithofacies depending on the field site. *Skolithos linearis* are long thin vertical burrows 10 to 30 cm long and 3 to 5 mm diameter (Bradshaw, 1981), while *Skolithos sp.* are shorter vertical burrows. Both types will be referred to as *Skolithos* and often form densely burrowed beds called piperock. *Thalassinoides* are also found within the Trough Cross-bedded Lithofacies and are much less common than *Skolithos. Thalassinoides* are horizontal burrows that weather with negative relief and do not have a median ridge (Fig 5-8, 5-9). U-shaped burrows, *Arenicolites* and *Tigillites* are also found rarely throughout the lithofacies. U-shaped burrows can only be seen in cross section and link paired holes that can be seen in plan view. *Tigillites* are short vertical burrows with a funnel shaped opening.

5.2.3 Cross-bedded Bioturbated Lithofacies (CBL)

The lower contact of the Cross-bedded Bioturbated Lithofacies of the Altar Mountain Formation with the Trough Cross-bedded Lithofacies of the Odin Arkose Member is gradational and the contact is placed at different heights dependent on changes within the stratigraphic section such as decrease in feldspar or grainsize.

The lithofacies is comprised of bedded (thin to thick), massive and trough cross-bedded fine to coarse sandstone with granules and very rare pebbles. Trough cross beds are 20 to 50 cm thick and occur interbedded with *Skolithos*, massive and bedded (0.2 to 4 m thick) sandstone layers. Granules are scattered or aligned along bounding surfaces between cross bed sets. Pebbles occur rarely as layers.

Skolithos linearis and *Skolithos sp.* are the most common and obvious trace fossil within the CBL. *Skolithos* are observed in two different ways, firstly *Skolithos* as piperock or secondly as singular vertical burrows through existing bedding. *Thalassinoides, Arenicolites* and U-shaped burrows are also present but to a lesser degree.

5.2.4 Bedded Fine Lithofacies (BFL)

The Bedded Fine Lithofacies is only observed at Mt Electra. The lithofacies is composed of laminated, bedded and cross-bedded medium and coarse sandstone. Sedimentary structures include mud rip ups, local ripples and polygonal sand filled mud cracks.

5.3 Overview

Throughout the field area the Trough Cross-bedded Lithofacies is observed in contact with the underlying Conglomerate Lithofacies. The thickness of the TCL varies from 8 to 20 m thick. There is no pattern in thickness changes across the field area but it is often due to the different thickness of the sections measured at each site. The TCL is conformably overlain by the Cross-bedded Bioturbated Lithofacies with a gradational contact. The CBL is observed at Mt Jason, Mt Aeolus, Mt Boreas, Mt Electra and Balham Lake. The CBL also varies in thickness across the field area due to the thickness of the measured sections. The Bedded Fine Lithofacies is only observed at Mt Electra and is 17 m thick. It is possible it is deposited

elsewhere in the field area, however it was not observed at other localities due to shorter measured sections.

5.4 Facies Distribution and Relationships in Observed Sections

5.4.1 Mt Jason

10 to 60 cm of Conglomerate Lithofacies is deposited on the jagged Heimdall Erosion Surface (Chapter 4.5.1). The overlying Trough Cross-bedded Lithofacies is 16 m thick. Directly overlying the conglomerate is a 1 m thick massive bed of coarse sand with weathered cavities. The lithofacies is also composed of alternating trough cross beds (20 to 50 cm thick) of 1) coarse sand with granules and 2) fine sand with granules. Massive beds (0.7 to 1.3 m thick) containing granules and weathered out cavities also occur. Cross beds indicate paleocurrent directions to the northwest (Fig 5-2). This is different from the cross beds and ripples within the Cross-bedded Sandstone Lithofacies of the New Mountain Sandstone below the Heimdall Erosion Surface at Mt Jason (Fig 3-7C, D).

Skolithos occur in the Trough Cross-bedded Lithofacies. *Skolithos* are observed in coarse to very coarse sand with granules and are often interbedded with cross beds (Appendix A1/1). *Skolithos* beds are 0.4 to 2 m thick and are either entirely *Skolithos* piperock or spaced burrows that leave the cross beds intact.

The contact between the Trough Cross-bedded Lithofacies and the overlying Cross-bedded Bioturbated Lithofacies is gradational and the actual contact is difficult to define. The contact is put at 16 m above the HES at the last observation of feldspar in the stratigraphic column (Appendix A1/1) and the end of obvious granules within the sediments.

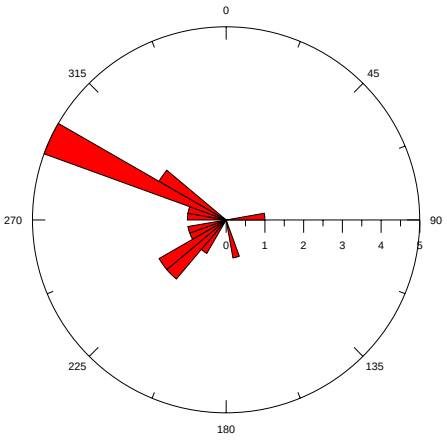

Figure 5-2: Paleocurrent directions within the Trough Cross-bedded Lithofacies, Mt Jason (n=18).

The Cross-bedded Bioturbated Lithofacies is 54.2 m thick to the top of the measured section (Appendix A1/1) at Mt Jason. The lithofacies is composed of trough cross-bedded (20 to 50 cm thick) medium to very coarse sandstone. Massive beds are from 0.2 to 2 m thick and composed of fine to very coarse sandstone. Some massive beds display normal grading across one or more grain sizes. Bedded horizons are 0.2 to 4 m thick and are composed of either thinly bedded medium to coarse sandstone or alternating medium and coarse sandstone. Cross beds alternate with massive sandstone, thin and thickly bedded sandstones and *Skolithos* layers. Granules are found in some massive beds and rarely as layers on the bounding surfaces of cross beds. One pebble layer is observed. *Skolithos* trace fossils are very prominent and occur in beds 0.3 to 3 m thick or as more separated vertical traces. U-shaped burrows occur at the very top of the lithofacies and overlie the pebble layer (Appendix A1/1).

The sequence at Mt Jason begins with 10 to 60 cm of Conglomerate Lithofacies overlain by 15.4 m of cross-bedded and massive Trough Cross-bedded Lithofacies followed by 54.2 m of Cross-bedded Bioturbated Lithofacies. The lower part of the section is dominated by thick *Skolithos* beds, which decrease in thickness up section. Further up section thinner *Skolithos* beds alternate with thick and thinly bedded, cross-bedded and massive sandstone. Cross beds dominate the top of the measured section. Overall there is a decrease feldspar and general fining up section.

5.4.2 Mt Hercules

The Conglomerate Lithofacies at Mt Hercules is 28 to 33 cm thick and is distinguished from other field sites by *Skolithos* burrows into the underlying New Mountain Sandstone (Chapter 4.5.2). Overlying the Conglomerate Lithofacies is 19 m of typical Trough Cross-bedded Lithofacies containing medium and coarse trough cross-bedded sandstone (Fig 5-3B) with coarse material along the foresets. *Skolithos*, broken up mud layers, minor planar thinly bedded sandstone and thin olive green shales are present (Appendix A1/2). *Skolithos* appear 10 m into the Trough Cross-bedded Lithofacies, which is the first occurrence after the *Skolithos* in the underlying Conglomerate Lithofacies

Paleocurrents from the Trough Cross-bedded Lithofacies indicate flow towards the southwest (Fig 5-3A). These are different to those in the TCL at Mt Jason (Fig 5-2), approximately 3 to 4 km away. The Cross-bedded Bioturbated Lithofacies and Bedded Fine Lithofacies were not observed at Mt Hercules.

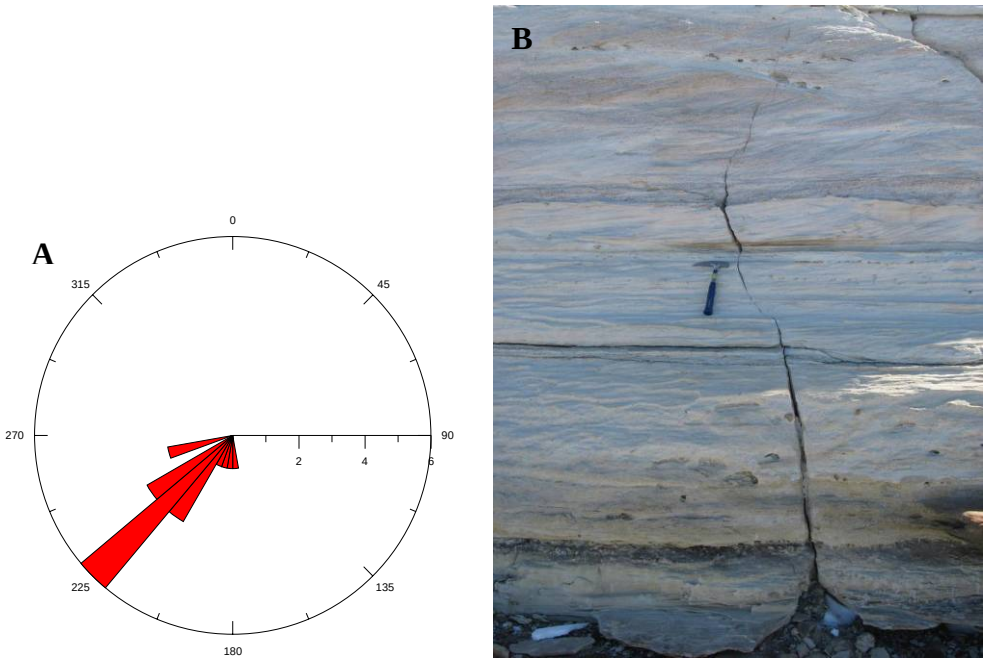

Figure 5-3: A) Paleocurrent directions from the Trough Cross-bedded Lithofacies (n=18). **B)** Trough Cross-bedded Lithofacies, Mt Hercules

5.4.3 Mt Aeolus

5 to 20 cm of Conglomerate Lithofacies is deposited directly on the Heimdall Erosion Surface either as pebbles or medium sand to granule sandstone (Chapter 4.5.3). Overlying this is 6 m (to the top of measured section) of Trough Cross-bedded Lithofacies (Appendix A1/3). The lithofacies is composed of massive and cross-bedded, fine and coarse sandstone with granules and pebbles. Cross beds are 20 to 40 cm thick and are more abundant than massive beds. Pebbles are scattered throughout cross bed sets and as layers on bounding surfaces. They are composed of grey sandstone, quartz, dark grey sandstone and pink sandstone. The unit is characterised by high feldspar content (7 to 20%). The overlying lithofacies of the Altar Mountain Formation were not observed at Mt Aeolus.

5.4.4 Mt Boreas

The Conglomerate Lithofacies at Mt Boreas is up to 20 cm thick and composed of pink sandstone, quartz, quartzite and feldspar (Chapter 4.5.4). Overlying the Conglomerate Lithofacies is the Trough Cross-bedded Lithofacies (Fig 5-4). The lithofacies is composed of cross-bedded (10 to 20 cm thick), medium to very coarse sandstone with granules (Appendix A1/4). Visible feldspar is 1 to 25%. The contact between the TCL and the Cross-bedded

Bioturbated Lithofacies is placed at the last occurrence of visible feldspar in the measured section, which is at 22 m (Appendix A1/4).

Figure 5-4: Trough Cross-bedded Lithofacies at Mt Boreas.

The measured thickness of Cross-bedded Bioturbated Lithofacies at Mt Boreas is only 5.2 m up to the obscured top of the measured section (Appendix A1/4). The CBL is composed of massive muddy medium sandstone with scattered coarse sand, which is 0.6 to 1.4 m thick. This is overlain by thinly bedded medium sandstone with scattered quartz sand (2 m thick). No trace fossils are observed in the Mt Boreas measured section.

5.4.5 Mt Electra

The Conglomerate Lithofacies is observed east below Mt Dido, in the measured section and west near the Wright Upper Glacier (Chapter 4.5.5). Below Mt Dido the lithofacies is 2 to 3 cm thick and deposited directly in the HES. In the measured section the actual erosion surface was not observed but pebbles of quartz and quartzite where collected from where the HES is inferred to be. Near the Wright Upper Glacier the Conglomerate Lithofacies is 1.4 m thick and has a layer of pebble cavities directly on the HES followed by two conglomerate layers and intervening sandstone layers. There is also a variation in the Conglomerate Lithofacies shown by non-deposition of a conglomerate on the HES.

The Trough Cross-bedded Lithofacies is deposited above the Conglomerate Lithofacies in the measured section at Mt Electra but the thickness is difficult to determine and is likely 8.5 m (Appendix A1/5a). The lithofacies is composed of cross beds 10 to 30 cm thick in fine to very coarse sandstone with granules. It also contains massive coarse and very coarse sandstone fining up to fine or medium sand; muddy sandstone containing white siltstone and pebble cavities; thin green shale layers; rare mudstone and rip-up clasts

(Appendix A1/5a). Three pebble layers occur at 2.8 m, 3.2 m and 8.5 m above the base of the section. Cross beds within the Trough Cross-bedded Lithofacies at Mt Electra show flow to the southwest (Fig 5-5). The upper contact with the Cross-bedded Bioturbated Lithofacies is very difficult to place at this location because there are no very obvious changes in sedimentation up section. The contact is placed at the last pebble layer in the section (Appendix A1/5a) at 8.5 m.

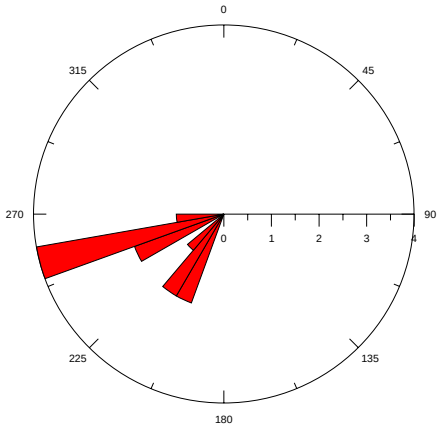

Figure 5-5: Paleocurrent directions within the Trough Cross-bedded Lithofacies, Mt Electra (n=12).

The Cross-bedded Bioturbated Lithofacies is 15 m thick and is composed of massive and cross-bedded sandstone. Cross beds are 0.2 to 1 m thick and are composed of medium or coarse sandstone with foreset beds rarely lined with granules (Fig 5-6A). Massive beds are 0.4 to 1.5 m thick and are composed of medium or coarse sandstone or muddy sandstone with minor granules and bioturbation. Mud beds are a minor unit and are 20 to 30 cm thick and laterally discontinuous. A pebble layer found at 23.4 m is composed of pink-stained quartz and pink sandstone. The pebble layer defines the boundary between the CBL and the Bedded Fine Lithofacies. *Skolithos* are first observed 2.5 m into the Cross–bedded Bioturbated Lithofacies and are not extensive. Undefined bioturbation is relatively more common and could be *Skolithos* but are poorly exposed due to erosion.

The Bedded Fine Lithofacies is 17 m thick. The lithofacies is composed of cross-bedded, massive and thick to thinly bedded, medium to coarse sandstone (Appendix A1/5a). Cross beds are 30 to 50 cm thick and massive beds are 20 cm thick. Both horizontally bedded and wavy thinly bedded sandstones occur (3 m thick). Sedimentary structures include polygonal sand filled mud cracks, mud rip up clasts (Fig 5-6B) and rare ripples.

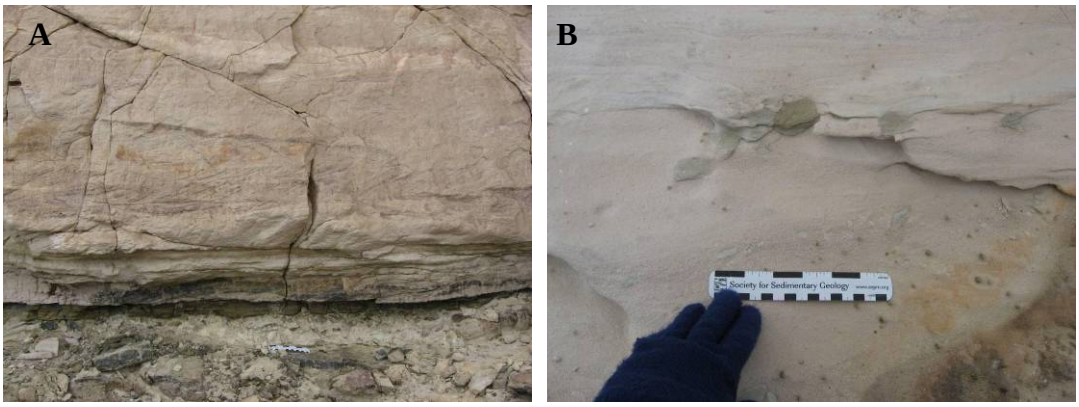

Figure 5-6: A) Green mudstone underlying cross-bedded sandstone with faint vertical burrows in the Cross-bedded Bioturbated Lithofacies in the Mt Electra measured section. **B)** Mud rip ups and clasts lining foresets in Bedded Fine Lithofacies.

In summary, the measured section at Mt Electra is composed of 8.5 m of Trough Cross-bedded Lithofacies overlain by the Cross-bedded Bioturbated Lithofacies. The CBL is composed of massive and cross-bedded medium to coarse sandstone alternating with mudstone layers. The upper part of the section is bedded, laminated and cross-bedded predominantly medium sandstone, typical of the Bedded Sandstone Lithofacies. Undefined bioturbation and *Skolithos* are commonly associated with massive sandstone and mudstone layers.

The Trough Cross-bedded Lithofacies is also observed below Mt Dido and above the Upper Wright Glacier overlying the Conglomerate Lithofacies, and is 2 to 3 cm and 1.4 m thick respectively, however the entire sequence was not investigated and therefore the thickness of the Trough Cross-bedded Lithofacies is unknown.

5.4.6 Balham Lake

The beginning of the succession at Balham Lake is identified as the Trough Cross-bedded Lithofacies and is 9.5 m thick. However, it is a lot more variable than at other localities. Exposure at Balham Lake is limited due to extensive scree cover (Appendix A1/6). The Heimdall Erosion Surface was located to within 1 to 2 m of outcrops of basement rocks (Koettlitz Group) and overlying sediments. Closest to the contact is a green-grey fine sand unit with rounded burrows infilled with coarse sand and granules. Overlying the fine sand is trough cross-bedded, pink coloured, poorly sorted, coarse sandstone, with granule to very coarse pebbles of white quartz, pink granite and feldspar. The section contains trough cross beds of medium sandstone and coarse sandstone with granule and pebbles. Rip ups of fine

sandstone are associated with the coarse sandstone beds (Fig 5-7). Cross beds are 20 to 50 cm thick.

Figure 5-7: Very coarse sandstone with granules, pebbles and fine thinly bedded sandstone rip up clasts (shown by arrow) typical of the Trough Cross-bedded Lithofacies at Balham Lake.

The lower contact of the Cross-bedded Bioturbated Lithofacies with the underlying Trough Cross-bedded Lithofacies is placed where the sedimentology changes to medium sandstone with larger scale cross beds (Appendix A1/6). The Cross-bedded Bioturbated Lithofacies is 43.3 m thick. The lithofacies is composed of cross-bedded medium sandstone (0.3 to 1 m thick), coarse sandstone (~50 cm thick) and fine sandstone (~1 m thick). Cross-bedded coarse sandstone has either scattered granules or very coarse sand and granules lining the foresets. Cross beds containing granule lined foresets are associated with clasts of thinly bedded fine sandstone and massive coarse sand layers up to 20 cm thick. One 30 cm thick very fine sandstone layer occurs between cross-bedded sandstones (Appendix A1/6). Undefined bioturbation occurs in some medium sandstone cross beds on the measured section.

Identifiable trace fossils were observed in fallen blocks up the slope and above the measured section; they included *Skolithos* and *Thalassinoides*. *Thalassinoides* (Fig 5-8) occurs independently and with *Skolithos* (Fig 5-9). The blocks could not have fallen far and are representative of trace fossils within the formation.

Figure 5-8: *Thalassinoides* at Balham Lake. Photo by: Margaret Bradshaw

Figure 5-9: *Thalassinoides* and *Skolithos* at Balham Lake. Photo by: Margaret Bradshaw

The sequence at Balham Lake begins with the cross beds of medium and coarse sandstone typical of the Trough Cross-bedded Lithofacies. This is overlain by the Cross-bedded Bioturbated Lithofacies, composed of cross-bedded fine sandstone and changes to cross-bedded medium to coarse sandstone. Cross beds are the dominant sedimentary structure at Balham Lake but there is no apparent dominant grainsize.

5.4.7 Sponsors Peak

The Conglomerate Lithofacies is observed on the col between Sponsors and Nickel Peaks and southwest of the campsite (Fig 1-10). The lithofacies is very thin (>10 cm) and composed mainly of pink sandstone and quartz. Green very fine sandstone is observed in the Conglomerate Lithofacies to the southwest of camp (Chapter 4.5.8).

The Trough Cross-bedded Lithofacies overlies the Conglomerate Lithofacies and is well exposed in cliffs on either side of the col between Sponsors and Nickel Peaks (Fig 5-10). The lithofacies is composed of alternating beds of trough cross-bedded (10 to 30 cm thick) medium sand to granule and fine to medium sandstone. Scattered grey sandstone and thinly bedded fine sandstone clasts are scattered in the cross bed sets. The lithofacies also contains thin (3 to 4cm thick) discontinuous shale layers. Paleocurrent data indicates current flow in directions between south and west, but is inconclusive due to the low number of measurements (Fig 5-11).

The Cross-bedded Bioturbated and Bedded Fine Lithofacies are not observed at Sponsors Peak.

Figure 5-10: Trough Cross-bedded Lithofacies on the western side of the col between Sponsors and Nickel Peaks.

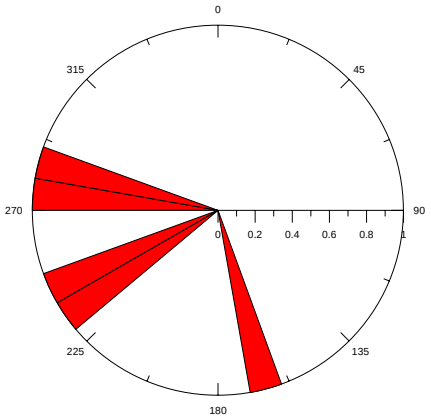

Figure 5-11: Flow directions within the Trough Cross-bedded Lithofacies at Sponsors Peak (n=5).

5.5 Composition

Examination of thin sections from samples of Trough Cross-bedded and Cross-bedded Bioturbated Lithofacies gives information as to the provenance of the material that makes up the sediments. Point count data can be found in Appendix B1. There are several samples of the Trough Cross-bedded Lithofacies but only three samples of the Cross-bedded Bioturbated Lithofacies; as these are all from Mt Electra, they do not provide a valid representation of the lithofacies.

5.5.1 Conglomerate Lithofacies

The sample of Conglomerate Lithofacies matrix from Mt Jason is a quartzarenite (Fig 5-12). Thin sections of the matrix show that it contains quartz (mono and polycrystalline) and altered feldspar. Contacts between some of the grains are stylolitic. Further information can be found in Chapter 4.5.1.

5.5.2 Trough Cross-bedded Lithofacies

The Trough Cross-bedded Lithofacies covers the spectrum from subarkose to quartzarenite (Fig 5-12).

Sample H11 (directly above Conglomerate Lithofacies) from Mt Hercules is a quartzarenite and is composed of 95% quartz (mostly monocrystalline) and minor feldspar (plagioclase and alkali). Fig 5-13A shows the quartz is rounded and irregular in shape and is supported in a fine greenish matrix, which could be clay.

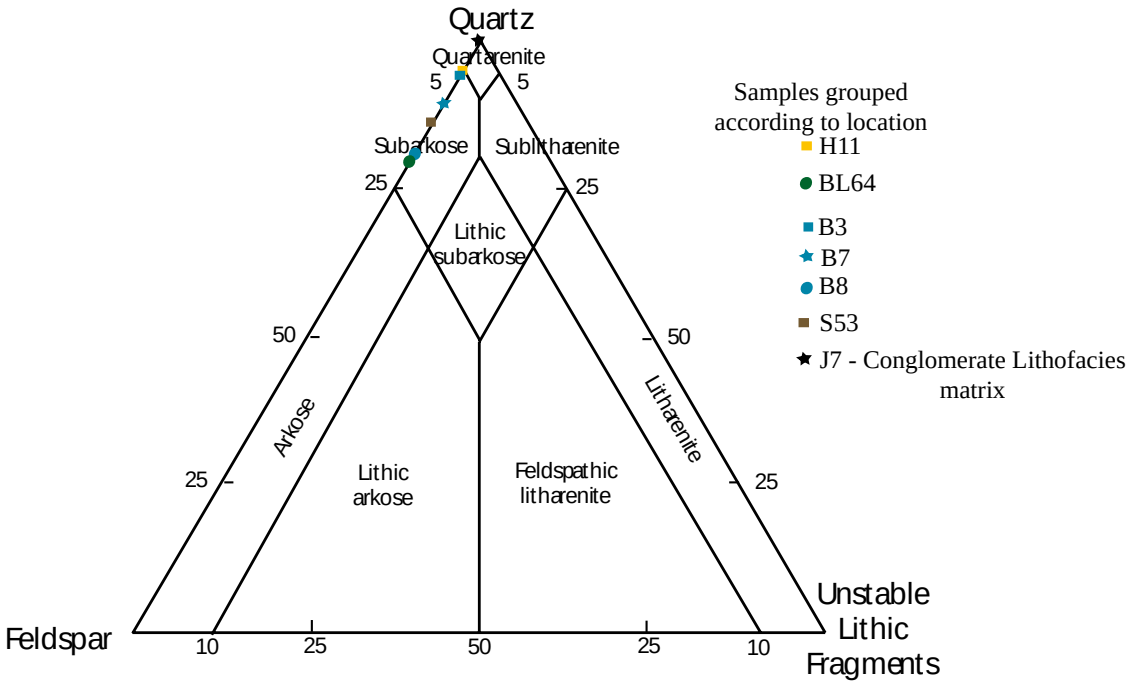

Figure 5-12: QFL plot of Trough Cross-bedded Lithofacies samples. Adapted from Blatt and Tracey (1996)

The sample from Balham Lake (BL64) is a subarkose and is composed of quartz (79%) and feldspar (21%), which is predominantly alkali. The thin sections show stylolitic contacts between quartz grains (Fig 5-13B), rounded quartz and rounded altered feldspar.

There are two samples from Mt Aeolus and they cover the spectrum from subarkose to quartzarenite (Fig 5-12). Sample B8 is composed of quartz (81%) and alkali feldspar (19%). The thin sections show quartz overgrowths, monocrystalline rounded quartz and dust rims (Fig 5-14A, B). B7 is also a subarkose but contains less alkali feldspar (11%). Quartz (89%) also shows dust rims and quartz overgrowths and is monocrystalline (Fig 5-14A, B). Sample B3 (from Mt Boreas) is just outside the boundary of a quartzarenite and is composed of quartz (94%) and minor alkali feldspar (6%) (Fig 5-12).

There does not seem to be a pattern that relates to sandstone composition and position in the stratigraphic column within the Trough Cross-bedded Lithofacies. Both plagioclase and alkali feldspar are found in this lithofacies, though alkali feldspar is more common. The more arkosic samples come from Balham Lake and Mt Aeolus and the more quartzose from Mt

Boreas and Mt Hercules. The Trough Cross-bedded Lithofacies varies in composition laterally and vertically within the lithofacies.

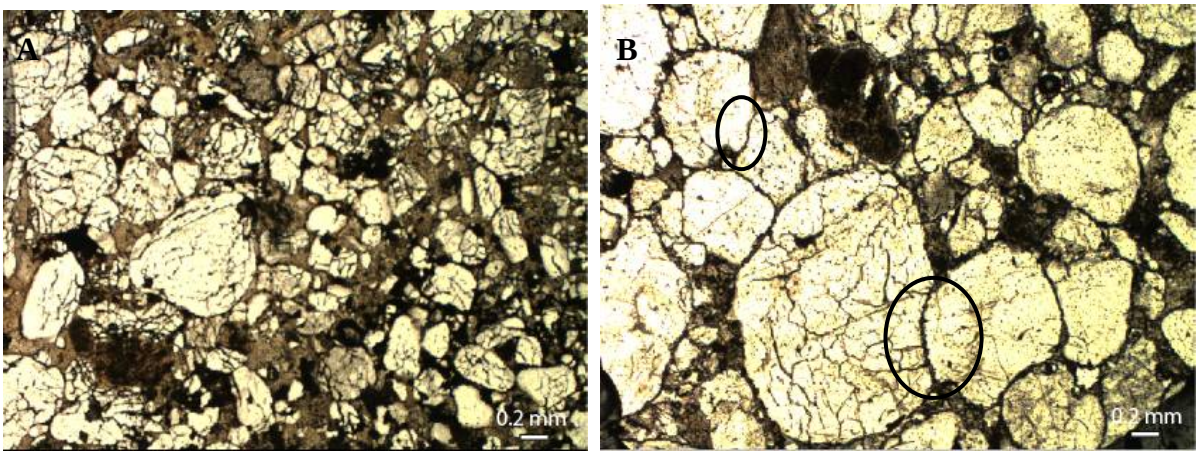

Figure 5-13: A) Trough Cross-bedded Lithofacies, Mt Hercules. **B)** Stylolitic contacts (circled) within the Trough Cross-bedded Lithofacies, Balham Lake.

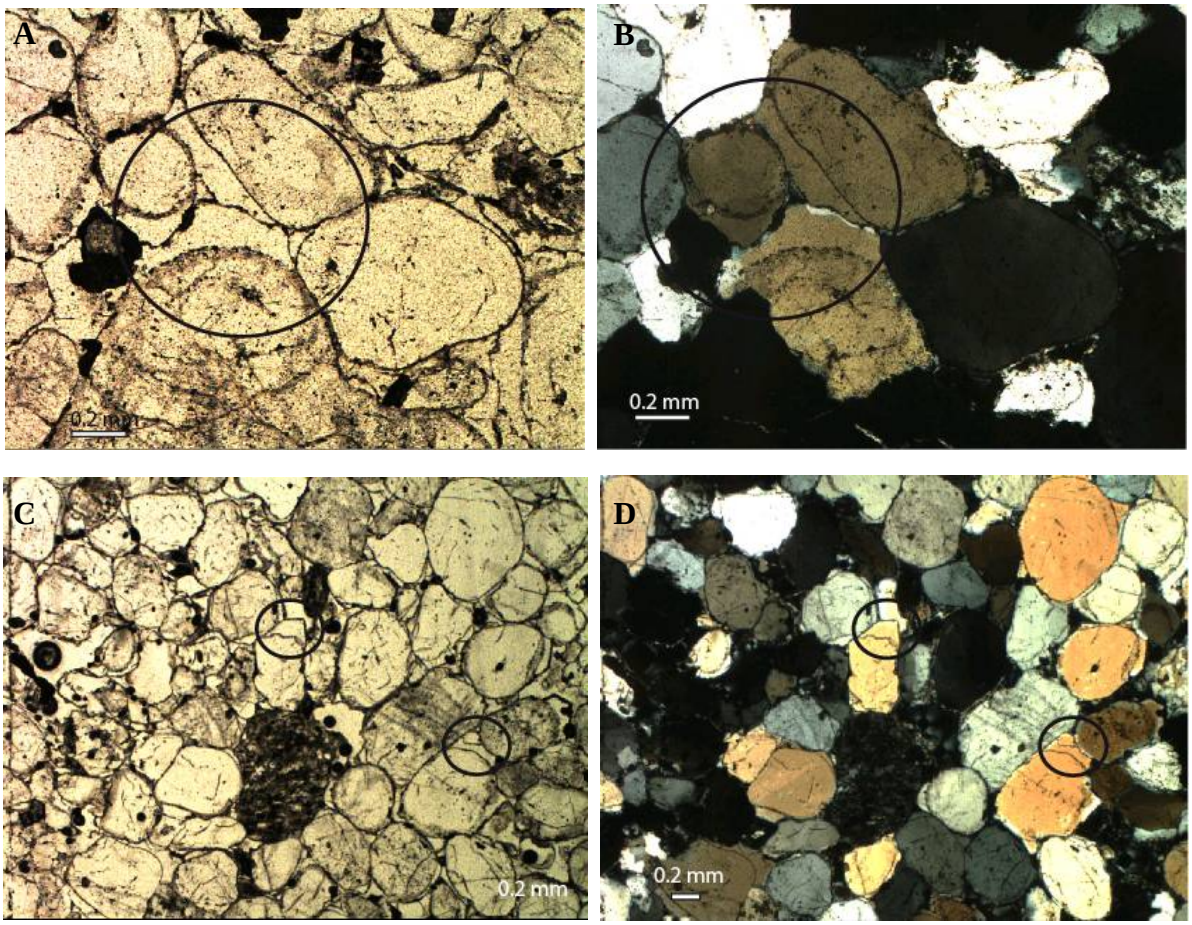

Figure 5-14: Trough Cross-bedded Lithofacies with good examples of quartz overgrowths circled, Mt Aeolus. **A)** Plain polarised light and **B)** Cross-polarised light. **C)** Plain polarised light and **D)** Cross-polarised light.

5.5.3 Cross-bedded Bioturbated Lithofacies

Sample E27 is from the Cross-bedded Bioturbated Lithofacies and is composed of 71% quartz and 29% feldspar (both plagioclase and alkali). Sample E27 is an arkose as is E24 (Fig 5-16), which is not located in the measured section. E24 occurs much higher in the Altar Mountain Formation (top of outcrop below Mt Electra camp). The feldspar grains (yellow colour) are more rounded than the quartz grains (Fig 5-15A). The quartz grains show no overgrowths but have pressure-solution contacts. There is a minor amount of fine matrix material supporting the sand grains.

Sample E28 (Fig 5-15B) is from the Bedded Fine Lithofacies and is composed of 4% feldspar (plagioclase) and 96% quartz. The lithofacies is a quartzarenite (Fig 5-16). Quartz grains are the dominant feature and are mainly sub-angular. There is a fine matrix supporting the quartz. Fracturing and shattering of the quartz grains could be a product of deposition.

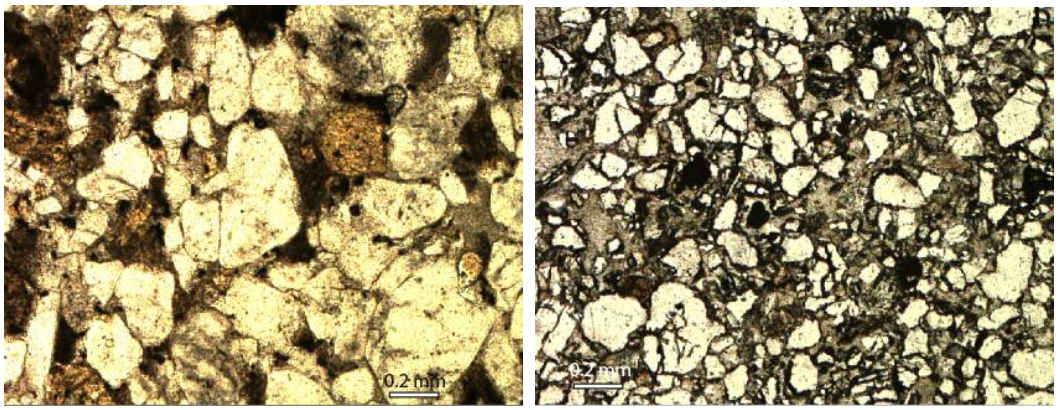

Figure 5-15: Representative images of the Cross-bedded Bioturbated Lithofacies. **A)** Feldspar stained yellow and quartz grains. **B)** Fractured and shattered quartz supported by matrix.

The QFL diagram (Fig 5-16) shows that although the visible feldspar content may decrease, the amount within the sediments remains high (Sample E27 and E28). This suggests that putting a boundary between the Trough Cross-bedded Lithofacies and Cross-bedded Bioturbated Lithofacies based on feldspar content could be more problematic than is apparent in the field and may require redefinition or renaming of the Odin Arkose Member.

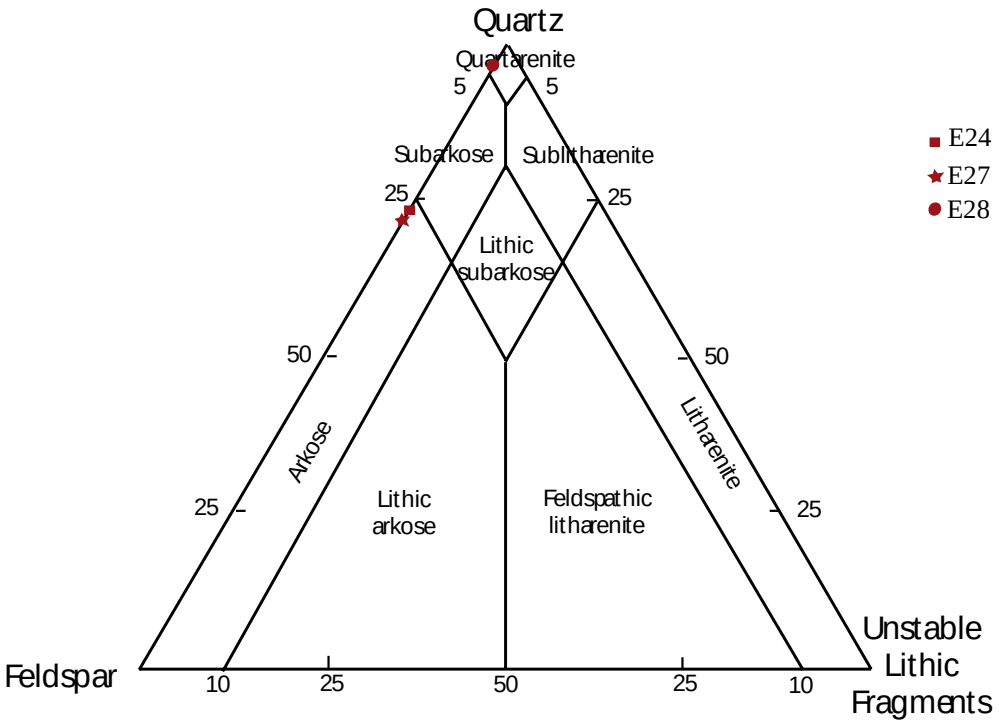

Figure 5-16: QFL plot of lithofacies within the Altar Mountain Formation. Adapted from Blatt and Tracey (1996)

5.6 Interpretation

The contact between the Trough Cross-bedded Lithofacies and the underlying Conglomerate Lithofacies is gradational and indicates that they were deposited in laterally adjacent environments as sea level rose.

The Trough Cross-bedded Lithofacies is a shallow marine deposit probably from a shoreface environment. This conclusion is based on the sedimentary structures, grainsize and sorting and trace fossils. The sedimentary structures within the Trough Cross-bedded Lithofacies are similar to those found in shoreface deposits described by Boggs (2001) and are summarised in Chapter 3.5. The deposits include sediments ranging from fine sand to gravel, trough cross beds and *Skolithos*.

Skolithos linearis, *Skolithos sp.* and *Tigillites* are diagnostic of marine environments (Webby, 1968; Martino and Curran, 1990; Gourmanis *et al*, 2003; Mangano *et al*, 2005; Metz, 2006). *Skolithos linearis* are found predominantly in higher energy environments associated with continuously shifting sands and storm events (Gouramanis *et al*, 2003; Mangano *et* al, 2005). The high-energy environment could be within the shoreface or at the

shoreface to inner shelf transition. The shoreface area is high energy due to interaction of waves and currents during both fair-weather and storm events. In the shoreface to inner shelf transition, *Skolithos* beds could indicate storm events with waves interacting with sediment within the storm wave base. This leads to alteration between *Skolithos* beds and trough cross beds or massive beds. There is not a huge amount of *Skolithos* in the TCL suggesting that the lithofacies was deposited in a middle shoreface environment with cross beds formed by longshore currents and *Skolithos* colonising due to the high energy conditions. Cross beds within the Trough Cross-bedded Lithofacies show flows towards an area between the southwest and northwest. Decrease in visible feldspar up section shows that the feldspar is being broken down prior to deposition and it is no longer big enough to see with the naked eye. This indicates the feldspars travelled further before being deposited. The finer grainsize could also indicate deepening water over time as the sea transgresses northward across the shore platform (Heimdall Erosion Surface). The finer sediment could be deposited in deeper water due to the lesser degree of energy needed to transport the sediment further (as opposed to coarser grain sizes, which are deposited in relatively shallower water).

Therefore, the Trough Cross-bedded Lithofacies was deposited in a shallow marine environment with longshore currents flowing in a westerly direction as the sea moved across the shore platform (Heimdall Erosion Surface). Storm events lead to cross-bedded units with *Skolithos* bioturbation after storms.

The Trough Cross-bedded Lithofacies is a subarkose and quartzarenite that is composed of quartz and alkali feldspar. Samples show overgrowths, dust rims and stylolitic contacts. The occurrence of feldspar within the lithofacies suggests rejuvenation of an old sediment source or switch to a new sediment source. The source was most likely basement rocks to the north of the depositional area, though the lower Taylor Group could also be considered.

The contact between the Trough Cross-bedded Lithofacies and overlying Cross-bedded Bioturbated is gradational and indicates a gradual change in environment over time that lead to a change in sedimentation pattern. As the CBL is gradational with the underlying TCL, which has been interpreted as shallow marine (shoreface), the Cross-bedded Bioturbated Lithofacies and overlying Bedded Fine Lithofacies are also most likely marine in origin.

Trace fossils found within the Cross-bedded Bioturbated Lithofacies and Bedded Fine Lithofacies provide strong evidence for a marine origin of the lithofacies. *Skolithos linearis* has been proved to be an indicator for shallow marine environments (see above) and commonly indicates higher energy environments such as those present on the shoreface or during storm events. *Thalassinoides* are also found in marine environments (Gouramanis *et al*, 2003). The lack of trace fossils in some stratigraphic columns does not indicate the unit is non-marine, rather that the high-energy environment typical of *Skolithos* was not the dominant condition at time of deposition.

Sedimentary structures within the Cross-bedded Bioturbated Lithofacies and Bedded Fine Lithofacies also suggest a marine depositional environment. Cross beds are the dominant feature of the lithofacies and are similar in size and structure to those found in shallow marine (middle to lower shoreface) or inner shelf environments (Bezerra *et al*, 1998; Boggs, 2001). These deposits also include trough cross beds, planar bedding, horizontal bedding and *Skolithos* and *Thalassinoides* (Bezerra *et al*, 1998; Boggs, 2001; Gouramanis *et al*, 2003). Cross beds most likely indicate rips or longshore currents in the depositional area or remobilisation of sediment in deeper water by wave action during storms. In terms of an inner shelf environment the cross beds could also indicate storm deposits, with waves reaching down to the sediment within the storm wave base. Muddy sandstone and mudstone layers are common at Mt Electra and Mt Boreas but mud cracks are not observed. Massive beds of sandstone, muddy sandstone and mud beds indicate periods of deposition in a lower energy environment, out of the influence of waves and currents. Therefore, deposition of the CBL could have occurred in an inner shelf environment, with relatively quiet deposition (massive, bedded and laminated beds) but reworking of sediments during storms creating the cross beds.

The Bedded Fine Lithofacies is also a marine deposit. The lithofacies indicates an intertidal or shallower marine environment. Sedimentary structures within the lithofacies include a higher proportion of thick and thinly bedded sandstones, polygonal cracks, mud rip up clasts and ripples. The lithofacies is interpreted as an intertidal deposit due to these structures, which indicate exposure to air and shallower water. The BFL shows local shallowing at Mt Electra in the upper part of the Altar Mountain Formation. The Bedded Fine Lithofacies could exist at other field sites but not enough section was measured.

Depositional patterns vary across the field due to the distance between outcrops. This variation is to be expected as deposition along a modern coast varies. For example, the stratigraphic column at Mt Jason shows alternating massive, cross-bedded and *Skolithos* rich horizons. Cross-bedded and *Skolithos* rich horizons indicate influence of storm waves or currents and the massive and bedded beds show times of quieter deposition during fair-weather or changing in current patterns. This pattern is repeated at the other field sites where the Cross-bedded Sandstone Lithofacies is observed, however, the relative amounts of cross beds, trace fossils and other beds vary.

The Cross-bedded Bioturbated Lithofacies is an arkose to quartzarenite and is composed of rounded feldspar and sub-rounded quartz in a fine matrix. There is a large proportion of matrix material in sample E28 in comparison to E27. Quartz overgrowths are not very common. The composition reflects source of sediment from the same area as the underlying Trough Cross-bedded Lithofacies.

The lithofacies of the Altar Mountain Formation are composed of sediment derived from the same source. However, the grainsize decreases up section indicating a change in environment, lowering of environmental energy or weathering of old sediment. The sediment source is probably a rejuvenated basement area due to the presence of abundant feldspar at the base of the formation. The nearshore facies commonly receive the coarser sediment (Odin Arkose Member) and offshore facies the finer sediment (rest of Altar Mountain Formation).

The Altar Mountain Formation has three parts; the lower is the Trough Cross-bedded Lithofacies (Odin Arkose Member), the Cross-bedded Bioturbated Lithofacies makes up the middle and the Bedded Fine Lithofacies comprises the upper portion. The lower portion is a shallow marine (probably upper shoreface) deposit. The middle part is shallow marine to inner shelf deposit comprised of cross-bedded and massive sandstones and the Bedded Fine Lithofacies is an intertidal or shallow marine marine deposit, seen only at Mt Electra. The lithofacies is composed of sedimentary structures typical of intertidal deposits and associated with exposure to air and coarser deposits associated with shallower water.

Overall, deposition of the Altar Mountain Formation reflects fining upwards of sediment and increase in massive, bedded or laminated sandstones and mudstone associated with deeper water or lower energy conditions followed by shallowing.

5.7 Summary

- The Altar Mountain Formation and Odin Arkose Member are divided into four lithofacies: Conglomerate Lithofacies (Chapter 4), Trough Cross-bedded Lithofacies, Cross-bedded Bioturbated Lithofacies and Bedded Fine Lithofacies
- The Trough Cross-bedded Lithofacies is a shallow marine deposit, probably deposited in the upper shoreface by longshore currents flowing to the west.
- The Cross-bedded Bioturbated Lithofacies was deposited in a shallow marine to inner shelf environment.
- The Bedded Fine Lithofacies is an intertidal to shallow marine deposit.
- Overall the formation decreases in grainsize up section.
- There is a deepening in water from the Heimdall Erosion Surface followed by a shallowing in the upper Altar Mountain Formation.

Chapter Six: Provenance

6.1 Introduction

Little is known of the provenance of the Beacon Supergroup sediments. The age of zircons found within the New Mountain Sandstone and Odin Arkose Member of the Altar Mountain Formation could constrain the sediment source and show if changes occur across the Heimdall Erosion Surface. A change in source could reflect either exhumation and deeper erosion (of the same source) or a switch in sediment source over time associated with changing paleocurrent directions (see previous chapters) and tectonics. This chapter presents and analyses results of LA-ICP-MS dating and cathodoluminescence images of zircon and quartz grains from the same samples. The techniques complement the basic composition and QFL data that were presented in the previous chapters.

6.2 LA-ICP-MS

LA-ICP-MS was undertaken on detrital zircons from New Mountain Sandstone and Odin Arkose Member samples from Mt Electra. Dates obtained from the zircons can be used to identify the source rocks.

6.2.1 Samples

Dr. Robert Bolhar collected three samples from Mt Electra during the 2007 field season. All the samples are from one locality to better constrain the stratigraphic change in composition up section. The samples are described in the table below.

Zircons from samples were taken to the Research School of Earth Sciences, Australian National University (ANU) and analysed using the LA-ICP-MS (outlined in Chapter 1.3.5). Results for each zircon and the method by which these data were reduced and convoluted can be seen in Appendix B2.

Table 6-1: Description and location of samples used in LA-ICP-MS. Source: Dr Robert Bolhar.

Sample	Fieldsite	GPS	Formation	Lithofacies	Description
E207	Mt Electra	77°30.805'S 160°59.073'E	New Mountain Sandstone	Cross-bedded Sandstone Lithofacies	yellow, med-grained sandstone from large-scale cross-bedded
E206	Mt Electra	77°30.760'S 160°58.805'E	Odin Arkose Member	Conglomerate Lithofacies	rounded-subangular clasts; matrix supported; clasts: mainly qrt, quarzite, matrix: granular to coarse-sand; reddish cement (hematite?)
E205	Mt Electra	77°30.760'S 160°58.805'E	Odin Arkose Member	Trough Cross-bedded Lithofacies	pale coloured, medium sand to granule, poorly sorted, feldspathic.

6.2.2 Results

All the samples from Mt Electra show similar age peaks that correspond to the ages of the Granite Harbour Intrusives (Chapter 2.2), which are the local basement rocks. Fig 6.1 shows the age peaks for each sample from Mt Electra. All samples have a single peak around 500 to 530 Ma in common.

Sample E207 (New Mountain Sandstone) has four minor age peaks at approximately 620, 680, 990, and 1080 Ma and a broad peak between approximately 1420 and 1820 Ma (Fig 6-1A). Sample E206 (Odin Arkose Member) has five minor peaks at approximately 380, 700, 750, 1180 and 1420 Ma (Fig 6-1B). Sample E205 (Odin Arkose Member) has only one age peak at 530 Ma, which corresponds to the main age peak for all the samples. Both E207 and E206 contain older grains (>590 Ma). These peaks indicate possible influence of older source material but are very small compared to the main age peak. The older grains (>590 Ma) also decrease in number between the two samples; E207 contains a greater proportion of older grains than E206. Overall the number of older grains decreases across the Heimdall Erosion Surface but the main age peak remains the same.

Fig 6-2 shows age and relative probability plots of the main age peaks for each sample. Sample E207 has only one narrow main age peak, which centres around 520 Ma (Fig 6-2A). Sample E206 has a double age peak at 500 Ma and 530 Ma (Fig 6-2B). Sample E205 (Fig 6-2C) has one broad peak centred on 530 Ma.

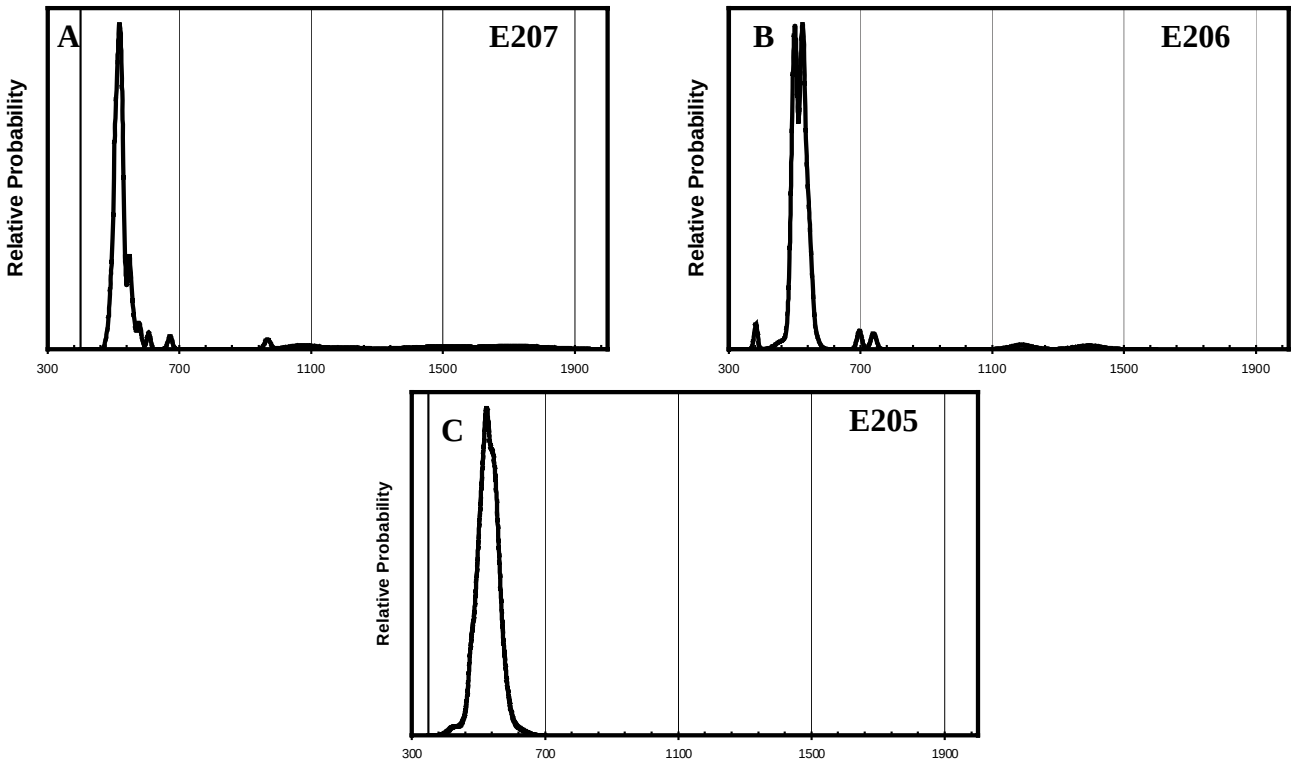

Figure 6-1: Age and relative probability plots for samples **A)** E207 - Cross-bedded Sandstone Lithofacies of the New Mountain Sandstone **B)** E206 - Conglomerate Lithofacies of the Odin Arkose Member **C)** E205 - Trough Cross-bedded Lithofacies of the Odin Arkose Member, from Mt Electra. Age (Ma) is on horizontal axis.

Allibone *et al* (1993, 1993a) and Allibone and Wysoczanski (2002) have divided the Granite Harbour Intrusives (Chapter 2.2) into suites based on date of emplacement and composition. DV1a suite was emplaced between 490 and 589 Ma; DV1b suite was emplaced around 490 Ma and DV2 suite was emplaced between 455 and 489 Ma. These divisions are shown on Fig 6-2. It is safe to conclude that the lower Taylor Group is mainly derived from Granite Harbour Intrusives, which is the local basement.

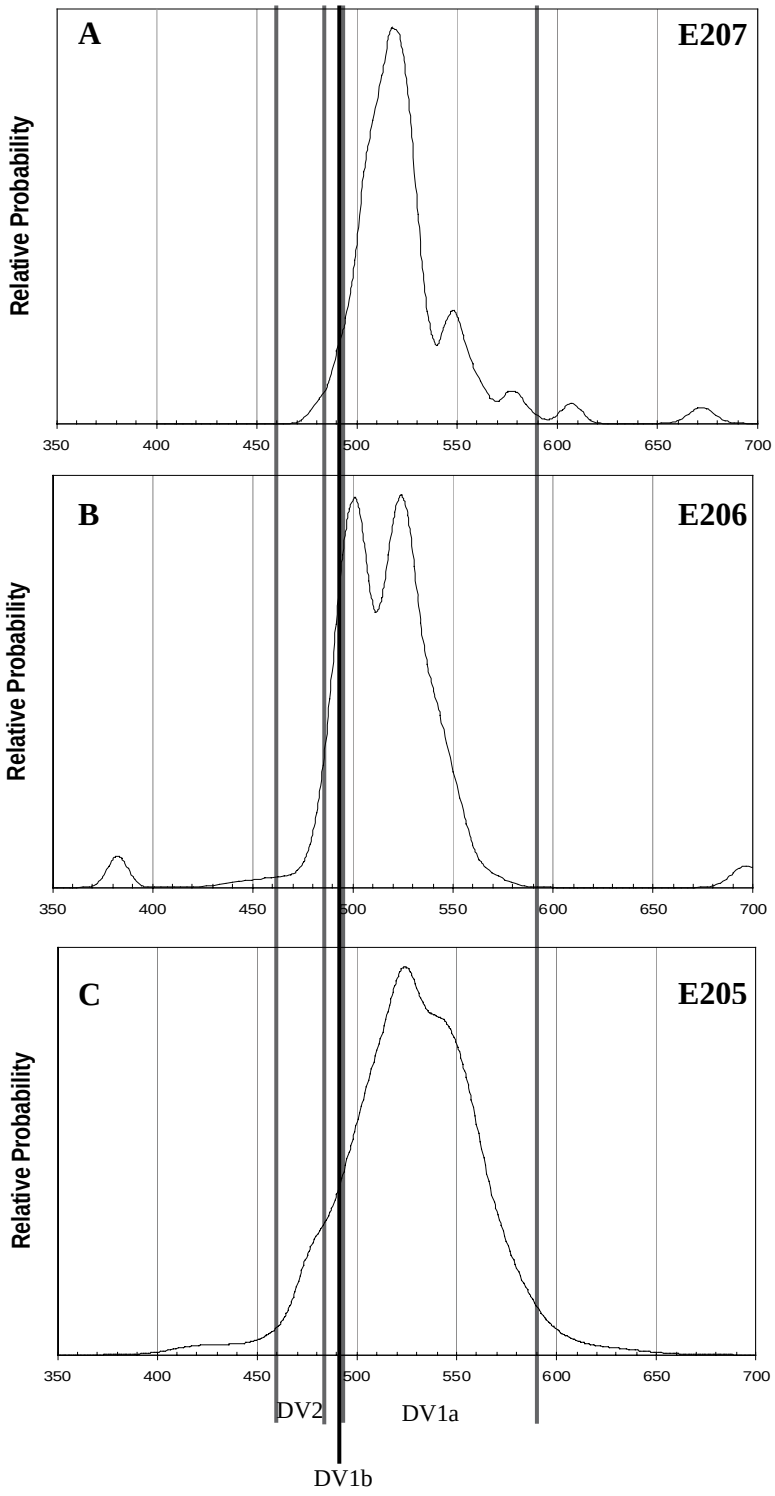

Figure 6-2: Age and relatively probability plots of samples **A)** E207 - Cross-bedded Sandstone Lithofacies of the New Mountain Sandstone **B)** E206 - Conglomerate Lithofacies of the Odin Arkose Member **C)** E205 - Trough Cross-bedded Lithofacies of the Odin Arkose Member, from Mt Electra. Age (Ma) is on horizontal axis. Divisions between the different suites within the Granite Harbour Intrusives are shown (see Chapter 2.2).

The 380 Ma age from sample E206 could be due to lead loss in the zircon grains or input from a younger source such as granites from Tasmania. SHRIMP dating by Black *et al* (2005) indicates ages between 350 and 400 Ma for Tasmania granites, which could have been supplying sediment to the Ross Sea region.

All main age peaks in the samples from Mt Electra correspond with the DV1a suite of Allibone *et al* (1993). However, the 490 Ma age from the double age peak in sample E206 could also correspond with DV1b and DV2 due to the overlap in ages.

6.3 Cathodoluminescence (SEM-CL)

The same samples (E207, E206, E205) were also examined using a scanning electron microscope to obtain cathodoluminescence images (methods described in Chapter 1.3.6). Zircons were examined in the mount that was used for dating. Thin sections were made to examine quartz from the same samples. The pits in the SEM-CL images of the zircons are from the LA-ICM-PS.

6.3.1 Zircons

SEM-CL images of the zircons show zoning that is typical of zircon crystals (Fig 6-3). The zircons have an irregular rounded shape due to weathering and abrasion during transport. Some zircons have retained close to the original shape (Fig 6-3B, D), however others have been broken and only retain a portion of the original zoning (Fig 6-3A, C). The zoning of the zircons is important because it can indicate if the core of the zircon is older (inherited) than the rim, which is shown by crosscutting relationships in the zircon zoning. Fig 6-3C shows a zircon with an inherited core. The location of the pits from dating shows that a variety of different zones within the zircons were targeted, this is important when dating detrital zircons.

6.3.2 Quartz

SEM-CL images of the thin sections show quartz grains with spidery micro cracks, rare sharp zonation and large brittle cracks filled with silica cement (Fig 6-4, 6-5). Highly luminescent grains, some with twinning, are feldspar.

Zoning in quartz (Fig 6-5) is common in volcanic and vein quartz and rare in plutonic quartz (Bernet and Bassett, 2005; Boggs and Krinsley, 2006). The zoning in a quartz grain in E205 is sharp and pointy indicating it is vein quartz. Spidery micro cracks form in plutonic quartz and rarely in high-grade metamorphic quartz from cracking and healing during the late stages of crystallization and cooling (Bernet and Bassett, 2005). Their spidery healed microstructure differentiates them from later brittle deformation fabrics. The majority of the quartz grains in all samples contain spidery micro cracks indicating plutonic quartz (Fig 6-5).

Many of the plutonic quartz grains were crushed during compaction (Fig 6-4, 6-5). High pressures at grain point contacts cause dissolution of the quartz, which reprecipitates into the quartz grains as 'veins' and as overgrowths (Dickinson and Milliken, 1995) this is part of the diaganatic process forming the abundant concave-convex grain contacts and quartz overgrowths observed in thin sections.

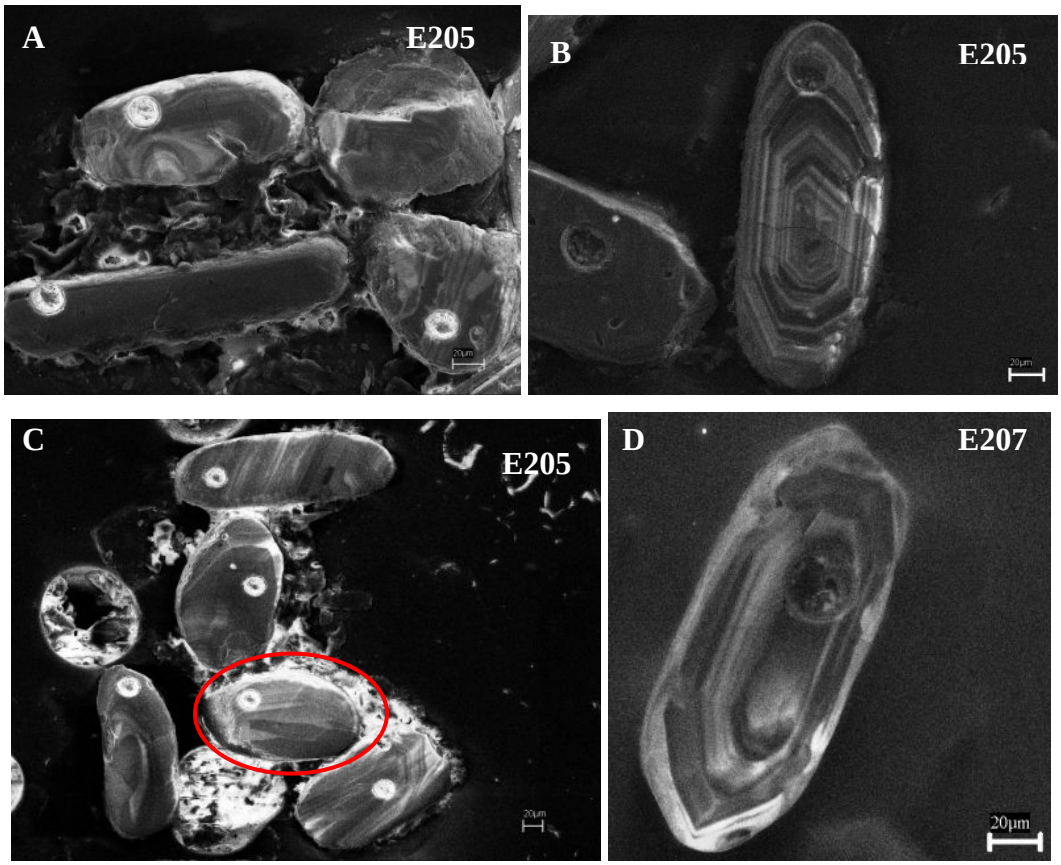

Figure 6-3: SEM-CL images of detrital zircons from Mt Electra. **C)** Zircon with an inherited core shown by crosscutting relationship with the outer zones (circled).

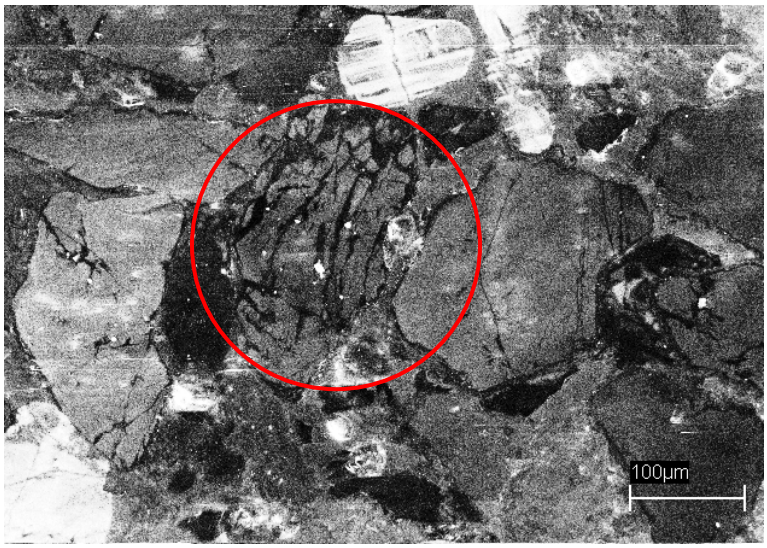

Figure 6-4: Diagenetic quartz (circled) in sample E205 (Odin Arkose Member).

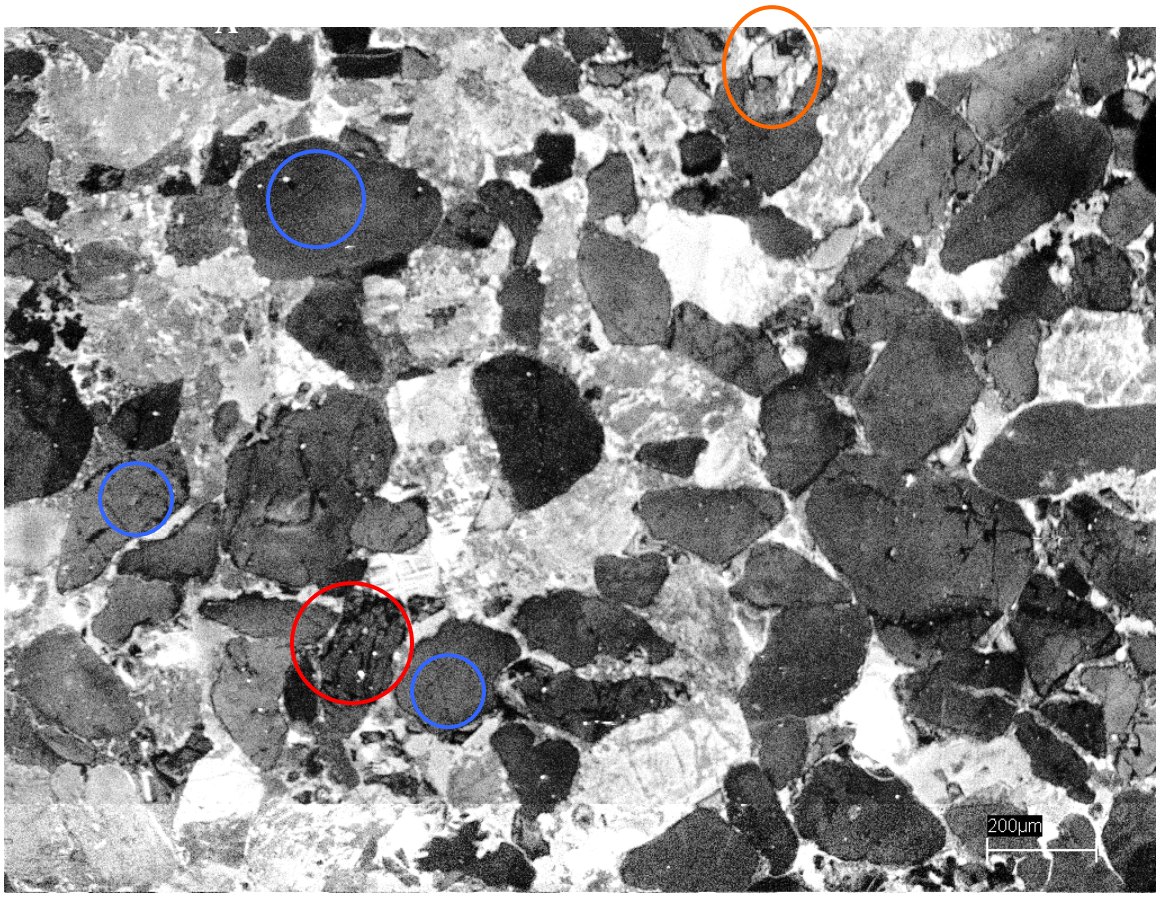

Figure 6-5: SEM-CL image of Sample E205 (Odin Arkose Member) showing spidery micro cracks (blue circles), sharp zonation (orange circle) and brittle deformation (red circle).

6.4 Composition

The composition of the lithofacies of the New Mountain Sandstone and Odin Arkose Member of the Altar Mountain Formation has been covered in Chapters 3.5, 4.6 and 5.5 but will be briefly outlined here.

Overall, the New Mountain Sandstone becomes more quartzose up section (Fig 3-18). The Cross-bedded Sandstone Lithofacies (E207) of the New Mountain Sandstone is a quartzarenite (Fig 3-18). This lithofacies is composed of quartz and cemented with overgrowths. The quartz is mainly monocrystalline but some polycrystalline grains are observed. Where the lithofacies is close to a dolerite intrusion the samples contain zeolite cement.

The matrix of the Conglomerate Lithofacies (E206) of the Odin Arkose Member is quartzarenite (Fig 5-12). The lithofacies is mainly composed of a variety of pebbles including quartz (milky, smoky and pink-stained), plagioclase feldspar, quartzite, pink sandstone, dark grey coarse sandstone, green very fine sandstone, white siltstone, grey-pink poorly sorted sandstone, grey sandstone, jasper, red medium sandstone, rhyolite and granite. The grey, red and pink sandstone clasts from the Conglomerate Lithofacies are subarkose to quartzarenites (Fig 4-17).

The Trough Cross-bedded Lithofacies (E205) of the Odin Arkose Member is a subarkose to quartzarenite (Fig 5-12). The lithofacies is composed of mono and polycrystalline quartz and alkali and plagioclase feldspar. Dust rims, matrix material and stylolitic grain contacts are observed in some thin sections.

Tectonic discrimination diagrams from Dickinson *et al* (1982) constrain the source for the New Mountain Sandstone, Altar Mountain Formation and Odin Arkose Member to a continental provenance (Fig 6-6). The sediment that makes up the sandstone clasts found in the Conglomerate Lithofacies is also from a continental source (Fig 6-6).

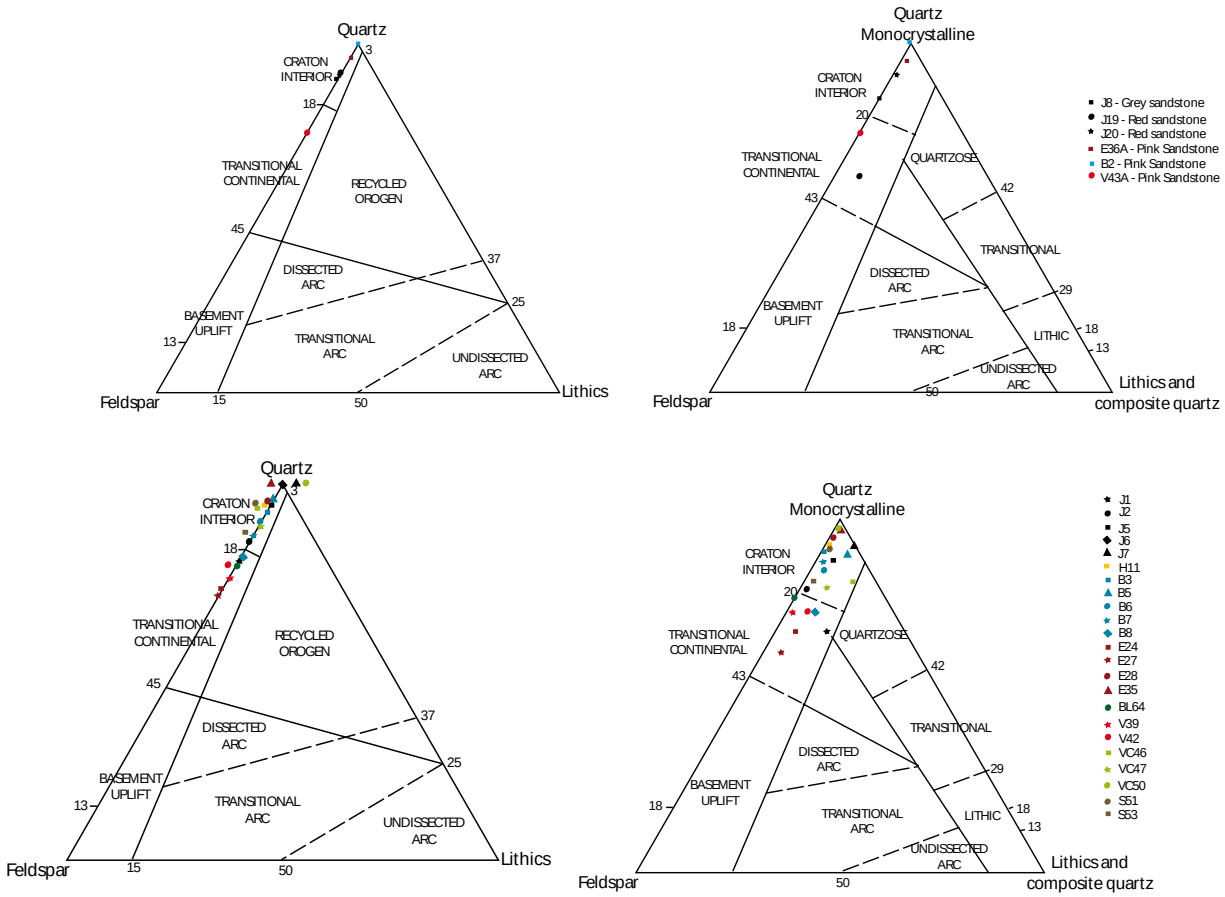

Figure 6-6: Tectonic discrimination diagrams of Dickinson *et al* (1982). Top diagrams show counts of sandstone pebbles of the Conglomerate Lithofacies (Odin Arkose Member). The bottom two diagrams show counts from New Mountain Sandstone, Altar Mountain and Odin Arkose Member samples.

6.5 Discussion

The age peaks for all samples from Mt Electra correspond to the crystallisation ages of the Granite Harbour Intrusives (Allibone *et al*, 1993, 1993a; Allibone and Wysoczanski, 2002). This is strongly supported by the fact that most of the quartz grains are plutonic as shown by SEM-CL. Micro cracks are the most common feature and are typical of plutonic quartz (Bernet and Bassett, 2005; Boggs and Krinsley, 2006). Diagenetic textures indicate early alteration of quartz grains due to compaction. Rare vein quartz grains are observed and support evidence of vein quartz (milky quartz) pebbles that are found in conglomerate layers and scattered through out the New Mountain Sandstone and Odin Arkose Member. Plutonic zoning was also seen rarely in quartz

grains. Quartz overgrowths, which were observed under plain polarised and cross-polarised light, did not show up well in SEM-CL.

The basement rocks in the field area are Koettlitz Group and Granite Harbour Intrusives. The sediments of the New Mountain Sandstone and Odin Arkose Member are sourced from rocks similar to those on which they were deposited. This is possible because the Granite Harbour Intrusives are extensive throughout southern Victoria Land. At the time of deposition of the New Mountain Sandstone the basement rocks to the west and northwest were exposed (Savage, 2005) and could have been supplying sediment. During Odin Arkose Member deposition in both the Olympus Range and Bulls Pass-St Johns Range area (of Savage, 2005) basement rocks could have been exposed further north and supplying sediment.

SHRIMP zircon dating by Savage (2005) on the Sperm Bluff Formation (correlative to the Odin Arkose Member of the Altar Mountain Formation) show dominant age peaks at 500-600 Ma and minor peaks at ~1000-1500 Ma and ~2000 Ma. The older age peaks are large in comparison to the samples from Mt Electra, but minor in comparison to the influence of the Granite Harbour Intrusives (Savage, 2005). The peaks are very similar to the samples from Mt Electra.

The Junction Sandstone of the Beacon Supergroup in the Darwin Glacier correlates with the lower Taylor Group in the Dry Valleys (Woolfe, 1989). SHRIMP dating of detrital zircons within the sandstone by Wysoczanski *et al* (1997) shows that the Junction Sandstone has similar age peaks to those from Mt Electra. However, the Junction Sandstone shows a greater influence from older sources with age peaks at 1100 Ma and 1600 Ma (Wysoczanski *et al*, 1997). The age peak pattern shows sediments were sourced from both Ross Orogen rocks (Granite Harbour Intrusives) and Grenville-age zircons and several sources were feeding into the depositional basin.

A combination of LA-ICP-MS, SEM-CL and tectonic discrimination diagrams indicate that the sediment of the New Mountain Sandstone and Odin Arkose Member are from a plutonic, continental source that is most likely the Granite Harbour Intrusives. Older age peaks seen in Wysoczanski *et al* (1997) are not recorded in the Mt Electra

samples suggesting that the basin within which the sandstones were being deposited was only fed by sediment from the Granite Harbour Intrusives. Inherited cores observed in the zircons could be the source for minor older age peaks in the Mt Electra samples; alternatively age peaks could be due to minor influx of sediments from an older source, such as the Koettlitz Group. The younger age peak in E206 could be caused by lead loss in the zircons or minor influx of younger sediment possibly from Tasmanian granites (Black *et al*, 2005). Textures seen in SEM-CL images show that the quartz grains are from a plutonic source. Both the New Mountain Sandstone and Odin Arkose Member at Mt Electra and Sperm Bluff Formation (Savage, 2005) only have one major source (Granite Harbour Intrusives). The depositional basin was probably closed to other sources except for a low amount of older sediment.

Zircon dates also show that the source of the sediment for the New Mountain Sandstone and the Odin Arkose Member of the Altar Mountain Formation is the same and did not change across the Heimdall Erosion Surface even though there was a break in sedimentation. The length of the break in deposition between the New Mountain Sandstone and Odin Arkose Member is unknown. However, as the New Mountain Sandstone was partially or totally lithified prior to erosion (see Chapter 3) it is likely that the lapse was considerable.

6.6 Summary

- The sediment of the Cross-bedded Sandstone Lithofacies (New Mountain Sandstone), Conglomerate Lithofacies and Trough Cross-bedded Lithofacies (Odin Arkose Member) have zircon U-Pb dates similar to the Granite Harbour Intrusives and are probably sourced from them.
- SEM-CL shows micro cracks and minor zoning, which supports a plutonic origin of the sediments. Vein quartz is also observed.
- Crushing of quartz grains during compaction and early cementation is easily seen by SEM-CL.
- Tectonic discrimination diagrams show that the sediment has a continental block provenance.

Chapter Seven: Depositional Environments, Sequence Stratigraphy, Nomenclature and Conclusions

7.1 Introduction

The Devonian Taylor Group is widely developed throughout southern Victoria Land and is divided by an intraformational unconformity called the Heimdall Erosion Surface. Highly quartzose sandstones dominate the lower Taylor Group, though feldspathic sandstones are observed at the base of both the New Mountain Sandstone Formation and Altar Mountain Formation. Little is known of the source for the abundant feldspar and the quartz, which the formations are composed of. Identifying the source could help determine if it changes across the Heimdall Erosion Surface. Current depositional environment interpretations of the New Mountain Sandstone and Altar Mountain Formation are based on trace fossil and sedimentary analysis and have been either done on single locations or formations or after broad reconnaissance mapping. Detailed sedimentary analysis done on several formations over a larger area in this thesis better constrains the paleoenvironment of the formations of the lower Taylor Group. This is especially important for the New Mountain Sandstone Formation, as the depositional environment of the sandstone has been under contention since research on the Beacon Supergroup began. Interpretation of the paleoenvironments of the lower Taylor Group lead to a better understanding of the formation of the Heimdall Erosion Surface, as this has had little investigation.

7.2 Deposition of the New Mountain Sandstone Formation

7.2.1 My Interpretation

The New Mountain Sandstone is interpreted as a shoreface deposit that changes up section from upper shoreface to lower shoreface, with minor aeolian deposition. This interpretation is based on the size and shape of the cross beds, trace fossils, morphology of *Heimdallia* beds and style of slumping. The aeolian deposit is interpreted as dunes

adjacent to the coastline due to the size and shape of cross beds, pinstriping and style of slumping, which is different from the slumping seen in the shoreface deposits. The Heimdall Erosion Surface truncates the New Mountain Sandstone.

7.2.2 Previous Interpretations

7.2.2a Fluvial

Barrett (1979), Plume (1982) and Woolfe (1990) interpreted the New Mountain Sandstone as a fluvial deposit.

Plume's (1982) account is based on fieldwork done in the Ferrar-Taylor Glacier region, Asgard Range and two sites in the Olympus Range on the New Mountain Subgroup (Windy Gully Sandstone, Terra Cotta Siltstone and New Mountain Sandstone). He interprets the New Mountain Sandstone as a fluvial and minor aeolian deposit but does not include specifics of field sites or location of outcrops.

Cross bedding is very abundant in the New Mountain Sandstone and the cross beds observed by Plume (1982) are described as tabular and wedge planar, tangential and angular with erosional bases, which vary from 0.1 to 7 m thick. Plume (1982) separates the cross beds into three types: Type I - 20 to 50 cm thick, Type II - 0.5 to 2 m thick with a westerly trend and Type III - 2 to 8 m thick with an east or southeast trend. He also observed red beds (observed only at Table Mountain (20 cm thick and about 50 m across)), mud cracks, primary current lineation, penecontemporaneous slumping, horizontal burrows, walking traces and *Skolithos* (near the top of the formation) in the New Mountain Sandstone (Plume, 1982).

Plume (1982) interprets Type I cross beds as deposited in crevasse splay areas of a sandy braided river due to the presence of interbedded siltstone beds. The siltstone beds were interpreted as ephemeral lakes with winds creating ripples and sub aerial exposure leading to desiccation cracks. One scour and fill channel was observed in Type I cross bedding (25 cm deep and 50 cm wide) (Plume, 1982). Plume (1982) suggests Type II cross bedding was formed in a braided sandy river system, as shown by form of the cross beds (dip, thickness, lateral persistence), unimodal distribution of the paleocurrent direction, primary current lineation and thin siltstone interbeds. Type III cross beds are

interpreted as aeolian due to frosting of quartz grains, well sorted sediment, cross bed size and shape and paleocurrent pattern (Plume, 1982). He interprets the upper and middle parts of the New Mountain Sandstone as deposited by a sandy braided river (because they contain Type I and II cross beds). Important in his interpretation are olive green siltstone beds that are laterally persistent at the base of the formation (Plume, 1982). He argues that the presence of primary current lineation found in the New Mountain Sandstone shows disequilibrium in flow regime. This is because dunes (leading to formation of cross beds) and primary current lineation cannot be formed under the same flow conditions and therefore there must be a variation in flow conditions like those found in a river.

The location of the fieldwork done by Plume (1982) is principally to the south of my field area. The size of the cross beds and paleocurrent directions given by Plume (1982) could correspond with cross beds found in the lithofacies of the New Mountain Sandstone in my field area. However, he provides no sedimentological information on the lithofacies in which the cross beds were observed in. His Type I cross beds may match with those observed in the Pebbly Sandstone and Granule Cross-bedded Lithofacies, because they are a similar thickness (20 to 50 cm thick). However, no paleocurrent data is included in Plume (1982) for Type I cross beds and no indication of whether they are pebbly. Type II cross beds may correlate with cross beds within the Cross-bedded Sandstone Lithofacies because they are 0.5 to 2 m thick and have a westerly trend similar to the CSL (Fig 3-7C, D; 3-12B, C; 3-17A). Type III cross bedding probably corresponds with the Pinstripe Cross-bedded Lithofacies due to the thickness of the cross beds (2 to 8 m thick) and similar textural features. Plume's (1982) Type III cross beds have an east or southeast trend, which is different from the Pinstripe Cross-bedded Lithofacies at Lake Vashka, however this could be due to small sample size. Plume (1982) interprets Type III cross beds as aeolian, a conclusion consistent with my interpretation of the Pinstripe Cross-bedded Lithofacies (see Chapter 3).

The scale and paleocurrent directions of the Type I and II cross beds of Plume (1982) in the New Mountain Sandstone appear to correspond with lithofacies in my field area but the paleoenvironment interpretations are different. Plume's (1982) interpretation

relies on siltstone lithologies, scour channels, primary current lineation, desiccation cracks and symmetric ripple marks. No mention is made of pebbles or organic matter, which could have accumulated in the river sediments, or the extent of bioturbation and trace fossils. The lack of variation within the deposits of Plume (1982) could indicate that it is not a fluvial deposit. Only one scour and fill channel was recorded in Type I cross beds (Plume, 1982). This is not enough evidence for a secure interpretation of a fluvial environment and, as with the above discussion, the unit does not show much variation in facies (except between sandstone and thin siltstone) that would be expected in a braided river. Plume (1982) uses the presence of cross beds and primary current lineation as evidence for variation in flow conditions like those found in a river. Boggs (2001) however, states that parting lineations (primary current lineations) are probably related to the upper flow regime (as opposed to dunes which are formed in the lower flow regime) but the exact mechanism by which they are formed is poorly understood. The abundance of primary current lineations in Plume (1982) is unknown. If primary current lineation were not a common sedimentary structure then the interpretation of a variation in flow regime may not be valid. Plume (1982) suggests that mud cracks in the New Mountain Sandstone are subaerial desiccation cracks but also mentions that some subaqueous mud cracks may be present in the Terra Cotta Siltstone. It is difficult to differentiate between mud cracks formed by subaerial exposure and those formed in subaqueous conditions by loading, shearing (Cowan, 2001) or settling (Flower and Ives, 1946).

Barrett (1979) in a brief paper on the Taylor Group concluded that the New Mountain Sandstone was deposited in fluvial-aeolian environment. This is based on evidence given by Plume (1976, 1978, 1982). The evidence includes symmetrical ripple marks, small scale cross beds and desiccation cracks (fluvial) and large scale cross beds (aeolian) and intensely burrowed horizons (Barrett, 1979). This paper also does not include a detailed facies description.

The interpretation by Plume (1982) and Barrett (1979) of a fluvial and minor aeolian depositional environment for the New Mountain Sandstone is difficult to compare with my findings due to the distance between the two field areas. On the surface the description of the sedimentary structures are similar, however, more information on their

context within the facies observed would aid in correlation with the New Mountain Sandstone in my field area.

Woolfe (1990) used trace fossils within the Taylor Group from the Knobhead area to interpret the entire Taylor Group as non-marine. The trace fossils Woolfe (1990) used include *Beaconites, Diplichnites, Cruziana-Rusophycus* and *Skolithos*. *Diplichnites* were observed in the New Mountain Sandstone and *Skolithos* in the Altar Mountain Formation in my field area and only these ones will be focused on.

Diplichnites trackways are suggested to have been formed by trilobites, annelids, arthropods or myriapods (Bradshaw, 1981; Woolfe, 1990). Woolfe (1990) interprets *Diplichnites* as non-marine because of the association with sedimentary structures interpreted as of fluvial (and subaerial exposure) origin, including desiccation polygons, drainage rivulets, mud veneers and raindrop imprints (Plume, 1978; Woolfe *et* al, 1989; Woolfe, 1990).

Skolithos are found above the Heimdall Erosion Surface in the Olympus Range but it is unclear where Woolfe observed *Skolithos*. Woolfe (1990) suggests that *Tigillites, Cylindricum* and *Monocraterion* are junior synonyms of *Skolithos* and that diagenesis and weathering of the sandstone made it impossible to tell one type from another. Woolfe (1990) interprets *Skolithos* to be deposited in high-energy conditions due to the type of substrate it occurs in (trough cross-bedded sandstone and gritstone) but suggests that *Skolithos* may not be a marine indicator.

Overall, Woolfe (1990) suggests that trace fossils have limitations as paleoenvironment indicators because 1) similar trace fossils can be produced by different organisms, 2) each organism could produce a wide range of traces and 3) scientists are not always able to identify the trace maker. He goes on to add that ‘Although, the ichnogenera discussed can not be used to definitively distinguish marine, non-marine and subaerial environments, they do indicate biological activity within the depositional environment.’ Therefore, trace fossils reflect substrate consistency and energy conditions rather than water depth or salinity (Woolfe, 1990). However, after having indicated that trace fossils cannot be used to indicate paleoenvironment he interprets the entire Taylor

Group as non-marine based on the association of the trace fossils with interpreted fluvial deposits.

It is difficult to compare the findings of Woolfe (1990) with those herein because the distance between the two field areas is enough to create variations in the trace fossil assemblages. Woolfe (1990) also combines the entire Taylor Group in one paleoenvironment interpretation, rather than looking at separate formations. This is shown by the combination of trace fossils that are found in separate formations in my field area. Moreover, Woolfe (1990) does not include *Heimdallia,* which is one of the most abundant trace fossils in my field area and are recorded by Woolfe *et al* (1989) in the Knobhead map area. Another problem is that Woolfe (1990) does not recognize different *Skolithos* traces; those found in my field area are *Skolithos linearis* and *Skolithos sp.* and have been found in mainly marine environments (Gouramanis *et al*, 2003; Metz 2004; Mangano *et al*, 2005) while other *Skolithos* traces or the *Skolithos* ichnofacies imply marine influence but not necessarily dominantly marine environment (Trewin, 1993, 1993a; Trewin and McNamara, 1995; Uchman *et al*, 2004). Thus identifying different types of *Skolithos* is very important. By inferring that the entire Taylor Group is non-marine Woolfe (1990) has disregarded the presence of the Heimdall Erosion Surface in the middle of the group, which is found as far south as Table Mountain (Plume, 1978). The Heimdall Erosion Surface indicates a break in deposition, which means the sandstones above and below the erosion surface should be interpreted separately.

The New Mountain Sandstone in my field area is not interpreted as a fluvial deposit due to lack of organic material, fine sand or mud drapes and veneers and pebbles and gravels lags at the base of cross bed sets. The shape of the cross beds in the upper part of the New Mountain Sandstone are not similar to those found fluvial environments because they are tangential in shape, with flat bases. Slumping within the upper New Mountain Sandstone shows that the cross beds were water saturated when they were deformed and that deformation occurred across a whole bed (greater than 200 m laterally). If it were a sandy braided river deposit, slumps are likely to be confined to one cross bed set. They may vary in morphology because cross beds would be both

underwater and above the surface, creating different slump types within the deposit. The morphology of the *Heimdallia* beds throughout the New Mountain Sandstone also indicates that the depositional environment was not fluvial. This is because the *Heimdallia* beds form the bounding surface of several cross bed sets rather than only one and are not very lensoidal as might be expected if formed between dunes in a river or in pools. The other trace fossils (*Diplichnites,* scoop-like burrows, *?Metaichna* etc) may also be difficult to preserve in a high-energy environment like a braided river system

7.2.2b Aeolian

Wizevich (1997) examined the New Mountain Sandstone at Table Mountain and concluded that the formation was deposited in primarily an aeolian environment with subordinate fluvial and lacustrine deposition. Wizevich (1997) divides the New Mountain Sandstone at Table Mountain into three facies associations: lower, middle and upper.

The lower facies association (LFA) was interpreted as deposited in an aeolian environment with wet interdune areas and braided streams that periodically flooded the aeolian plain (Wizevich, 1997). The interpreted aeolian deposits are characterized by quartzose trough to tangential cross beds (up to 1 m thick) with foresets made of wind ripple laminae and grain flow strata, parallel laminated sandstone and rare mudstone laminae (Wizevich, 1997). The deposits also include adhesion, current and wave ripples, *Heimdallia, Diplichnites, Skolithos,* and *Cylindricum* (Wizevich, 1997). The units interpreted as braided stream deposits are composed of trough cross-bedded and horizontally laminated feldspar rich sandstone (20 to 50 cm thick) with thin gravel lags at the base (Wizevich, 1997). Ripple cross-laminations and mudstone beds are recorded in the lower part of the interpreted braided river deposits (Wizevich, 1997). Paleocurrents in the LFA indicate flow towards the east (Wizevich, 1997).

The middle facies association (MFA) was interpreted as deposited in a large dune field with interdune deposits (Wizevich, 1997). The deposits are primarily composed of planar to tangential cross-bedded (up to 9 m thick), pinstriped (inversely graded) fine to medium sandstone (Wizevich, 1997). Other deposits include low angle cross-laminated sandstone; horizontally laminated sandstone; mud beds with desiccation cracks; adhesion,

wave and current ripple marks; slumps and featureless sandstone in channel and tabular shapes often inversely graded (Wizevich, 1997). *Diplichnites, Skolithos, Beaconites* and *Cylindricum* trace fossils are found in MFA (Wizevich, 1997). The primary deposit is interpreted as deposition in transverse aeolian dunes (Wizevich, 1997). The other deposits are interpreted as deposition at the base of dunes, in interdune areas and as sandy gravity flows respectively (Wizevich, 1997). Paleocurrents in the MFA are predominantly to the west (Wizevich, 1997).

The upper facies association (UFA) was interpreted as deposited in a mixed aeolian and fluvial environment (Wizevich, 1997). Bioturbation obliterates much of the sedimentary structures (Wizevich, 1997). Low angle cross laminations with abundant *Skolithos* are interpreted as aeolian deposits (Wizevich, 1997). Tangential cross-bedded sandstone (1 to 2 m thick) with rare basal breccia is interpreted as a braided fluvial deposit (Wizevich, 1997).

There are no sedimentary structures diagnostic of a fluvial environment associated with the interpreted braided river deposits in the LFA and it seems their association with the interpreted aeolian deposits is the reason they have been interpreted as fluvial. The lower facies association (LFA) of Wizevich (1997) is similar to the lithofacies of the New Mountain Sandstone in this thesis. The braided river deposits of the LFA are similar to the Pebble Sandstone and Granule Sandstone Lithofacies with similar size of cross beds, feldspathic composition, *Heimdallia* and presence of pebbles. The interpreted aeolian deposits are similar to the Cross-bedded Sandstone Lithofacies (in my field area) in cross bed size, ripples, sorting and trace fossils. However, wind ripple laminae, grainflow strata and horizontally laminated sandstone are not observed in the CSL further north and are typical of aeolian deposits, which is likely why part of the LFA was interpreted as an aeolian deposit.

The interpreted aeolian deposits of the MFA are similar to the Pinstripe Cross-bedded Lithofacies at Lake Vashka. The size of the cross beds is similar and also the pinstriping. However, other sedimentary structures observed in the MFA were not observed at Lake Vashka. This could be due to the limited outcrop at Lake Vashka. The

Pinstripe Cross-bedded Lithofacies also contains none of the trace fossils found in the MFA.

Wizevich (1997) does not record the type of *Skolithos* found in the New Mountain Sandstone at Table Mountain. The variety of *Skolithos* trace is important as outlined in Chapter 5.2.2, 5.6 and 7.2.2a.

The lithofacies of the New Mountain Sandstone in the north have similarities to the LFA and MFA of Wizevich (1997) at Table Mountain in the south. The LFA is likely equivalent to the Pebbly Sandstone, Granule Cross-bedded and Cross-bedded Sandstone Lithofacies and the MFA is likely equivalent to the Pinstripe Cross-bedded Lithofacies. However, there are also many differences between the lithofacies. The distance between Table Mountain and Olympus Range could create the variation between the facies in each area and even variation in the depositional environment. Wizevich studied only one locality and therefore the extension of his conclusions to the whole of SVL is of doubtful validity.

The bulk of New Mountain Sandstone in my field area was not interpreted as aeolian because the type of slumping indicates the presence of water, the low degree of sorting (would expect extremely well sorted sand) and lack of frosted grains. The morphology of the *Heimdallia* beds is also important. They are not lensoidal shaped are would be expected if they were formed between aeolian dunes. Trace fossils are well preserved in the New Mountain Sandstone and this may be unlikely in an aeolian environment. The Pinstripe Cross-bedded Lithofacies of the New Mountain Sandstone that was interpreted as aeolian is due to pinstriping, different slumping type and cross bed size.

7.2.2c Shallow Marine

Barrett and Kohn (1975) did fieldwork between the Mackay and Taylor Glaciers and are some of the only authors who have data from within my field area. They suggest the New Mountain Sandstone was deposited by the migration of large sand waves in a shallow sea. This is supported by the size (0.5 to 2.5 m thick) and shape of the cross beds (trough in shape and 5 to 10 m across with foresets that curve downwards to a tangential

base), foreset dip (15º) and the penecontemporaneous slumping (Barrett and Kohn, 1975). Paleocurrents from the New Mountain Sandstone indicate flow to the northwest and northeast in the lower 150 m (Windy Gully and Terra Cotta) and south for the upper 100 m (Barrett and Kohn, 1975). The New Mountain Sandstone described above is very similar to the Cross-bedded Sandstone Lithofacies. Though the paleocurrent directions do not match up very well, the facies description is similar.

Bradshaw (1981) interprets the New Mountain Sandstone as marine due to cross beds (quartzose medium to coarse sandstone in sets 0.5 to 2 m thick) and horizontal layers of intensely bioturbated sandstones. Bradshaw (1981) did fieldwork over southern Victoria Land and included sites within my field area. The depositional environment is interpreted as tidally affected sand flats laced with channels; paleocurrent variations are interpreted as due to tide and wave action. *Heimdallia* and *Diplichnites* are taken to suggest subaqueous deposition. This description is similar to the Cross-bedded Sandstone Lithofacies but has been interpreted in this thesis as shoreface rather than sand flats due to the lack of mud.

7.3 Heimdall Erosion Surface

7.3.1 My Interpretation

The Heimdall Erosion Surface was probably formed due to relative sea level fall leading to regression and exposure of the large area of southern Victoria Land. I interpret the convergence of the HES with the basal Kukri Erosion Surface due to irregularities in the basal unconformity. The amount of material eroded from the underlying New Mountain Sandstone is unknown. The Heimdall Erosion Surface became a shore platform as relative sea level rose after an unconstrained amount of time.

7.3.2 Previous Interpretations

McKelvey *et al* (1970) first recognized the Heimdall Erosion Surface in Beacon Supergroup between the Olympus and Boomerang Ranges. They made no interpretations on how the surface was formed.

McKelvey *et al* (1977) describe the Heimdall Erosion Surface, between the Mackay Glacier and Boomerang Range, as a fossil surface with local relief. They suggest the surface has a paleoslope to the south and southeast. Though they offer no explanation for the formation of the Heimdall Erosion Surface they recognize irregularities in the Kukri Erosion Surface and suggest they are due to the paleoslope on the surface and that there is no evidence of faulting on the KES post formation. McKelvey *et al* (1977) highlight the variation in thickness of the Taylor Group formations between the two unconformities and record convergence with the Kukri Erosion Surface at Vashka Crag, Wheeler Valley, Balham Valley and Packhard Glacier.

Bradshaw (1981) interprets formation of the Heimdall Erosion Surface as due to relative uplift of the basement in the Balham Valley region. Bradshaw (1981, Fig 12) indicates a high in the Balham Valley due to convergence of the Heimdall Erosion Surface and the basal Kukri Erosion Surface but makes no other interpretations in regard to the Heimdall Erosion Surface.

The location of the Heimdall Erosion Surface in McKelvey *et al* (1970, 1977) and Bradshaw (1981) and description by McKelvey *et al* (1977) are consistent with observations of the erosion surface made in my field area. The surface was observed between the New Mountain Sandstone and Altar Mountain Formation and converging with the basal Kukri Erosion Surface. The truncation of the KES by the HES is observed at the same localities as Bradshaw (1981) and McKelvey *et al* (1977). Further investigation of the section of Balham Valley support the proposal put forward by Bradshaw (1981) for the Balham Valley high.

7.4 Depositional Setting and Correlation of the Altar Mountain Formation

7.4.1 My Interpretation

The Altar Mountain Formation with its Odin Arkose Member is interpreted as deposited on the Heimdall Erosion Surface as a shallow marine to inner shelf deposit. The Odin Arkose Member is a shoreface deposit due to the size and shape of the cross

beds, presence of pebbles and coarse material and dense *Skolithos*. A basal lag occurs directly on the Heimdall Erosion Surface at the base of the Odin Arkose Member. The Altar Mountain Formation is the shallow marine to inner shelf deposit due to *Skolithos*, cross beds, muddy sandstone, mud layers and massive and bedded sandstones. The formation changes upwards to an estuarine or intertidal deposit due to polygonal cracks, mud rip ups and thick and thinly bedded sandstone.

7.4.2 Previous Interpretations

Barrett and Kohn (1975) described the basal Odin Arkose Member of the Altar Mountain Formation as a feldspathic sandstone and grit with trough cross beds and pebbles deposited on the Heimdall Erosion Surface. Paleocurrents from the Odin Arkose Member showed flow predominantly towards the southeast (Barrett and Kohn, 1975). The Odin Arkose Member was interpreted as deposited by low sinuosity streams flowing southwards in response to uplift in the north (Barrett and Kohn, 1975). The rest of the overlying Altar Mountain Formation is a trough cross-bedded sandstone (flow predominantly to the northwest) with burrowed red and green siltstone and mud cracks. Barrett and Kohn (1975) interpreted the Altar Mountain as the result of non-marine deposition, possibly in a coastal environment. They did not, however, include any trace fossil data that points to marine origin. The facies descriptions of the Altar Mountain Formation and Odin Arkose Member are similar to the Trough Cross-bedded and Cross-bedded Bioturbated Lithofacies in my field area. Paleoenvironment interpretations in this thesis are different, due to recognition of marine trace fossils, but Barrett and Kohn (1975) recognized the influence of marine processes in the depositional environment.

Bradshaw (1981) described the Odin Arkose Member as trough cross-bedded feldsarenite, with conglomerates and siltstones. The member grades up into the Altar Mountain Formation, which is composed of small scale cross beds with *Tigillites*, *Diplocraterion* and *Skolithos.* The Altar Mountain Formation and Odin Arkose Member were interpreted as deposited in a shallow marine environment due to trace fossils and facies (Bradshaw, 1981). This description and interpretation agrees with the interpretation put forward in this thesis.

Savage (2005) correlated the Sperm Bluff Formation (formerly Sperm Bluff Conglomerate and the Informal Queer Member (Turnbull *et al*, 1994)) with the Odin Arkose Member of the Altar Mountain Formation. Her fieldwork was based in the Bull Pass – St Johns Range map area of Turnbull *et al* (1994). The correlation in Savage (2005) was based on then published data and interpretations on arkosic units in the Taylor Group. Only the basal Kukri Erosion Surface was observed in the field (Savage, 2005).

The Conglomerate Lithofacies Association sits directly on the basement of Granite Harbour Intrusives on the convergent Kukri and Heimdall Erosion Surface. It is a medium to coarse arkose to subarkose, with polymict conglomerate layers and trough and tabular cross beds (Savage, 2005). The lithofacies also contains shale and mudstone layers, granules, scattered pebbles and *Heimdallia, Diplichnites,* and *Zoophycus* trace fossils (Savage, 2005). Paleocurrent orientations are widespread but mainly trend to the east and west. The variation in paleocurrents is interpreted as the result of dominant long shore currents with variations caused by tidal influence (Savage, 2005). The Conglomerate Lithofacies Association has been interpreted as a deltaic deposit and is correlated with the Odin Arkose Member of the Altar Mountain Formation (Savage, 2005).

At one locality, the Interbedded Siltstone/Sandstone Lithofacies (formerly the Informal Queer Member of Turnbull *et* al, 1994) was deposited directly on the basement then overlain by the Conglomerate Lithofacies Association. The lithofacies is composed of alternating siltstone (grey, green-grey, brown, purplish-black and dark purpley brown) and cross-bedded sandstone beds (pink, whitish and green) (Savage, 2005). The sandstone contains vein quartz, alkali feldspar and rhyolite granules. Flaser bedding, pinch and swell morphologies, mud drapes, siltstone rip up clasts, syneresis cracks, finely laminated siltstone and sandstone and lenticular ripples are also present (Savage, 2005). Paleocurrent directions show flow to the south but are variable. Savage (2005) has interpreted the lithofacies as deposited in an estuarine or lagoon setting lateral to the Conglomerate Lithofacies Association.

Savage (2005) describes the Parallel-bedded Sandstone Lithofacies, which interfingers with the Conglomerate Lithofacies Association as containing massive and cross-bedded (up to 3 m thick) fine to medium sandstone with occasional quartzose, very coarse sandstone beds (Savage, 2005). *Diplocraterion, Didymaulyponomos, Heimdallia*, *Diplichnites*, *Tigillites*, *Skolithos* and U-shaped burrows are observed in this lithofacies (Savage, 2005). Paleocurrents show flow to the northeast but the sample size is very small. The Parallel-bedded Sandstone Lithofacies is interpreted as a shallow marine deposit and is correlated with the Altar Mountain Formation (Savage, 2005).

Overlying the Conglomerate Lithofacies Association and Parallel-bedded Sandstone Lithofacies at Mt Suess, is the Low-angle Cross-bedded Lithofacies, which has been interpreted as correlative with the Arena Sandstone Formation due to the presence of the characteristic sediments (medium to fine sandstone with clay cement) and *Beaconites antarcticus* trace fossils (Savage, 2005; M. Bradshaw, pers comms, 2008).

As mentioned above, Savage's (2005) interpretations are based on information then available on feldspathic units within the Taylor Group. At that time there was no significant information on the feldspathic and pebbly unit at the base of the New Mountain Sandstone and now that this has been recognized, there is a need to reconsider the correlation of the facies described by Savage. In addition, observation of only one erosion surface (Kukri Erosion Surface) makes correlation difficult because the lack of an upper contact to the sedimentary package also makes it difficult to establish whether the sediments were deposited above or below the Heimdall Erosion Surface (Fig 2-1). The Sperm Bluff Formation (Savage, 2005) could therefore be correlated to the lower New Mountain Sandstone or to the Odin Arkose Member of the Altar Mountain Formation.

The Interbedded Siltstone/Sandstone Lithofacies could be also be correlated with the Terra Cotta Siltstone, which has been interpreted as lagoon by Bradshaw (1981). If it were, the overlying lithofacies could be the New Mountain Sandstone due to the stratigraphic succession observed elsewhere in southern Victoria Land (Fig 2-1). If this were so, the underlying Windy Gully Sandstone is missing due to the Terra Cotta Siltstone being deposited directly on the basement.

The Conglomerate Lithofacies Association of the Sperm Bluff Formation could be correlated with the lower New Mountain Sandstone due to its feldspathic nature, presence of pebbles, trace fossils and proximity to the Kukri Erosion Surface. The amount of pebbles and feldspar in the Conglomerate Lithofacies Association is greater than in the lower New Mountain Sandstone in my field area but this could be due to lateral variation over SVL. Pebbles in the Basal Conglomerate Lithofacies (this thesis) include quartz with rod-like crystals, which is similar to those found in the Conglomerate Lithofacies Association of Savage (2005). However, rhyolites, which are very common in the Conglomerate Lithofacies Association (Savage, 2005), are rare or absent in the Basal Conglomerate Lithofacies (this thesis). Mudstone layers are also found very rarely in the New Mountain Sandstone in my field area. *Heimdallia* and *Diplichnites* are observed in the New Mountain Sandstone in my field area. These match trace fossils within the Conglomerate Lithofacies Association (Savage, 2005) and could aid in correlation with the New Mountain Sandstone because *Heimdallia* and *Diplichnites* are not found in the Altar Mountain Formation or Odin Arkose Member. If the Conglomerate Lithofacies Association were equivalent to the New Mountain Sandstone, this would indicate a change across the paleoenvironment from deltaic to shallow marine (shoreface) to the west.

The Parallel-bedded Sandstone Lithofacies could be correlated to the upper New Mountain Sandstone in my field area. Trace fossils found in the Parallel-bedded Sandstone Lithofacies are a mixture of those observed above and below the Heimdall Erosion Surface in the Olympus Range. *Heimdallia* in the Parallel-bedded Sandstone Lithofacies of Savage (2005) occur as densely burrowed horizons, whereas the *Skolithos* is only observed as faint single traces (M. Bradshaw, pers comms, 2008). The density of bioturbation is indicative of a depositional environment that favoured *Heimdallia* over *Skolithos.* A depositional environment more suited to *Heimdallia* was in existence in my field area, because the beds are denser and more pervasive. Although faint *Skolithos* are present, they do not provide a strong environment indicator because they are not the dominant trace present. The cross bed size and shape within the Parallel-bedded Sandstone Lithofacies is also similar to the upper New Mountain Sandstone in my field area.

However, the uppermost unit of Savage's (2005) Sperm Bluff Formation (the Low-angle Cross-bedded Sandstone Lithofacies) is quite different from my New Mountain Sandstone. The clay matrix and *Beaconites antarcticus* trace fossils are more typical of the Arena Sandstone Formation and Savage (2005) correlated the uppermost lithofacies with that. The Low-angle Cross-bedded Sandstone Lithofacies was only observed at Mt Suess. The lithofacies could overlie the Sperm Bluff Formation elsewhere in her field area but the pervasive nature of the dolerite sills has truncated the top of her measured sections. As the Low-angle Cross-bedded Lithofacies (Arena Sandstone Formation) conformably overlies the other lithofacies of the Sperm Bluff Formation at Mt Suess it supports the correlation of the Sperm Bluff Formation with the Altar Mountain. This is because no unconformity was observed between the Sperm Bluff Formation and Arena Sandstone so it can be assumed the two are conformable. Elsewhere in southern Victoria Land the Arena Sandstone conformably overlies the Altar Mountain Formation (Fig 2-1).

Although the New Mountain Sandstone and Sperm Bluff Formation are similar in lithology, trace fossils and paleocurrent directions correlation of the two remains ambiguous due to observation of a single erosion surface and the deposition of a unit very similar to the Arena Sandstone Formation conformably on top of the Sperm Bluff Formation. Trace fossils may not provide a valid means of correlating the two formations and the abundance of trace fossils observed by Savage (2005) appear to be less than in my field area. For the purposes of the block diagrams in the Chapter 7.5, I have agreed with Savage's (2005) correlation of the Sperm Bluff Formation with the Altar Mountain Formation. Possible correlation of the Sperm Bluff Formation with the New Mountain Sandstone needs to be kept open due to facies and trace fossil similarities. Until an upper contact is found or examination of a linking area, possibly at Bull Pass, is examined the above correlation stands.

7.5 Depositional Environment and Sequence Stratigraphy

The lithofacies of the New Mountain Sandstone represent deposition in a shallow marine environment. This is followed by sea level fall and erosion to form the Heimdall Erosion Surface. Deposited on the erosion surface is another cycle of rising and falling seas made up of the lithofacies of the Altar Mountain Formation and its basal Odin Arkose Member.

The Kukri Erosion Surface underlies the Taylor Group throughout my field area and is observed at the base of the Windy Gully Sandstone and New Mountain Sandstone. The New Mountain Sandstone is deposited directly on the Kukri Erosion Surface at Lake Vashka, Sponsors Peak and Vashka Crag. The KES has a large amount of relief.

The Basal Conglomerate Lithofacies of the New Mountain Sandstone was deposited both before and laterally coeval with deposition of the overlying lithofacies. The clasts within the lithofacies have been transported to the depositional site as shown by rounding and deposition of clasts on basement that is often of a different composition. The size of the boulders, especially at Lake Vashka, gives an indication of the large amount of relief on the Kukri Erosion Surface. The boulders have most likely been sourced from highs in the KES.

The Pebbly Sandstone and Granule Cross-bedded Lithofacies were deposited in a shallow marine environment similar to the upper to middle shoreface (Fig 7-1B). The two lithofacies are laterally correlative with each other (Fig 7-2, 7-3). The Pinstripe Cross-bedded Lithofacies was deposited at the same time at Lake Vashka due to similarities in composition (Fig 3-18) and location relative to the Kukri Erosion Surface (Fig 7-1B). Trough cross beds in the PSL and GCL were deposited by longshore currents flowing from the west moving sediment eastwards along the coastline aligned east-west between Balham Lake and Sponsors Peak (including Vashka Crag). Rip currents and wave action probably created variations in cross bed orientations. The lithofacies were deposited on underlying formations (Terra Cotta Siltstone and Windy Gully Sandstone) or where there were highs on the Kukri Erosion Surface. The depositional environment of the Granule Cross-bedded Lithofacies included periods of lower energy or non-deposition, which led

to bioturbation by *Heimdallia*. Variations in the PSL and GCL across the field area are due to variations in water depth, which can be expected in a shallow marine environment over a large area. The Pinstripe Cross-bedded Lithofacies is an aeolian deposit. The lithofacies was probably deposited by winds blowing northwards in dunes adjacent to the coastline (Fig 7-1B). The area to the north, including Sponsors Peak, Queer Mountain and Mt Suess, was exposed and being eroded and may have supplied sediment to the marine area. The Pebbly Sandstone and Granule Cross-bedded Lithofacies represent the beginning of a transgressive systems tract (Boggs, 2001; Coe and Church, 2003). This is characterized by marine sediments, which build in a landward direction (Boggs, 2001).

The Cross-bedded Sandstone Lithofacies was deposited next indicating relative sea level rise and migration of the coastline to the north (Fig 7-1C). The sandstone was deposited on the underlying PSL, GCL or basement rocks on Kukri Erosion Surface highs. The coastline moved north to include Sponsors Peak but aeolian deposition was still probably occurring at Lake Vashka (Fig 7-1C). The lithofacies is interpreted as deposited in the lower shoreface with the cross beds created by longshore currents flowing towards the west. Variations in paleocurrent directions also probably occurred due to rip currents and wave action. Relatively deeper water and/or periods of lower energy led to *Heimdallia* colonisation and other trace fossil formation. Slumping of the cross bed sets occurred due to shaking events indicated by the lateral extent of the slumped horizons. Slumping of single cross bed set was due to oversteepening or removal of support. Ripples were probably deposited by eddies over the crest of the sub-aqueous dunes or variations in current directions. The Cross-bedded Sandstone Lithofacies was deposited in a highstand systems tract.

Falling sea level is recorded at Mt Jason in the New Mountain Sandstone is shown by the presence of mud cracks and finer sediments. This shows the onset of relative sea level fall, which then led to exposure of the entire area and erosion by the Heimdall Erosion Surface and so, is interpreted as a regressive systems tract.

If the correlation of the Sperm Bluff Formation (Savage, 2005) with the Altar Mountain Formation is correct then there is no New Mountain Sandstone recorded at Mt

Cerberus and other locations to the northeast across the Bull Pass (Savage, 2005). If there is no intervening fault, the proximity to the Olympus Range suggests there may have been deposition of New Mountain Sandstone on a basement high that was subsequently eroded by the Heimdall Erosion Surface. Therefore, there is only a record of formations deposited above the Heimdall Erosion Surface in the Bull Pass-St Johns Range map area (Turnbull *et* al, 1994; Savage, 2005).

The Heimdall Erosion Surface was formed due to a drop in sea level (Fig 7-1D). The entire field area was exposed and the surface eroded removing both sediments and basement (Fig 7-2, 7-3). The removal of basement rocks from highs in the Kukri Erosion Surface caused the two erosion surfaces to appear to converge (Fig 7-2, 7-3, 7-4). The Cross-bedded Sandstone Lithofacies was partially or totally lithified before erosion allowing water to erode along the foreset beds creating an irregular pattern. The surface is clean indicating there was not prolonged exposure (leading to soil development) or the surface was cleaned before deposition of the overlying lithofacies. It is unknown how much of the New Mountain Sandstone has been removed by erosion. The Heimdall Erosion Surface is a sequence boundary shown by a fall in sea level and erosion of the underlying alluvial and coastal facies (Boggs, 2001; Coe and Church, 2003). It is probably a Type 1 sequence boundary (Boggs, 2001).

As sea level rose again, the Heimdall Erosion Surface became an eroding shore platform and the depositional environment once again reverted to shallow marine. The Conglomerate and Trough Cross-bedded Lithofacies of the Odin Arkose Member are interpreted as deposited on the shoreface in a high-energy environment leading to *Skolithos* colonisation (Fig 7-1E). The Conglomerate Lithofacies is a lag that was deposited directly on the shore platform (Heimdall Erosion Surface) by waves and currents. Sandstone pebbles from the Conglomerate Lithofacies were not sourced from the underlying New Mountain Sandstone but could have been sourced from older formations in the Taylor Group exposed laterally or exotic sandstones transported into the basin by longshore currents. The quartz, quartzite and feldspar pebbles are from the basement Granite Harbour Intrusives. The Trough Cross-bedded Lithofacies is interpreted as deposited in a shallow marine environment with currents flowing to the

west as the sea gradually moved across the shore platform and water deepened. The two lithofacies of the Odin Arkose Member represent deposition in a transgressive systems tract (Boggs, 2001; Coe and Church, 2003).

Both lithofacies are laterally equivalent to the Sperm Bluff Formation of Savage (2005). Savage (2005) interpreted this as a delta environment with associated lateral shoaling. The correlation of the Sperm Bluff Formation (Savage, 2005) with the Conglomerate and Trough Cross-bedded Lithofacies shows changing of the environment from deltaic in the east to shallow marine west across southern Victoria Land (Fig 7-1E).

The Cross-bedded Bioturbated Lithofacies, of the Altar Mountain Formation, was deposited in a shallow marine to inner shelf environment (Fig 7-1F) as sea level continued to gradually rise across the field area. It was a high energy environment that formed cross beds and lead to *Skolithos* colonization, alternating with a low energy environment that lead to the formation of massive, bedded and muddy units. The lithofacies is probably correlative with the Sperm Bluff Formation of Savage (2005). The Cross-bedded Bioturbated Lithofacies and Sperm Bluff Formation record sea level rise across the whole of the Olympus Range and Bull Pass-St Johns Range region. The Cross-bedded Bioturbated Lithofacies represents deposition in a highstand systems tract (Boggs, 2001; Coe and Church, 2003).

Relative sea level fall is recorded at Mt Electra by the Bedded Fine Lithofacies. This is a shallow water deposit shown by the sedimentary structures that record exposure to the air. This drop in sea level may have occurred across the whole field area but a larger section was measured at Mt Electra so it was only seen there. The Bedded Fine Lithofacies represents a regressive systems tract.

According to interpretations in this thesis deposition of the New Mountain Sandstone Formation across southern Victoria Land occurred in a shallow sea. The marine environment existed from the Olympus Range, southwards in the Asgard Range and included Vashka Crag. Quartz and feldspathic sediment was supplied from the exposed basement to the north (around Sponsors Peak) and northeast (around Mt Suess). Longshore currents transported sediment and created sub aqueous cross beds. As relative

sea level fell due to tectonic uplift or eustatic process the depositional environment changed to intertidal or estuarine as recorded at Mt Jason. Continual relative sea level fall led to exposure of the large proportion of southern Victoria Land, from Sponsors Peak to at least the Asgard Range, and formation of the Heimdall Erosion Surface. However, from correlation with adjacent areas it appears deposition of the New Mountain Sandstone continued further south as shown by the gradational contact between the New Mountain Sandstone and overlying Altar Mountain Formation. Relative sea level rise led to inundation of the Olympus Range and Bull Pass-St johns Range area again and deposition of the Altar Mountain Formation. The basal Odin Arkose Member was deposited in shallow seas with deltas to the east (in the Bull Pass-St Johns Range area) feeding feldspathic sediment into the depositional basin. Longshore currents once more dominated the depositional environment. As relative sea level continued to rise across the area the delta region in the east was drowned and shallow marine to inner shelf environment led to deposition of the rest of the Altar Mountain Formation. Correlation with previous work shows that this environment existed over southern Victoria Land, from Sponsors Peak in the north to Rotunda in the south.

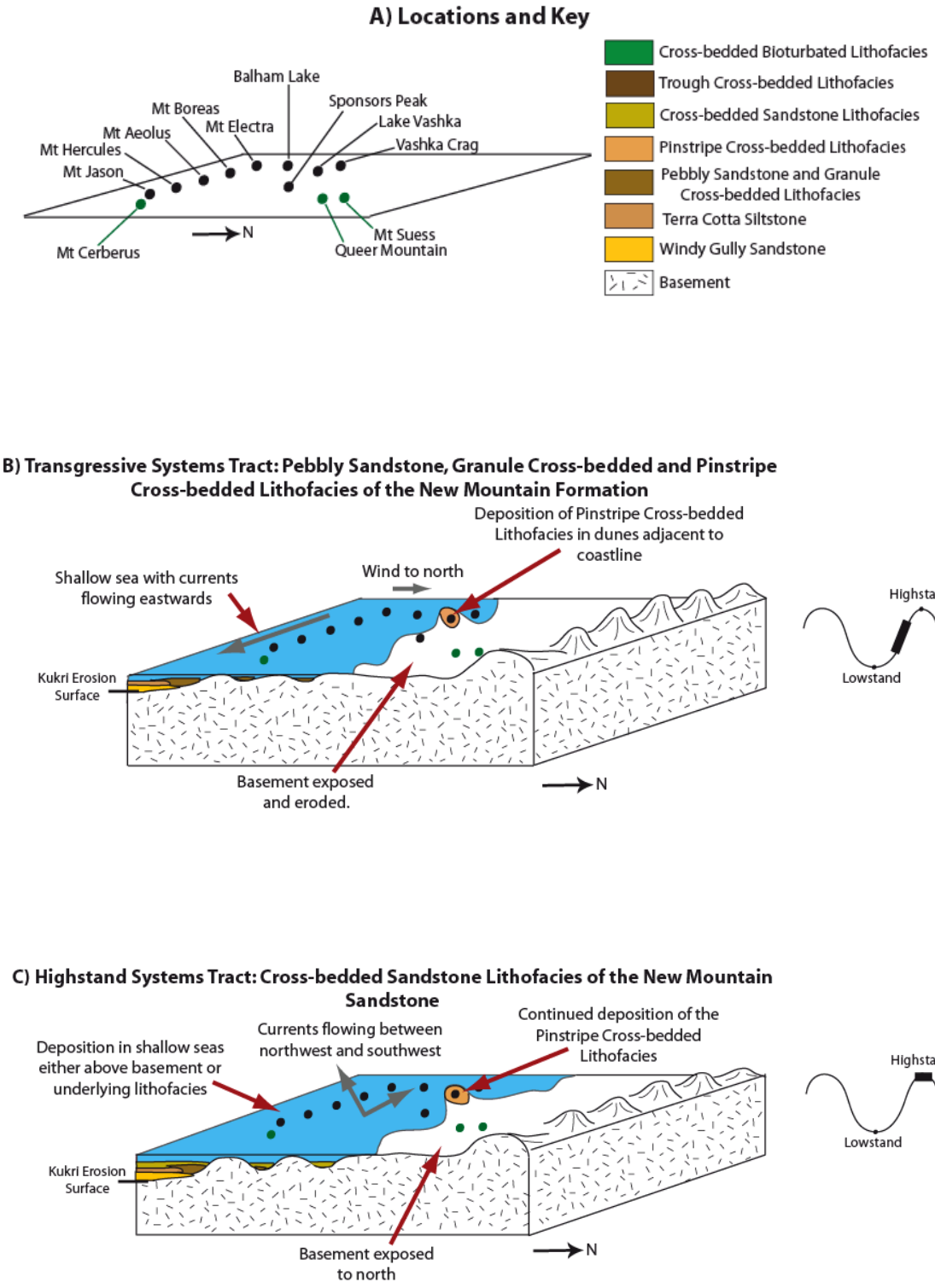

Figure 7-1: Depositional environment of the New Mountain Sandstone and overlying Altar Mountain Formation and Odin Arkose Member including formation of the Heimdall Erosion Surface.

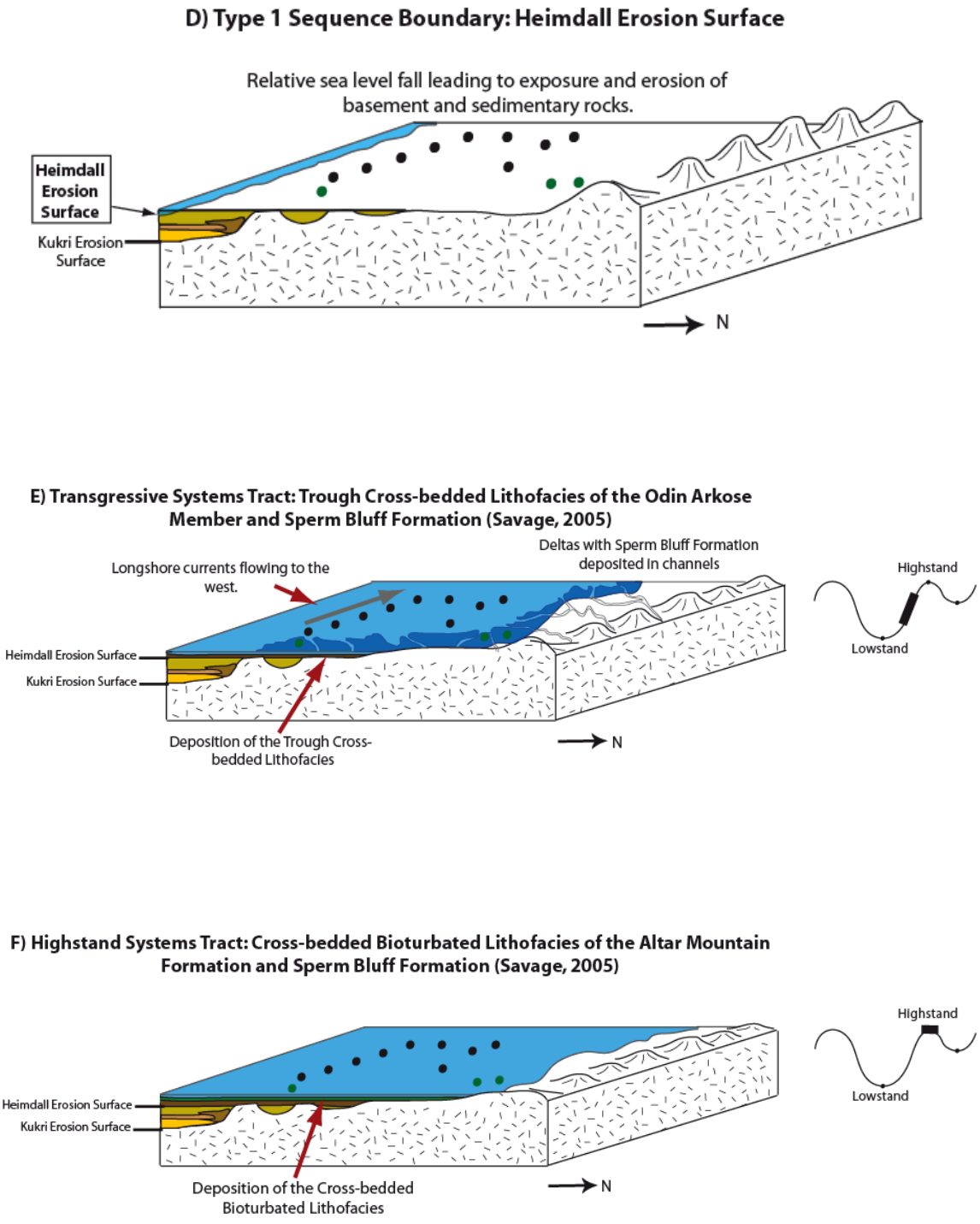

Figure 7-1: Depositional environment of the New Mountain Sandstone and overlying Altar Mountain Formation and Odin Arkose Member including formation of the Heimdall Erosion Surface.

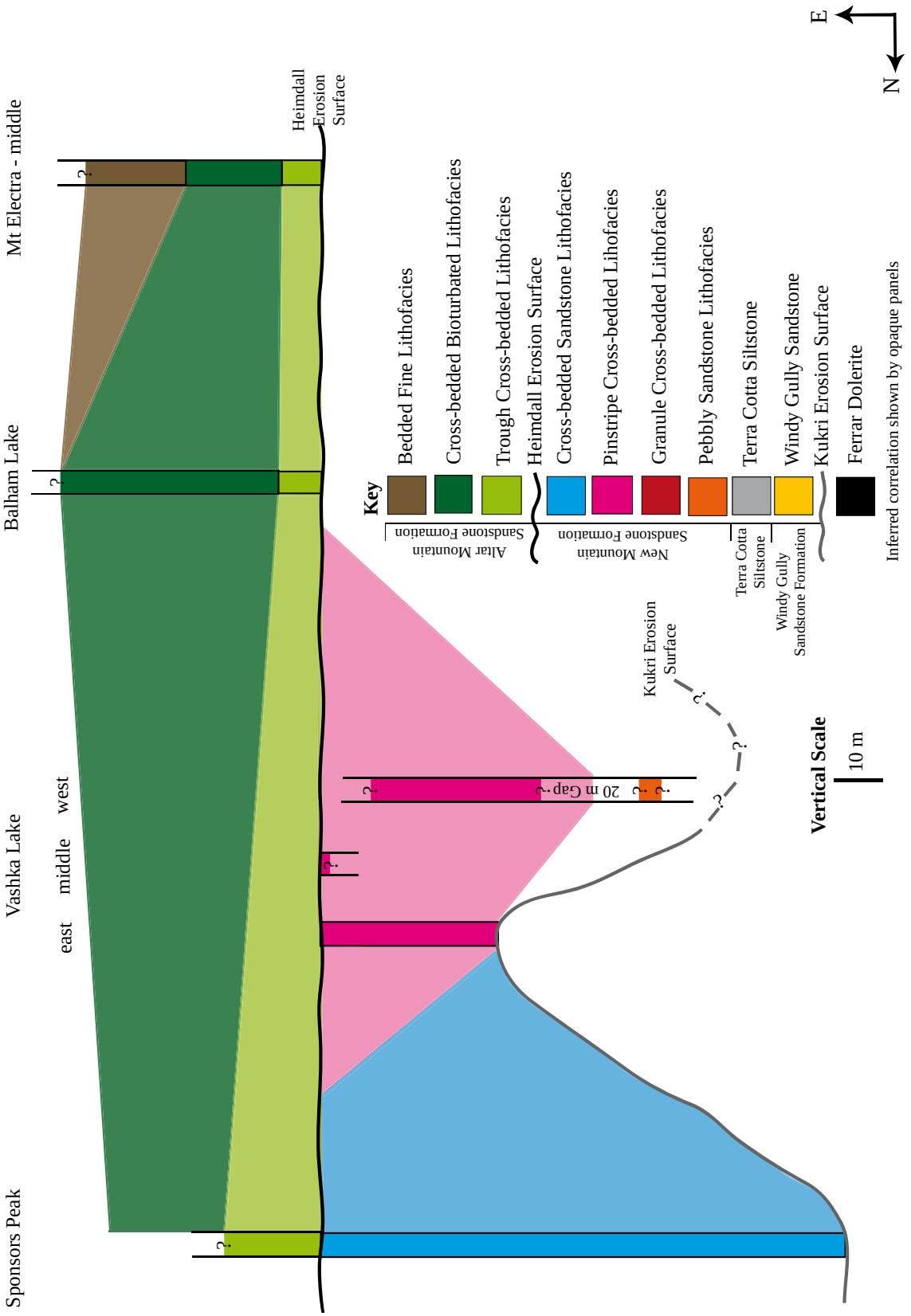

Figure 7-2: Correlation of stratigraphy north-south through field area.

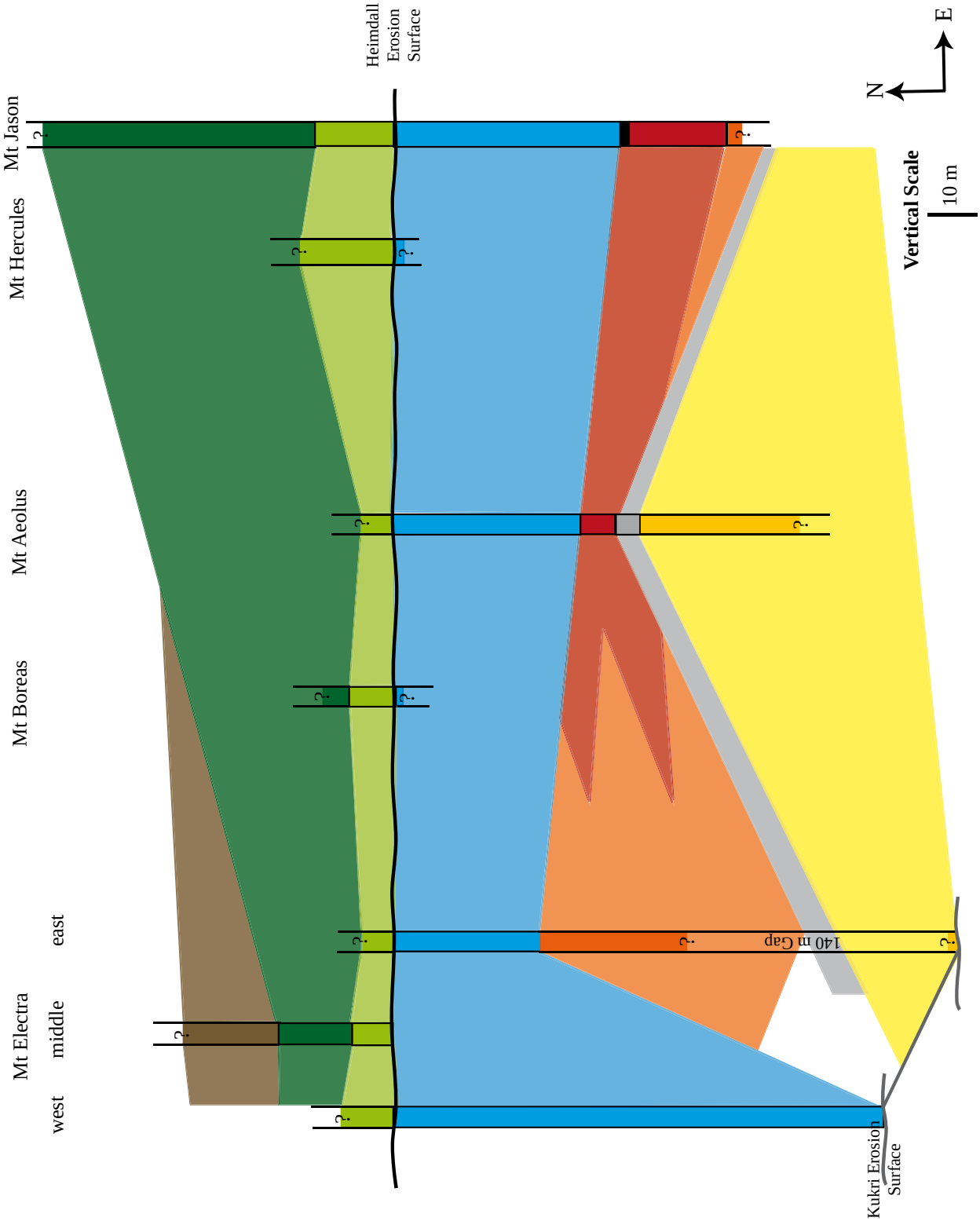

Figure 7-3: Correlation of stratigraphy east-west along Olympus Range.

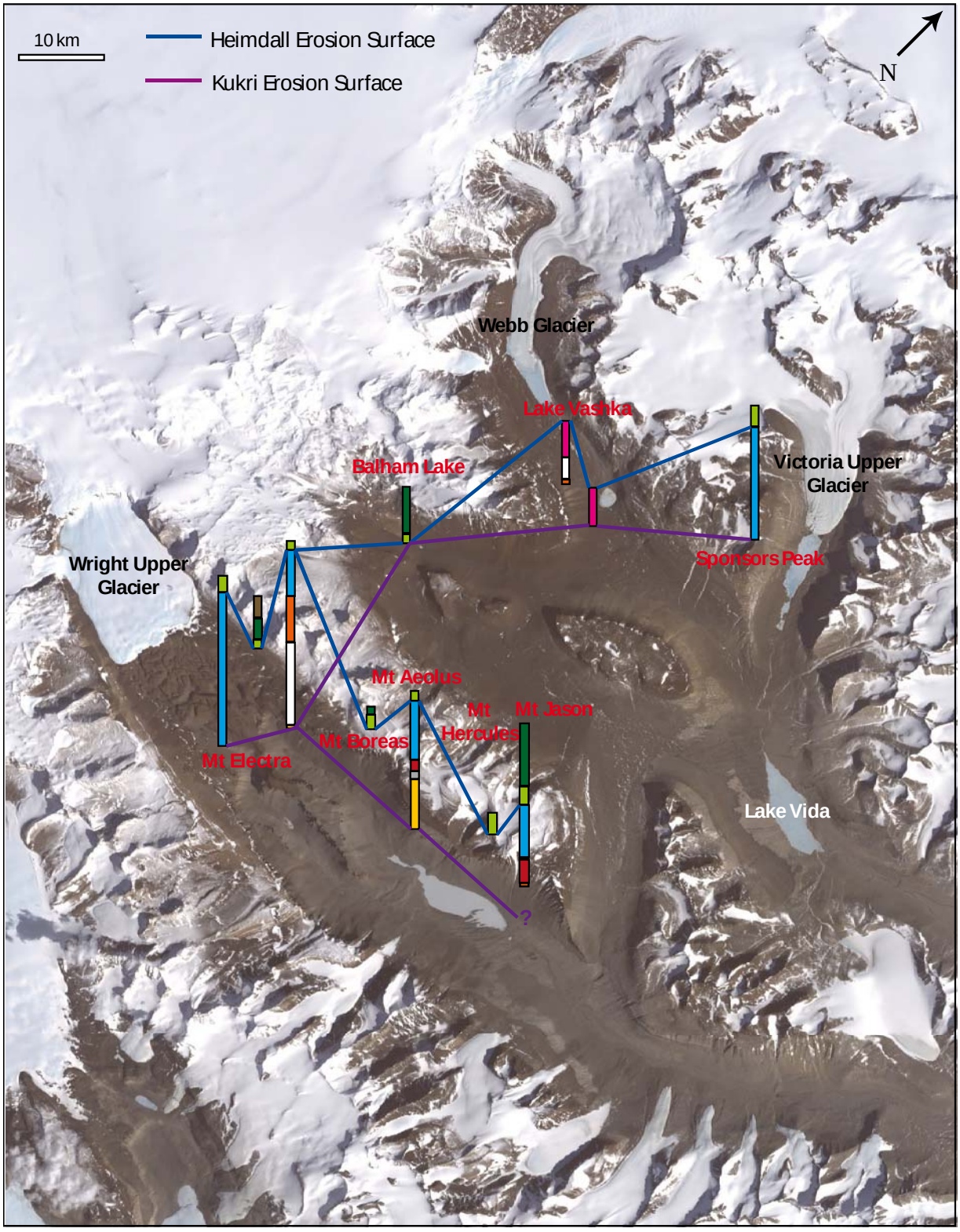

Figure 7-4: Correlation of stratigraphic columns across field area showing change in position of erosion surfaces across the field area.

7.6 Nomenclature Changes

After examination of the formations within the lower Taylor Group I feel that some minor nomenclature changes are needed to clarify the status of different rock units. My thesis has also discovered the lateral extent of a previously unrecognized unit.

Examination of thin sections shows that the Odin Arkose Member is not an arkose but a subarkose to quartzarenite (see Fig 5-12). Consequently, it is suggested that the name be changed to Odin Member, as the description of the member as an arkose is misleading.

The feldspathic and pebbly unit at the base of the New Mountain Sandstone (Pebbly Sandstone Lithofacies and Granule Cross-bedded Lithofacies) also should be raised to member status. I designate Mt Jason as the type locality and suggest the name Mt Jason Member. The Mt Jason Member is distinguished from the overlying New Mountain Sandstone proper by its subarkosic composition, greater proportion of pebbles and granules and smaller cross bed size. The contact between the New Mountain Sandstone and the Mt Jason Member is gradational. The lower contact of the Mt Jason Member is with the Kukri Erosion Surface, Terra Cotta Siltstone or underlying formations of the lower Taylor Group. The nature of the contact with underlying sedimentary rocks is unknown.

Due to division of the Taylor Group by the Heimdall Erosion Surface I propose that the formations over and underlying the Heimdall Erosion Surface be grouped separately. I propose that the name Lower Taylor Group be formalized for those formations and associated members underlying the HES, including the Windy Gully Sandstone, Terra Cotta Siltstone and New Mountain Sandstone. The formations between the Heimdall Erosion Surface and Maya Erosion Surface would then be named the Upper Taylor Group. Although these names may have been used before, it is not if clear they have been formalized.

7.7 Conclusions

- The New Mountain Sandstone was deposited in a predominantly shallow marine environment with deepening water over time as the sea moved north across the field area. Subordinate aeolian deposition took place in dunes adjacent to the coastline.
- The Heimdall Erosion Surface was formed due to a drop in relative sea level that lead to exposure and erosion of the New Mountain Sandstone and basement. As the sea transgressed across the field area the HES became a shore platform and the overlying Altar Mountain Formation was deposited in a shallow marine environment. To the north and east deltas fed sediment into the shallow marine setting but as sea level continued to rise the deltas of the Sperm Bluff Formation were flooded and shallow marine to inner shelf deposition occurred over the entire field area.
- The New Mountain Sandstone Formation and Altar Mountain Formation represent two transgressive to highstand system tracts separated by the Heimdall Erosion Surface, which is a type 1 sequence boundary.
- The sediment and pebbles of the New Mountain Sandstone and its Mt Jason Member and the Altar Mountain Formation and its Odin Member were primarily sourced from the Granite Harbour Intrusives or the underlying Taylor Group rocks.

Appendices

Appendix A: Field Data

APPENDIX A1: STRATIGRAPHIC COLUMNS

Key to all Stratigraphic Columns

Lithologies

- Sandstone
- Sandstone with granules
- Sandstone with mud
- Shale
- Conglomerate and pebbles
- Mudstone
- Volcanic
- Granite

Contacts

- Sharp planar
- Sharp irregular
- Sharp erosional
- Gradational
- Shale lined
- Obscured
- Top and bottom contact

Biologic

- Undefined bioturbation
- Infilled burrows
- *Skolithos*
- *Heimdallia*
- *Diplichnites*
- U-shaped burrows

Cross beds (Drawn to approx scale unless overwise indicated)

- Trough and tangential cross beds
- Trough cross beds with pebble lined foresets

Other

B3 Rock Samples

Sedimentary Structures

- Parallel bedding (thick and thin)
- Slumping
- Trough
- Pebble impression
- Rip up clasts (mudstone unless stated)
- Load cast
- Iron cementation
- Mud filled cavity
- Cavity left by weathered out sandstone
- Fine sand wedge
- Ripples
- Symmetrical ripples
- Asymmetrical ripples
- Polygonal cracks
- Mud clasts or rip ups

Scale (unless stated)

1 cm:1 m (when drawn)

Vertical scale on all columns is in metres.

1. Mt Jason

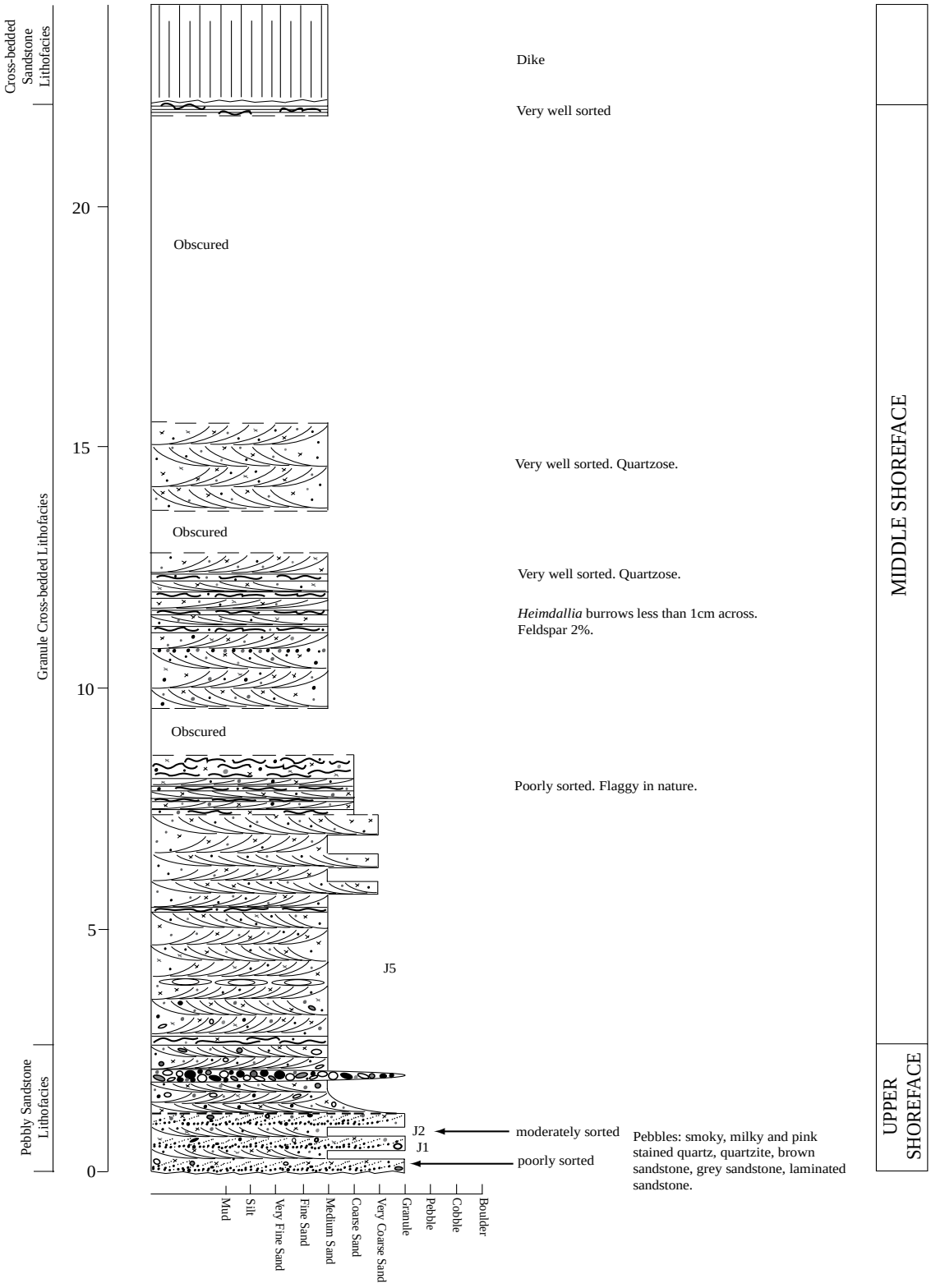
Cross-bedded Sandstone Lithofacies
Granule Cross-bedded Lithofacies
Pebbly Sandstone Lithofacies
20
15
10
5
0
Dike
Very well sorted
Obscured
Very well sorted. Quartzose.
Obscured
Very well sorted. Quartzose.
Heimdallia burrows less than 1cm across.
Feldspar 2%.
Obscured
Poorly sorted. Flaggy in nature.
J5
J2
J1
moderately sorted
poorly sorted
Pebbles: smoky, milky and pink stained quartz, quartzite, brown sandstone, grey sandstone, laminated sandstone.
Mud
Silt
Very Fine Sand
Fine Sand
Medium Sand
Coarse Sand
Very Coarse Sand
Granule
Pebble
Cobble
Boulder
MIDDLE SHOREFACE
UPPER SHOREFACE

1. Mt Jason

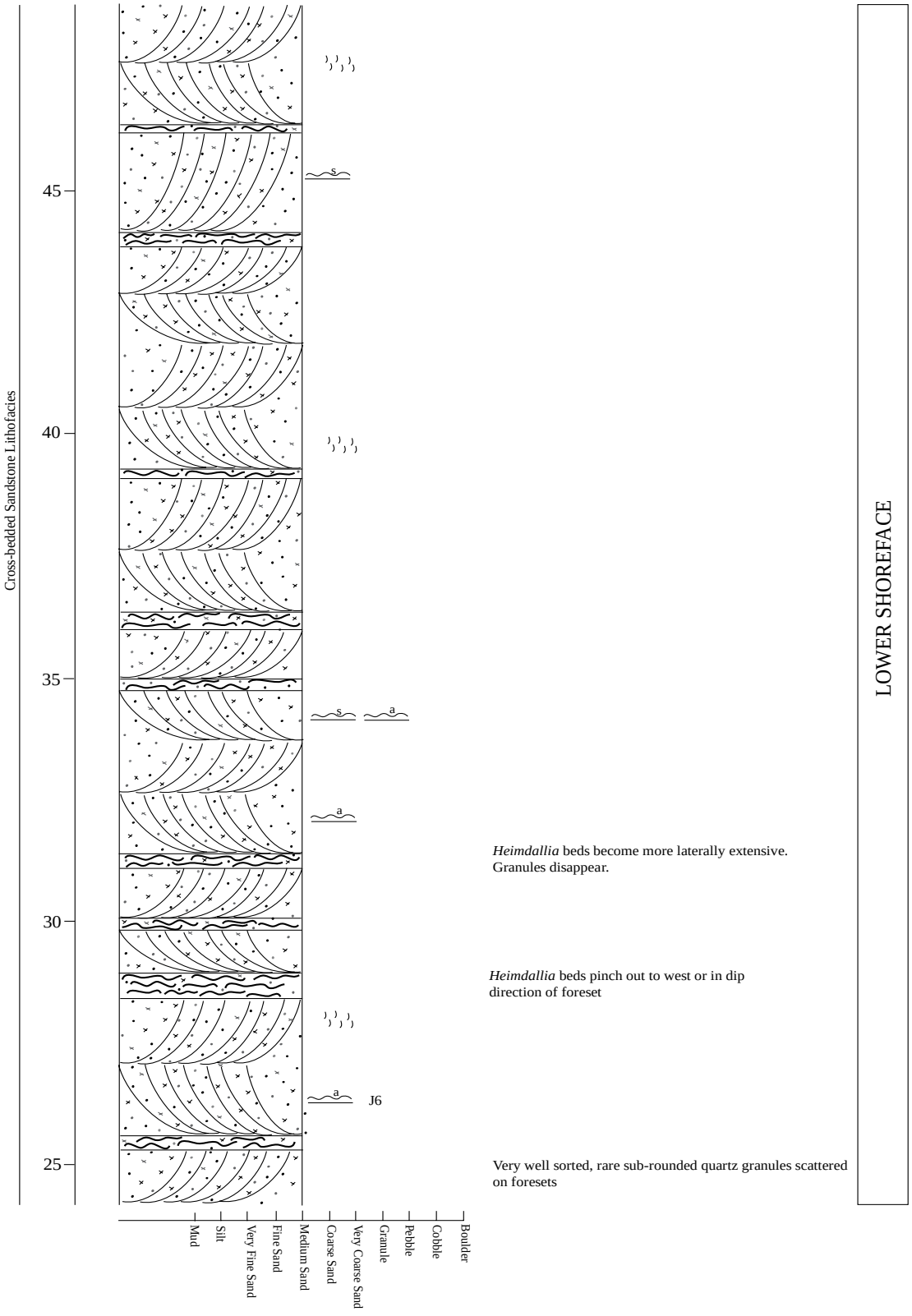
Cross-bedded Sandstone Lithofacies
45
40
35
30
25
s
s
a
a
a
J6
Heimdallia beds become more laterally extensive. Granules disappear.
Heimdallia beds pinch out to west or in dip direction of foreset
Very well sorted, rare sub-rounded quartz granules scattered on foresets
LOWER SHOREFACE
Mud
Silt
Very Fine Sand
Fine Sand
Medium Sand
Coarse Sand
Very Coarse Sand
Granule
Pebble
Cobble
Boulder

1. Mt Jason

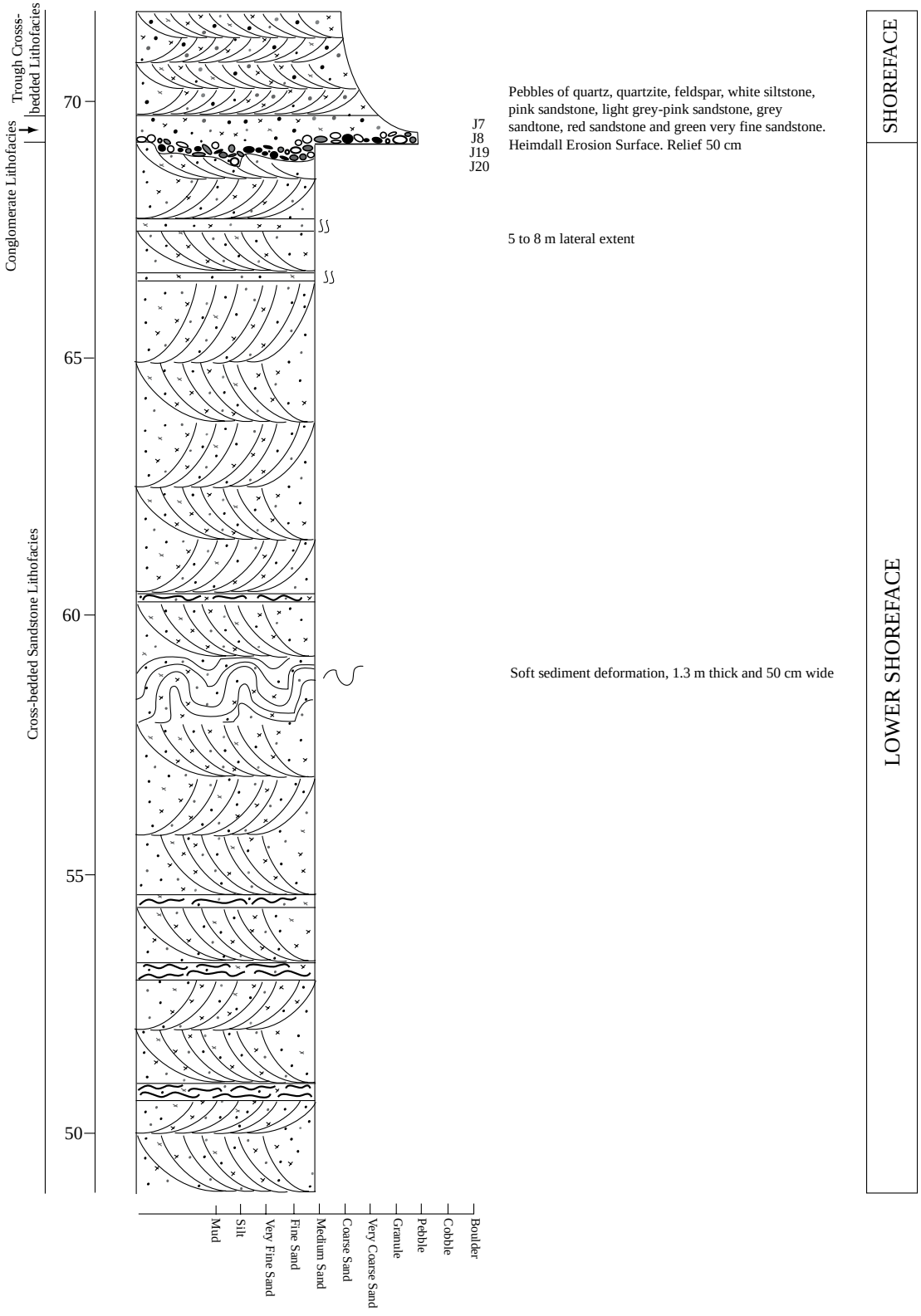
Trough Crosss-bedded Lithofacies
Conglomerate Lithofacies
Cross-bedded Sandstone Lithofacies
70
65
60
55
50
J7
J8
J19
J20
Pebbles of quartz, quartzite, feldspar, white siltstone, pink sandstone, light grey-pink sandstone, grey sandtone, red sandstone and green very fine sandstone.
Heimdall Erosion Surface. Relief 50 cm
5 to 8 m lateral extent
Soft sediment deformation, 1.3 m thick and 50 cm wide
SHOREFACE
LOWER SHOREFACE
Mud
Silt
Very Fine Sand
Fine Sand
Medium Sand
Coarse Sand
Very Coarse Sand
Granule
Pebble
Cobble
Boulder

1. Mt Jason

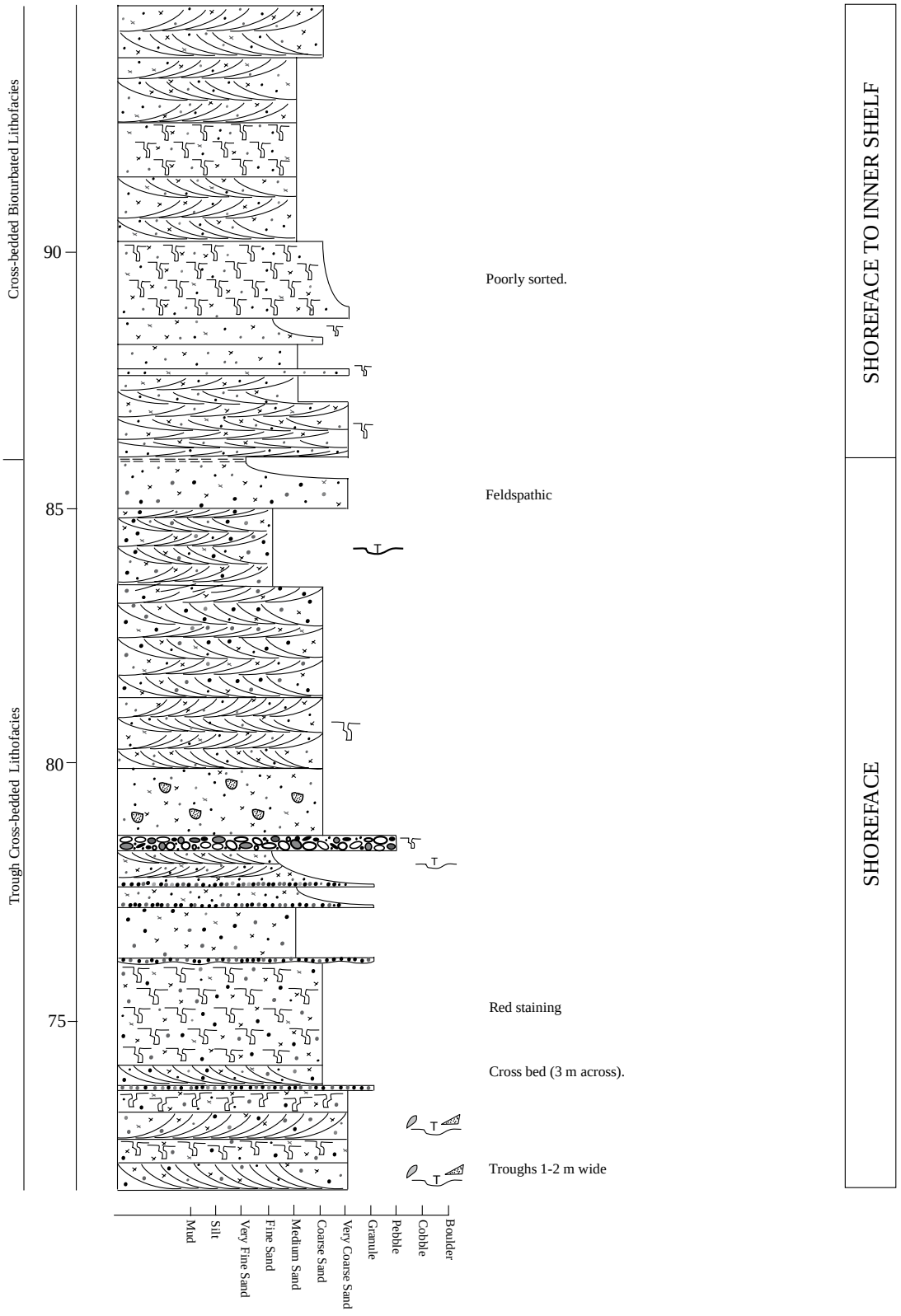
Cross-bedded Bioturbated Lithofacies
Trough Cross-bedded Lithofacies
90
85
80
75
Poorly sorted.
Feldspathic
Red staining
Cross bed (3 m across).
Troughs 1-2 m wide
SHOREFACE TO INNER SHELF
SHOREFACE
Mud
Silt
Very Fine Sand
Fine Sand
Medium Sand
Coarse Sand
Very Coarse Sand
Granule
Pebble
Cobble
Boulder

1. Mt Jason

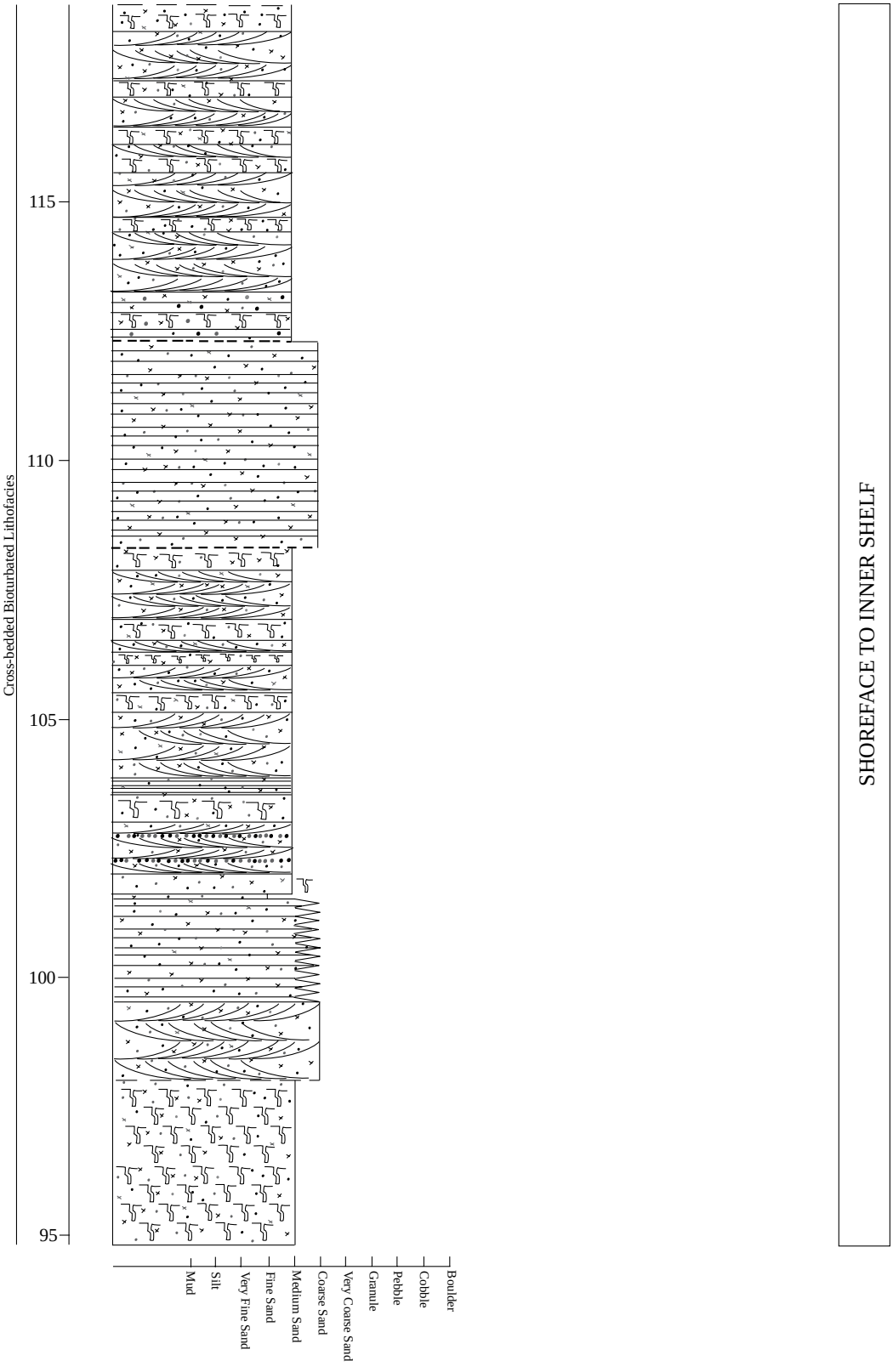
Cross-bedded Bioturbated Lithofacies
115
110
105
100
95
Mud
Silt
Very Fine Sand
Fine Sand
Medium Sand
Coarse Sand
Very Coarse Sand
Granule
Pebble
Cobble
Boulder
SHOREFACE TO INNER SHELF

1. Mt Jason

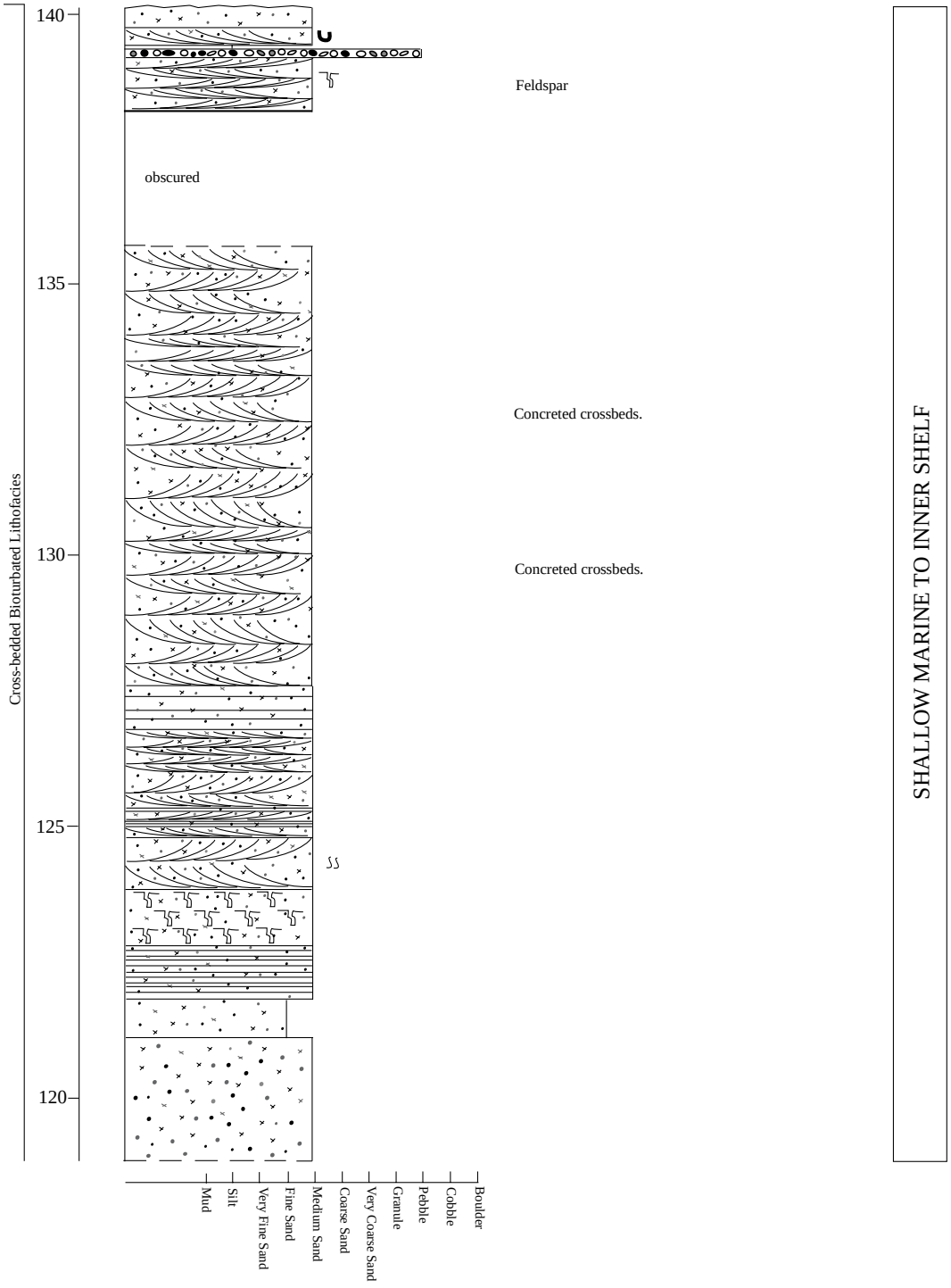
140
135
130
125
120
Cross-bedded Bioturbated Lithofacies
Feldspar
obscured
Concreted crossbeds.
Concreted crossbeds.
SHALLOW MARINE TO INNER SHELF
Mud
Silt
Very Fine Sand
Fine Sand
Medium Sand
Coarse Sand
Very Coarse Sand
Granule
Pebble
Cobble
Boulder

2. Mt Hercules

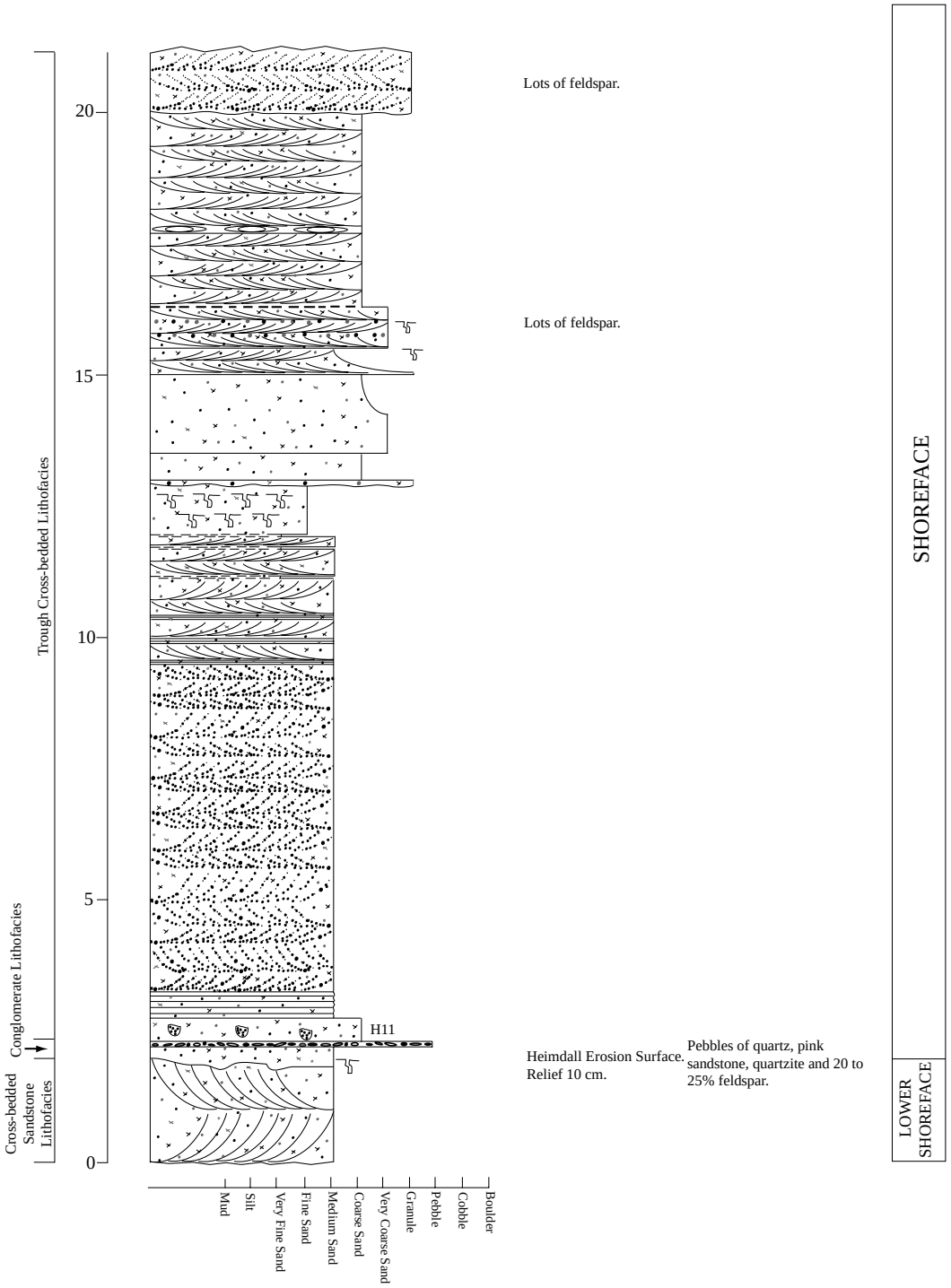

3. Mt Aeolus

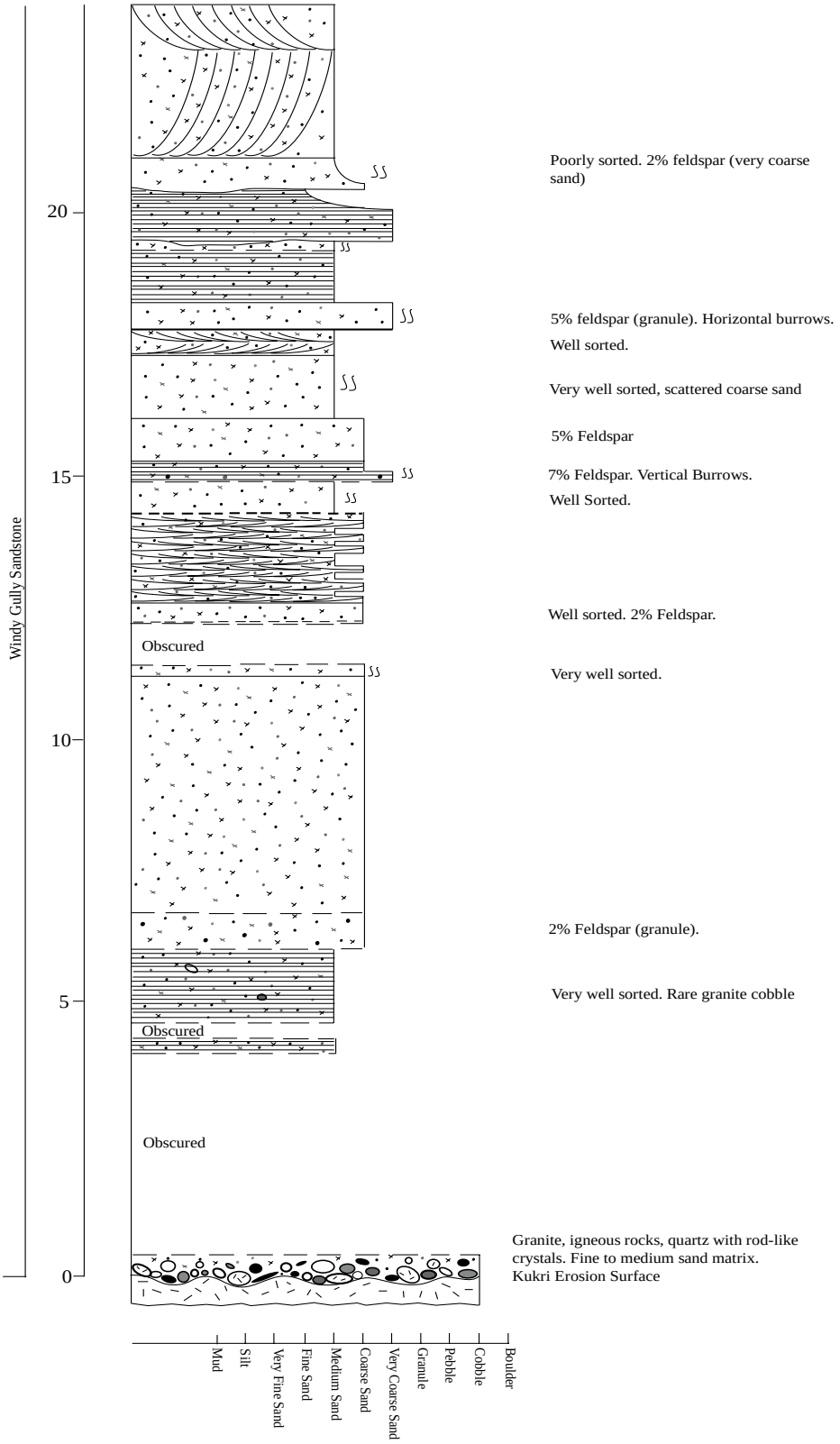
Windy Gully Sandstone
20
15
10
5
0
Poorly sorted. 2% feldspar (very coarse sand)
5% feldspar (granule). Horizontal burrows.
Well sorted.
Very well sorted, scattered coarse sand
5% Feldspar
7% Feldspar. Vertical Burrows.
Well Sorted.
Well sorted. 2% Feldspar.
Obscured
Very well sorted.
2% Feldspar (granule).
Very well sorted. Rare granite cobble
Obscured
Obscured
Granite, igneous rocks, quartz with rod-like crystals. Fine to medium sand matrix.
Kukri Erosion Surface
Mud
Silt
Very Fine Sand
Fine Sand
Medium Sand
Coarse Sand
Very Coarse Sand
Granule
Pebble
Cobble
Boulder

3. Mt Aeolus

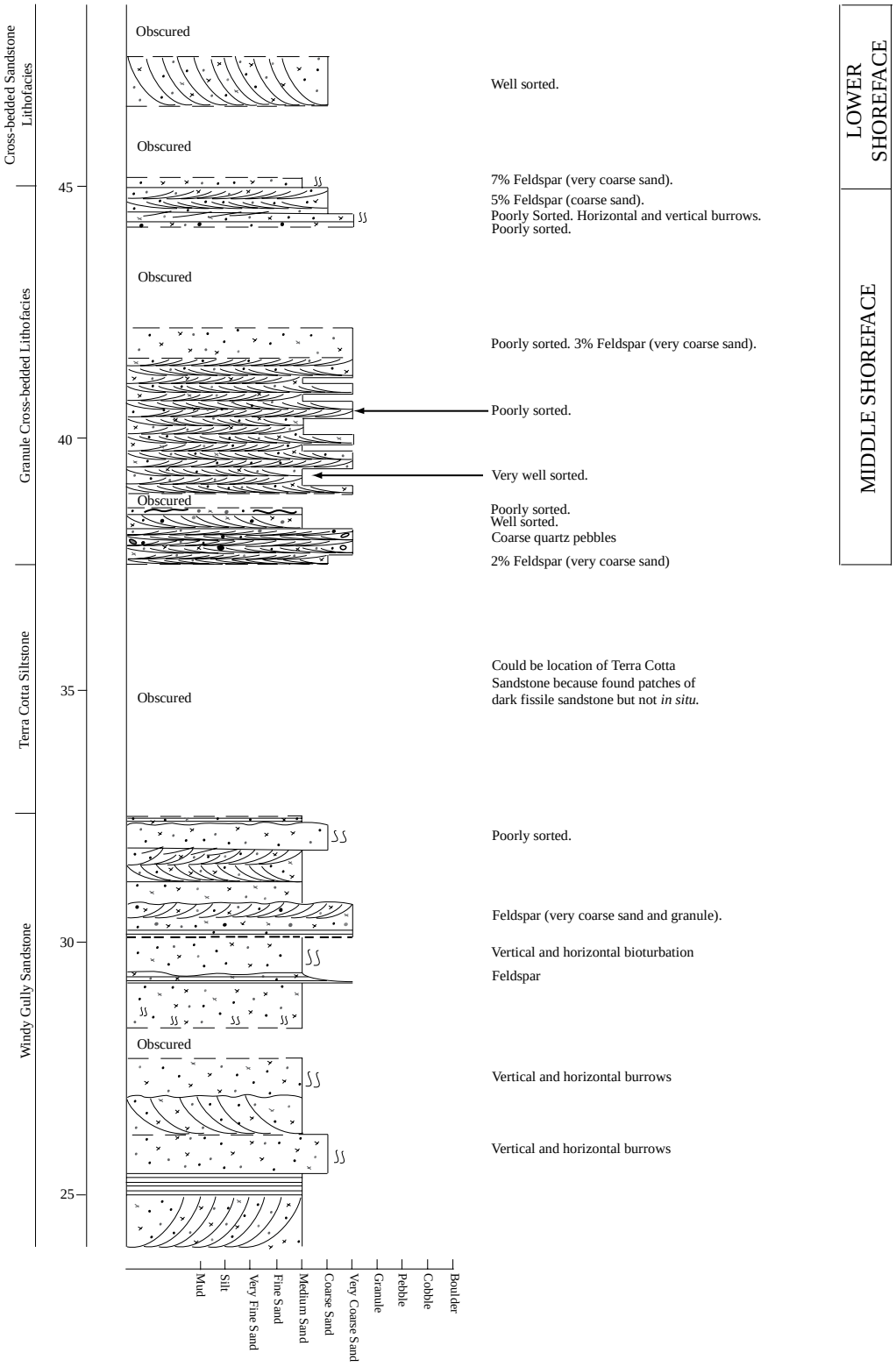
Cross-bedded Sandstone Lithofacies
Granule Cross-bedded Lithofacies
Terra Corta Siltstone
Windy Gully Sandstone
45
40
35
30
25
Obscured
Obscured
Obscured
Obscured
Obscured
Obscured
Well sorted.
7% Feldspar (very coarse sand).
5% Feldspar (coarse sand).
Poorly Sorted. Horizontal and vertical burrows.
Poorly sorted.
Poorly sorted. 3% Feldspar (very coarse sand).
Poorly sorted.
Very well sorted.
Poorly sorted.
Well sorted.
Coarse quartz pebbles
2% Feldspar (very coarse sand)
Could be location of Terra Cotta Sandstone because found patches of dark fissile sandstone but not in situ.
Poorly sorted.
Feldspar (very coarse sand and granule).
Vertical and horizontal bioturbation
Feldspar
Vertical and horizontal burrows
Vertical and horizontal burrows
LOWER SHOREFACE
MIDDLE SHOREFACE
Mud
Silt
Very Fine Sand
Fine Sand
Medium Sand
Coarse Sand
Very Coarse Sand
Granule
Pebble
Cobble
Boulder

3. Mt Aeolus

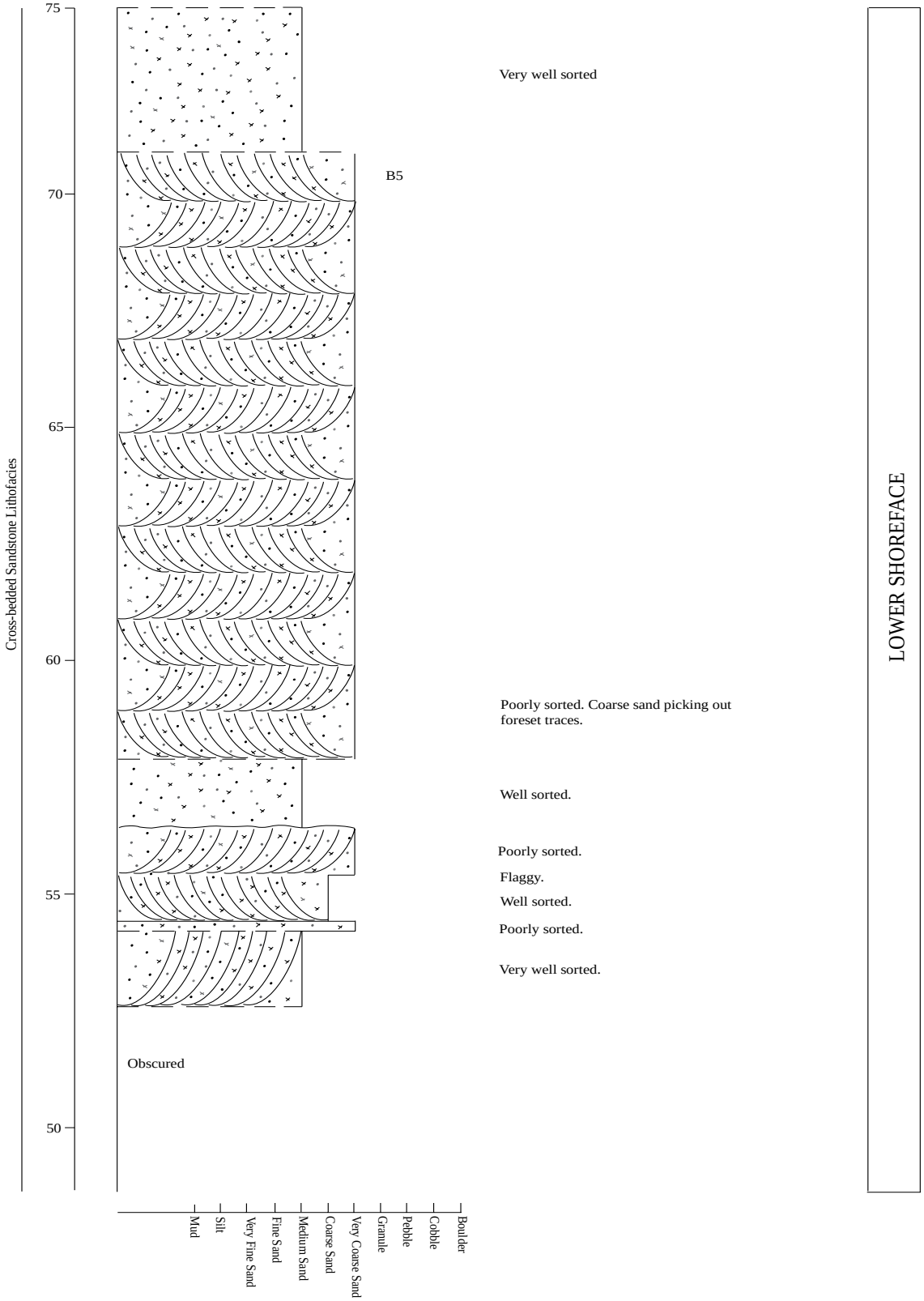
75
70
65
60
55
50
Cross-bedded Sandstone Lithofacies
B5
Very well sorted
Poorly sorted. Coarse sand picking out foreset traces.
Well sorted.
Poorly sorted.
Flaggy.
Well sorted.
Poorly sorted.
Very well sorted.
Obscured
LOWER SHOREFACE
Mud
Silt
Very Fine Sand
Fine Sand
Medium Sand
Coarse Sand
Very Coarse Sand
Granule
Pebble
Cobble
Boulder

3. Mt Aeolus

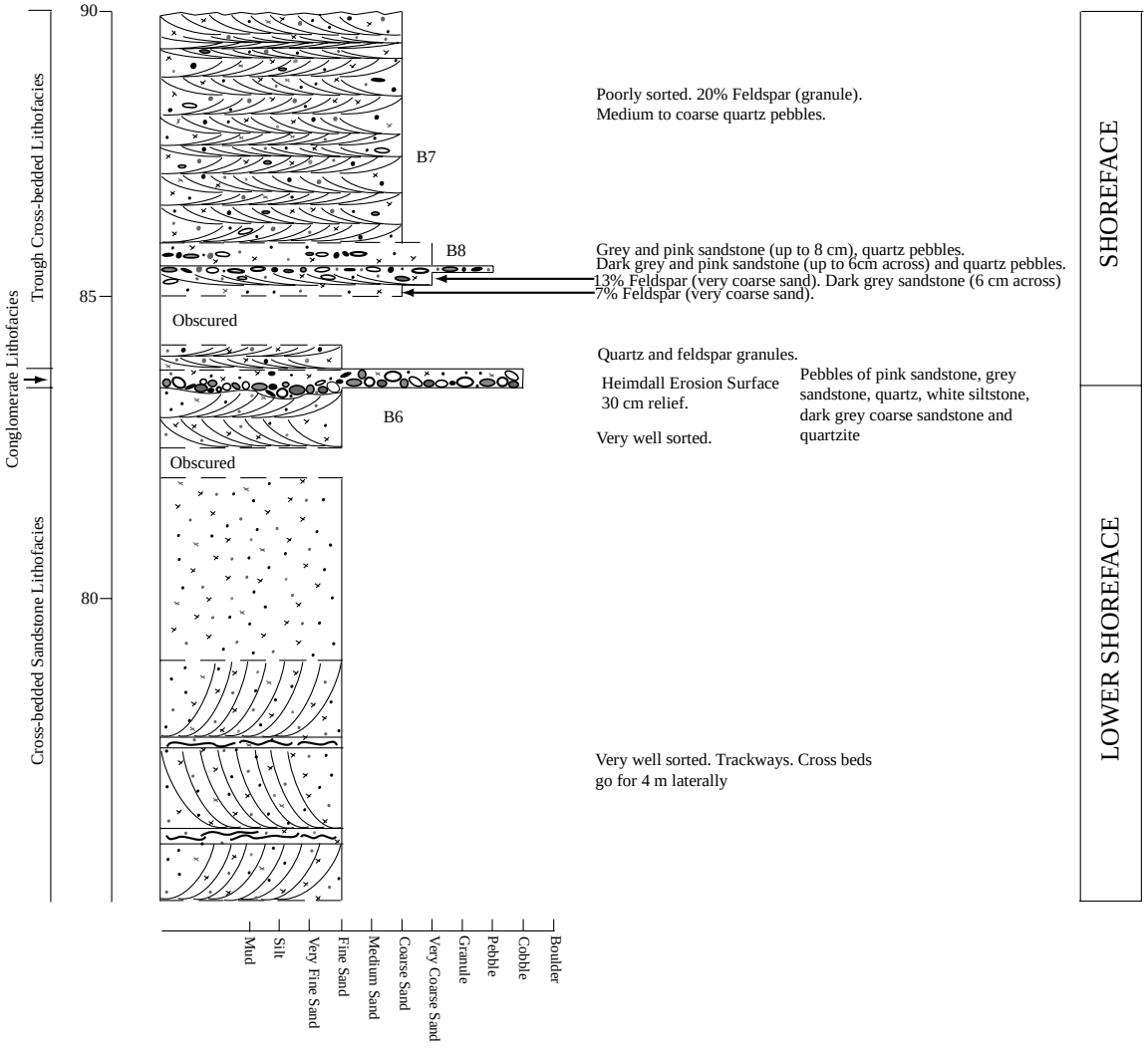
90
85
80
Conglomerate Lithofacies
Trough Cross-bedded Lithofacies
Cross-bedded Sandstone Lithofacies
B7
B8
B6
Obscured
Obscured
Poorly sorted. 20% Feldspar (granule).
Medium to coarse quartz pebbles.
Grey and pink sandstone (up to 8 cm), quartz pebbles.
Dark grey and pink sandstone (up to 6cm across) and quartz pebbles.
13% Feldspar (very coarse sand). Dark grey sandstone (6 cm across)
7% Feldspar (very coarse sand).
Quartz and feldspar granules.
Heimdall Erosion Surface
30 cm relief.
Pebbles of pink sandstone, grey sandstone, quartz, white siltstone, dark grey coarse sandstone and quartzite
Very well sorted.
Very well sorted. Trackways. Cross beds go for 4 m laterally
SHOREFACE
LOWER SHOREFACE
Mud
Silt
Very Fine Sand
Fine Sand
Medium Sand
Coarse Sand
Very Coarse Sand
Granule
Pebble
Cobble
Boulder

4. Mt Boreas

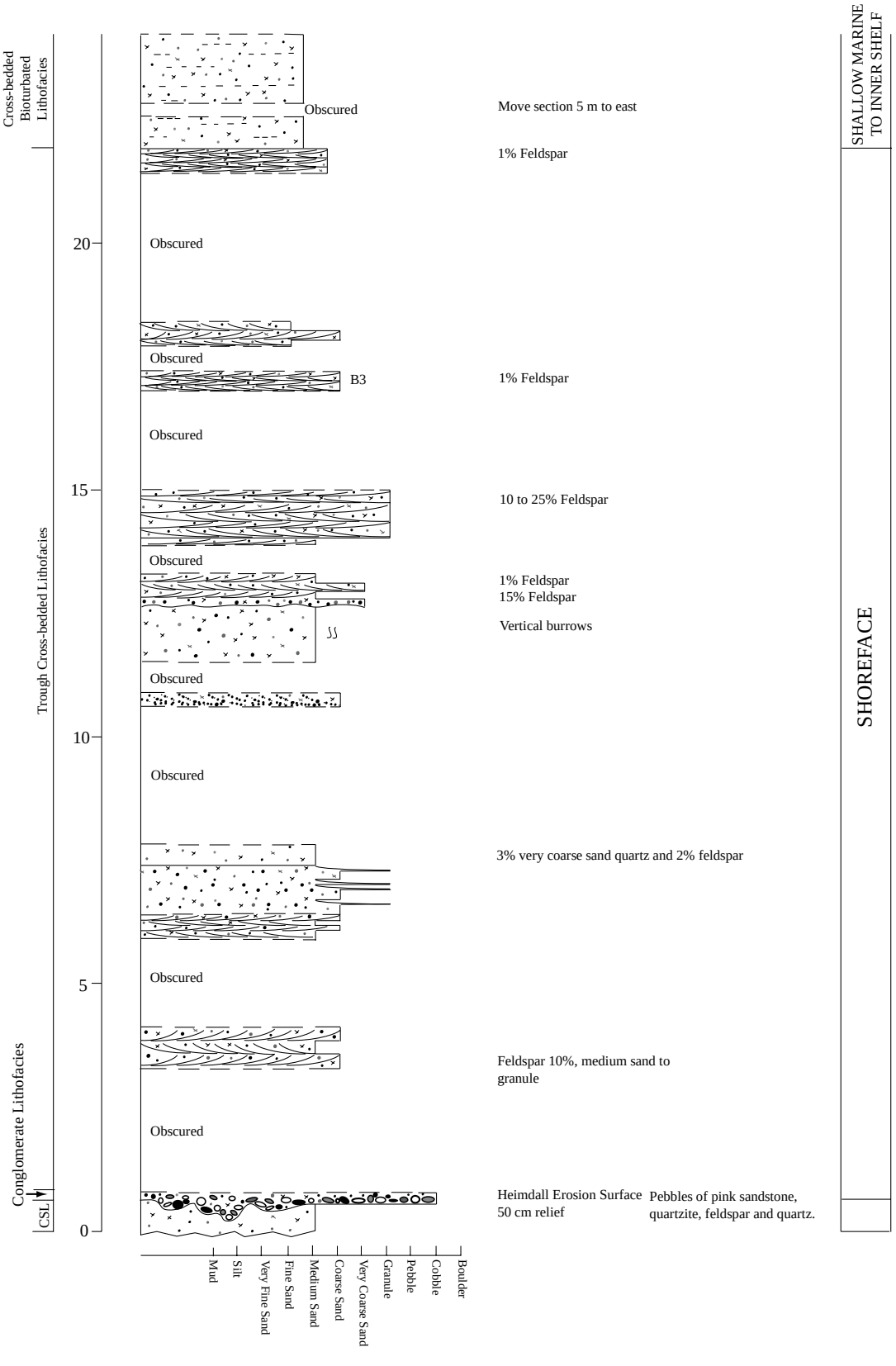
Cross-bedded Bioturbated Lithofacies
Trough Cross-bedded Lithofacies
Conglomerate Lithofacies
CSL
SHALLOW MARINE TO INNER SHELF
SHOREFACE
0
5
10
15
20
Obscured
Move section 5 m to east
1% Feldspar
Obscured
Obscured
B3
1% Feldspar
Obscured
10 to 25% Feldspar
Obscured
1% Feldspar
15% Feldspar
Vertical burrows
Obscured
Obscured
3% very coarse sand quartz and 2% feldspar
Obscured
Feldspar 10%, medium sand to granule
Obscured
Heimdall Erosion Surface
50 cm relief
Pebbles of pink sandstone, quartzite, feldspar and quartz.
Mud
Silt
Very Fine Sand
Fine Sand
Medium Sand
Coarse Sand
Very Coarse Sand
Granule
Pebble
Cobble
Boulder

4. Mt Boreas

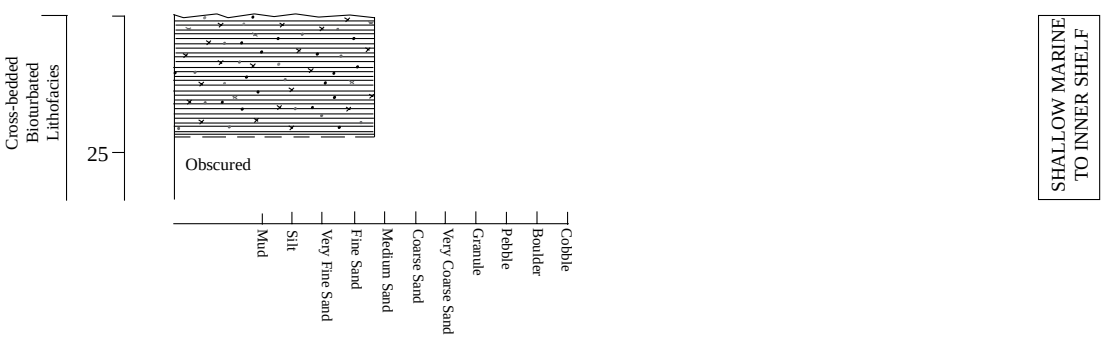
Cross-bedded
Bioturbated
Lithofacies
25
Obscured
Mud
Silt
Very Fine Sand
Fine Sand
Medium Sand
Coarse Sand
Very Coarse Sand
Granule
Pebble
Boulder
Cobble
SHALLOW MARINE
TO INNER SHELF

5a. Mt Electa - middle

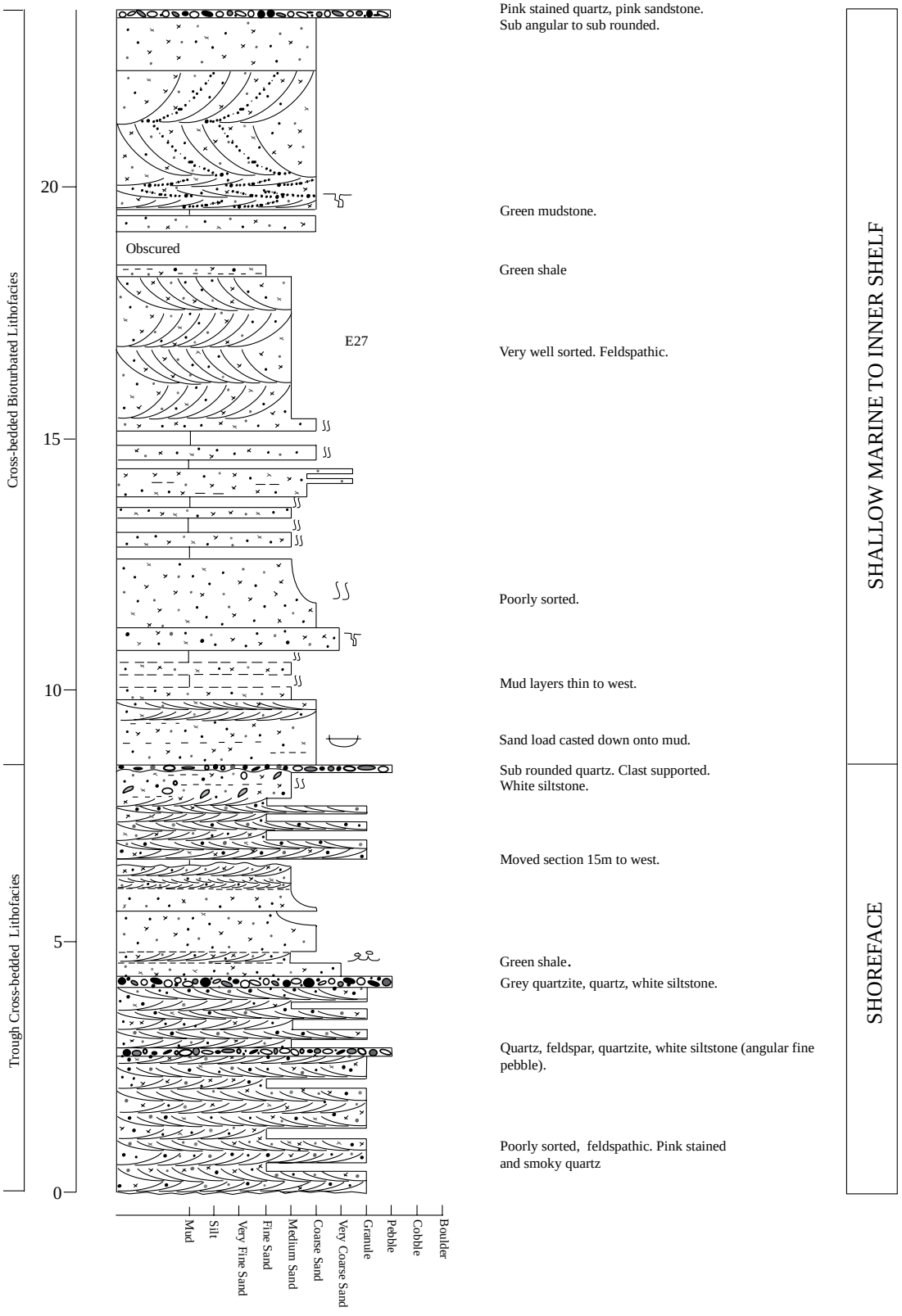

5a. Mt Electra - middle

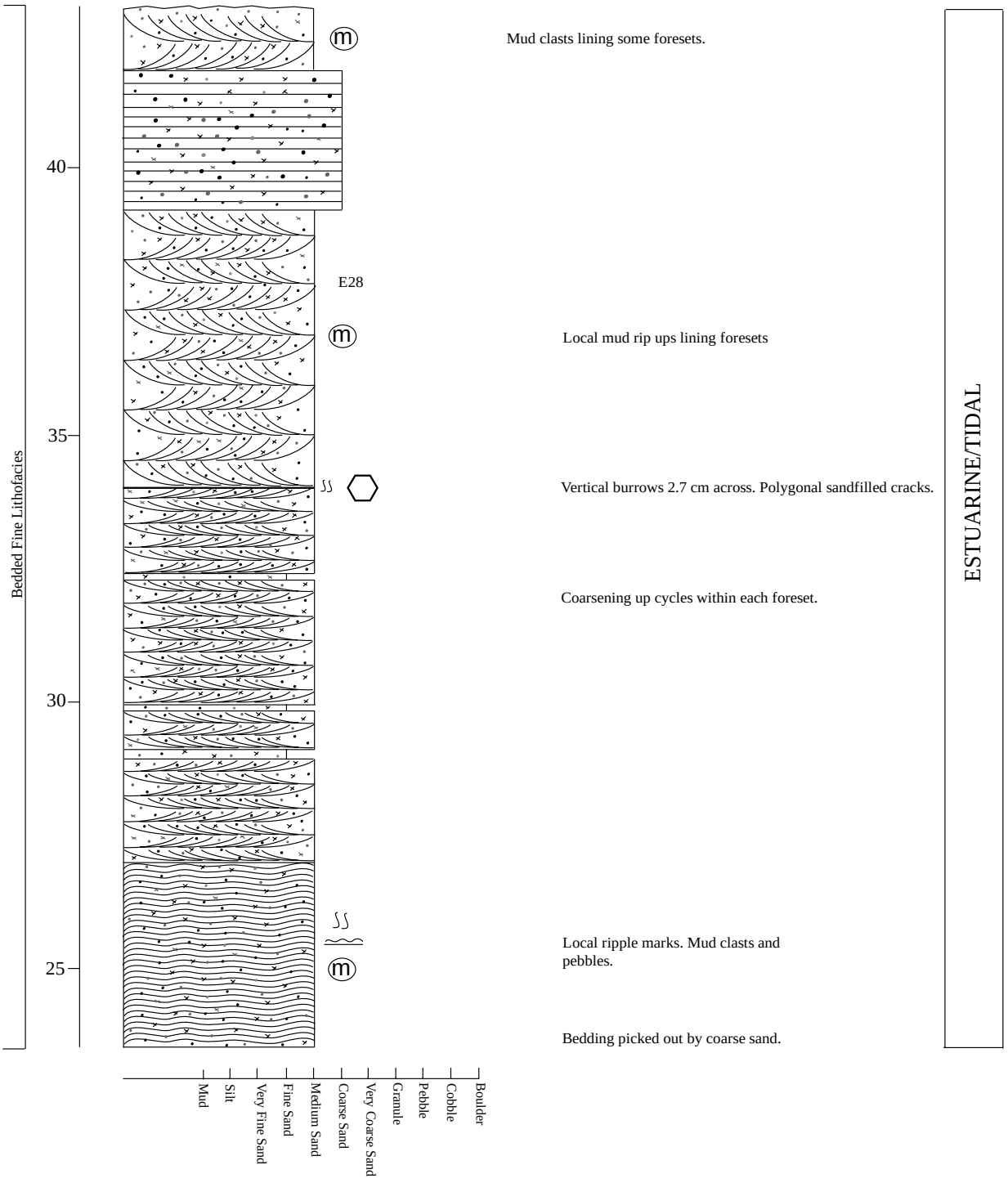

5b. Mt Electra - west

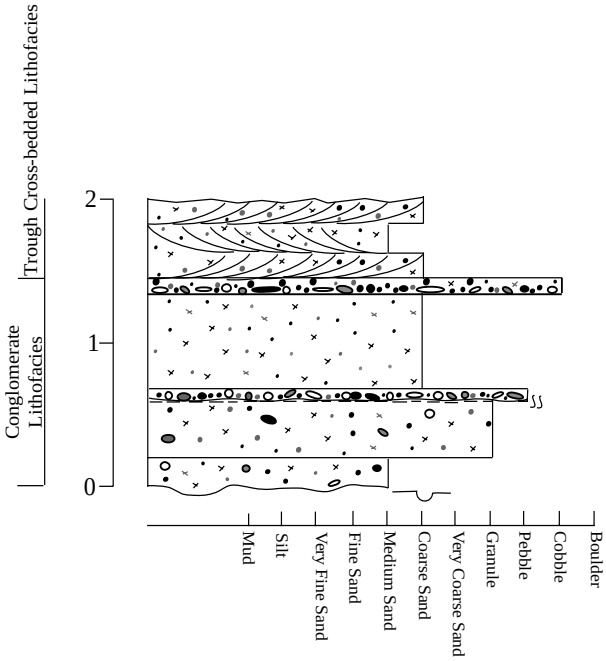

1 cm = 0.5 m

Pink sandstone, grey sandstone, white, light grey and dark grey quartzite, quartz, white siltstone.

Poorly sorted.

Vertical burrows through green shale.

Very poorly sorted. Quartz, pink sandstone (up to medium pebble), angular to sub rounded.

Quartz, pink sandstone.

Heimdall Erosion Surface. Cavities 1 to 4 cm across.

SHOREFACE

6. Balham Lake

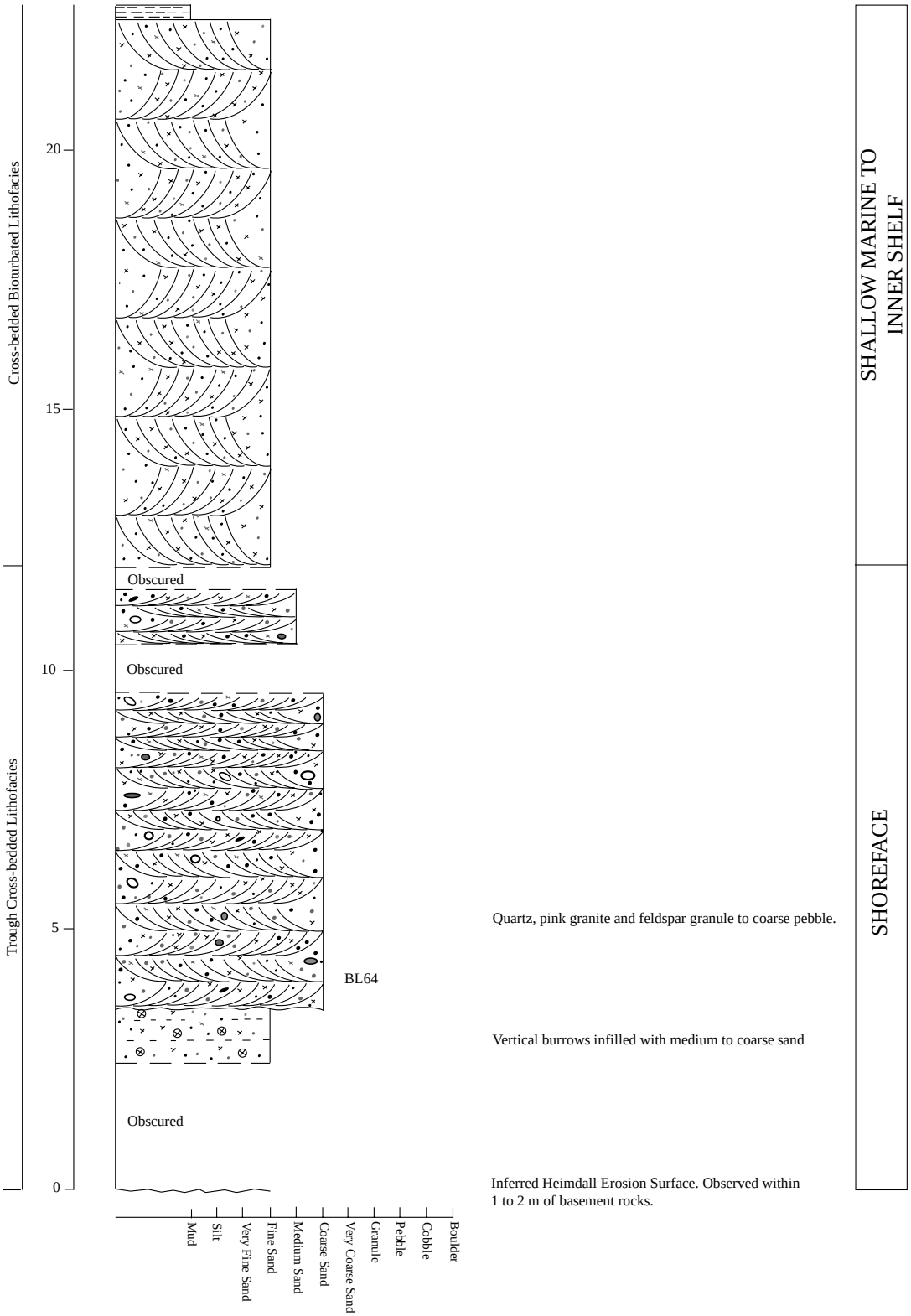

6. Balham Lake

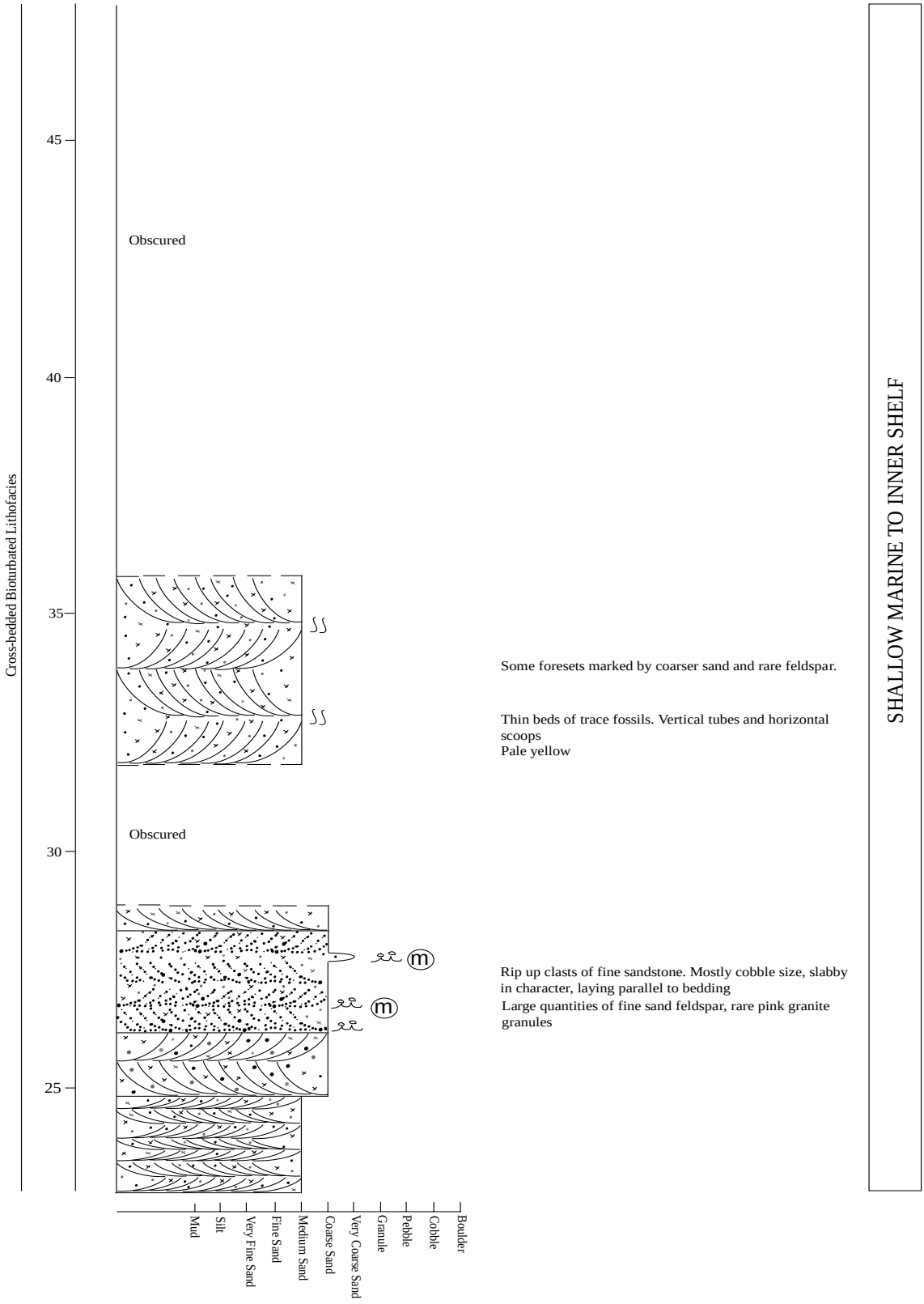

6. Balham Lake

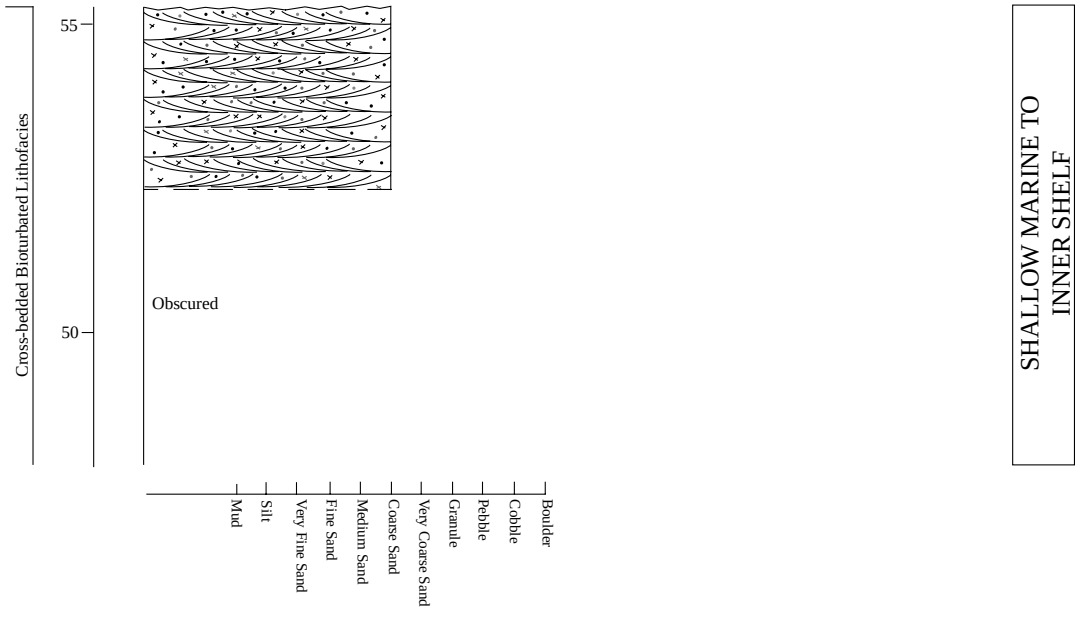

7a. Lake Vashka - west

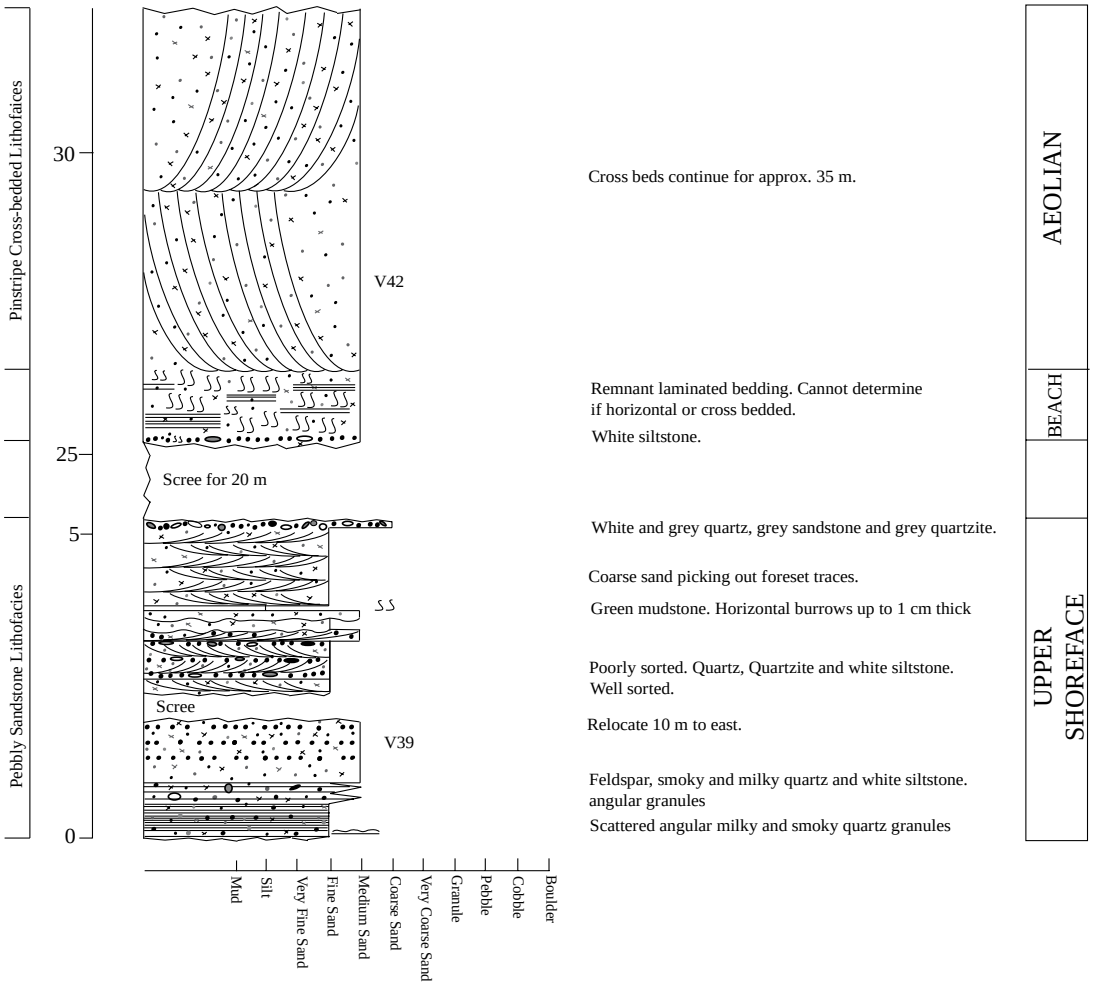

7b. Lake Vashka - middle

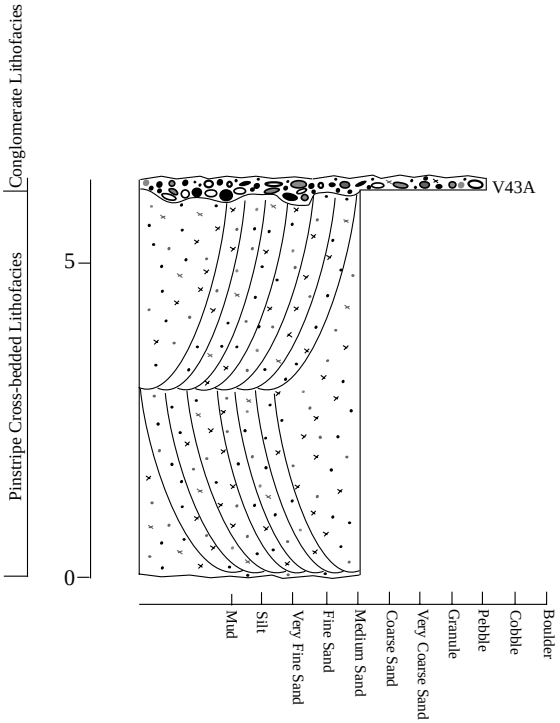

Pebbles of pink sandstone, grey sandstone, feldspar, granite, rhyolite, quartz and quartzite

Heimdall Erosion Surface. Relief 10 cm.

AEOLIAN

7c. Lake Vashka - east

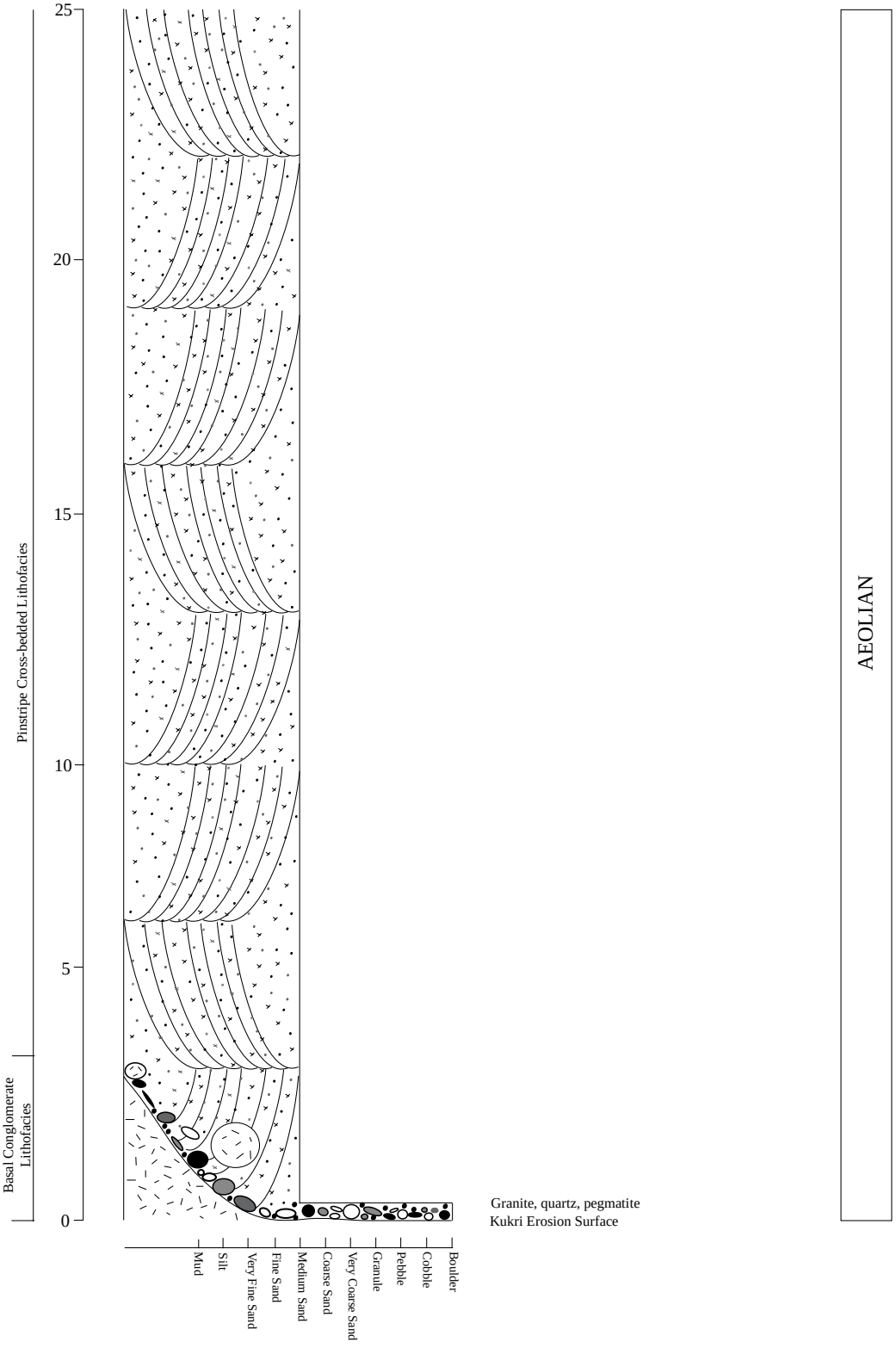

7c. Lake Vashka - east

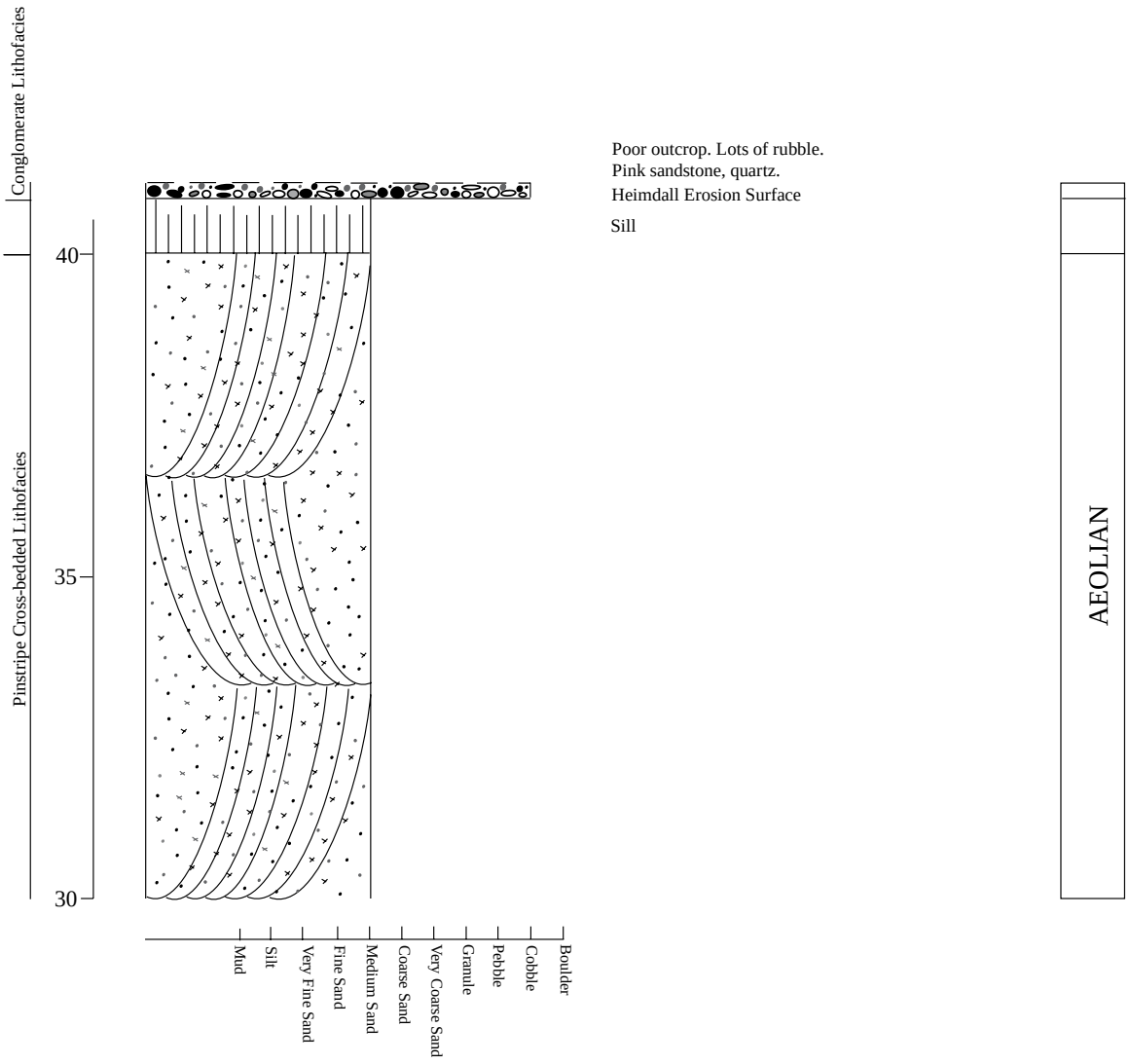

APPENDIX A2: PALEOCURRENT DATA

GJG = Greer Gilmer. MAB = Margaret Bradshaw
Data from GJG and MAB have been corrected for New Zealand declination of 21º

1. Pebbly Sandstone Lithofacies

Date and location	Measurer	Feature	Shape	Dip	Wavelength (mm)	Amplitude (mm)	Strike/Trend	Corrected Strike/Trend	Flow Direction	
Mt Jason										
12/1/07	**GJG**	Cross bed		N			130	260	170	S
		Cross bed		NE			50	180	90	E
		Cross bed		N			150	280	10	N
		Cross bed		NE			156	286	16	N
		Cross bed		N			110	240	330	N-NW
		Cross bed		NE			130	260	350	N-NW
		Cross bed		NE			128	258	348	N-NW
		Cross bed		NE			119	249	339	N-NW
		Cross bed		E			34	164	74	E-NE
		Cross bed		E			172	302	32	E-NE
		Cross bed		E			52	182	92	E
		Cross bed		E			166	296	26	N-NE
		Cross bed		NE			142	272	2	N
		Cross bed		E			46	176	86	E
		Cross bed		E			64	194	104	E-SE
		Cross bed		E			36	166	76	E-NE
		Cross bed		NE			104	234	144	S-SE
		Cross bed		E			40	170	80	E
		Cross bed		E			52	182	92	E
		Cross bed		SE			105	235	145	S-SE
		Cross bed		SE			42	172	82	E
		Cross bed		ESE			58	188	98	E
		Cross bed		SE			78	208	118	E-SE
		Cross bed		S			115	245	155	S-SE
		Cross bed		E			35	165	75	E-NE
		Cross bed		SSE			109	239	149	S-SE
		Cross bed		NE			10	140	50	NE
		Cross bed		SE			93	223	133	SE
		Cross bed		NE			2	132	42	NE
	JDB	Cross bed		NE			2	153	63	E-NE
		Cross bed		SE			93	244	154	S-SE
		Cross bed		E			35	186	96	E
		Cross bed		NE			10	161	71	E-SE
		Cross bed		SE			78	229	139	SE
		Cross bed		SE			58	209	119	E-SE
		Cross bed		SE			42	193	103	E-SE
		Cross bed		SE			105	256	166	S-SE
		Cross bed		SSE			109	260	170	S-SE
Mt Electra										
20/1/07	**JDB**	Cross bed		12E			38	189	99	E
		Cross bed		23E			34	185	95	E
		Cross bed		20E			42	193	103	E-SE
		Cross bed		8SW			1	152	242	W-SW
		Cross bed		16E			45	196	106	E-SE
		Cross bed		13E			54	205	115	E-SE
		Cross bed		20SE			95	246	156	E-SE
		Cross bed		21SE			67	218	128	SE
	GJG	Cross bed		20E			95	226	136	SE
		Cross bed		12E			102	233	143	S-SE

2. Granule Cross-bedded Lithofacies

Date	Measurer	Feature	Shape	Dip	Wavelength (mm)	Amplitude (mm)	Strike/Trend	Corrected Strike/Trend	Flow Direction	
Mt Jason										
12/1/07	**GJG**	Cross beds		S			2	132	222	SW
		Cross beds		SE			56	186	96	E
		Cross beds		S			120	250	160	S-SE
		Cross beds		SE			88	218	128	E-SE
		Cross beds		N			130	260	350	N
		Cross beds		N			112	242	332	N-NW
		Cross beds		SW			142	272	182	S
		Cross beds		NE			154	284	14	N
		Cross beds		S			122	252	162	S-SE
		Cross beds		E			60	190	100	E
		Cross beds		S			110	240	150	S-SE
		Cross beds		N			78	208	298	W-NW
		Cross beds		5W			49	179	269	W
	MAB	Cross beds		5W			49	179	269	W
	MAB	Cross beds		N			154	284	14	N-NE
				NE			164	294	24	N-NE
	GJG			4W			52	182	272	W

3. Pinstripe Cross-bedded Sandstone

Date and location	Measurer	Feature	Shape	Dip	Wavelength (cm)	Amplitude (cm)	Strike/Trend	Corrected Strike/Trend	Flow Direction	
Lake Vashka	**GJG**	Cross bed		15N			132	263	353	N
24/1/07		Cross bed		12NW			131	262	352	N
		Cross bed		16NW			118	269	359	N
		Cross bed		17W			63	194	284	NW
		Cross bed		21SW			55	186	96	E
		Cross bed		20NE			176	307	37	NE
		Cross bed		20W			50	181	271	W

4. Cross-bedded Sandstone Lithofacies

Date and location	Measurer	Feature	Shape	Dip	Wavelength (mm)	Amplitude (mm)	Strike/Trend	Corrected Strike/Trend	Flow Direction	
Mt Jason										
13/1/07	**GJG**	Cross beds		3W			8	138	228	SW
		Cross beds		12W			12	142	232	SW
		Cross beds		7W			169	299	209	S-SW
		Cross beds		17W			4	134	224	SW
		Cross beds		14SW			134	264	174	S
		Cross beds		4W			3	133	223	SW
		Cross beds		11SW			141	271	181	S
		Cross beds		4W			52	182	272	W
		Cross beds								
	JDB	Cross beds		11SW			141	292	202	S
		Cross beds		9W			33	184	274	W
		Cross beds		15W			173	324	234	SW
		Cross beds		15W			167	318	228	SW
		Cross beds		24S			115	266	176	S
		Cross beds		18NW			66	217	307	NW
		Cross beds		9NW			100	251	351	N-NW
	GJG	Cross beds		4NW			56	186	276	W
		Cross beds		4W			42	172	262	W
		Cross beds		15W			173	303	213	S-SW
		Cross beds		10E			150	280	10	N
		Cross beds		15W			167	297	207	S-SW
		Cross beds		1W			21	151	241	W-SW
		Cross beds								
	GJG	Cross beds		14W			176	306	216	SW
		Cross beds								
	GJG	Cross beds		12N			108	238	328	N-NW
		Cross beds		8N			104	234	324	NW
		Cross beds		2NW			100	230	320	NW
		Cross beds		20W			6	136	226	SW
		Cross beds								
	GJG	Cross beds		24S			115	245	155	S-SE
		Cross beds		15W			7	137	227	SW
	JDB	Cross beds		24W			23	174	264	S-SE
		Cross beds		19NW			121	272	182	W
		Cross beds		17NW			67	218	308	W
		Cross beds		10E			171	322	52	NW
		Cross beds		10NW			141	292	22	W
		Cross beds		15W			168	319	49	NW
		Cross beds		23W			69	220	310	SW
		Cross beds		23W			79	230	320	SW
		Cross beds		7W			72	223	313	SW
		Cross beds		28W			166	317	47	NW
		Cross beds		11NW			75	226	316	NW
		Cross beds		29SW			36	187	277	S
		Cross beds		12NW			112	263	173	W
		Cross beds		23NW			74	225	315	SW
		Cross beds		8NW			99	250	340	W

Mt Electra

19/1/07	**JDB**	Cross bed	24N	23	175	265	W
		Cross bed	19NW	121	273	3	N
		Cross bed	17NW	67	219	309	W-NW
		Cross bed	10E	171	323	53	E-NE
		Cross bed	10NW	141	293	23	N-NE
		Cross bed	15W	168	320	230	SW
		Cross bed	23W	69	221	311	NW
		Cross bed	23W	79	231	321	N-NW
		Cross bed	7W	72	224	314	NW
		Cross bed	28W	166	318	228	SW
		Cross bed	11NW	75	227	317	NW
		Cross bed	29SW	36	188	278	W
		Cross bed	12NW	112	264	354	N
		Cross bed	23NW	74	226	316	NW
		Cross bed	8NW	99	251	341	N-NW

Sponsors Peak

28/1/07	**GJG**	Cross bed	18S	14	144	234	S-SW
		Cross bed	12S	21	151	241	W-SW
		Cross bed	18SW	48	178	268	W
		Cross bed	30SW	0	130	220	SW

4. Cross-bedded Sandstone Lithofacies Ripples and other things

Date and location	Measurer	Feature	Shape	Dip	Wavelength (mm)	Amplitude (mm)	Trend	Corrected Trend	Flow Direction
Mt Jason									
11/1/07	**GJG**	Ripples	S		100	10	130	260	
		Ripples	A		30		122	252	
		Ripples	A		33	5	65	195	
		Ripples			50		154	284	
		Ripples					156	286	
		Ripples			55		150	280	
		Ripples	A		48		112	242	
	MAB	Ripples					145	275	
		Ripples					144	274	
		Ripples	S				10	140	
		Ripples	A		75	7	140	270	
		Ripples	S		20	4	47	177	
		Ripples					136	266	
		Parting Lineation					160		
12/1/07	**JDB**	Trough					55	206	
13/1/07									
	GJG	Ripples	A		80		157	287	
	JDB	Parting Lineation					49	200	
	GJG	Ripples	A		40		154	284	
		Ripples	A		50		90	220	
		Ripples	S		40		140	270	
		Ripples					85	215	
		Ripples	A		35	5	82	212	
		Ripples	S			5	30	160	
	JDB	Ripples	S		50	5	140	291	
	GJG	Ripples	A		75	7	140	270	
		Ripples	S		20	4	47	177	
		Ripples	A		85	6	136	266	
	GJG	Ripples	S		35	5	102	232	
	MAB	Ripples	A		11	3	132	262	
		Ripples			11	3	45	175	
		Ripples			30	4	108	238	
		Ripples			35	5	102	232	
17/1/01									
	GJG	Ripples	A			50	5	52	
		Ripples	A		70	6	136	266	
		Ripples	S		20	3	59	189	
		Ripples	S		60	7	161	291	
		Cross beds		2			52	182	
		Cross beds		10			80	210	
		Cross beds		10			42	172	
		Cross beds		14			84	214	
		Ripples	S		15	3	85	215	
		Ripples	A		120	11	51	181	
		Ripples	A		65	8	159	289	
		Ripples	A		110	13	171	301	
		Ripples	S		20	2	159	289	
		Ripples	A		40	3	85	215	
		Ripples	S		55	5	24	154	

5. Trough Cross-bedded Lithofacies

Date and location	Measurer	Feature	Shape	Dip	Wavelength (mm)	Amplitude (mm)	Strike/Trend	Corrected Strike/Trend	Flow Direction	
Mt Jason										
13/1/07	**GJG**	Channel					158	288		NW
West Face										
		Cross beds		W			0	130	220	SW
		Cross beds		S			126	256	166	S
		Cross beds		E			44	174	84	E
	JDB			SW			175	326	236	W-SW
				SW			160	311	221	SW
				SW			165	316	226	SW
				SW			175	326	236	W-SW
				SW			45	196	286	W
		Cross bed strike in axis of small troughs		SW			50	201	291	W-NW
				SW			54	205	295	W-NW
				SW			15	166	256	W-SW
				SW			60	211	301	W-NW
				SW			61	212	302	W-NW
				SW			50	201	291	W-NW
				SW			52	203	293	W-NW
				SW			58	209	299	W-NW
				SW			5	156	246	W-SW
				SW			30	181	271	W
Mt Hercules										
14/1/07										
	JDB	Trough		Approx S			65	217		S
		Trough		Approx S			75	227		SW
		Trough		Approx S			60	212		S
		Trough		Approx S			62	214		S
		Trough		Approx S			104	256		SW
		Trough		Approx S			82	234		SW
		Trough		Approx S			86	238		SW
		Trough		Approx S			72	224		SW
	GJG	Cross bed		S			0	131	221	SW
		Cross bed		S			194	325	235	W-SW
		Cross bed		S			140	271	181	S
		Cross bed		S			156	287	197	S-SW
		Cross bed		S			0	131	221	S-SW
		Cross bed		SW			36	167	257	W-SW
		Cross bed		S			162	293	203	S-SW
		Cross bed		S			4	135	225	SW
		Cross bed		S			138	269	179	S
		Cross bed		S			4	135	225	SW
Mt Electra										
19/1/07	**JDB**	Cross bed		16SW			4	156	246	W-SW
	GJG	Cross bed		SW			30	161	251	W-SW
		Cross bed		SW			37	168	258	W-SW
		Cross bed		SW			28	159	249	W-SW
		Cross bed		SW			39	170	260	W-SW
		Cross bed		W			38	169	259	W-SW
		Cross bed		W			40	171	219	S-SW
		Cross bed		W			358	129	219	S-SW
		Cross bed		NW			40	171	261	W-SW

20/1/07	**JDB**	Cross bed	24SW	144	296	206	S
		Cross bed	19SW	166	318	228	S-SW
		Cross bed	18SW	140	292	202	S
Sponsors Peak							
28/1/07	**GJG**		S	23	153	243	SW
			S	13	143	233	SW
			SW	53	183	273	W
			SW	63	193	283	W
			SE	123	253	163	S

Appendix B: Laboratory Data

APPENDIX B1: POINT COUNT DATA

1. Sample Descriptions

Field Site	Sample Number	Formation	Lithofacies	Description
Mt Jason	**J1**	New Mountian Sandstone	Pebbly Sandstone Lithofacies	Sandstone with pebbles.
	J2	New Mountian Sandstone	Pebbly Sandstone Lithofacies	Fine sand to granule quartzose and feldspathic sandstone. Coarse sand to granule smoky quartz and feldspar.
	J5	New Mountian Sandstone	Granule Cross-bedded Lithofacies	Coarse sandstone.
	J6	New Mountian Sandstone	Cross-bedded Sandstone Lithofacies	Sandstone foreset.
	J7	Odin Arkose Member	Conglomerate Lithofacies - matrix	Granule sandstone
	J8	Odin Arkose Member	Conglomerate Lithofacies	Grey sandstone megaclast
	J19	Odin Arkose Member	Conglomerate Lithofacies	Red sandstone clast
	J20	Odin Arkose Member	Conglomerate Lithofacies	Red sandstone clast
Mt Electra	**E24**	Altar Mountain Formation	Cross-bedded Bioturbated Lithofacies	Green sandstone from close to camp
	E27	Altar Mountain Formation	Cross-bedded Bioturbated Lithofacies	Fine to medium quartzose and feldspathic sandstone
	E28	Altar Mountain Formation	Cross-bedded Bioturbated Lithofacies	Sandstone
	E35	New Mountain Sandstone	Cross-bedded Sandstone Lithofacies	Granule sandstone
	E36A	Odin Arkose Member	Conglomerate Lithofacies	Pink sandstone clast
	E36B	Odin Arkose Member	Conglomerate Lithofacies	Grey sandstone clast
	E207	New Mountain Sandstone	Cross-bedded Sandstone Lithofacies	Medium quartzose sandstone
	E206	Odin Arkose Member	Conglomerate Lithofacies	Subrounded to subangular quartz, quartzite. Matrix granule to coarse sand. Matrix supported.
	E207	Odin Arkose Member	Arkosic Sandstone Lithofacies	Feldspathic medium sand to granule sandstone.
Vashka Lake	**V39**	New Mountain Sandstone	Pebbly Sandstone Lithofacies	Fine sandstone. Angular coarse to small pebble milky and smoky quartz and feldspar
	V42	New Mountain Sandstone	Pinstripe Cross-bedded Lithofacies	Fine to medium quartzose sandstone. Predominantly fine sand.
	V43A	Odin Arkose Member	Conglomerate Lithofacies	Pink sandstone clast
Vashka Crag	**VC46**	New Mountain Sandstone	Granule Cross-bedded Lithofacies	Medium sand to granule quartzose sandstone. Coarse sand to granule smoky and milky quartz
	VC47	New Mountain Sandstone	Granule Cross-bedded Lithofacies	Fine to medium quartzose sandstone. Medium to coarse sand feldspar.
	VC50	New Mountain Sandstone	Granule Cross-bedded Lithofacies	Fine to granule quartzose sandstone. Coarse sand to granule smoky quartz. Rare coarse to very coarse sand feldspar.
Mt Hercules	**H11**	Odin Arkose	Arkosic Sandstone Lithofacies	Medium to coarse sand quartzose and feldspathic sandstone. Magnetic minerals.
Sponsors Peak	**S51**	New Mountain Sandstone	Cross-bedded Sandstone Lithofacies	
	S53	Odin Arkose Member	Arkosic Sandstone Lithofacies	Medium to granule quartzose and feldspathic sandstone. White feldspar, smoky and milky quartz.
Mt Boreas	**B2**	Odin Arkose	Conglomerate Lithofacies	Pink sandstone pebble
	B3	Odin Arkose	Arkosic Sandstone Lithofacies	Medium sand to fine pebble. Smoky and milky quartz and feldspar coarse sand to fine pebble.
Mt Aeolus	**B5**	New Mountain Sandstone	Cross-bedded Sandstone Lithofacies	Well sorted fine to medium sand.
	B6	New Mountain Sandstone	Cross-bedded Sandstone Lithofacies	Well sorted fine sand.
	B7	Odin Arkose	Arkosic Sandstone Lithofacies	Fine cross bed

	B8	Odin Arkose	Arkosic Sandstone Lithofacies	Coarse cross bed
Balham Lake	**BL64**	Altar Mountain Formation	Cross-bedded Bioturbated Lithofacies	Trough cross-bedded sandstone

2. Raw Data

Sample Number	**J1**	**J2**	**J5**	**J7**	**J8**	**J6**	**J19**	**J20**	**H11**	**BL64**	**V39**	**V42**	**V43A**	**S51**	**S53**
Quartz	142	187	221	157	153	251	166	145	189	199	163	205	173	205	168
Polycrystalline Quartz	16	12	14	1	34	0	17	2	3	0	0	13	0	4	0
Undulose Quartz	6	5	4	19	8	3	2	41	9	6	10	0	0	0	17
Plagioclase Feldspar	2	6	12	0	21	0	0	18	6	3	15	9	4	4	4
Alkali Feldspar	41	27	2	0	0	0	23	0	5	51	44	50	54	7	44
Matrix	62	42	17	2	79	0	6	91	77	13	46	17	62	75	29
Hole	19	19	29	6	5	46	21	0	11	4	11	6	0	1	34
Epoxy	0	0	0	5	0	0	0	3	0	23	0	0	7	4	0
Epidote	1	0	1	0	0	0	0	0	0	0	0	0	0	0	0
Magnetic Minerals	0	1	0	0	0	0	0	0	0	0	0	0	0	0	0
Large Polycrystalline Quartz	11	1	0	11	0	0	65	0	0	1	2	0	0	0	4
Fibrous Minerals	0	0	0	0	0	0	0	0	0	0	9	0	0	0	0
Grey	0	0	0	0	0	0	0	0	0	0	0	0	0	0	0
Red Stuff	0	0	0	0	0	0	0	0	0	0	0	0	0		
Total	300	300	300	201	300	300	300	300	300	300	300	300	300	300	300
Total Feldspar	43	33	14	0	21	0	23	18	11	54	59	59	58	11	33
Percentage	20	14	6	-	10	-	8	9	5	21	25	21	25	5	15
Total Quartz	175	205	239	188	195	297	250	188	201	206	175	218	173	209	189
Percentage	80	86	94	100	90	100	92	91	95	79	75	79	75	95	85
Lithics	0	0	0	0	0	0	0	0	0	0	0	0	0	0	0
Percentage	-	-	-	-	-	-	-	-	-	-	-	-	-	-	-
Total	218	238	253	188	216		273	206	212	260	234	277	231	220	222

Sample Number	**E207**	**E206**	**E205**	**E24**	**E27**	**E28**	**E35**	**E36A**	**VC46**	**VC47**	**VC50**	**B2**	**B3**	**B5**	**B6**	**B7**	**B8**
Quartz	226	160	183	160	136	205	206	192	185	156	230	200	242	258	235	233	169
Polycrystalline Quartz	15	3	4	11	18	2	2	1	14	20	3	0	0	18	10	2	0
Undulose Quartz	9	15	0	0	4	0	8	8	18	40	14	1	5	4	0	9	10
Plagioclase Feldspar	20	0	9	3	27	8	0	9	0	11	0	0	1	0	0	0	0
Alkali Feldspar	0	0	27	61	38	0	0	0	16	17	0	0	14	9	28	30	45
Matrix	13	105	58	45	71	73	53	86	33	32	24	96	1	2	0	8	23
Hole	13	0	3	0	4	12	0	0	0	24	12	3	19	1	6	1	4
Epoxy	0	3	0	13	0	0	27	4	20	0	8	0	0	8	21	17	35
Epidote	4	0	5	0	0	0	0	0	0	0	0	0	0	0	0	0	0
Magnetic Minerals	0	0	0	0	2	0	0	0	0	0	0	0	0	0	0	0	0
Large Polycrystalline Quartz	0	14	0	0	0	0	4	0	14	0	9	0	3	0	0	0	14
Fibrous Minerals	0	0	0	0	0	0	0	0	0	0	0	0	0	0	0	0	0
Grey	0	0	11	0	0	0	0	0	0	0	0	0	0	0	0	0	0
Red Stuff	0	0	0	7	0	0	0	0	0	0	0	0	0	0	0	0	0
Total	300	300	300	300	300	300	300	300	300	300	300	300	285	300	300	300	300
Total Feldspar	20	0	36	64	65	8	0	9	16	28	0	0	15	9	28	30	45
Percentage	7	0	16	27	29	4	-	4	6	11	-	-	6	3	10	11	19
Total Quartz	250	192	187	171	158	207	220	201	231	216	247	200	250	280	245	244	193
Percentage	93	100	84	73	71	96	100	96	94	89	100	100	94	97	90	89	81
Lithics	0	0	0	0	0	0	0	0	0	0	0	0	0	0	0	0	0
Percentage	-	-	-	-	-	-	-	-	-	-	-	-	-	-	-	-	-
Total	270	192	223	235	223	215	220	210	247	244	247	200	265	289	273	274	238

APPENDIX B2: LA-ICP-MS RESULTS

1. U-Th-Pb isotope data for Sample E207.

Spot No.	Pb* (ppm)	U (ppm)	atomic Th/U	Measured isotope ratios and 1σ (%) internal errors								Corrected ages and 1σ absolute internal errors (Ma)						6*/38 -7*/35 concord-ance(%)	% common 206Pb	Spot MSW D	Selected age and 1σ absolute external error (Ma)	
				206Pb/238U	±	207Pb/235U	±	207Pb/206Pb	±	208Pb/232Th	±	206Pb*/238U	±	207Pb*/235U	±	207Pb*/206Pb*	±					
88	97.67	1513	0.78	0.05780	2.2	1.0150	4.4	0.1274	3.8	0.02264	2.5	352.7	7.9	563.9	37.1	1566.2	65.9	63	3.89	115.2	d,x	
58	114.3	1461	0.61	0.07156	1.3	0.9641	1.6	0.0977	1.0	0.02931	1.3	436.3	5.4	534.1	10.7	997.3	14.1	82	3.11	57.72	d,x	
61	58.33	717	1.00	0.07118	0.8	0.8248	1.4	0.0840	1.2	0.01606	2.2	468.4	3.8	825.0	13.2	1981.7	18.9	57	-4.92	10.05	d,x	
31	82.16	989	0.81	0.07412	1.0	0.8312	1.6	0.0813	1.3	0.02157	1.5	469.1	4.7	658.0	12.5	1391.8	18.0	71	-0.89	23.64	d,x	
57	104.2	1136	1.05	0.07671	0.7	0.8953	1.2	0.0846	1.0	0.02559	1.0	477.3	3.3	581.1	14.7	1041.2	21.1	82	1.31	15.59	d,x	
69	67.70	823	0.60	0.07647	0.9	0.6485	1.2	0.0615	0.8	0.02263	1.7	480.7	4.2	538.8	8.6	807.1	10.2	89	-0.55	20.10	d,x	
12	39.35	440	0.94	0.07632	0.6	0.6378	1.5	0.0606	1.4	0.02293	1.1	481.7	3.2	531.0	22.5	772.9	29.3	91	-0.53	3.16	481.7	5.0
51	28.03	290	1.14	0.07824	0.4	0.6364	1.3	0.0590	1.2	0.02472	0.8	491.4	2.3	479.8	16.4	459.7	15.7	102	0.34	2.76	491.4	4.5
43	42.06	517	0.34	0.07983	0.4	0.7357	1.3	0.0668	1.2	0.02948	1.4	492.7	2.1	501.7	7.4	553.7	7.8	98	0.99	3.61	492.7	4.4
44	15.39	164	1.03	0.07832	0.6	0.6234	1.7	0.0577	1.6	0.02413	0.9	493.0	2.9	499.6	15.1	559.0	16.2	99	-0.13	2.24	493.0	4.8
32	37.28	434	0.78	0.07815	0.7	0.9766	1.8	0.0906	1.7	0.02062	1.4	498.0	3.6	782.8	16.1	1727.9	23.7	64	-1.93	6.94	d	
16	21.29	238	0.75	0.07977	0.4	0.6588	1.7	0.0599	1.6	0.02465	0.8	499.5	2.1	517.4	17.7	617.3	20.1	97	-0.06	1.18	499.5	4.5
68	27.43	293	0.91	0.08055	0.9	0.9103	3.2	0.0820	3.1	0.02678	2.3	499.6	4.5	592.3	26.5	991.0	36.9	84	1.20	5.96	d	
15	15.51	180	0.71	0.07858	0.8	0.7020	2.2	0.0648	2.0	0.02040	2.6	501.1	3.9	657.7	16.6	1252.9	24.0	76	-2.17	2.31	d	
21	21.55	242	0.71	0.08027	0.4	0.6426	1.4	0.0581	1.4	0.02469	0.9	502.4	2.1	510.0	8.8	562.7	9.3	99	-0.10	1.97	502.4	4.5
13	15.55	177	0.64	0.08042	0.6	0.6539	2.3	0.0590	2.2	0.02484	1.2	502.6	3.2	515.7	13.7	590.3	14.9	97	-0.08	1.94	502.6	5.1
64	49.85	419	2.22	0.07825	0.6	0.7360	1.5	0.0682	1.4	0.02428	0.8	502.9	3.9	564.1	33.8	892.8	46.1	89	-0.07	6.35	502.9	5.6
14	73.22	774	0.99	0.07993	0.4	0.6456	1.0	0.0586	0.9	0.02387	0.7	504.5	2.2	544.3	9.3	739.6	11.4	93	-0.65	4.91	504.5	4.5
60	43.22	487	0.66	0.08075	0.4	0.6436	1.1	0.0578	1.0	0.02466	0.8	505.4	2.1	516.0	9.2	580.7	9.8	98	-0.19	2.90	505.4	4.5
83	39.54	454	0.59	0.08084	0.5	0.6403	1.5	0.0574	1.4	0.02446	1.3	505.6	2.6	516.3	9.8	579.1	10.4	98	-0.23	2.81	505.6	6.6
67	30.88	334	0.84	0.08067	0.4	0.6507	1.3	0.0585	1.3	0.02493	0.8	505.6	2.2	512.7	12.2	567.6	13.0	99	-0.06	2.29	505.6	4.5
41	8.35	97	0.51	0.08131	0.8	0.6483	2.8	0.0578	2.7	0.02570	1.7	506.3	4.2	499.7	21.3	483.4	20.5	101	0.12	2.24	506.3	5.8
50	32.20	356	0.91	0.07915	0.5	0.6814	1.2	0.0624	1.2	0.02056	1.1	507.1	2.6	661.3	13.8	1248.2	20.0	77	-2.44	2.58	d	
76	40.36	501	0.26	0.08183	0.6	0.7042	1.8	0.0624	1.6	0.02451	1.9	509.1	3.3	550.3	13.0	730.5	15.6	93	-0.15	4.49	509.1	6.9
65	30.70	336	0.75	0.08148	0.5	0.6740	1.2	0.0600	1.1	0.02540	0.9	509.4	2.6	521.2	13.3	593.3	14.4	98	0.03	3.14	509.4	4.8
78	47.17	560	0.42	0.08171	0.4	0.6545	1.4	0.0581	1.4	0.02474	1.1	509.5	2.0	521.8	7.3	586.2	7.7	98	-0.17	1.78	509.5	6.4
30	14.15	164	0.52	0.08151	0.6	0.6506	2.1	0.0579	2.0	0.02412	1.4	510.0	3.1	533.6	10.0	648.1	11.1	96	-0.41	2.07	510.0	5.1

Spot No.	Pb* (ppm)	U (ppm)	atomic Th/U	Measured isotope ratios and 1σ (%) internal errors								Corrected ages and 1σ absolute internal errors (Ma)						6*/38 -7*/35 concord-ance(%)	% common 206Pb	Spot MSW D	Selected age and 1σ absolute external error (Ma)	
				206Pb/238U	±	207Pb/235U	±	207Pb/206Pb	±	208Pb/232Th	±	206Pb*/238U	±	207Pb*/235U	±	207Pb*/206Pb*	±					
01	30.51	260	1.97	0.08015	0.5	0.6463	1.6	0.0585	1.5	0.02502	0.7	510.0	4.3	491.5	42.6	471.6	41.1	104	0.24	3.89	510.0	5.9
79	38.91	407	0.99	0.08086	0.5	0.6519	1.8	0.0585	1.7	0.02383	1.0	511.0	2.7	559.3	12.0	785.5	14.9	91	-0.83	2.82	511.0	6.7
17	89.81	1072	0.35	0.08262	0.4	0.7011	1.2	0.0615	1.1	0.02695	0.8	512.4	2.1	520.9	9.0	567.8	9.4	98	0.30	7.11	512.4	4.6
34	25.69	281	0.82	0.08088	0.5	0.6572	1.6	0.0589	1.5	0.02215	1.1	513.4	2.7	605.5	14.5	985.2	19.8	85	-1.59	2.62	d	
49	68.87	766	0.58	0.08316	0.4	0.7596	1.0	0.0662	0.9	0.02823	1.1	514.5	2.1	522.3	7.8	573.2	8.2	99	0.85	4.04	514.5	4.5
86	8.04	92	0.55	0.08247	0.9	0.6925	3.4	0.0609	3.3	0.02469	2.4	515.3	4.4	551.2	19.1	715.4	22.6	93	-0.28	1.52	515.3	7.6
82	47.89	571	0.36	0.08282	0.5	0.6554	1.5	0.0574	1.4	0.02508	1.2	515.5	2.5	519.9	8.2	547.4	8.3	99	-0.13	3.22	515.5	6.7
40	82.52	970	0.41	0.08272	0.4	0.6679	0.9	0.0586	0.8	0.02477	0.8	515.8	2.0	533.6	5.0	620.7	5.3	97	-0.23	5.71	515.8	4.5
45	34.53	412	0.34	0.08295	0.4	0.6482	1.1	0.0567	1.0	0.02545	0.9	515.9	1.9	511.1	5.2	498.1	4.9	101	-0.06	2.26	515.9	4.5
18	88.34	1046	0.37	0.08312	0.5	0.7467	0.8	0.0652	0.7	0.02622	0.7	516.4	2.6	560.3	4.5	752.1	4.9	92	0.10	9.85	516.4	4.8
26	77.21	857	0.60	0.08326	0.6	0.8009	1.3	0.0698	1.1	0.02715	1.0	516.9	3.0	568.5	8.3	796.8	10.0	91	0.49	12.55	d,x	
05	95.14	1095	0.44	0.08357	0.6	0.8050	1.3	0.0699	1.2	0.02799	1.9	517.5	3.0	568.4	9.3	789.2	11.2	91	0.53	8.08	517.5	5.1
38	26.39	247	1.42	0.08170	0.4	0.6604	1.6	0.0586	1.5	0.02490	0.7	518.0	2.6	541.0	22.1	680.9	26.0	96	-0.43	2.47	518.0	4.8
36	13.22	142	0.70	0.08334	0.5	0.6667	2.3	0.0580	2.2	0.02678	1.4	518.5	2.6	492.7	14.9	395.2	12.4	105	0.41	1.56	518.5	4.9
07	24.75	303	0.23	0.08355	0.4	0.6638	1.6	0.0576	1.5	0.02536	1.6	518.9	1.8	521.7	7.1	539.4	7.2	99	-0.08	1.10	518.9	4.5
02	86.38	913	0.87	0.08260	0.8	0.8503	1.2	0.0747	0.9	0.02475	1.0	519.2	4.0	651.8	9.4	1163.3	12.3	80	-0.49	15.20	d,x	
04	16.39	175	0.75	0.08319	0.6	0.6494	1.8	0.0566	1.7	0.02570	1.4	519.4	3.5	503.0	26.9	450.4	24.6	103	0.08	1.97	519.4	5.4
74	52.55	582	0.64	0.08299	0.6	0.6705	1.5	0.0586	1.4	0.02460	1.2	519.9	3.2	549.1	11.7	687.7	13.4	95	-0.46	4.29	519.9	7.0
66	70.86	805	0.47	0.08402	0.4	0.7201	1.6	0.0622	1.6	0.02632	1.0	521.4	2.1	552.7	11.2	688.5	13.0	94	-0.03	3.42	521.4	4.6
81	32.72	388	0.33	0.08384	0.6	0.6520	1.9	0.0564	1.8	0.02512	1.5	521.7	3.1	520.3	9.4	522.0	9.1	100	-0.17	2.62	521.7	7.0
48	21.77	261	0.28	0.08406	0.4	0.6642	1.4	0.0573	1.3	0.02629	1.3	521.7	2.2	514.7	7.1	491.1	6.6	101	0.04	1.74	521.7	4.6
39	47.07	517	0.76	0.08208	0.6	0.7140	1.2	0.0631	1.1	0.02171	1.1	521.8	3.2	657.3	10.2	1170.0	14.0	79	-1.95	5.45	d	
56	44.72	509	0.49	0.08370	0.3	0.6735	1.1	0.0584	1.1	0.02508	0.7	522.2	1.7	538.7	5.9	620.9	6.4	97	-0.26	2.22	522.2	4.4
73	17.01	186	0.66	0.08347	0.7	0.6817	2.4	0.0592	2.3	0.02509	1.8	522.3	3.4	547.7	15.0	671.5	17.1	95	-0.32	1.63	522.3	7.1
20	84.10	986	0.37	0.08387	0.6	0.6882	1.1	0.0595	0.9	0.02476	1.8	523.7	3.1	562.2	11.9	729.6	14.0	93	-0.50	8.90	523.7	5.2
33	56.80	581	0.91	0.08390	0.4	0.7150	1.5	0.0618	1.4	0.02579	0.8	525.6	2.4	553.6	15.2	694.9	17.7	95	-0.10	3.94	525.6	4.8
28	32.05	350	0.61	0.08438	0.4	0.6911	1.2	0.0594	1.1	0.02631	0.8	525.7	2.0	529.3	7.2	561.3	7.3	99	0.07	nd	525.7	4.6
53	26.03	263	0.94	0.08403	0.4	0.6778	1.4	0.0585	1.4	0.02611	0.8	526.2	2.2	525.0	11.0	546.2	11.1	100	0.01	nd	526.2	4.7
19	44.93	447	1.02	0.08392	0.4	0.6840	1.1	0.0591	1.0	0.02599	0.7	526.3	2.3	530.6	15.7	578.1	16.7	99	-0.02	3.54	526.3	4.8

Spot No.	Pb* (ppm)	U (ppm)	atomic Th/U	Measured isotope ratios and 1σ (%) internal errors								Corrected ages and 1σ absolute internal errors (Ma)						6*/38 -7*/35 concord-ance(%)	% common 206Pb	Spot MSW D	Selected age and 1σ absolute external error (Ma)	
				206Pb/238U	±	207Pb/235U	±	207Pb/206Pb	±	208Pb/232Th	±	206Pb*/238U	±	207Pb*/235U	±	207Pb*/206Pb*	±					
70	31.84	364	0.40	0.08501	0.4	0.6832	1.3	0.0583	1.2	0.02713	1.0	527.5	2.2	517.6	7.1	485.0	6.5	102	0.17	2.45	527.5	4.7
27	56.40	621	0.55	0.08497	0.4	0.7133	1.2	0.0609	1.1	0.02710	1.2	527.9	2.3	531.1	8.8	559.4	9.0	99	0.25	3.73	527.9	4.7
77	81.16	907	0.48	0.08527	0.9	0.7133	1.5	0.0607	1.2	0.02675	1.4	530.0	4.6	540.8	9.5	599.3	9.4	98	0.09	12.01	x	
10	11.79	119	0.89	0.08494	0.7	0.6991	2.4	0.0597	2.3	0.02668	1.1	530.1	3.7	524.2	21.9	523.5	21.6	101	0.22	1.96	530.1	5.6
59	33.72	376	0.47	0.08552	0.4	0.6771	1.4	0.0574	1.3	0.02708	0.8	531.1	2.1	514.6	8.6	454.9	7.6	103	0.16	2.59	531.1	4.7
63	63.68	697	0.53	0.08590	0.4	0.6907	1.0	0.0583	0.9	0.02659	0.7	534.5	1.9	533.9	5.6	545.2	5.5	100	-0.01	3.21	534.5	4.6
89	24.07	255	0.63	0.08632	0.8	0.7493	2.2	0.0630	2.1	0.02790	1.6	535.5	4.6	535.4	29.8	554.0	30.4	100	0.52	3.86	535.5	7.9
35	89.93	957	0.57	0.08747	0.5	0.7649	1.2	0.0634	1.1	0.02716	0.8	544.1	2.7	575.8	7.4	717.8	8.2	94	0.02	9.40	544.1	5.1
46	75.12	809	0.54	0.08741	0.5	0.7248	1.0	0.0601	0.9	0.02626	1.0	544.8	2.7	570.4	5.8	686.9	6.1	96	-0.27	7.08	544.8	5.1
25	50.45	544	0.50	0.08796	0.4	0.7447	1.2	0.0614	1.2	0.02693	1.1	547.3	2.5	573.7	12.8	692.1	14.5	95	-0.14	3.89	547.3	5.0
52	17.23	181	0.53	0.08898	0.5	0.7932	1.9	0.0647	1.8	0.03007	0.9	549.2	2.6	544.0	12.2	538.2	11.9	101	0.77	1.77	549.2	5.1
62	24.28	214	1.39	0.08729	0.4	0.7045	1.6	0.0585	1.6	0.02681	0.9	550.5	2.6	554.8	18.2	613.6	19.4	99	-0.21	2.24	550.5	5.0
90	38.48	402	0.59	0.08892	0.4	0.7289	1.4	0.0595	1.4	0.02663	1.2	554.4	2.4	575.8	9.8	675.4	10.8	96	-0.31	1.87	554.4	7.1
75	96.49	995	0.62	0.08935	0.6	0.7527	1.3	0.0611	1.2	0.02724	1.3	556.4	3.2	580.0	8.9	689.2	9.6	96	-0.16	6.96	556.4	7.4
71	36.85	380	0.65	0.08916	0.6	0.7934	1.9	0.0645	1.8	0.02527	1.3	559.0	3.4	647.0	11.2	981.7	14.2	86	-0.89	3.63	d	
22	20.82	217	0.49	0.09077	0.5	0.7291	1.9	0.0583	1.8	0.02925	1.2	561.7	3.0	535.3	12.0	438.1	10.0	105	0.31	2.76	561.7	5.4
55	36.83	374	0.82	0.08851	0.5	0.7751	1.2	0.0635	1.1	0.02051	1.3	568.8	3.1	777.1	10.8	1448.4	14.6	73	-3.43	4.52	d	
24	51.91	582	0.14	0.09343	0.3	0.7676	1.0	0.0596	0.9	0.02859	1.1	576.7	1.8	579.9	4.4	595.6	4.3	99	-0.02	2.47	576.7	4.9
80	30.14	337	0.12	0.09422	0.5	0.7738	1.8	0.0596	1.7	0.02724	2.2	581.7	2.8	589.5	8.1	622.1	8.1	99	-0.11	1.87	581.7	7.5
37	53.98	559	0.23	0.09840	0.3	0.8210	0.8	0.0605	0.8	0.02978	0.9	606.9	1.9	613.4	4.5	642.7	4.4	99	-0.07	2.36	606.9	5.1
54	33.31	319	0.09	0.11010	0.6	0.9960	1.3	0.0656	1.1	0.04437	2.2	671.8	3.7	676.3	7.6	693.8	7.1	99	0.36	4.52	671.8	6.5
29	29.25	171	0.50	0.16118	0.5	1.9038	1.2	0.0857	1.1	0.04965	1.0	967.4	4.7	1073.1	10.1	1306.1	10.5	90	0.13	nd	967.4	9.0
08	48.53	275	0.44	0.16827	0.3	1.7231	1.0	0.0743	1.0	0.05024	1.0	1007.8	3.1	1023.2	8.6	1066.0	8.5	98	-0.08	1.82	1066.0	43.6
09	88.26	471	0.54	0.17691	1.1	1.8783	1.4	0.0770	0.9	0.04332	2.2	1070.5	11.2	1194.4	17.0	1435.8	16.4	90	-1.60	3.99	d	
06	112.0	610	0.19	0.18710	0.4	1.9693	0.9	0.0763	0.7	0.05708	1.0	1106.7	4.8	1097.5	18.0	1083.2	17.6	101	0.09	1.72	1083.2	46.9
85	274.7	1340	0.51	0.19697	2.5	2.8902	2.7	0.1064	0.9	0.04007	3.9	1191.7	27.7	1547.1	26.7	2079.5	19.3	77	-2.73	15.43	d,x	
23	66.19	269	0.73	0.21699	0.4	2.4342	0.8	0.0814	0.7	0.06530	0.7	1274.3	4.5	1242.8	9.2	1205.4	8.7	103	0.12	2.51	1205.4	49.1
72	115.0	508	0.30	0.22366	0.6	2.6380	1.0	0.0855	0.8	0.05859	1.4	1310.3	7.6	1351.9	8.1	1423.3	6.7	97	-0.51	1.49	1423.3	68.6
84	177.2	762	0.05	0.24358	1.0	3.1661	1.2	0.0943	0.8	0.05634	5.7	1409.2	12.1	1470.9	10.0	1561.6	6.9	96	-0.28	nd	1561.6	75.2

Spot No.	Pb* (ppm)	U (ppm)	atomic Th/U	Measured isotope ratios and 1σ (%) internal errors								Corrected ages and 1σ absolute internal errors (Ma)						6*/38 -7*/35 concord-ance(%)	% common 206Pb	Spot MSW D	Selected age and 1σ absolute external error (Ma)	
				206Pb/238U	±	207Pb/235U	±	207Pb/206Pb	±	208Pb/232Th	±	206Pb*/238U	±	207Pb*/235U	±	207Pb*/206Pb*	±					
87	112.2	415	0.66	0.24346	1.4	3.2046	1.6	0.0955	0.9	0.07349	1.1	1411.6	17.8	1445.2	20.4	1508.5	17.6	98	0.17	3.55	1508.5	74.4
47	153.1	562	0.26	0.27232	0.6	3.7737	0.8	0.1005	0.5	0.05751	1.7	1568.1	8.9	1664.5	7.1	1789.9	4.9	94	-1.03	1.69	d	
11	140.4	496	0.10	0.28753	0.3	4.3556	0.6	0.1099	0.5	0.12110	1.1	1622.6	4.7	1659.0	5.5	1708.1	4.8	98	0.60	1.29	1708.1	68.6
42	98.54	345	0.24	0.28367	0.3	3.8253	0.6	0.0978	0.5	0.06372	1.4	1623.2	4.9	1657.1	5.5	1703.8	4.7	98	-0.75	1.17	1703.8	68.5
03	50.43	130	0.79	0.33138	0.4	5.1172	1.0	0.1120	0.9	0.09709	0.8	1855.3	6.2	1824.8	11.7	1805.2	11.1	102	0.19	1.39	1805.2	73.2

All errors are 1σ, * = radiogenic component only, nd = not determined, d = discordant, rd = reversely discordant, x = excess within grain MSWD.

2. U-Th-Pb isotope data for Sample E206.

Spot No.	Pb* (ppm)	U (ppm)	atomic Th/U	Measured isotope ratios and 1σ (%) internal errors								Corrected ages and 1σ absolute internal errors (Ma)						6*/38 -7*/35 concord-ance(%)	% common 206Pb	Spot MSW D	Selected age and 1σ absolute external error (Ma)	
				206Pb/238U	±	207Pb/235U	±	207Pb/206Pb	±	208Pb/232Th	±	206Pb*/238U	±	207Pb*/235U	±	207Pb*/206Pb*	±					
85	131.7	2081	0.83	0.05655	1.7	0.6050	1.9	0.0776	0.8	0.01570	1.9	363.4	6.1	548.6	11.4	1434.3	15.7	66	-1.62	76.99	d,x	
20	7.89	103	1.17	0.06137	1.0	0.5397	4.1	0.0638	4.0	0.02093	1.7	382.6	3.9	336.2	27.6	63.3	5.9	114	1.97	1.94	382.6	5.1
87	106.0	1539	1.46	0.05655	2.9	0.6892	3.3	0.0884	1.6	0.00973	3.6	402.2	11.7	956.3	26.1	2634.5	27.7	42	-12.72	112.9	d,x	
57	107.3	1565	0.83	0.06285	1.2	0.6496	2.5	0.0750	2.2	0.01192	3.0	416.1	5.0	738.1	16.2	1909.7	24.4	56	-5.47	31.01	d,x	
31	96.84	1437	1.62	0.05545	1.5	0.5552	2.5	0.0726	1.9	0.00551	1.9	422.7	6.5	1118.7	14.5	2953.4	13.9	38	-21.51	13.19	d,x	
46	80.98	1119	0.51	0.06897	1.0	0.5941	1.6	0.0625	1.3	0.02048	2.0	434.2	4.1	498.4	11.8	816.9	15.9	87	-0.47	10.75	d,x	
89	145.2	2028	4.24	0.03367	2.0	0.5548	2.5	0.1195	1.5	0.00385	2.0	443.7	13.1	1814.5	29.4	4288.1	16.4	24	-107.48	65.13	d,x	
04	69.62	962	0.31	0.07204	1.5	0.5863	1.8	0.0590	1.0	0.02456	1.3	448.0	6.6	440.3	7.5	409.4	4.9	102	0.49	48.09	x	
17	41.98	529	1.14	0.06753	1.1	0.6299	1.8	0.0676	1.4	0.01344	2.7	457.7	5.0	846.6	12.9	2088.4	17.1	54	-8.14	nd	d	
74	72.95	982	0.34	0.07356	1.6	0.6230	1.9	0.0614	1.1	0.02290	1.7	460.2	7.0	496.1	9.8	676.3	9.5	93	-0.08	nd	460.2	18.5
58	61.60	739	1.10	0.07118	1.8	0.6897	2.4	0.0703	1.6	0.01557	3.5	473.6	8.4	810.5	21.1	1915.8	28.5	58	-6.11	nd	d	
07	22.15	279	1.90	0.06101	0.8	0.5289	2.1	0.0629	1.9	0.00733	1.7	474.0	4.2	1218.1	10.7	2997.7	11.6	39	-23.97	3.14	d	
03	75.03	998	1.53	0.06286	1.5	0.5762	2.1	0.0665	1.5	0.00570	3.9	475.0	8.0	1182.3	23.8	2904.7	28.0	40	-21.15	16.50	d,x	
06	10.98	125	1.16	0.07293	1.1	0.6625	3.1	0.0659	2.9	0.01793	3.0	479.9	5.7	750.5	21.5	1692.9	31.7	64	-4.83	2.66	d	
45	108.1	1352	0.42	0.07745	1.1	0.6573	1.4	0.0615	0.9	0.02372	1.3	483.9	5.2	530.1	7.5	741.4	7.4	91	-0.30	14.03	x	

Spot No.	Pb* (ppm)	U (ppm)	atomic Th/U	Measured isotope ratios and 1σ (%) internal errors								Corrected ages and 1σ absolute internal errors (Ma)						6*/38 -7*/35 concord-ance(%)	% common 206Pb	Spot MSWD	Selected age and 1σ absolute external error (Ma)	
				206Pb/238U	±	207Pb/235U	±	207Pb/206Pb	±	208Pb/232Th	±	206Pb*/238U	±	207Pb*/235U	±	207Pb*/206Pb*	±					
33	4.97	57	0.79	0.07757	0.8	0.6247	3.9	0.0584	3.8	0.02360	1.8	487.0	4.1	506.4	21.0	615.2	24.0	96	-0.23	1.24	487.0	5.9
42	13.72	134	0.94	0.08404	1.1	1.4279	4.8	0.1232	4.7	0.04094	4.7	488.1	6.3	472.3	66.4	437.5	62.3	103	8.12	2.45	488.1	7.6
13	8.93	91	1.19	0.07846	0.7	0.6652	2.8	0.0615	2.7	0.02495	1.2	491.7	3.8	483.5	22.3	480.5	22.0	102	0.57	1.74	491.7	5.6
81	16.03	156	1.52	0.07727	1.0	0.6872	3.7	0.0645	3.6	0.02323	2.0	493.3	6.8	583.2	59.0	990.7	83.6	85	-0.94	2.20	493.3	9.0
48	23.30	248	1.00	0.07874	0.5	0.6329	1.8	0.0583	1.7	0.02448	0.9	494.3	2.7	496.6	12.8	534.0	13.4	100	0.02	2.35	494.3	5.0
19	5.88	65	0.87	0.07887	0.9	0.6722	3.7	0.0618	3.6	0.02422	1.7	495.0	4.2	530.2	21.5	706.8	26.1	93	-0.14	1.51	495.0	6.0
30	21.24	226	0.99	0.07893	0.7	0.6057	2.1	0.0557	2.0	0.02443	1.1	496.2	3.9	490.8	30.2	491.9	30.1	101	-0.16	3.24	496.2	5.8
53	6.39	73	0.66	0.07948	0.9	0.6025	3.3	0.0550	3.2	0.02449	2.0	497.0	4.5	481.8	21.7	428.0	19.4	103	-0.05	1.56	497.0	6.2
86	6.99	76	0.91	0.07917	1.0	0.6027	3.7	0.0552	3.6	0.02361	1.6	498.9	5.1	510.3	24.0	585.4	26.1	98	-0.52	2.02	498.9	7.9
16	86.32	1044	0.42	0.08023	0.8	0.6902	1.2	0.0624	0.9	0.02507	1.1	499.2	3.6	537.2	6.4	707.9	6.8	93	-0.07	7.47	499.2	5.6
22	3.96	46	0.54	0.08013	1.1	0.6282	3.9	0.0569	3.8	0.02493	2.2	499.5	5.2	490.7	20.1	463.8	18.8	102	0.07	1.57	499.5	6.7
54	6.95	73	0.99	0.07966	0.9	0.6334	2.9	0.0577	2.8	0.02450	1.6	500.3	4.6	504.0	21.0	547.2	22.0	99	-0.10	1.95	500.3	6.3
82	9.55	103	1.42	0.07390	1.2	0.7074	3.2	0.0694	3.0	0.01631	2.9	501.8	6.7	910.2	30.5	2119.3	43.3	55	-8.20	5.00		
55	6.92	71	1.08	0.07995	0.9	0.6481	3.3	0.0588	3.2	0.02485	1.5	502.0	4.3	503.0	22.2	537.4	23.1	100	0.07	1.71	502.0	6.1
12	4.77	51	0.94	0.07952	0.9	0.6392	3.9	0.0583	3.8	0.02325	1.6	502.3	4.7	550.1	22.3	775.6	28.0	91	-0.82	5.00	502.3	6.4
35	20.34	217	0.92	0.08016	0.5	0.6321	1.9	0.0572	1.8	0.02454	1.0	503.4	2.7	510.1	12.4	564.4	13.1	99	-0.21	2.19	503.4	5.1
44	32.96	355	0.87	0.08029	0.5	0.6448	1.6	0.0582	1.6	0.02470	0.8	503.5	2.5	512.3	12.4	574.6	13.3	98	-0.12	2.72	503.5	5.0
25	19.08	188	1.27	0.08005	0.5	0.6514	2.0	0.0590	1.9	0.02476	0.8	504.6	2.7	512.7	15.7	585.1	17.2	98	-0.06	5.00	504.6	5.1
77	45.92	543	0.46	0.08103	0.7	0.6431	1.4	0.0576	1.2	0.02585	1.0	504.7	3.5	491.6	7.0	447.2	5.9	103	0.20	6.70	504.7	19.0
76	16.76	177	0.91	0.08087	0.7	0.6339	2.9	0.0569	2.8	0.02583	1.1	506.4	3.3	468.8	16.8	324.0	12.3	108	0.48	2.39	506.4	19.1
84	38.45	424	0.77	0.08068	0.7	0.6537	1.9	0.0588	1.8	0.02423	1.4	506.4	3.7	534.0	16.0	673.0	18.6	95	-0.39	4.29	506.4	7.1
65	110.5	1252	1.01	0.07685	0.7	0.6714	1.4	0.0634	1.2	0.01640	2.3	507.2	3.9	802.0	14.6	1757.3	21.0	63	-5.64	22.42	d,x	
88	16.15	168	0.99	0.08089	0.6	0.6565	2.5	0.0589	2.5	0.02459	1.3	509.3	3.2	533.3	16.6	664.6	19.3	95	-0.35	1.67	509.3	6.9
36	112.9	1322	1.19	0.07376	1.2	0.7912	1.6	0.0778	1.2	0.01158	2.8	510.1	6.5	1039.6	21.0	2435.3	27.1	49	-10.97	23.23	d,x	
34	50.43	543	0.84	0.08118	0.5	0.6441	1.2	0.0575	1.1	0.02403	0.8	510.5	3.2	543.4	27.7	702.3	33.2	94	-0.64	3.46	510.5	5.4
63	39.83	465	0.74	0.07863	0.9	0.6815	1.5	0.0629	1.2	0.01668	3.3	511.5	5.0	759.5	19.8	1591.1	28.6	67	-4.47	5.32	d	
75	56.44	681	0.89	0.07613	0.7	0.6626	1.9	0.0631	1.8	0.01088	1.4	512.5	3.5	897.2	11.2	2030.4	15.2	57	-8.10	3.16	d	
90	7.05	77	0.70	0.08204	1.1	0.6859	3.5	0.0606	3.3	0.02543	2.2	513.0	5.5	537.8	21.5	662.3	24.4	95	-0.12	5.00	513.0	8.3
69	94.66	1094	0.93	0.07738	1.1	0.6680	1.6	0.0626	1.1	0.01425	2.5	514.5	5.7	848.0	14.9	1874.2	19.9	61	-6.71	22.26	d,x	

Spot No.	Pb* (ppm)	U (ppm)	atomic Th/U	Measured isotope ratios and 1σ (%) internal errors								Corrected ages and 1σ absolute internal errors (Ma)						6*/38 -7*/35 concord-ance(%)	% common 206Pb	Spot MSW D	Selected age and 1σ absolute external error (Ma)	
				206Pb/238U	±	207Pb/235U	±	207Pb/206Pb	±	208Pb/232Th	±	206Pb*/238U	±	207Pb*/235U	±	207Pb*/206Pb*	±					
80	26.54	262	1.16	0.08150	0.8	0.6501	1.9	0.0579	1.7	0.02570	1.2	514.5	4.0	502.0	20.5	490.6	19.9	102	0.11	3.33	514.5	19.5
14	46.79	534	0.50	0.08291	0.5	0.6506	1.4	0.0569	1.3	0.02592	1.0	516.0	2.4	504.5	8.1	465.4	7.4	102	0.07	3.98	516.0	5.0
59	30.85	327	1.12	0.07958	1.0	0.8876	1.9	0.0809	1.6	0.02007	2.1	517.4	5.5	830.0	17.1	1815.4	23.8	62	-3.86	5.27	d	
18	60.14	644	0.79	0.08247	0.5	0.6627	1.1	0.0583	1.0	0.02485	1.3	517.7	2.6	545.8	12.5	684.3	14.5	95	-0.48	3.76	517.7	5.1
60	10.83	125	0.45	0.08314	0.7	0.6530	2.3	0.0570	2.2	0.02538	1.6	517.9	3.4	516.9	11.5	523.6	11.3	100	-0.11	1.54	517.9	5.6
43	36.55	365	1.12	0.08193	0.5	0.6468	1.5	0.0573	1.4	0.02446	1.0	518.0	2.7	552.8	12.3	727.5	14.7	94	-0.76	3.15	518.0	5.2
24	28.68	308	0.90	0.08117	0.7	0.6659	1.6	0.0595	1.5	0.02166	1.5	518.1	3.4	643.8	12.0	1131.5	16.5	80	-2.20	3.13	d	
67	49.71	559	0.58	0.08310	0.5	0.6695	1.3	0.0584	1.2	0.02438	1.3	520.4	2.6	553.0	8.3	703.1	9.5	94	-0.53	3.65	520.4	5.1
09	43.22	466	0.78	0.08255	0.5	0.6571	1.4	0.0577	1.3	0.02329	1.0	521.4	2.6	584.1	10.6	853.6	13.4	89	-1.19	3.52	521.4	5.2
73	41.81	504	0.24	0.08437	0.5	0.6732	1.1	0.0579	1.0	0.02719	1.6	523.3	2.6	514.6	6.5	484.2	5.9	102	0.13	3.15	523.3	19.6
21	39.30	438	0.49	0.08456	0.4	0.6654	1.3	0.0571	1.2	0.02843	1.0	523.3	2.7	479.2	21.1	287.8	13.8	109	0.60	2.66	523.3	5.2
26	59.08	687	0.37	0.08435	0.4	0.6700	1.2	0.0576	1.1	0.02634	0.9	524.0	2.0	518.2	6.0	502.1	5.6	101	0.04	3.22	524.0	4.9
62	24.38	268	0.59	0.08435	0.5	0.6811	1.6	0.0586	1.5	0.02636	1.0	525.2	2.7	523.7	9.1	532.3	9.0	100	0.06	2.40	525.2	5.3
50	83.51	954	0.36	0.08559	1.5	0.7601	2.3	0.0644	1.8	0.03148	2.2	526.1	7.4	503.3	13.7	411.7	10.6	105	1.13	19.22	x	
39	34.15	392	0.41	0.08468	0.4	0.6663	1.3	0.0571	1.2	0.02599	1.2	526.7	2.3	522.4	8.6	513.6	8.2	101	-0.06	2.41	526.7	5.1
64	80.57	930	0.39	0.08467	0.4	0.6634	1.0	0.0568	0.9	0.02564	0.9	526.9	2.1	526.4	7.2	533.4	7.0	100	-0.15	4.63	526.9	5.0
61	18.84	188	0.93	0.08483	0.7	0.6736	1.9	0.0576	1.8	0.02758	1.1	526.9	3.7	471.8	16.0	240.0	8.9	112	0.79	5.00	526.9	5.8
23	38.49	387	0.94	0.08450	0.4	0.6722	1.4	0.0577	1.3	0.02628	1.1	528.1	3.5	512.3	35.7	468.9	33.2	103	0.15	2.29	528.1	5.7
27	40.47	348	1.65	0.08551	1.0	1.1527	3.9	0.0978	3.8	0.02860	1.7	528.8	5.5	645.3	38.9	1127.8	55.0	82	2.52	nd	d	
47	29.79	321	0.65	0.08487	0.7	0.7118	1.8	0.0608	1.7	0.02599	1.4	529.4	3.7	559.2	16.1	695.6	18.5	95	-0.22	nd	529.4	5.8
29	19.47	217	0.64	0.08346	0.7	0.6908	1.9	0.0600	1.7	0.02105	2.0	529.9	3.9	654.5	13.6	1122.3	18.4	81	-2.09	3.00	d	
52	18.19	210	0.38	0.08506	0.6	0.6664	1.7	0.0568	1.6	0.02436	1.9	530.8	3.3	549.9	9.4	638.2	10.0	97	-0.50	2.29	530.8	5.6
10	116.7	1329	0.49	0.08442	0.9	0.6998	1.3	0.0601	0.9	0.02186	1.6	531.4	4.5	618.2	8.5	959.2	10.0	86	-1.33	21.46	d	
68	68.38	819	0.21	0.08572	0.4	0.6771	1.1	0.0573	1.0	0.02632	1.2	531.5	2.2	526.8	5.0	511.9	4.5	101	-0.03	4.25	531.5	5.1
56	14.15	157	0.48	0.08588	0.5	0.6890	2.4	0.0582	2.3	0.02685	1.5	533.7	2.8	528.3	12.3	517.8	11.9	101	0.06	nd	533.7	5.4
28	34.43	355	0.85	0.08505	0.6	0.7324	1.6	0.0625	1.4	0.02475	1.1	535.5	3.3	610.7	11.9	919.9	15.2	88	-0.88	4.61	d	
11	41.08	449	0.86	0.08222	0.9	0.7774	2.3	0.0686	2.1	0.01728	2.4	537.3	5.1	837.1	22.5	1759.2	31.9	64	-4.97	5.69	d	
15	10.37	111	0.61	0.08622	0.7	0.6614	2.7	0.0556	2.6	0.02603	1.6	537.9	3.7	532.0	16.3	521.4	15.7	101	-0.26	1.57	537.9	5.9
78	27.87	285	0.79	0.08611	0.6	0.6879	1.6	0.0579	1.5	0.02680	1.1	538.6	3.0	528.4	13.5	512.3	13.0	102	0.05	2.47	538.6	20.2

Spot No.	Pb* (ppm)	U (ppm)	atomic Th/U	Measured isotope ratios and 1σ (%) internal errors								Corrected ages and 1σ absolute internal errors (Ma)						6*/38 -7*/35 concord-ance(%)	% common 206Pb	Spot MSW D	Selected age and 1σ absolute external error (Ma)	
				206Pb/238U	±	207Pb/235U	±	207Pb/206Pb	±	208Pb/232Th	±	206Pb*/238U	±	207Pb*/235U	±	207Pb*/206Pb*	±					
41	71.74	821	0.33	0.08677	0.5	0.6902	1.1	0.0577	0.9	0.02602	0.8	539.1	2.6	543.4	5.3	569.3	5.1	99	-0.16	5.17	539.1	5.3
05	27.27	289	0.54	0.08783	0.7	0.7365	1.8	0.0608	1.7	0.03031	1.2	541.3	3.7	498.6	20.1	322.7	14.0	109	0.95	3.22	541.3	5.9
08	18.09	202	0.39	0.08747	0.5	0.7152	1.7	0.0593	1.6	0.02715	1.3	542.7	2.9	546.4	11.2	571.1	11.3	99	0.02	1.96	542.7	5.5
02	24.88	255	0.72	0.08732	0.6	0.6983	1.7	0.0580	1.6	0.02678	1.0	544.7	3.3	544.7	11.1	563.2	11.0	100	-0.11	3.39	544.7	5.7
40	63.26	622	0.84	0.08826	0.6	0.6833	1.2	0.0561	1.0	0.02764	1.0	549.8	3.5	518.0	10.6	403.3	8.4	106	0.16	6.84	549.8	5.8
32	104.9	1148	0.37	0.08900	0.6	0.7098	1.1	0.0578	0.9	0.02913	1.1	550.4	3.4	525.8	14.3	430.5	12.0	105	0.29	10.09	x	
66	37.14	399	0.47	0.08897	0.5	0.7078	1.4	0.0577	1.3	0.02684	1.1	553.2	2.8	555.5	7.7	576.2	7.5	100	-0.19	3.46	553.2	5.5
49	3.25	30	0.93	0.09087	1.7	0.8175	5.5	0.0652	5.3	0.02962	2.6	561.9	9.4	544.9	38.4	500.8	35.4	103	0.96	2.48	561.9	10.6
72	102.8	1123	0.15	0.09655	0.8	0.8166	1.1	0.0613	0.8	0.01471	4.2	602.1	4.7	690.2	9.8	990.8	11.2	87	-1.31	17.08	d,x	
79	78.06	708	1.79	0.08420	0.8	0.7703	1.9	0.0664	1.7	0.01117	6.6	644.0	14.5	1468.3	54.6	3024.1	63.9	44	-23.71	72.90	d,x	
37	24.87	214	0.37	0.11362	0.6	0.9885	1.6	0.0631	1.5	0.03467	1.5	696.6	4.2	699.9	12.7	719.2	12.6	100	-0.03	2.95	696.6	7.3
38	57.73	419	0.77	0.12050	0.6	1.1765	1.6	0.0708	1.5	0.03918	2.7	739.6	5.4	790.9	35.1	956.0	39.3	94	-0.02	4.22	739.6	8.3
83	38.57	301	3.01	0.08115	1.0	1.0666	5.1	0.0953	5.0	0.00702	3.4	776.6	38.8	2090.3	77.8	3870.4	69.5	37	-56.71	82.03	d,x	
70	52.69	231	0.67	0.20460	0.5	2.2168	1.0	0.0786	0.9	0.06020	0.9	1209.1	5.3	1196.9	15.2	1188.9	14.8	101	-0.13	nd	1188.9	32.0
71	97.25	430	0.28	0.22245	1.4	2.8462	1.5	0.0928	0.7	0.07438	1.0	1293.9	15.9	1328.6	12.9	1393.2	8.2	97	0.50	nd0	1393.2	37.8
51	240.0	948	1.46	0.21052	0.9	3.3303	1.1	0.1147	0.6	0.02593	2.7	1398.0	12.0	2151.0	15.0	2984.4	13.3	65	-14.33	7.42	d	
01	388.0	1166	0.81	0.30988	1.0	9.2928	1.1	0.2175	0.3	0.04086	1.6	1841.2	16.3	2601.5	11.0	3267.8	5.6	71	-6.26	3.09	d	

All errors are 1σ, * = radiogenic component only, nd = not determined, d = discordant, rd = reversely discordant, x = excess within grain MSWD.

3. U-Th-Pb isotope data for Sample E205.

Spot No.	Pb* (ppm)	U (ppm)	atomic Th/U	Measured isotope ratios and 1σ (%) internal errors								Corrected ages and 1σ absolute internal errors (Ma)						6*/38 -7*/35 concord-ance(%)	% common 206Pb	Spot MSW D	Selected age and 1σ absolute external error (Ma)	
				206Pb/238U	±	207Pb/235U	±	207Pb/206Pb	±	208Pb/232Th	±	206Pb*/238U	±	207Pb*/235U	±	207Pb*/206Pb*	±					
04	5.77	153	2.48	0.02562	1.8	0.2884	6.1	0.0816	5.9	0.00441	2.7	211.3	4.0	761.9	16.9	3179.5	24.2	28	-26.98	2.53	d	
79	101.1	1841	0.55	0.05204	0.8	0.5222	1.3	0.0728	1.0	0.01547	2.4	331.1	2.7	454.2	8.2	1149.4	14.3	73	-0.67	11.70	d,x	
13	128.0	1995	0.67	0.05844	0.6	0.6099	1.7	0.0757	1.6	0.02012	2.4	366.1	2.4	433.9	13.4	834.1	21.2	84	1.08	9.67	d	

Spot No.	Pb* (ppm)	U (ppm)	atomic Th/U	Measured isotope ratios and 1σ (%) internal errors								Corrected ages and 1σ absolute internal errors (Ma)						6*/38 -7*/35 concord-ance(%)	% common 206Pb	Spot MSW D	Selected age and 1σ absolute external error (Ma)	
				206Pb/238U	±	207Pb/235U	±	207Pb/206Pb	±	208Pb/232Th	±	206Pb*/238U	±	207Pb*/235U	±	207Pb*/206Pb*	±					
87	81.38	1219	0.88	0.05817	1.0	0.6783	1.8	0.0846	1.5	0.01874	2.0	366.8	3.8	505.7	18.2	1218.0	31.5	73	0.46	11.91	d,x	
67	111.0	1660	0.66	0.06126	1.3	0.6035	1.9	0.0715	1.4	0.02037	1.7	385.0	4.9	442.4	10.7	779.3	14.5	87	0.77	18.52	d,x	
65	81.27	1107	0.71	0.06573	1.6	0.6249	2.1	0.0690	1.4	0.02266	1.9	411.0	6.7	435.7	26.2	595.6	32.4	94	1.11	53.58	d,x	
02	62.47	796	0.88	0.06777	1.4	0.6514	2.6	0.0697	2.2	0.02218	1.5	425.9	5.8	471.7	15.3	732.9	19.9	90	0.73	nd	425.9	16.8
24	109.6	1521	0.60	0.06728	0.6	0.6415	1.3	0.0692	1.1	0.01911	1.8	427.2	2.6	549.9	10.0	1114.8	15.3	78	-0.94	5.47	d	
78	113.8	1612	0.69	0.06634	0.8	0.5974	1.4	0.0653	1.2	0.01210	1.6	434.8	3.3	693.4	7.4	1665.5	10.2	63	-4.72	11.83	d,x	
54	15.81	168	0.99	0.07599	0.8	1.2074	3.1	0.1152	3.0	0.03801	2.1	439.9	3.8	269.8	41.6	0.1	0.0	163	9.74	3.54	rd	
57	68.76	856	0.94	0.07058	0.7	0.6081	1.3	0.0625	1.1	0.01624	1.6	462.6	3.2	692.7	9.4	1555.3	13.7	67	-4.29	7.78	d	
76	74.45	950	0.55	0.07427	1.1	0.6733	1.7	0.0658	1.4	0.02040	1.5	468.9	4.9	578.0	9.4	1045.1	12.0	81	-1.03	25.69	d,x	
18	34.16	383	0.96	0.07510	0.7	0.6193	1.6	0.0598	1.4	0.02429	1.3	471.2	3.2	452.4	12.9	394.4	11.3	104	0.63	4.41	471.2	17.8
37	55.85	730	0.53	0.07388	1.1	0.6045	1.6	0.0593	1.2	0.01560	3.2	475.0	5.0	637.8	12.9	1277.0	18.2	74	-2.98	11.98	d,x	
83	38.37	486	0.46	0.07594	0.5	0.6158	1.4	0.0588	1.3	0.02273	1.3	475.5	2.2	502.7	7.7	639.5	9.0	95	-0.27	2.26	475.5	6.1
70	78.14	964	0.56	0.07595	0.6	0.6493	1.2	0.0620	1.1	0.02323	1.4	476.5	2.7	516.6	8.2	716.0	10.0	92	-0.15	6.27	476.5	17.9
35	55.17	713	0.57	0.07407	1.4	0.6245	1.9	0.0611	1.3	0.01558	2.8	477.2	6.4	657.2	13.4	1347.4	17.8	73	-3.15	23.72	d,x	
30	64.94	780	0.66	0.07650	0.6	0.6111	1.2	0.0579	1.0	0.02177	1.3	483.7	3.0	537.6	6.9	792.3	8.4	90	-0.93	5.96	483.7	18.2
80	30.01	342	0.74	0.07796	1.0	0.6493	2.0	0.0604	1.8	0.02586	1.4	484.7	4.7	461.2	16.9	367.9	13.7	105	0.78	7.42	484.7	7.5
55	65.93	785	0.47	0.07981	0.7	0.6894	1.9	0.0627	1.7	0.02802	1.6	493.9	3.6	469.2	14.2	369.1	11.5	105	1.04	13.20	d,x	
56	57.78	676	0.58	0.07929	0.5	0.6568	1.4	0.0601	1.3	0.02505	1.0	495.6	3.0	503.4	21.7	559.5	23.4	98	0.15	nd	495.6	18.6
90	43.59	490	0.78	0.07900	0.6	0.6434	1.6	0.0591	1.5	0.02342	1.2	497.3	2.7	539.1	10.3	739.3	12.6	92	-0.59	3.32	497.3	6.5
27	10.51	128	0.40	0.08029	0.7	0.6592	2.4	0.0595	2.3	0.02500	1.7	500.6	3.4	512.1	11.9	576.8	12.6	98	0.03	nd	500.6	18.9
77	128.0	1469	0.68	0.07961	0.5	0.7131	1.2	0.0650	1.0	0.02288	1.6	501.5	2.8	596.2	11.4	990.1	15.5	84	-0.88	5.16	d	
59	35.25	399	0.67	0.08009	0.5	0.6305	1.6	0.0571	1.5	0.02495	1.0	501.5	2.3	494.2	9.3	483.8	8.9	101	0.04	2.62	501.5	18.8
58	10.05	113	0.75	0.07940	1.7	0.6764	3.2	0.0618	2.7	0.02411	3.2	502.2	8.8	580.8	32.8	922.8	43.6	86	-0.98	7.83	502.2	20.6
23	73.57	868	0.49	0.08071	1.2	0.7275	1.7	0.0654	1.2	0.02546	1.7	503.6	5.6	550.6	10.5	765.8	11.8	91	0.08	25.49	d,x	
20	46.81	564	0.43	0.08066	0.5	0.6685	1.1	0.0601	1.0	0.02305	1.5	505.6	2.3	553.1	6.5	766.1	7.8	91	-0.56	2.45	505.6	18.9
73	23.00	266	0.56	0.08096	0.6	0.6249	1.9	0.0560	1.8	0.02439	1.6	506.2	3.1	508.5	11.3	533.0	11.4	100	-0.25	2.42	506.2	6.8
34	24.66	278	0.63	0.08109	0.5	0.6354	1.7	0.0568	1.6	0.02536	1.2	507.0	2.6	494.7	10.2	460.2	9.4	102	0.08	nd	507.0	19.0
44	16.44	188	0.57	0.08128	0.6	0.6366	1.8	0.0568	1.7	0.02526	1.2	507.9	3.2	499.9	12.3	482.8	11.7	102	0.00	nd	507.9	19.1
64	48.52	463	1.42	0.07999	0.6	0.6313	1.4	0.0572	1.3	0.02475	0.9	508.3	3.3	499.9	22.9	516.2	23.3	102	-0.05	5.25	508.3	19.1

Spot No.	Pb* (ppm)	U (ppm)	atomic Th/U	Measured isotope ratios and 1σ (%) internal errors								Corrected ages and 1σ absolute internal errors (Ma)						6*/38 -7*/35 concord-ance(%)	% common 206Pb	Spot MSW D	Selected age and 1σ absolute external error (Ma)	
				206Pb/238U	±	207Pb/235U	±	207Pb/206Pb	±	208Pb/232Th	±	206Pb*/238U	±	207Pb*/235U	±	207Pb*/206Pb*	±					
26	74.90	761	1.09	0.08072	0.5	0.6493	1.3	0.0583	1.2	0.02514	0.8	509.1	2.8	505.2	18.6	527.6	19.0	101	0.05	6.23	509.1	19.1
89	51.04	579	0.60	0.08171	0.5	0.6776	1.5	0.0601	1.4	0.02446	1.0	511.4	3.1	547.5	18.9	714.7	22.7	93	-0.37	3.79	511.4	6.9
86	69.63	831	0.55	0.08032	0.6	0.6989	1.3	0.0631	1.1	0.01822	1.3	511.5	3.1	666.1	7.9	1241.1	10.7	77	-2.31	nd	d	
45	60.04	649	0.75	0.08212	0.5	0.6502	1.1	0.0574	1.0	0.02604	1.0	513.4	2.5	492.1	9.1	421.4	7.8	104	0.26	4.45	513.4	19.2
62	16.32	179	0.67	0.08247	0.7	0.6328	2.6	0.0556	2.5	0.02649	1.5	514.2	3.6	472.7	18.0	301.3	12.3	109	0.39	2.07	514.2	19.4
60	73.36	787	0.80	0.08214	0.8	0.6890	1.3	0.0608	1.0	0.02524	1.3	515.7	4.5	539.1	27.4	666.7	31.7	96	-0.11	11.02	x	
17	74.18	883	0.34	0.08309	0.5	0.6551	1.0	0.0572	0.8	0.02621	1.0	516.6	2.4	506.1	5.1	470.3	4.5	102	0.09	4.96	516.6	19.3
42	25.87	270	0.88	0.08259	0.6	0.6645	1.7	0.0584	1.6	0.02609	1.0	517.3	3.1	500.1	12.4	454.4	11.2	103	0.28	2.83	517.3	19.4
19	65.86	722	0.64	0.08318	0.6	0.6721	1.2	0.0586	1.0	0.02636	0.9	519.0	2.8	508.2	7.3	482.5	6.7	102	0.22	6.27	519.0	19.5
43	21.90	250	0.47	0.08353	0.6	0.6663	2.0	0.0579	1.9	0.02675	1.2	519.5	3.1	502.7	11.0	443.4	9.7	103	0.25	2.39	519.5	19.5
12	30.69	365	0.32	0.08361	0.5	0.6613	1.5	0.0574	1.4	0.02571	1.3	520.2	2.5	518.1	8.1	518.8	7.8	100	-0.04	2.52	520.2	19.5
88	52.95	610	0.47	0.08341	0.5	0.6765	1.5	0.0588	1.4	0.02456	1.2	520.9	2.6	547.7	7.9	671.7	8.8	95	-0.38	3.60	520.9	6.8
32	59.61	669	0.54	0.08362	0.4	0.6699	1.0	0.0581	0.9	0.02581	0.8	522.0	2.2	523.4	8.9	547.4	9.0	100	-0.04	3.40	522.0	19.5
07	36.08	411	0.47	0.08386	0.5	0.6761	1.3	0.0585	1.2	0.02617	1.1	522.4	2.6	521.4	7.4	532.2	7.2	100	0.05	2.80	522.4	19.6
81	12.00	131	0.65	0.08361	0.7	0.7106	2.8	0.0616	2.7	0.02533	1.7	522.6	3.7	559.2	15.9	727.1	18.8	93	-0.23	1.56	522.6	7.2
28	49.46	543	0.63	0.08351	0.5	0.6645	1.4	0.0577	1.3	0.02533	1.0	522.9	2.3	531.3	8.2	588.2	8.5	98	-0.22	3.11	522.9	19.5
68	41.41	425	0.86	0.08406	0.9	0.6606	1.8	0.0570	1.5	0.02719	1.3	524.4	4.7	475.3	15.2	278.7	9.5	110	0.62	7.83	524.4	20.0
74	64.38	739	0.44	0.08425	0.5	0.6732	1.2	0.0579	1.1	0.02511	1.0	525.2	2.3	539.2	6.6	609.2	7.0	97	-0.27	3.55	525.2	6.7
25	30.67	336	0.57	0.08459	0.5	0.6773	1.6	0.0581	1.6	0.02749	1.3	525.9	2.5	497.2	10.5	388.1	8.4	106	0.44	2.30	525.9	19.7
82	27.04	295	0.63	0.08418	0.6	0.6758	1.8	0.0582	1.7	0.02541	1.0	526.0	2.9	540.4	9.8	617.1	10.5	97	-0.26	2.17	526.0	6.9
40	7.16	83	0.37	0.08484	0.7	0.6930	2.8	0.0592	2.7	0.02751	2.2	526.4	3.3	516.2	14.9	484.1	14.0	102	0.29	1.08	526.4	19.8
15	18.58	208	0.51	0.08441	0.6	0.6510	2.2	0.0559	2.1	0.02579	1.3	526.8	3.0	517.1	13.6	491.2	12.8	102	-0.13	1.93	526.8	19.8
03	23.75	248	0.78	0.08443	0.5	0.7182	2.0	0.0617	2.0	0.02683	1.2	527.2	2.8	529.2	13.6	565.0	14.1	100	0.33	2.38	527.2	19.8
39	43.29	495	0.40	0.08515	0.4	0.6950	1.2	0.0592	1.1	0.02723	1.0	528.9	2.2	523.6	6.5	514.2	6.2	101	0.19	2.66	528.9	19.8
49	6.62	77	0.32	0.08564	0.9	0.7176	3.5	0.0608	3.4	0.02791	2.6	530.9	4.7	532.3	18.5	549.4	18.5	100	0.27	4.00	530.9	20.2
69	40.32	449	0.46	0.08579	0.4	0.6795	1.3	0.0574	1.2	0.02827	0.9	532.0	2.3	497.2	7.4	357.1	5.5	107	0.45	2.29	532.0	19.9
14	27.96	301	0.61	0.08538	0.5	0.6842	1.6	0.0581	1.6	0.02685	0.9	532.2	2.4	519.9	9.2	487.0	8.6	102	0.15	1.92	532.2	19.9
06	14.72	168	0.36	0.08592	0.7	0.7137	2.3	0.0602	2.2	0.02775	1.7	533.0	3.4	532.8	11.4	543.9	11.2	100	0.22	1.97	533.0	20.1
29	24.59	278	0.39	0.08632	0.7	0.6746	2.2	0.0567	2.1	0.02635	1.4	536.9	3.7	527.6	15.5	500.2	14.6	102	-0.06	3.19	536.9	20.3

Spot No.	Pb* (ppm)	U (ppm)	atomic Th/U	Measured isotope ratios and 1σ (%) internal errors								Corrected ages and 1σ absolute internal errors (Ma)						6*/38 -7*/35 concord-ance(%)	% common 206Pb	Spot MSW D	Selected age and 1σ absolute external error (Ma)	
				206Pb/238U	±	207Pb/235U	±	207Pb/206Pb	±	208Pb/232Th	±	206Pb*/238U	±	207Pb*/235U	±	207Pb*/206Pb*	±					
10	53.71	612	0.33	0.08686	0.5	0.6947	1.2	0.0580	1.1	0.02729	1.1	953.1	2.6	531.1	6.2	508.0	5.6	102	0.07	4.03	539.1	20.2
85	56.48	624	0.46	0.08699	0.5	0.7179	1.2	0.0599	1.0	0.02578	1.1	541.9	2.7	568.8	6.7	688.4	7.3	95	-0.31	3.59	541.9	7.0
38	50.40	510	0.80	0.08675	0.4	0.6845	1.3	0.0572	1.2	0.02707	0.9	542.4	2.3	523.5	10.6	470.3	9.6	104	0.09	2.53	542.4	20.3
63	12.93	126	0.92	0.08692	0.7	0.7040	3.0	0.0587	2.9	0.02781	1.4	542.5	3.8	506.5	20.6	382.6	16.3	107	0.54	1.59	542.5	20.5
01	25.14	260	0.68	0.08727	0.5	0.6898	1.7	0.0573	1.6	0.02816	1.2	542.6	2.9	502.2	13.9	347.4	10.1	108	0.47	2.19	542.6	20.3
75	50.53	537	0.61	0.08706	0.7	0.7423	1.5	0.0618	1.3	0.02592	1.2	544.0	3.8	591.1	12.5	790.6	14.8	92	-0.44	6.80	544.0	7.5
33	12.34	134	0.48	0.08765	0.7	0.6840	2.5	0.0566	2.4	0.02792	1.7	544.4	3.7	514.3	14.3	400.0	11.5	106	0.23	1.97	544.4	20.5
53	26.54	303	0.27	0.08812	0.7	0.6850	1.9	0.0564	1.8	0.02887	1.7	545.4	3.7	516.1	20.0	397.7	16.1	106	0.21	2.89	545.4	20.6
05	21.48	226	0.60	0.08780	0.6	0.7325	1.7	0.0605	1.6	0.02783	1.0	546.2	3.2	543.0	10.7	550.1	10.5	101	0.24	2.45	546.2	20.5
52	31.27	344	0.40	0.08833	1.0	0.7294	2.1	0.0599	1.9	0.02800	1.7	548.0	5.1	547.6	17.0	558.8	16.8	100	0.13	6.39	548.0	21.0
47	23.97	258	0.53	0.08774	0.8	0.7240	1.7	0.0599	1.5	0.02541	1.7	549.2	4.3	591.8	13.1	773.8	15.2	93	-0.62	3.96	549.2	20.8
84	18.85	192	0.74	0.08805	0.9	0.6816	2.4	0.0561	2.3	0.02586	1.5	551.6	4.7	566.1	16.6	643.0	17.7	97	-0.60	3.27	551.6	8.1
08	57.13	623	0.41	0.08903	0.5	0.7120	1.1	0.0580	1.0	0.02814	1.0	552.4	2.4	537.9	7.1	490.7	6.4	103	0.12	3.49	552.4	20.6
16	29.81	320	0.45	0.08915	0.4	0.7065	1.5	0.0575	1.5	0.02809	1.1	553.6	2.4	535.2	9.2	473.1	8.2	103	0.11	1.85	553.6	20.7
36	26.44	257	0.86	0.08883	0.5	0.7373	1.5	0.0602	1.5	0.02809	1.0	554.4	2.7	540.9	11.9	515.7	11.3	102	0.31	2.06	554.4	20.7
66	25.04	260	0.57	0.08935	0.5	0.7127	1.7	0.0578	1.7	0.02807	1.2	555.7	2.7	537.8	10.5	482.4	9.5	103	0.13	1.91	555.7	20.8
61	14.14	152	0.43	0.08950	0.6	0.6951	2.4	0.0563	2.3	0.02792	1.8	555.7	3.3	532.1	12.6	446.8	10.8	104	0.06	1.43	555.7	20.9
72	33.16	352	0.49	0.08958	0.5	0.7319	1.4	0.0593	1.3	0.02775	1.1	556.0	2.5	557.4	8.2	575.1	8.1	100	0.00	1.92	556.0	7.1
22	44.66	488	0.39	0.08947	0.5	0.7145	1.2	0.0579	1.1	0.02658	1.0	556.7	2.7	563.3	13.7	602.0	14.2	99	-0.24	3.11	556.7	20.8
31	13.23	141	0.45	0.09006	0.6	0.7195	2.4	0.0579	2.3	0.02892	1.5	558.2	3.4	533.1	12.1	442.4	10.2	105	0.26	1.56	558.2	21.0
48	19.45	197	0.63	0.09029	0.7	0.7331	2.1	0.0589	2.0	0.02913	1.7	560.5	3.8	530.6	16.2	426.8	13.4	106	0.42	2.65	560.5	21.1
21	22.36	237	0.46	0.09037	0.6	0.7548	1.8	0.0606	1.7	0.02847	1.3	560.8	3.0	562.2	10.0	583.3	10.0	100	0.14	2.19	560.8	21.0
09	18.31	184	0.67	0.09014	0.7	0.7303	2.0	0.0588	1.9	0.02816	1.3	561.4	3.7	548.4	13.8	518.2	12.9	102	0.13	2.82	561.4	21.2
50	6.09	63	0.48	0.09134	0.8	0.7649	3.3	0.0607	3.2	0.02935	2.4	565.7	4.6	553.5	20.4	520.6	19.2	102	0.36	1.51	565.7	21.5
11	30.37	308	0.58	0.09135	0.7	0.7377	1.8	0.0586	1.6	0.02831	1.4	568.3	3.6	559.9	11.6	545.7	11.0	102	0.02	3.46	568.3	21.4
46	31.32	318	0.52	0.09241	0.8	0.7281	1.9	0.0571	1.8	0.03050	1.2	571.3	4.2	517.2	10.9	304.2	6.8	110	0.56	5.25	571.3	21.6
41	19.10	180	0.47	0.10039	0.8	0.8136	2.0	0.0588	1.9	0.03389	1.7	617.4	5.1	560.2	28.0	351.0	19.1	110	0.62	3.19	617.4	23.5
71	99.54	800	1.40	0.09561	2.4	1.8180	5.9	0.1379	5.4	0.03065	6.9	621.7	17.5	1219.8	67.7	2548.7	84.4	51	-4.28	nd	d	
51	109.3	763	0.84	0.12113	2.4	1.2412	2.7	0.0743	1.1	0.04740	1.7	725.4	17.1	565.7	56.3	18.8	3.4	128	3.28	135.7	d,x	

All errors are 1σ, * = radiogenic component only, nd = not determined, d = discordant, rd = reversely discordant, x = excess within grain MSWD.

4. LA-ICP-MS Methodology (J. Michael Palin, March 2008)

Dating was undertaken at the Research School of Earth Sciences at the Australian National University following procedures established by Ballard et al. (2001) and described in detail by Bryan et al. (2004). Laser ablation was conducted with a pulsed LambdaPhysik LPX 120I UV ArF excimer laser operated at a constant energy of 120 mJ and 5 Hz, using a spot diameter of 32 μm. Ablated material was carried by a mixed He-Ar gas from a custom-designed sample cell and flow homogeniser to an Agilent 7500 ICP-MS. Data for 18 mass peaks were collected in time-resolved mode with one point per peak. Integration times were 40 ms for ^{206}Pb, ^{207}Pb, and ^{208}Pb; 25 ms for ^{232}Th, ^{235}U, and ^{238}U; 5 ms for ^{29}Si and ^{91}Zr; 10 ms for ^{31}P, ^{89}Y, ^{139}La, ^{140}Ce, ^{147}Sm, ^{153}Eu, ^{163}Dy, ^{175}Lu, and ^{177}Hf; 20 ms for ^{49}Ti, giving a total scan time of 396 ms per analysis. Because of a high ^{204}Hg blank, ^{204}Pb was not included. Background data were acquired for 20 s followed by 40 s with the laser on, giving about 100 mass scans and a penetration depth of c. 20 μm. A purge time of 30 - 60 s was allowed between each spot analysis to permit return to background signal levels.

Outlier data (> 3 σ from mean) were excluded, backgrounds subtracted and corrections made for elemental fractionation, instrumental mass bias and common Pb using an offline spreadsheet. Correction factors also were applied to each spot analysis to simultaneously correct for instrumental mass bias and depth-related elemental fractionation. After laser triggering, it took several seconds for a steady signal to be obtained, so the first 10 scans were routinely excluded. Depth-related inter-element fractionation of Pb, Th, and U were corrected by reference to TEMORA-2 standard zircon and NIST610 silicate glass. Standards were measured twice at the beginning of each session and then twice after every ten unknown analyses. Measured ^{207}Pb/^{206}Pb, ^{206}Pb/^{238}U, and ^{208}Pb/^{232}Th ratios in the zircon standard and ^{232}Th/^{238}U in NIST610, analysed at regular intervals over the course of each analytical session, were averaged and used to calculate correction factors based on accepted values (Pearce et al. 1997; Black et al. 2003).

Internal errors for individual spot analyses were taken as the standard error of the mean of the corrected isotopic ratios over the particular interval of mass scans selected for age calculation. These internal errors were compared with errors estimated from

counting statistics for the isotope ratios from each mass scan to calculate within-spot mean squared weighted deviates (MSWD) that were monitored during data interval selection. Spot analyses with resolvable age zonation or disturbance exhibiting internal MSWD values in excess of 10 were rejected from further consideration. Overall errors for each of the isotope ratios used for U-Pb geochronology were calculated by combining internal errors with the standard deviation in the same isotope ratios measured in the TEMORA-2 zircon standard over the course of each analytical session (typically 1 - 3%) as an estimate of external error (Stern & Amelin 2003). Compared to these errors, the reported uncertainty in the age of the TEMORA-2 zircon standard is negligible (Black et al. 2003).

Ages older than 800 Ma were calculated from $^{207}Pb^*/^{206}Pb^*$ ratios whereas younger ages were based on $^{206}Pb^*/^{238}U$ ratios, where * indicates radiogenic Pb, the total Pb minus common Pb). Common Pb corrections were applied based on the difference between measured and expected $^{208}Pb/^{206}Pb$ ratios for the measured $^{232}Th/^{238}U$ value, according to methods described by Compston et al. (1984). Concordance was calculated on the basis of agreement between $^{207}Pb^*/^{235}U$ and $^{206}Pb^*/^{238}U$ ages within their reported 1 σ internal errors. Analyses greater than 10% discordant were not included in the age calculation. Concordance was calculated on the basis of agreement between $^{207}Pb^*/^{235}U$ and $^{206}Pb^*/^{238}U$ ages, and has a typical uncertainty of 5 to 10%.

REFERENCES

Ballard, J.R.; Palin, J.M.; Williams, I.S.; Campbell, I.H.; Faunes, A. 2001: Two ages of porphyry intrusion resolved for the super-giant Chuquicamata copper deposit in northern Chile by ELA- ICP-MS and SHRIMP. *Geology* 29: 383–386.

Black, L.P.; Kamo, S.L.; Allen, C.M.; Aleinikoff, J.N.; Davis, D.W.; Korsch, R.J.; Foudoulis, C. 2003: TEMPORA 1: a new zircon standard for Phanerozoic U-Pb geochronology. *Chemical Geology* 200: 155-170.

Compston, W.; Williams, I.S.; Meyer, C. 1984: U-Pb geochronology of zircons from lunar breccia 73217 using a sensitive high mass-resolution ion microprobe. *Journal of Geophysical Research* 89: Supplement B525-B524.

Pearce, N.J.G.; Perkins, W.T.; Westgate, J.A.; Gorton, M.P.; Jackson, S.E.; Neal, C.R.; Chenery, S.P. 1997: A compilation of new and published major and trace element data for NIST SRM 610 and NIST SRM 612 glass reference materials. *Geostandards Newsletter* 21: 115-144.

Bryan, S.E., Allen, C.M., Holcombe, R.J., and Fielding, C.R. 2004: U–Pb zircon geochronology of Late Devonian to Early Carboniferous extension-related silicic volcanism in the northern New England Fold Belt. *Australian Journal of Earth Sciences* 51: 645-664.

Stern, R.A.; Amelin, Y. 2003: Assessment of errors in SIMS zircon U-Pb geochronology using a natural zircon standard and NIST SRM 610 glass. *Chemical Geology* 197: 111-142.

Appendix C: Rock Sample List

Field Site	Sample number	UC number	GPS	Elevation	Formation	Hand Specimen	Thin Section
Samples Collected by Greer Gilmer							
Mt Jason	**J1**	18727	77º 28.918' S 161º 36.006'E ±5 m	1647 m	New Mountian Sandstone	Y	Y
	J2	18728	77º 28.918' S 161º 36.006'E ±5 m	1647 m	New Mountian Sandstone	Y	Y
	J3	18729			New Mountian Sandstone	Y	
	J4	18730	77º 28.902'S 161º 35.746'E ±7 m	1644 m	New Mountian Sandstone	Y	
	J5	18731	77º 28.902'S 161º 35.746'E ±7 m	1644 m	New Mountian Sandstone	Y	Y
	J6	18732	77º 29.065'S 161º 34.958'E ±5 m	1703 m	New Mountian Sandstone	Y	Y
	J7	18733	77º 29.164'S 161º 34.198'E	1748 m	Odin Arkose Member	Y	Y
	J8	18734			Odin Arkose Member	Y	Y
	J12	18735	77º 28.799'S 161º 37.409'E ±5 m	1628 m	Terra Cotta Siltstone?	Y	
	J13	18736	77º 28.799'S 161º 37.409'E ±5 m	1628 m	New Mountian or Windy Gully Sandstone	Y	
	J14	18737	77º 28.799'S 161º 37.409'E ±5 m	1628 m	Windy Gully Sandstone?	Y	
	J15	18738	77º 28.799'S 161º 37.409'E ±5 m	1628 m	Windy Gully Sandstone?	Y	
	J16	18739	Close to above		New Mountain Sandstone	Y	
	J17	18740	Close to above		New Mountain Sandstone	Y	
	J18	18741			New Mountain Sandstone	Y	
	J19	18742			Odin Arkose Member	Y	Y
	J20	18743	77º 29.536'S 161º 33.884'E ±7 m	1761 m	Odin Arkose Member		Y
	J21	18744	77º 30.084'S 161º 34.338'E ±5 m	1663 m	New Mountain Sandstone	Y	
	J22	18745	77º 30.084'S 161º 34.338'E ±5 m	1663 m	New Mountain Sandstone	Y	
Mt Hercules	**H10**	18746	77º 29.117'S 161º 26.854'E ±6 m	1647 m	Odin Arkose Member	Y	
	H11	18747	77º 29.117'S 161º 26.854'E ±6 m	1647 m	Odin Arkose Member		Y
	H23	18748			Odin Arkose Member	Y	
Mt Aeolus	**B4**	18749	Close to 77º 30.391'S 161º 18.205'E ±8.5 m	1439 m	Windy Gully Sandstone	Y	Y
	B5	18750			New Mountain Sandstone	Y	Y
	B6	18751	77º 30.128'S 161º 18.371'E ±7 m	1550 m	New Mountain Sandstone	Y	Y
	B7	18752			Odin Arkose Member	Y	Y
	B8	18753			Odin Arkose Member	Y	Y
Mt Boreas	**B1**	18754	77º 28.136'S 161º 05.861'E ±6 m	1344 m	Odin Arkose Member	Y	
	B2	18755	77º 28.136'S 161º 05.861'E ±6 m	1344 m	Odin Arkose Member	Y	Y
	B3	18756			Odin Arkose Member	Y	Y
Mt Electra	**E24**	18757	77º 30.812'S 161º 51.066'E ±7 m	1269 m	Altar Mountain Formation?	Y	Y
	E25	18758	77º 30.941'S 160º 51.559'E ±8 m	1215 m	Odin Arkose Member	Y	
	E26	18759			Odin Arkose Member	Y	
	E27	18760			Altar Mountain Formation	Y	Y
	E28	18761			Altar Mountain Formation		Y
	E29	18762	Close to 77º 31.002'S 160º 56.685'E	1104 m	Boreas Subgreywacke Member	Y	
	E30	18763	Close to 77º 31.002'S 160º 56.685'E	1104 m	Boreas Subgreywacke Member	Y	
	E31	18764	Close to 77º 31.002'S 160º 56.685'E	1104 m	Boreas Subgreywacke Member	Y	
	E32	18765	Close to 77º 31.002'S 160º 56.685'E	1104 m	Boreas Subgreywacke Member	Y	
	E33	18766	77º 30.916'S 160º 59.039'E ±11 m	1244 m	New Mountain Sandstone	Y	
	E34	18767	77º 30.764'S 160º 58.829'E ±6 m	1297 m	Odin Arkose Member	Y	
	E35	18768			Odin Arkose Member?		Y
	E36	18769	77 31.029'S 160 44.933'E 5 m	1045 m	Odin Arkose Member	Y	Y
	E37	18770	77 31.029'S 160 44.933'E 5 m	1045 m	Odin Arkose Member	Y	
	E38	18771	77 31.029'S 160 44.933'E 5 m	1045 m	Odin Arkose Member	Y	

Lake Vashka	**V39**	18772				New Mountain Sandstone	Y	Y
	V40	18773				New Mountain Sandstone	Y	
	V41	18774	Not in section line			Odin Arkose Member?	Y	
	V42	18775				New Mountain Sandstone	Y	Y
	V43	18776	77 21.660'S	161 06.071'E	6 m	918 m Odin Arkose Member	Y	Y
	V44	18777				New Mountain Sandstone	Y	
Vashka Crag	**VC46**	18778	77 19.983'S	161 05.722'E	8 m	932 m New Mountain Sandstone	Y	Y
	VC47	18779	77 20.149'S	161 08.041'E	6 m	869 m New Mountain Sandstone	Y	Y
	VC48	18780	77 20.107'S	161 08.581'E	9 m	741 m New Mountain Sandstone	Y	
	VC49	18781	Close to above sample			New Mountain Sandstone?	Y	
	VC50	18782	77 19.788'S	161 05.460'E	6 m	1000 m New Mountain Sandstone	Y	Y
Sponsors Peak	**S51**	18783	77 19.083'S	161 24.451'E	6 m	1096 m New Mountain Sandstone	Y	Y
	S52	18784	77 19.083'S	161 24.451'E	6 m	1096 m Odin Arkose Member	Y	
	S53	18785	77 19.083'S	161 24.451'E	6 m	1096 m Odin Arkose Member	Y	Y
	S54	18786	77 18.725'S	161 27.298'E	7 m	1203 m Odin Arkose Member	Y	
	S55	18787	77 18.725'S	161 27.298'E	7 m	1203 m Odin Arkose Member	Y	
	S66	18788	77 29.782'S	161 17.503'E	5 m	1225 m New Mountain Sandstone	Y	
	S68	18789	77 18.797'S	161 10.558'E	6 m	1366 m Odin Arkose Member	Y	
Balham Lake	**BL56**	18790				Salmon Marble	Y	
	BL58	18791				Pink granite	Y	
	BL59	18792				Schist	Y	
	BL60	18793				Basement rocs	Y	
	BL61	18794	77 25.823'S	160 53.733'E	6 m	863 m Odin Arkose Member	Y	
	BL62	18795	77 25.823'S	160 53.733'E	6 m	863 m Odin Arkose Member	Y	
	BL63	18796				Odin Arkose Member?	Y	
	BL64	18797				Odin Arkose Member	Y	Y
	BL65	18798				Altar Mountain Formation	Y	
	Lab1	18799				White Siltstone/Rhyolite		Y

Samples Colected by Dr Robert Bolhar

Mt Jason	**J201**	18800	77°28.918'S	161°36.006'E		Odin Arkose Member	Y	
	J202	18801	77°28.801'S	161°37.404'E		Terra Cotta Siltstone?	Y	Y
	J203	18802	77°29.260'S	161°34.285'E		Odin Arkose Member	Y	Y
	J204	18803	77°29.210'S	161°34.478'E		New Mountain Sandstone	Y	Y
Mt Electra	**E205**	18804	77° 30.760'S	160° 58.805'E		Odin Arkose Member	Y	Y
	E206	18805	77° 30.760'S	160° 58.805'E		Odin Arkose Member	Y	Y
	E207	18806	77° 30.805'S	160° 59.073'E		New Mountain Sandstone	Y	Y
Sponsors Peak	**SP210**	18807				?	Y	